SANDIA REPORT

SAND94—0361 • UC—610
Unlimited Release
Printed July 1994

MELCOR 1.8.3 Assessment: GE Large Vessel Blowdown and Level Swell Experiments

Lubomyra Nadia Kmetyk

Prepared by
Sandia National Laboratories
Albuquerque, New Mexico 87185 and Livermore, California 94550
for the United States Department of Energy
under Contract DE-AC04-94AL85000

Issued by Sandia National Laboratories, operated for the United States Department of Energy by Sandia Corporation.

Available to DOE and DOE contractors from
Office of Scientific and Technical Information
PO Box 62
Oak Ridge, TN 37831

Prices available from (615) 576-8401, FTS 626-8401

Available to the public from
National Technical Information Service
US Department of Commerce
5285 Port Royal RD
Springfield, VA 22161

NTIS price codes
Printed copy: A11
Microfiche copy: A06

Distribution
Category UC-610

SAND94-0361
Unlimited Release
Printed July 1994

MELCOR 1.8.3 Assessment: GE Large Vessel Blowdown and Level Swell Experiments

Lubomyra Nadia Kmetyk
Thermal/Hydraulic Analysis Department
Sandia National Laboratories
Albuquerque, NM 87185-0745

Abstract

MELCOR is a fully integrated, engineering-level computer code, being developed at Sandia National Laboratories for the USNRC, that models the entire spectrum of severe accident phenomena in a unified framework for both BWRs and PWRs. As part of an ongoing assessment program, the MELCOR computer code has been used to analyze a series of blowdown tests performed in the early 1980s at General Electric. The GE large vessel blowdown and level swell experiments are a set of primary system thermal/hydraulic separate effects tests studying the level swell phenomenon for BWR transients and LOCAs; analysis of these GE tests is intended to validate the new implicit bubble separation algorithm added since the release of MELCOR 1.8.2. Basecase MELCOR results are compared to test data, and a number of sensitivity studies on input modelling parameters and options have been done. MELCOR results for these experiments also are compared to MAAP and TRAC-B qualification analyses for the same tests. Time-step and machine-dependency calculations were done to identify whether any numeric effects exist in our GE large vessel blowdown and level swell assessment analyses.

Contents

List of Figures

List of Tables

1 Introduction

MELCOR [1] is a fully integrated, engineering-level computer code, being developed at Sandia National Laboratories for the U. S. Nuclear Regulatory Commission (USNRC), that models the progression of severe accidents in light water reactor (LWR) nuclear power plants. The entire spectrum of severe accident phenomena, including reactor coolant system and containment thermal/hydraulic response, core heatup, degradation and relocation, and fission product release and transport, is treated in MELCOR in a unified framework for both boiling water reactors and pressurized water reactors.

The MELCOR computer code has been developed to the point that it is now being successfully applied in severe accident analyses. Some limited technical assessment activities were performed early in the MELCOR development process [2]; more recently, a systematic program of verification and validation has been underway. To this end, a number of assessment calculations have been and are being done [3-11]. One of these assessment activities is analysis of a series of blowdown tests performed in the early 1980s at General Electric (GE) [12].

The GE large vessel blowdown and level swell experiments are a set of primary system thermal/hydraulic separate effects tests studying the level swell phenomenon for BWR transients and LOCAs. This experiment series includes both top blowdown tests with vapor blowdown, characteristic of accidents such as steam line breaks, and bottom blowdown tests with liquid and two-phase blowdown, more characteristic of recirculation line breaks. Assessment against this data allows an evaluation of the ability of MELCOR to predict the inventory loss, and hence time to core uncovery and heatup, in the early stages of transients and accidents in BWRs. Also, an implicit bubble separation algorithm has been implemented recently in the CVH package in MELCOR. Prior to the implementation of this algorithm, MELCOR was experiencing problems with natural circulation phenomena in the COR package; it is expected that the problems with calculating natural circulation will be eliminated with the implementation of the implicit bubble separation algorithm. Analysis of the GE tests is intended to validate this algorithm for general use.

MELCOR version 1.8OO was used for all the calculations described in this report, except for a sensitivity study on the effect of the implicit bubble separation algorithm which compares results from MELCOR version 1.8OO to results from the release version of MELCOR 1.8.2, which was MELCOR 1.8NM. Note that these MELCOR calculations were done as an open post-test study, with both the experimental data and other code results [13, 14, 15, 16] available to guide the selection of code input.

The test facility, experimental configuration and experimental procedure are outlined briefly in Section 2. Section 3 describes the input used for these MELCOR assessment analyses. The results of our basecase calculations are given in Section 4, while sensitivity studies on MELCOR modelling options and input parameters in the CVH and FL packages, respectively, are presented in Section 5 and 6. Section 7 contains the results of our time step and machine dependency sensitivity studies, and compares results obtained with a recent code version with the implicit bubble separation algorithm with results obtained using the release version of MELCOR 1.8.2 (in which the bubble rise calculation

is explicitly coupled to the rest of the thermal/hydraulics analysis). Comparison with results obtained by other codes is done in Section 8. A summary and conclusions of this MELCOR assessment study are presented in Section 9. A listing of the input used for the Test 5801-13 basecase calculation is given in Appendix A.

2 Facility and Test Description

Void-fraction distribution and level-swell phenomena have been measured during blowdown tests conducted at General Electric [12]. These experiments were conducted in two vessels designated as the "small blowdown vessel" and the "large blowdown vessel". These blowdown tests were primarily separate effects tests investigating such basic phenomena as critical flow and transient liquid-vapor level swell during a blowdown. Important parameters controlling void distribution and level swell include initial fluid conditions, vessel depressurization rate, break size and location and vessel geometry. A brief description of the large blowdown vessel test facility is given in this section, together with descriptions of the various blowdown tests performed in the large vessel and important test parameters.

A schematic of the large blowdown vessel test apparatus, including the vessel, the blowdown line and instrumentation locations, is shown in Figure 2.1. The pressure vessel was 1.19m (47in) in diameter, 4.3m (14ft) long, and contained a volume of 4.5m^3 (160ft^3). The cylindrical body and hemispherical end caps of the vessel were 1in-thick carbon steel and insulated on the outside. Initially saturated water at over 7.14MPa (>1000psia) partially filled the vessel; saturated steam filled the remainder of the tank. The vessel had provision for a dip tube as part of the blowdown line. The dip tube had a 26.35cm (10.374in) inner diameter and was 0.4775cm (0.188in) thick.

A number of blowdown tests were conducted, some with blowdown occurring near the top of the vessel and others with blowdown occurring near the bottom of the vessel. Figure 2.1 shows the dip tube inserted so that a top-level blowdown is represented. When the dip tube was installed, the blowdown flow left the vessel above the two-phase level and a vapor blowdown occurred. For the bottom blowdown tests, the vertical dip tube shown in the figure was removed so that the blowdown line extended from the vessel in the horizontal direction only. Without the dip tube, the first part of the blowdown was a liquid blowdown because the break was covered; later in the blowdown, the break uncovered and a vapor blowdown followed. Flow-limiting Venturi nozzles with various throat diameters were inserted into the horizontal blowdown line to vary the break area and hence the blowdown flow rate and resulting vessel depressurization rate. Rupture discs were used to initiate the blowdown.

Table 2.1 summarizes the test matrix for the large vessel blowdown tests. The tests indicating top break were those with the dip tube installed, while the bottom break tests were with the dip tube removed.

There were three basic types of measurements made during each test: pressures, pressure differences, and temperatures. Figure 2.1 includes the instrumentation arrangement used. Strain-gage pressure transducers were used for measuring vessel pressure and differential pressure. Iron-Constantan thermocouples were used for determining the fluid temperatures. Two-phase mixture densities in the measurement nodes were obtained from the measurements of the axial differential pressure, *i.e.*, hydrostatic head of the fluid.

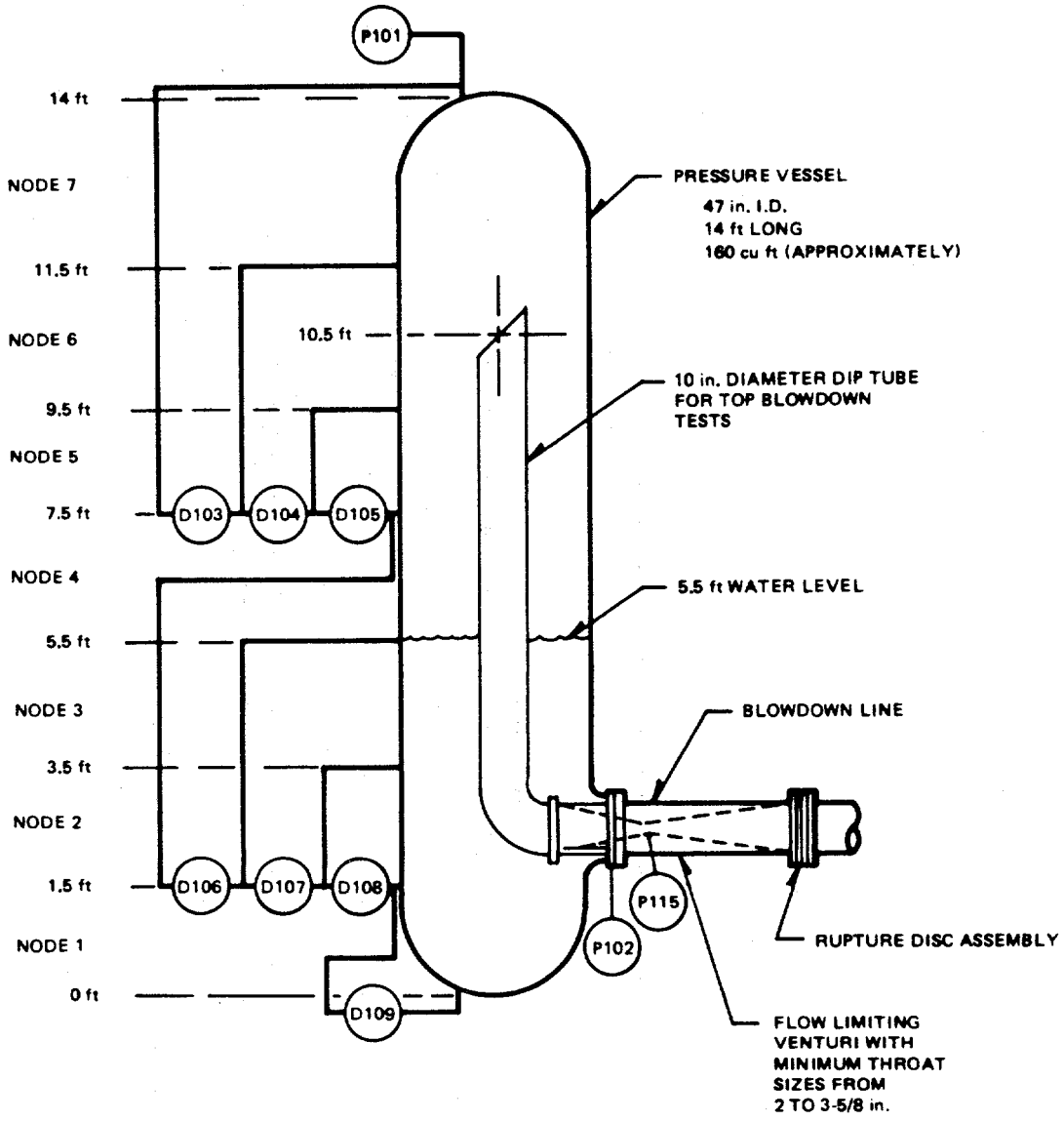

Figure 2.1. Schematic of GE Large Blowdown Vessel Test Facility

Table 2.1. Test Parameter Matrix for GE Large Vessel Blowdown Tests

Test No.	Blowdown Nozzle Size	Break Location	Initial Conditions Pressure	Initial Conditions Level
5801-13	5.3975cm (2-1/8in)	Top	7.3046MPa (1060psia)	1.6764m (5.5ft)
5801-15	3.81cm (2-1/2in)	Top	7.3046MPa (1060psia)	1.6764m (5.5ft)
5801-19	7.62cm (3in)	Top	7.3046MPa (1060psia)	1.6764m (5.5ft)
5802-16	9.2075cm (3-5/8in)	Top	7.3046MPa (1060psia)	1.6764m (5.5ft)
5803-1	5.3975cm (2-1/8in)	Bottom	7.2357MPa (1050psia)	2.28m (7.5ft)
5803-2	7.62cm (3in)	Bottom	7.2357MPa (1050psia)	2.8956m (9.5ft)

3 MELCOR Computer Model

The basecase MELCOR input model used for these GE large vessel experiment calculations is shown in Figure 3.1. Two control volumes, one flow path, and one heat structure are used in the basecase MELCOR model. (A copy of the input used for the 5801-13 top blowdown test basecase calculation is given in the appendix, for documentation.)

One control volume represents the vessel itself, with a volume-altitude table used to represent the hemispherical ends and the cylindrical body. The vessel control volume is specified to use nonequilibrium thermodynamics and to be a vertical volume. The other control volume is a time-independent volume used to model a constant, ambient environment serving as the blowdown flow sink.

A single flow path is used for the blowdown line, with two segments specified for the top blowdown test analyses (one representing the dip tube and the other the horizontal line containing the Venturi nozzle); for the bottom blowdown test analyses, only one flow segment is used (for the horizontal blowdown line). The flow path area is set to the nozzle throat area, while the segment flow areas are set to the dip tube and blowdown line pipe open areas.

A single heat structure is included to represent the cylindrical body of the vessel; the hemispherical end caps are neglected, because structural heat transfer is not expected to be a significant phenomenon at the short time scales characteristic of these blowdown and level swell experiments. The structure is specified to use "internal" heat transfer coefficient correlations on the inside surface, with the vessel diameter input as the characteristic length, while on the outside surface the heat structure is specified to be adiabatic. Five equally-spaced nodes are used in the wall. Radiation heat transfer using the gray gas model is enabled with an emissivity of 0.8. The heat structure uses MELCOR's steady-state temperature-gradient self-initialization option.

Bubble rise in the MELCOR thermal/hydraulics model is accounted for only in nonequilibrium volumes, such as normally used. As part of this assessment, a sensitivity study was done in which the vessel control volume was specified to use equilibrium, rather than nonequilibrium, thermodynamics; results are presented in Section 5.1. Other sensitivity studies on parameters directly affecting level swell were done varying the maximum allowed pool bubble fraction and the pool bubble rise velocity, as discussed in Sections 5.2 and 5.3.

Another sensitivity study was done in which the single vessel control volume was subdivided into a stack of control volumes, 11 for the cylindrical section, each 0.3048m (1ft) high, and one each for the hemispherical ends, as illustrated in Figure 3.2 for a bottom blowdown experiment configuration. Vertical flow paths were added as needed to connect the stacked volumes, with flow areas equal to the vessel cylinder area and lengths set to 0.3048m (1ft). The heat structure modelling the vessel cylinder was subdivided correspondingly, also. Since there is no obvious geometrically "correct" value for junction opening heights in flow paths connecting such a stack of volumes, both large (1ft) and

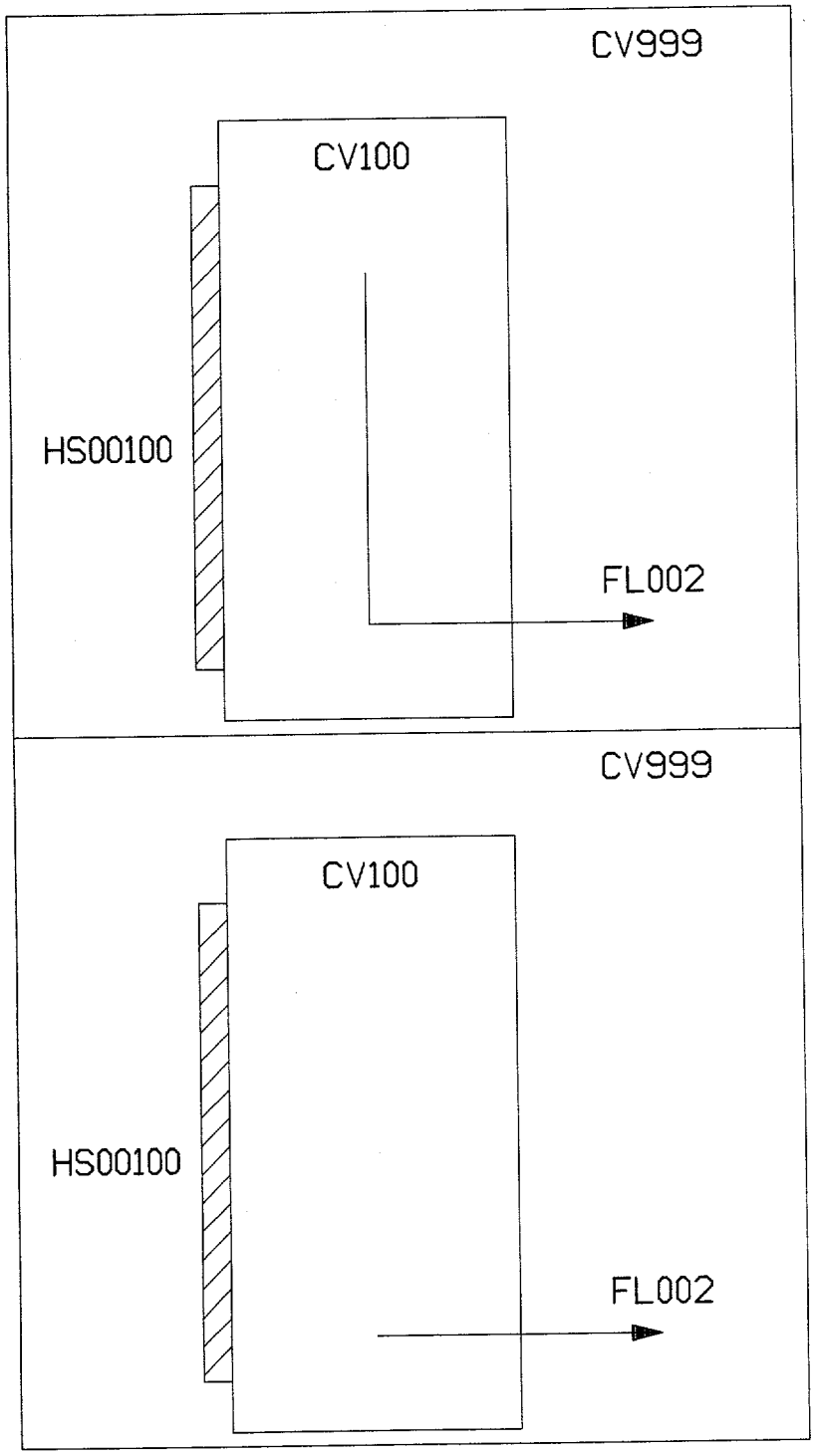

Figure 3.1. Reference MELCOR Model for GE Large Vessel Test Facility – Top Blowdown Configuration (top) and Bottom Blowdown Configuration (bottom)

small (1cm) junction opening heights were tried. Results using this more refined vessel nodalization are discussed in Section 5.4.

Other sensitivity studies were done varying the discharge coefficients and form loss coefficients in the blowdown line flow path, with results given in Sections 6.1 and 6.2, and with SPARC bubble rise physics turned on (as for the basecase calculations) and off (the code default) in the blowdown line flow path, with results given in Section 6.3.

The user-specified maximum time step in the basecase calculations was 2s, and the calculations were set to begin with a time step of 1ms at t=0. The code generally ran at an internally-determined time step in the basecase calculations. Results of a time-step study are given in Section 7.2. The majority of these GE large vessel blowdown and level swell MELCOR calculations were run on a 486PC. Results of a machine-dependency study are given in Section 7.1.

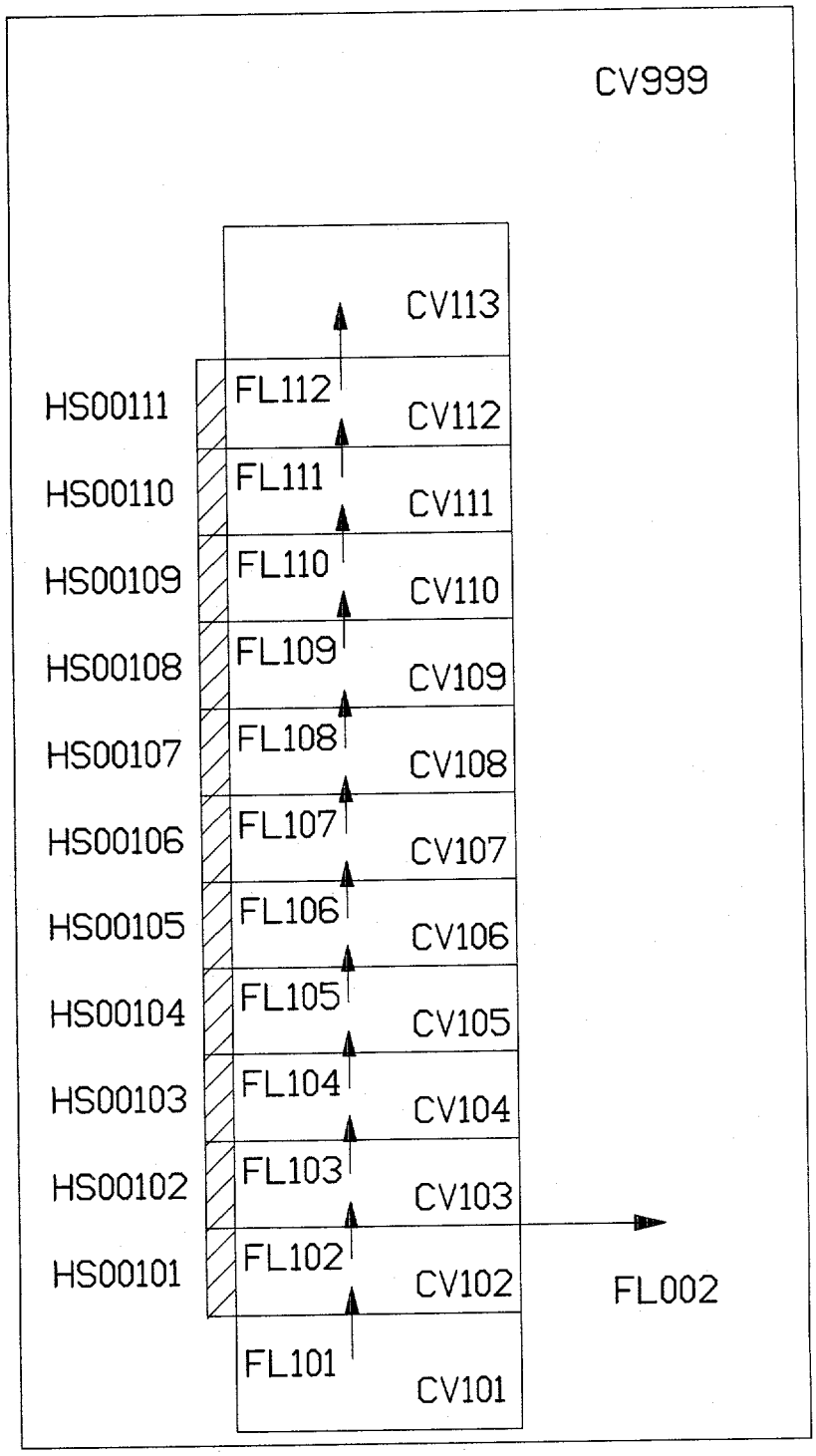

Figure 3.2. Stacked-Volume MELCOR Model for GE Large Vessel Test Facility – Bottom Blowdown Configuration

4 Basecase Calculation Results

This section gives basecase MELCOR assessment analysis results for the GE large vessel blowdown and level swell experiments. The results for both top blowdown tests and bottom blowdown tests are discussed for one test in more detail, and for the other tests more briefly, in comparison only.

4.1 Top Blowdown Tests

Test 5801-13 is a top blowdown test in the large blowdown vessel, with a nozzle diameter of 5.3975cm (2-1/8in). Initially the vessel is at 7.305MPa (1060psia) and the water level is at 1.6764m (5.5ft), at the interface between measurement nodes 3 and 4 in Figure 2.1. The void fraction is 0.0 below and 1.0 above this interface initially. The blowdown is initiated by bursting the rupture discs at time t=0.

The predicted vessel pressure history is compared with test data in Figure 4.1.1. The calculated pressure transient generally agrees well with the measurement. There is a relatively fast depressurization for the first few seconds, with progressively slower depressurization later in the transient.

One difference between the calculated and observed system pressure response is visible early in the transient. The test data indicates a sharp pressure dip and subsequent recovery in the first few seconds. This pressure dip occurs because steam is lost from the upper region of the vessel through the dip tube and blowdown line, locally depressurizing the system. As the pressure is reduced, flashing occurs in the initially saturated liquid region in the lower portion of the vessel; vapor bubbles nucleate and grow, and the expansion of the bubbles displaces liquid, causing the level to rise. As the two-phase mixture level swells, the steam remaining in the upper vessel is compressed and the system repressurizes.

This observed pressure dip and recovery is not predicted because delayed nucleation is not modelled in the code. The observed brief pressure undershoot is a strong function of the depressurization rate, the magnitude of the initial pressure, and of the amount of heterogeneity such as pre-existing voids and impurities present in the fluid. It is not expected to be a significant phenomenon in a BWR LOCA because of the presence of voids in the core and upper plenum, and due to the short time scale.

Figure 4.1.2 gives the swollen and collapsed liquid levels in the vessel control volume predicted by MELCOR, together with test data on the two-phase mixture level. The elevation of the entrance to the blowdown line (*i.e.*, the top of the dip tube) is also included in Figure 4.1.2, for reference. An error bar is included with the two-phase liquid level test data, providing a measurement accuracy and uncertainty estimate.

As discussed above, the two-phase level swells up initially due to flashing in the saturated liquid in the lower vessel as the pressure is reduced. The mixture level continues to rise until the free separation rate at the mixture-vapor interface exceeds the vapor

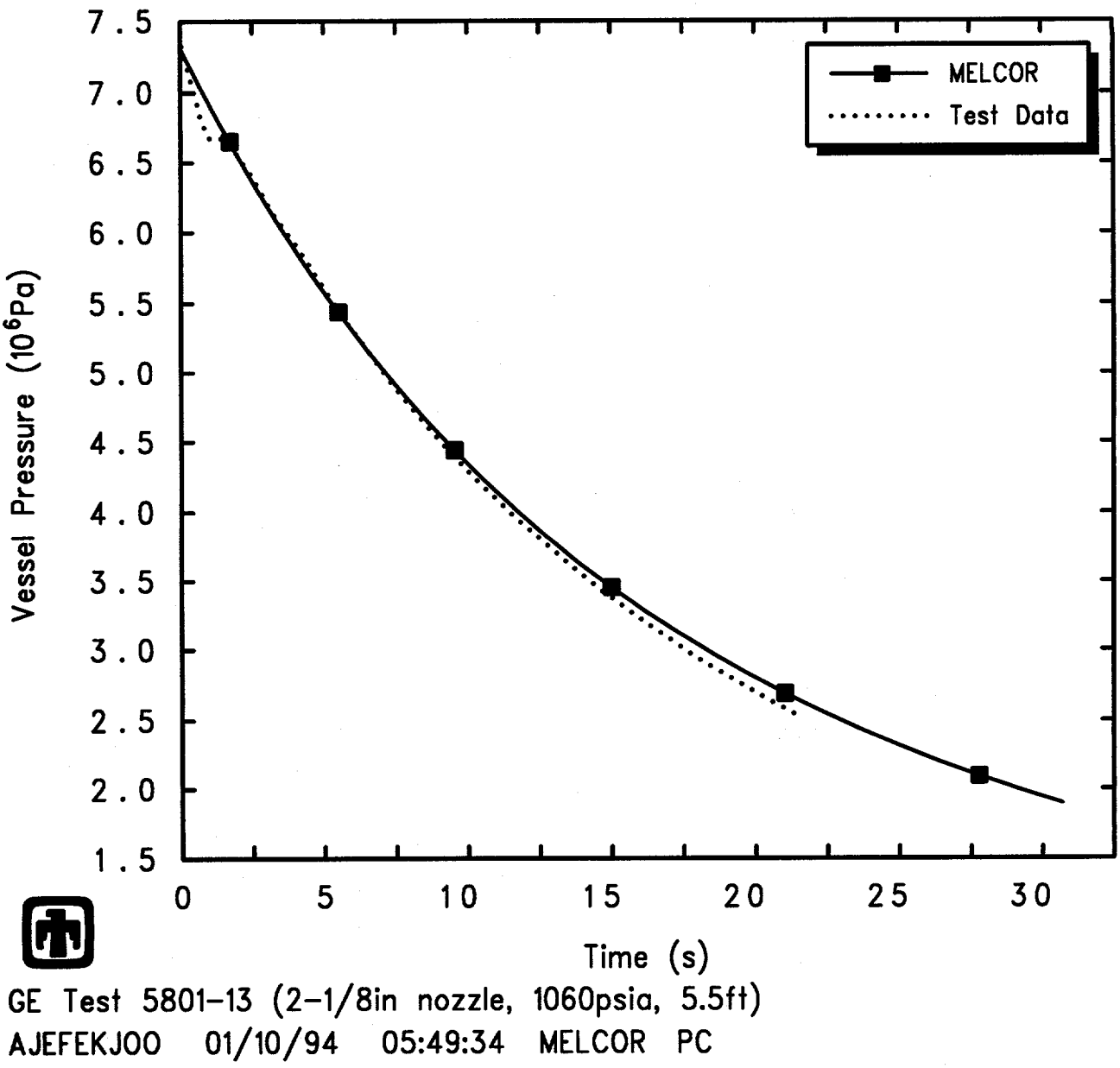

Figure 4.1.1. Vessel Pressure for GE Large Vessel Top Blowdown Test 5801-13 – Basecase Calculation Compared to Test Data

generation rate; when the separation rate exceeds the generation rate, the level falls. The two-phase mixture, or swollen, level calculated by MELCOR qualitatively correctly reproduces the observed initial swelling, and the predicted two-phase level initially increases at about the rate determined from measurement. However, the vessel swollen level calculated by MELCOR reaches a maximum visibly below the maximum two-phase level in the test data, and begins decreasing earlier in the calculation than observed in the test. The swollen liquid level in the calculation later decreases less rapidly than observed for the measured two-phase liquid level.

The maximum swollen level in the MELCOR calculation corresponds to the bubble fraction in the pool reaching a value of $\leq$0.40, as indicated in Figure 4.1.3. As discussed in more detail in Section 5.2, this is the default maximum allowed value in the CVH package in MELCOR for the pool bubble fraction; for numerical stability reasons, the maximum amount of bubbles which can exist in a pool has been limited to 40%. The swollen liquid level of the pool in the vessel is subsequently calculated to drop as the collapsed liquid level drops, due to continued inventory loss out the blowdown line, to maintain a pool bubble fraction of $\sim$0.40.

Figure 4.1.4 presents the flow calculated in the blowdown line. Because the top of the dip tube remains above the swollen level in the vessel, as indicated in Figure 4.1.2, the blowdown outflow is vapor throughout the transient, for this top blowdown test.

The results found for test 5801-13 are generally typical of the behavior seen in the other top blowdown test analyses. The predicted vessel pressure histories are compared with test data for all four top blowdown test analyses in Figure 4.1.5. Qualitatively, the MELCOR calculations correctly reproduce the increase in vessel depressurization rate as the nozzle throat diameter and area increase, in the top blowdown experiment set. Quantitatively, there is progressively more difference between the calculated and measured vessel pressures as the nozzle throat diameter and area increases and the depressurization rate increases. This difference is due partly to the fact that the single value of form loss and discharge coefficients used in all these basecase calculations may not be optimum for all test conditions (as indicated by sensitivity studies described in Sections 6.1 and 6.2), and partly due to increased discrepancies between measured and predicted level swelling as the nozzle throat diameter and area, and hence the depressurization rate, is increased.

Figure 4.1.6 gives the swollen liquid levels in the vessel control volume predicted by MELCOR, together with test data on the two-phase mixture level, for all four top blowdown tests. Again, the elevation of the entrance to the blowdown line (*i.e.*, the top of the dip tube) is included in Figure 4.1.6, for reference. Error bars are included with the two-phase liquid level test data for tests 5801-13 and 5801-15, providing a measurement accuracy and uncertainty estimate. No two-phase level data were available for test 5801-19.

The test data show the two-phase mixture levels increasing more rapidly early in the transient as the nozzle throat diameter and area, and hence the depressurization rate, is increased, and also shows the two-phase mixture level reaching progressively greater

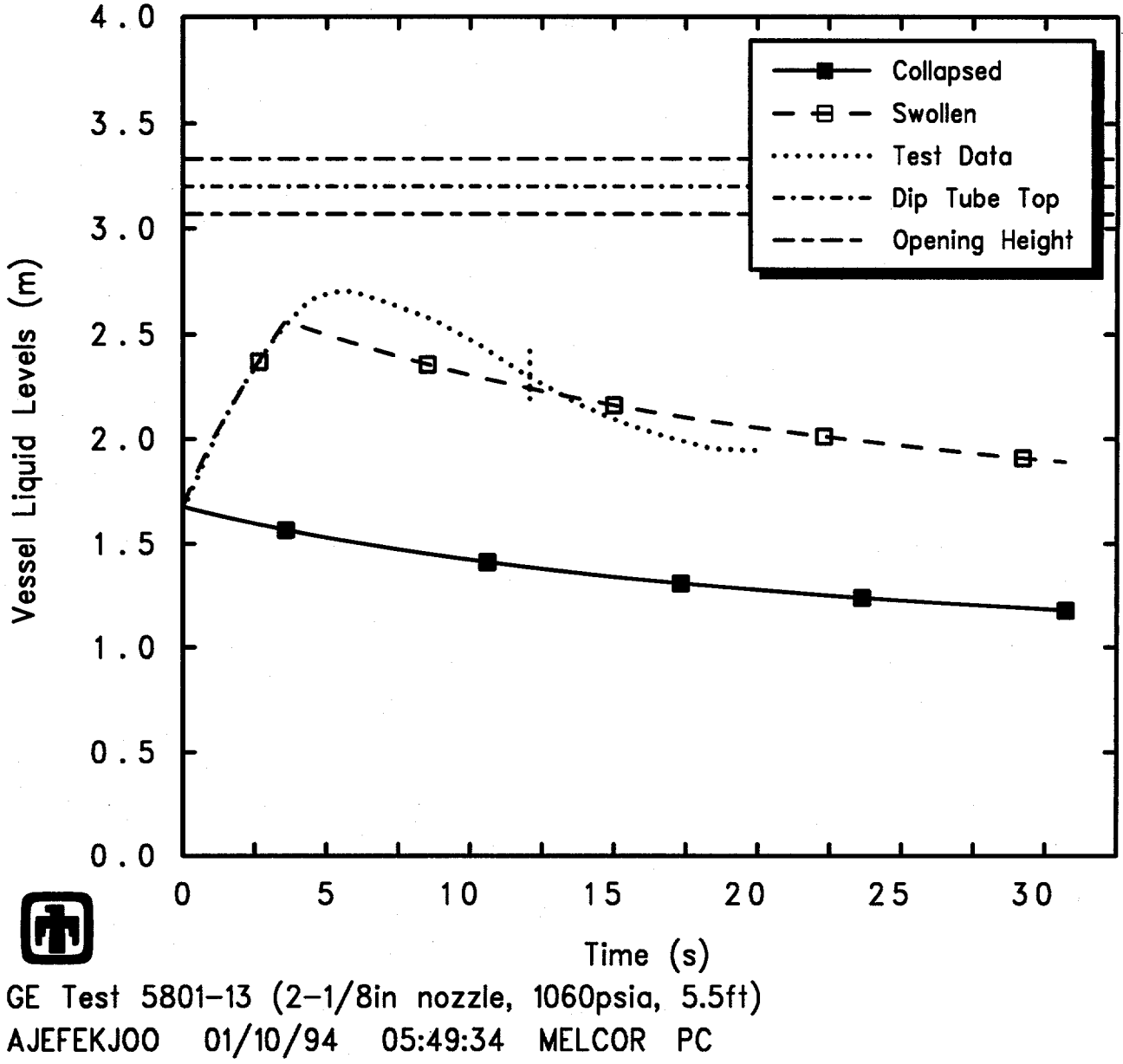

Figure 4.1.2. Vessel Levels for GE Large Vessel Top Blowdown Test 5801-13 – Basecase Calculation Compared to Test Data

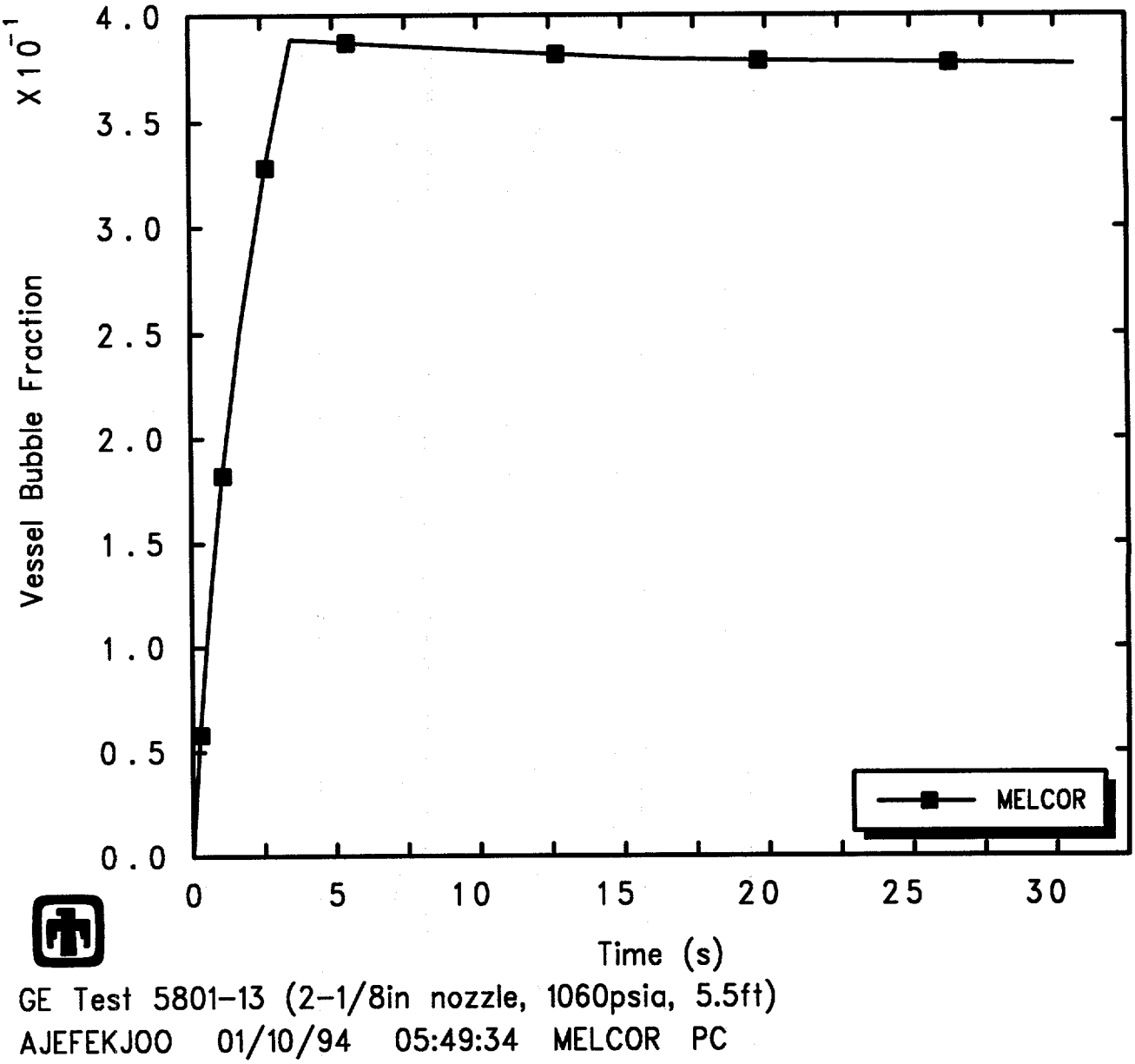

Figure 4.1.3. Vessel Two-Phase Liquid Level Bubble Fraction for GE Large Vessel Top Blowdown Test 5801-13 – Basecase Calculation

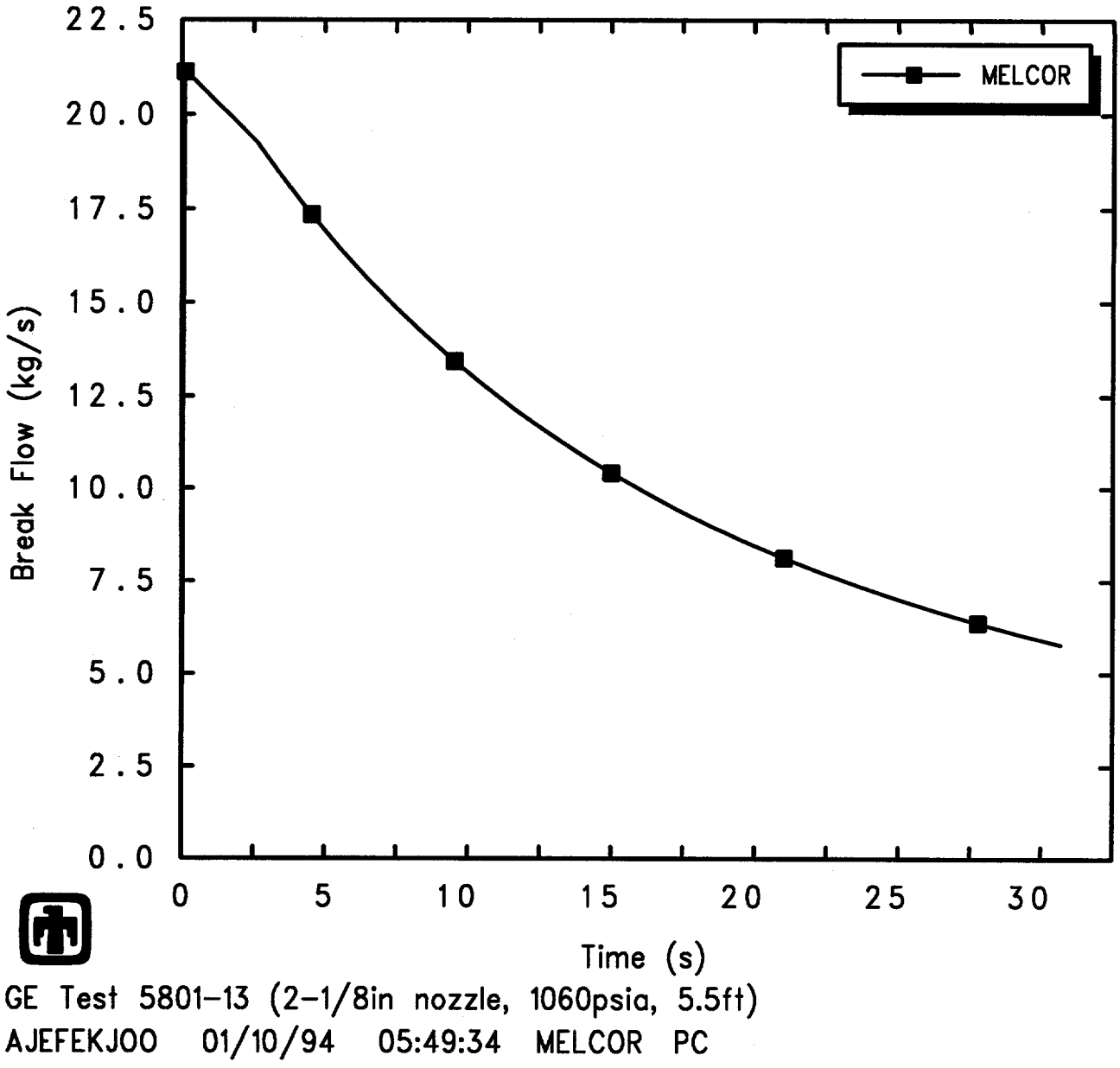

Figure 4.1.4. Blowdown Mass Flow for GE Large Vessel Top Blowdown Test 5801-13 – Basecase Calculation

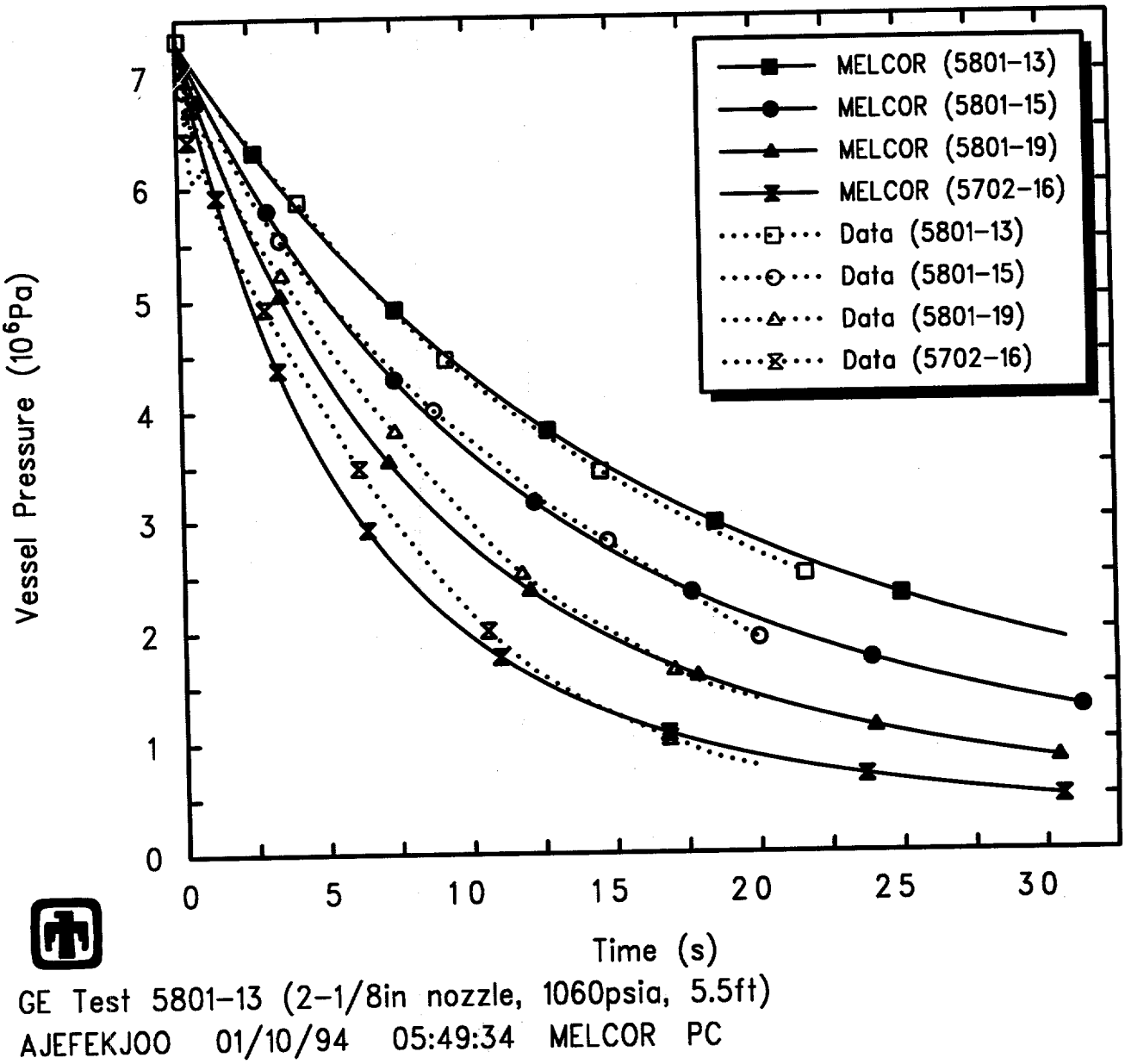

Figure 4.1.5. Vessel Pressure for GE Large Vessel Top Blowdown Tests – Basecase Calculations Compared to Test Data

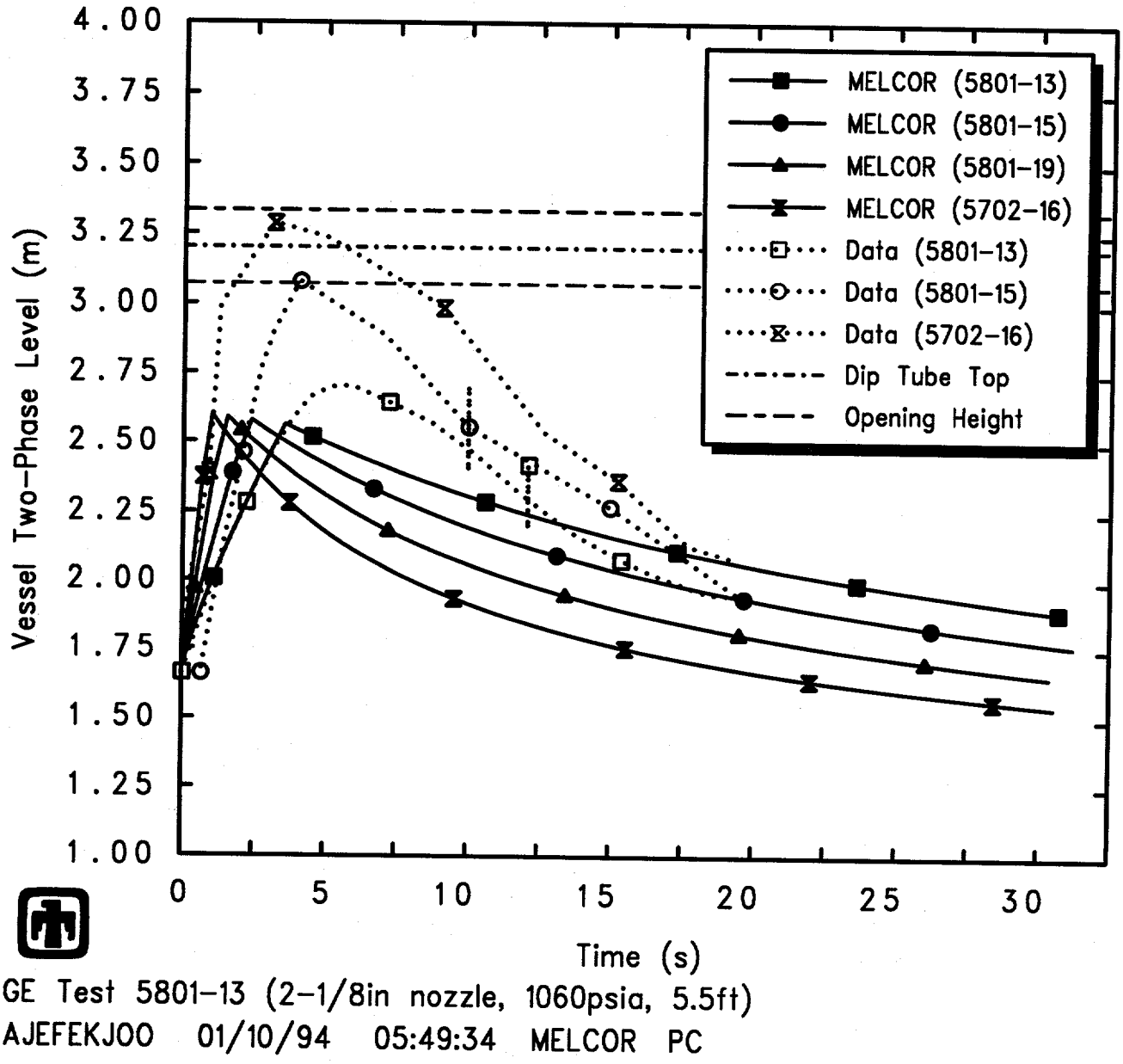

Figure 4.1.6. Vessel Levels for GE Large Vessel Top Blowdown Tests – Basecase Calculation Compared to Test Data

maximum heights before beginning to drop off; for the test with the largest blowdown nozzle dimensions (5702-16), the observed two-phase liquid level reaches above the top of the dip tube. The two-phase mixture, or swollen, levels calculated by MELCOR correctly reproduce the observed initial swelling, and the predicted two-phase levels initially increase at about the rate determined from measurement in each test. However, the vessel swollen levels calculated by MELCOR for the different nozzle dimensions all reach a similar maximum value which is significantly below the maximum two-phase levels in the test data, and the two-phase levels begin decreasing earlier in the calculations than observed in the test. MELCOR does correctly reproduce the qualitative trend seen in the test data that the measured two-phase liquid levels peak progressively earlier in the transient as the nozzle throat diameter and area, and hence the depressurization rate, is increased. The swollen liquid levels in the calculation later decrease less rapidly than observed for the measured two-phase liquid levels, for all these top blowdown tests. After the swollen levels begin to drop, the MELCOR calculations show progressively lower swollen levels at any particular time as the nozzle throat diameter and area, and hence the depressurization rate, is increased; the test data in contrast show the two-phase mixture levels in tests with larger blowdown nozzle diameters remaining above two-phase mixture levels in tests with smaller nozzle diameters throughout the entire period when test data are available.

The discrepancies found in measured *vs* calculated two-phase mixture levels are generally all attributable to the limiting in the MELCOR CVH package of the maximum allowed pool bubble fraction to 40%. The maximum swollen levels in each of the four MELCOR top blowdown test analyses correspond to the bubble fraction in the pool reaching a value of $\leq$0.40, as indicated in Figure 4.1.7. As the blowdown nozzle dimensions and hence the vessel depressurization rates increase, the swollen vessel level is predicted to reach that limiting value earlier in the transient and the swollen liquid level of the pool in the vessel then drops more rapidly as the vessel loses inventory more rapidly drops, due to continued inventory loss out the blowdown line, to maintain that pool bubble fraction of $\sim$0.40. (Section 5.2 presents results of a sensitivity study varying this maximum allowed pool bubble fraction in MELCOR.)

Figure 4.1.8 presents the flows calculated in the blowdown line for all four top blowdown test analyses. Because the top of the dip tube remains above the calculated swollen levels in the vessel in all four test analyses, as indicated in Figure 4.1.6, the blowdown flows are predicted to be vapor throughout the transient for all four top blowdown tests. The outflow increases as the blowdown line nozzle throat diameter is increased, especially early in the transient, as would be expected.

4.2 Bottom Blowdown Tests

Test 5803-1 is a bottom blowdown test in the large blowdown vessel, with a nozzle diameter of 5.3975cm (2-1/8in). Initially the vessel is at 7.2357MPa (1050psia) and the water level is at 2.28m (7.5ft), at the interface between measurement nodes 4 and 5 in Figure 2.1. The void fraction is 0.0 below and 1.0 above this interface, initially. The

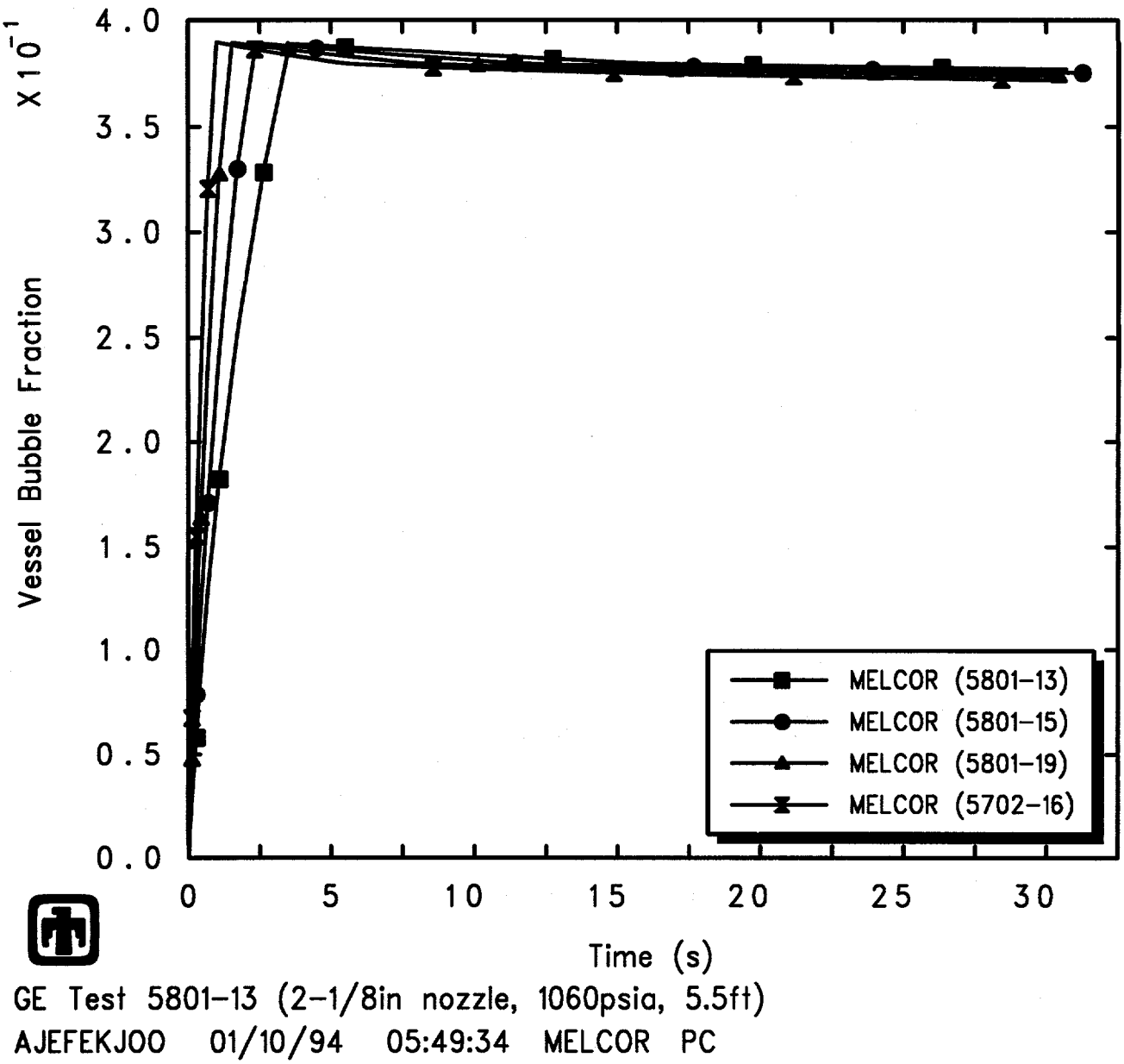

Figure 4.1.7. Vessel Two-Phase Liquid Level Bubble Fraction for GE Large Vessel Top Blowdown Tests – Basecase Calculation

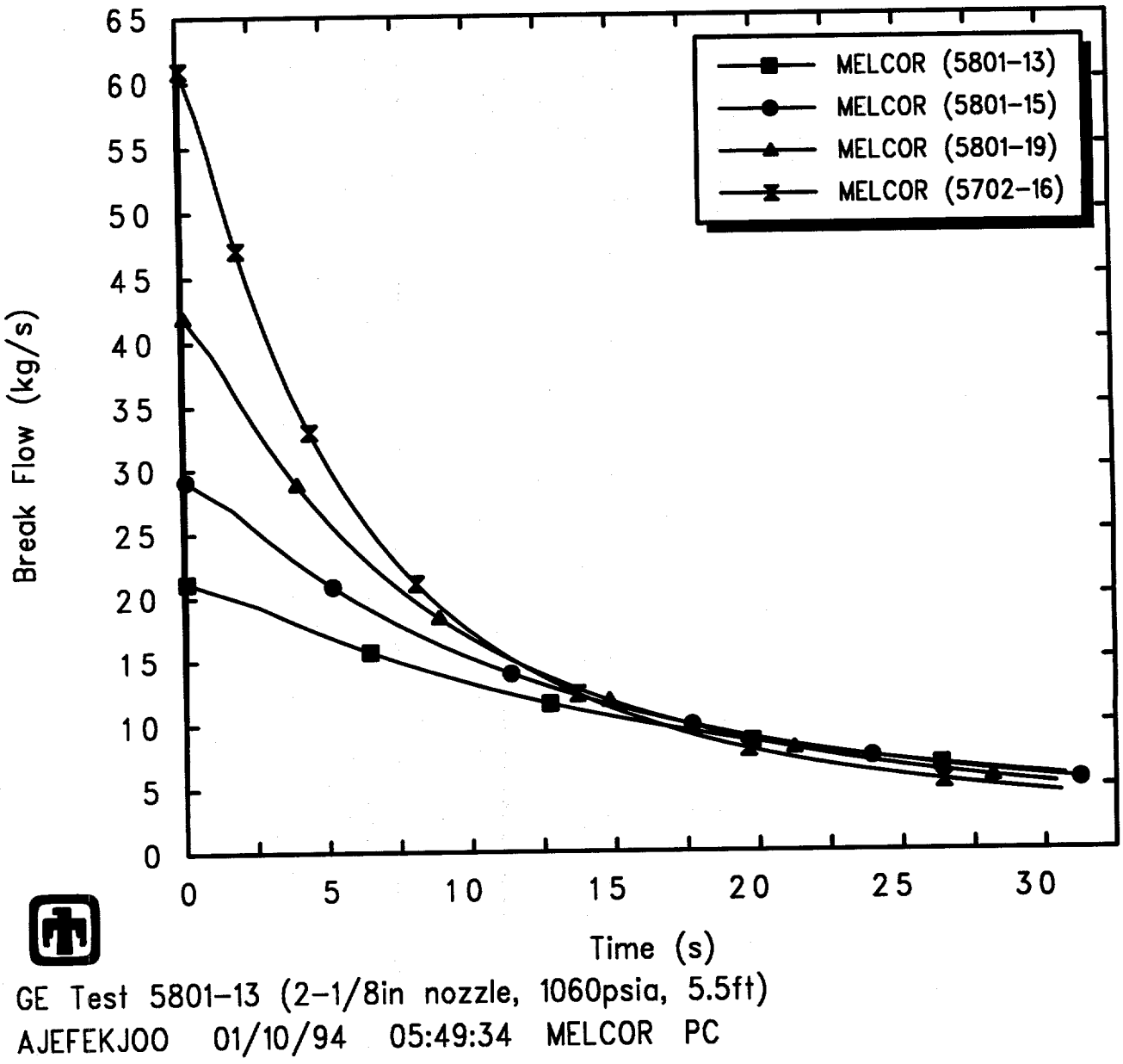

Figure 4.1.8. Blowdown Mass Flow for GE Large Vessel Top Blowdown Tests – Basecase Calculation

dip tube is removed, so that the blowdown line simply extends horizontally out from the vessel with its centerline at 0.762m elevation. The blowdown is initiated by bursting the rupture discs at time t=0.

The predicted vessel pressure history is compared with test data in Figure 4.2.1. The calculated pressure transient generally agrees very well with the measurement. There is a relatively slow depressurization for the first $\leq$20s seconds, followed by a more rapid depressurization beginning to slow again late in the transient.

Figure 4.2.2 gives the swollen and collapsed liquid levels in the vessel control volume predicted by MELCOR, together with test data on the two-phase mixture level. The elevation of the entrance to the blowdown line (both the centerline and the opening height) is also included in Figure 4.2.2, for reference. The relatively slow depressurization during the first $\leq$20s seconds is seen to correspond to the time period where the two-phase mixture level is above the entrance to the blowdown line, so that liquid is being lost directly out the blowdown line. The subsequent more rapid depressurization begins when the mixture level drops below the blowdown line elevation, so that vapor blowdown can occur. As with the vessel pressure histories presented in Figure 4.2.1, the calculated mixture level transient generally agrees very well with measurement; the agreement is excellent both during the earlier liquid blowdown and the later vapor blowdown periods.

The agreement of predicted level swell with test data is much better in this bottom blowdown test analysis than in any of the top blowdown test analyses discussed in Section 4.1 because the pool bubble fraction is not being controlled within MELCOR by the maximum allowed value of 40%, as indicated in Figure 4.2.3. There is significantly less level swell in this bottom blowdown test than in any of the top blowdown tests, and the pool bubble fraction is not affected by the maximum allowed value of 40% until very late in the transient, when little pool is left.

Figure 4.2.4 presents the flow calculated in the blowdown line, compared to the measured blowdown flow. There is a period of relatively high outflow during the first $\leq$20s, corresponding to the two-phase mixture level being above the entrance to the blowdown line, so that liquid is being lost directly out the blowdown line, resulting in the relatively slow depressurization seen during the first $\leq$20s seconds. The magnitude of the blowdown flow decreases dramatically when the mixture level drops below the blowdown line elevation, so that vapor blowdown occurs; the greater energy loss carried by the vapor outflow causes the more rapid depressurization seen after this transition. The calculated blowdown flow transient generally agrees well with measurement, although the transition from liquid to vapor outflow in the MELCOR calculation appears more abrupt and more oscillatory than the measured flow.

The results found for test 5803-1 are generally typical of the behavior seen in the other bottom blowdown test analysis. The predicted vessel pressure histories are compared with test data for both bottom blowdown test analyses in Figure 4.2.5. (Recall that, not only does test 5803-2 have a larger blowdown nozzle diameter, it also starts with a larger liquid pool in the vessel than test 5803-1.) Qualitatively, the MELCOR calculations correctly reproduce the increase in vessel depressurization rate as the nozzle

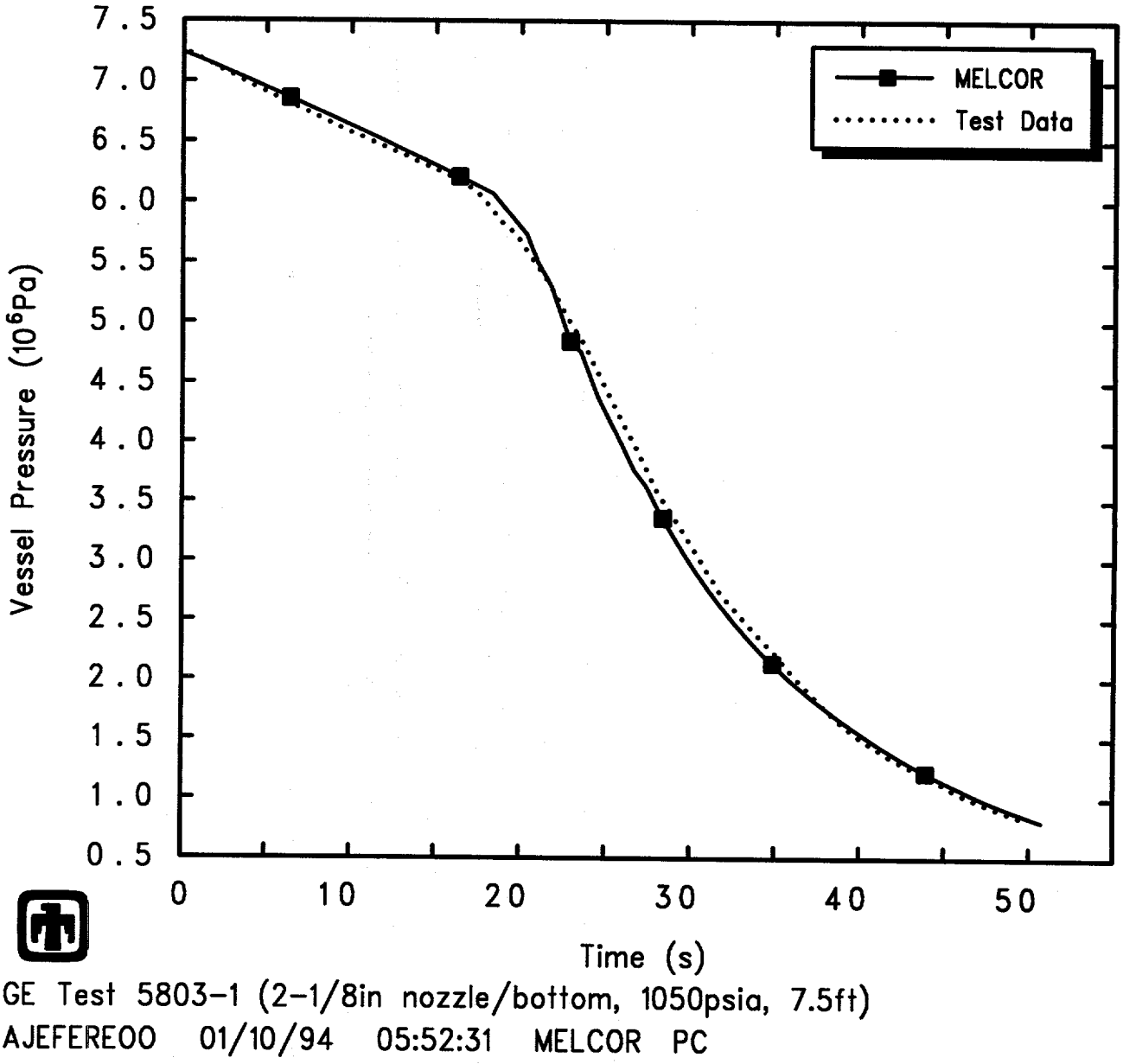

Figure 4.2.1. Vessel Pressure for GE Large Vessel Bottom Blowdown Test 5803-1 – Basecase Calculation Compared to Test Data

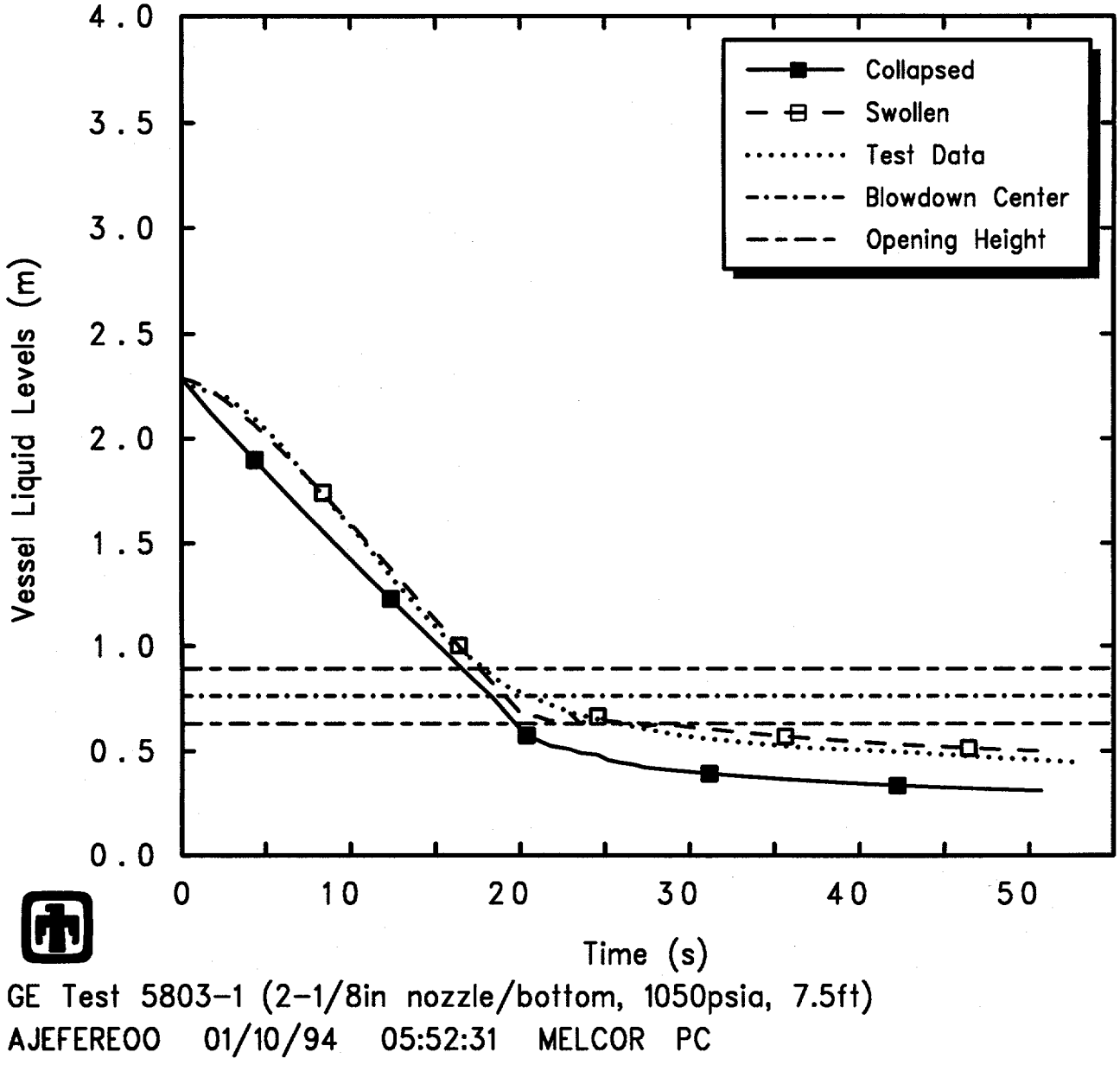

Figure 4.2.2. Vessel Levels for GE Large Vessel Bottom Blowdown Test 5803-1 – Basecase Calculation Compared to Test Data

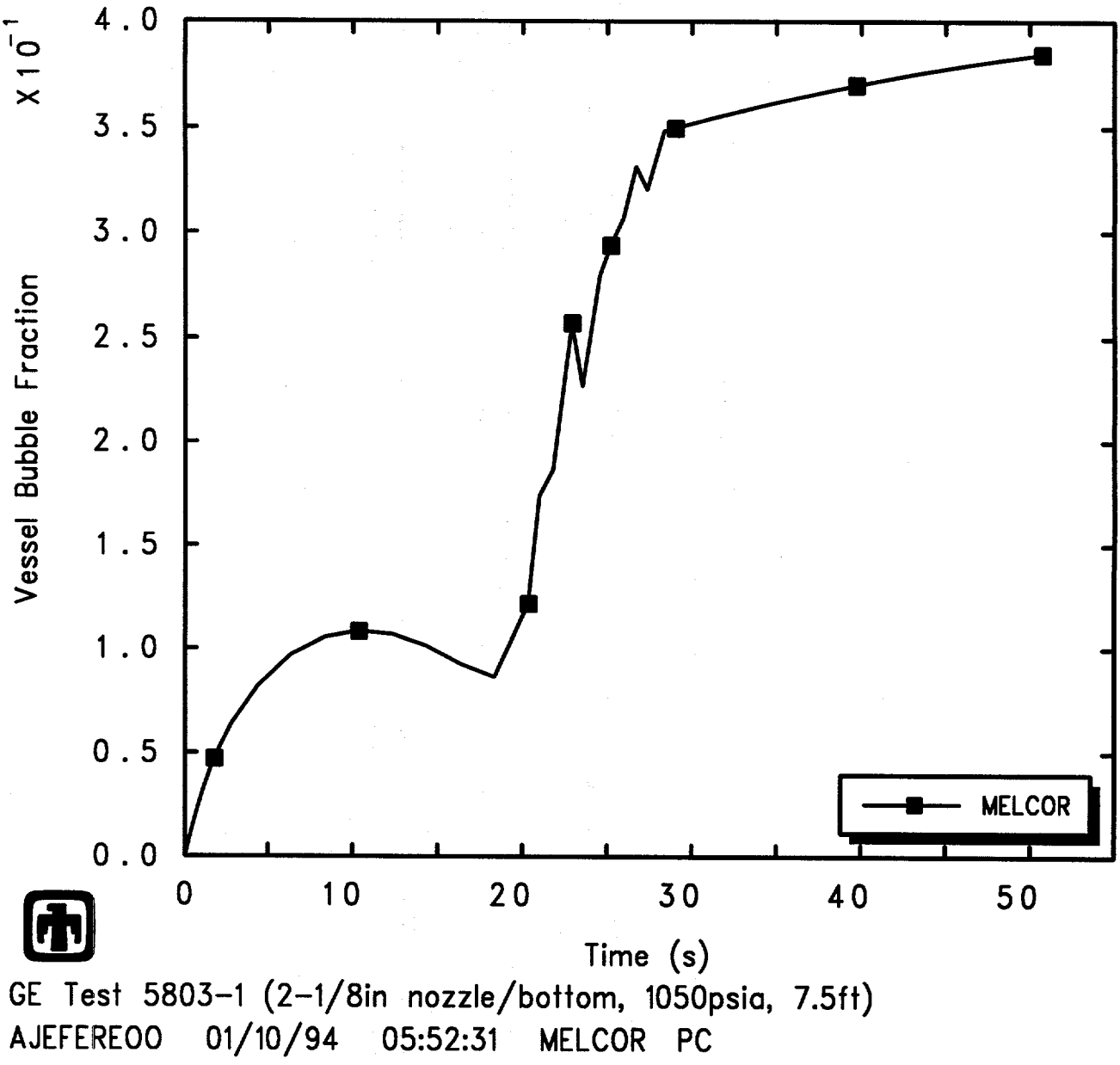

Figure 4.2.3. Vessel Two-Phase Liquid Level Bubble Fraction for GE Large Vessel Bottom Blowdown Test 5803-1 – Basecase Calculation

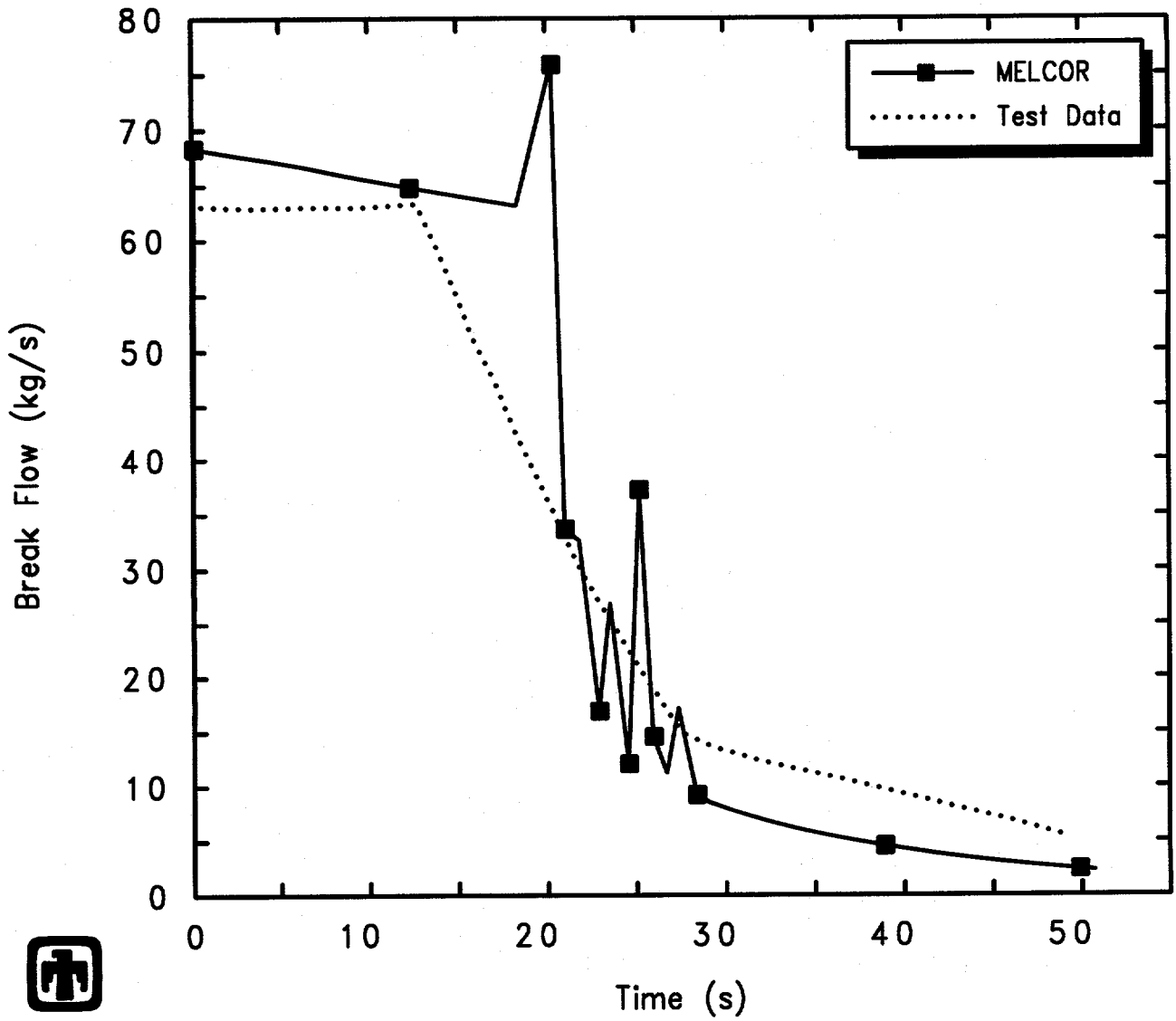

Figure 4.2.4. Blowdown Mass Flow for GE Large Vessel Bottom Blowdown Test 5803-1 – Basecase Calculation Compared to Test Data

throat diameter and area increase. Quantitatively, there is more difference between the calculated and measured vessel pressures as the nozzle throat diameter and area increases and the depressurization rate increases in test 5803-2 than found for test 5803-1. This difference is due primarily to the fact that the single value of form loss and discharge coefficients used in all these basecase calculations may not be optimum for all test conditions (as indicated by sensitivity studies described in Sections 6.1 and 6.2). The same trend was seen in the top blowdown test analyses discussed in Section 4.1, with MELCOR predicting progressively faster vessel depressurization than observed in the experiments with increased nozzle size.

Figure 4.2.6 gives the swollen liquid levels in the vessel control volume predicted by MELCOR, together with test data on the two-phase mixture level, for both bottom blowdown tests. Again, the elevation of the entrance to the blowdown line (centerline and opening height) is included in Figure 4.2.6, for reference. The agreement between calculation and measurement is somewhat worse for test 5803-2 than for test 5803-1, but still the agreement between test data and predicted two-phase liquid levels is quite good throughout the blowdown.

In neither case does the calculated pool bubble fraction reach the limiting, maximum allowed pool bubble fraction of 40% until very late in the blowdown, as indicated in Figure 4.2.7. As the blowdown nozzle dimension and hence the vessel depressurization rate increase, the swollen vessel level is predicted to reach that limiting value earlier, but there is so little pool left at that time that limiting the pool swell does not have any significant effect on the overall results calculated for the bottom blowdown tests.

Figure 4.2.8 presents the flows predicted in the blowdown line for both bottom blowdown test analyses, compared to test data. In both experiment and calculation, the outflow increases as the blowdown line nozzle throat diameter is increased, especially during the liquid blowdown in the first part of the transient, as would be expected. The calculated blowdown flows generally agree well with measurement for both bottom blowdown tests, although the transition from liquid to vapor outflow in the MELCOR calculations appear more abrupt than seen in the measured flows during this transition, and flow oscillations such as calculated during this transition period in the test 5803-1 analysis are not visible in the test 5803-2 analysis.

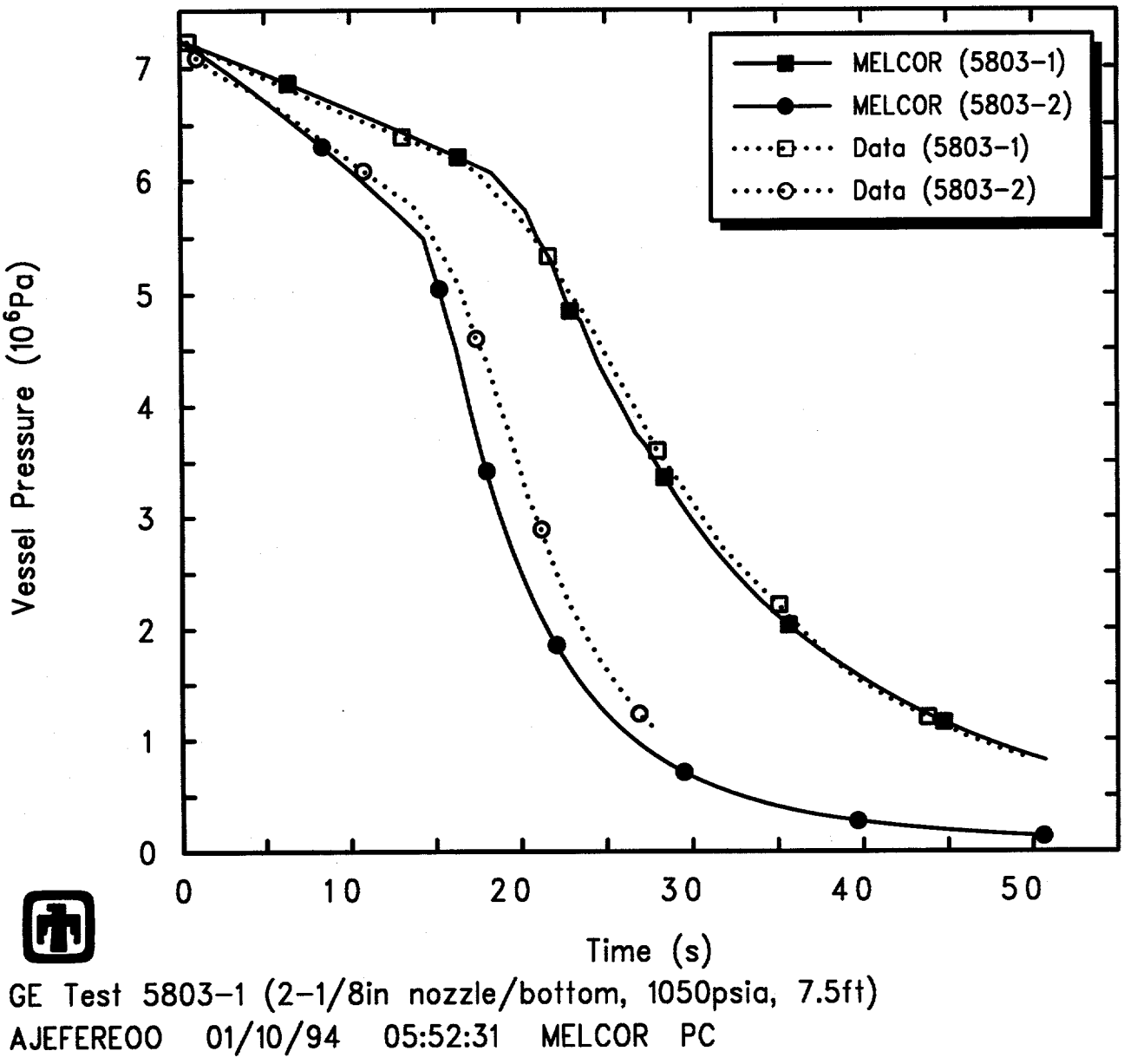

Figure 4.2.5. Vessel Pressure for GE Large Vessel Bottom Blowdown Tests – Basecase Calculations Compared to Test Data

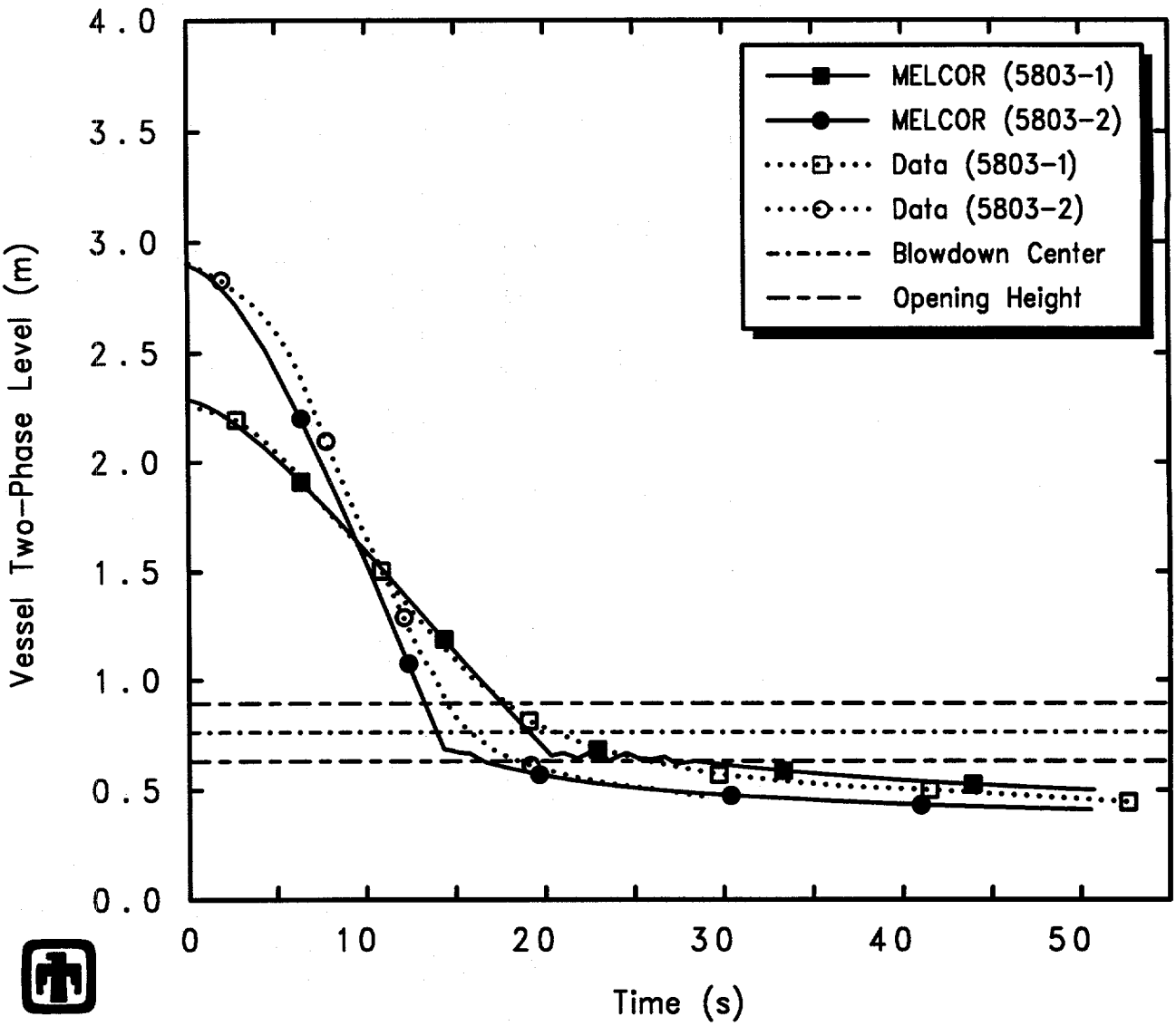

Figure 4.2.6. Vessel Levels for GE Large Vessel Bottom Blowdown Tests – Basecase Calculation Compared to Test Data

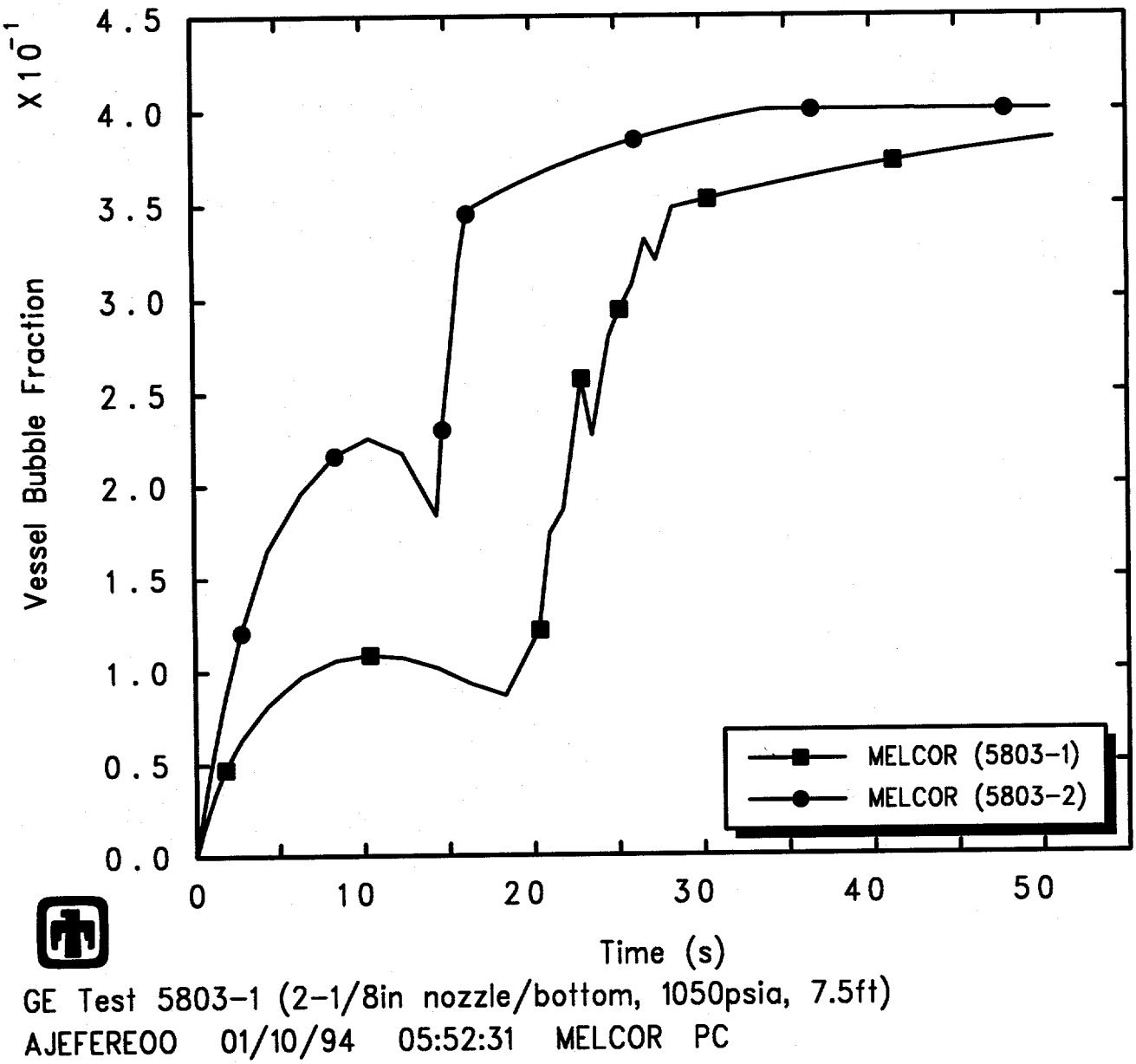

Figure 4.2.7. Vessel Two-Phase Liquid Level Bubble Fraction for GE Large Vessel Bottom Blowdown Tests – Basecase Calculation

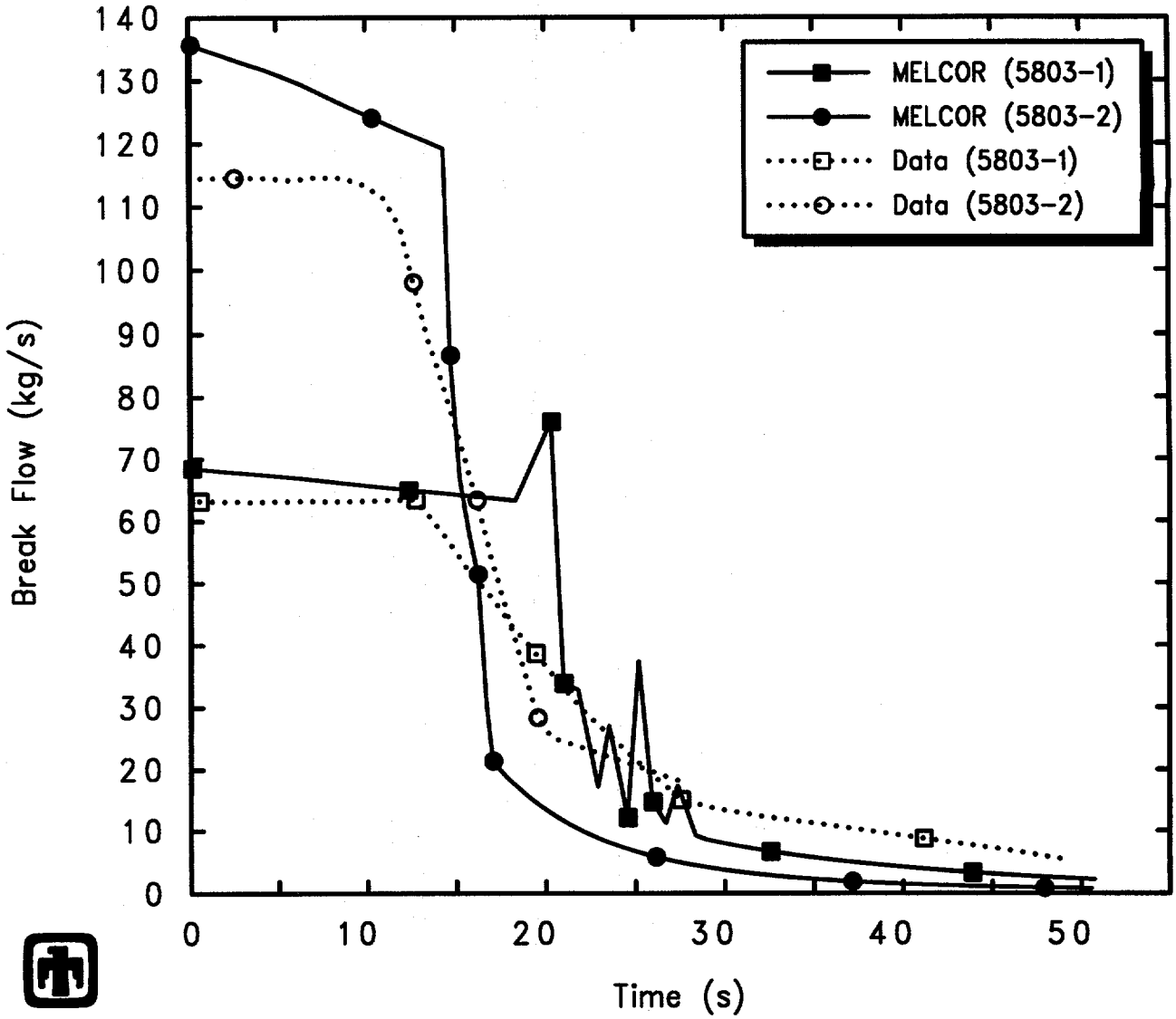

Figure 4.2.8. Blowdown Mass Flow for GE Large Vessel Bottom Blowdown Tests – Basecase Calculation Compared to Test Data

5 CVH Sensitivity Studies

There are options and uncertainties both in some MELCOR input values and in the modelling approach taken to represent test conditions. As described in this and the next section, a set of sensitivity studies has been done varying some parameters to determine how the results could be affected by such modelling variations and uncertainties. This section investigates modelling variations affecting the control volume thermal/hydraulics (CVH) package, while the following section presents results varying modelling parameter and options affecting the FL package.

5.1 Equilibrium *vs* Nonequilibrium Thermodynamics

There are two basic options available in the CVH package in MELCOR. Equilibrium thermodynamics assumes that the pool and atmosphere in a control volume are in thermal and mechanical equilibrium (*i.e.*, that they have the same temperature and pressure; the pool and atmosphere are also assumed to be in equilibrium with respect to evaporation and condensation of water. Non-equilibrium thermodynamics assumes that, while they are each in internal equilibrium, the pool and atmosphere are only in mechanical equilibrium; neither thermal nor phase equilibrium is assumed. Bubble rise in the MELCOR thermal/hydraulics model is accounted for only in nonequilibrium volumes.

Most MELCOR calculations, including these GE large vessel blowdown and level swell assessment analyses, are routinely done using the nonequilibrium thermodynamics model. To determine the importance and effect of modelling nonequilibrium phenomena, a sensitivity study has been done repeating the GE large vessel blowdown and level swell assessment analyses using the equilibrium modelling option in the CVH package.

The vessel pressures predicted by MELCOR using the nonequilibrium and the equilibrium thermodynamics options are compared with each other and with test data in Figure 5.1.1, for the four top blowdown experiments; Figure 5.1.2 compares the corresponding calculated break flows. The pressure histories and the break flows predicted by MELCOR using the nonequilibrium and the equilibrium thermodynamics options for each of these top blowdown tests appear identical.

Figure 5.1.3 gives the swollen and collapsed liquid levels in the vessel control volume predicted by MELCOR using the nonequilibrium and the equilibrium thermodynamics options for the top blowdown test 5801-13, together with test data on the two-phase mixture level, for reference. (The results and conclusions for the calculated vessel levels in the other three top blowdown test analyses are the same). The collapsed liquid levels appear identical in every case whichever of the two thermodynamics options are used. However, with the equilibrium thermodynamics assumption, the calculated swollen (two-phase) liquid level is the same as the collapsed liquid level; the maximum allowed pool bubble fraction is identically zero. The results for two-phase level calculated using the nonequilibrium thermodynamics assumption are obviously in much better qualitative and

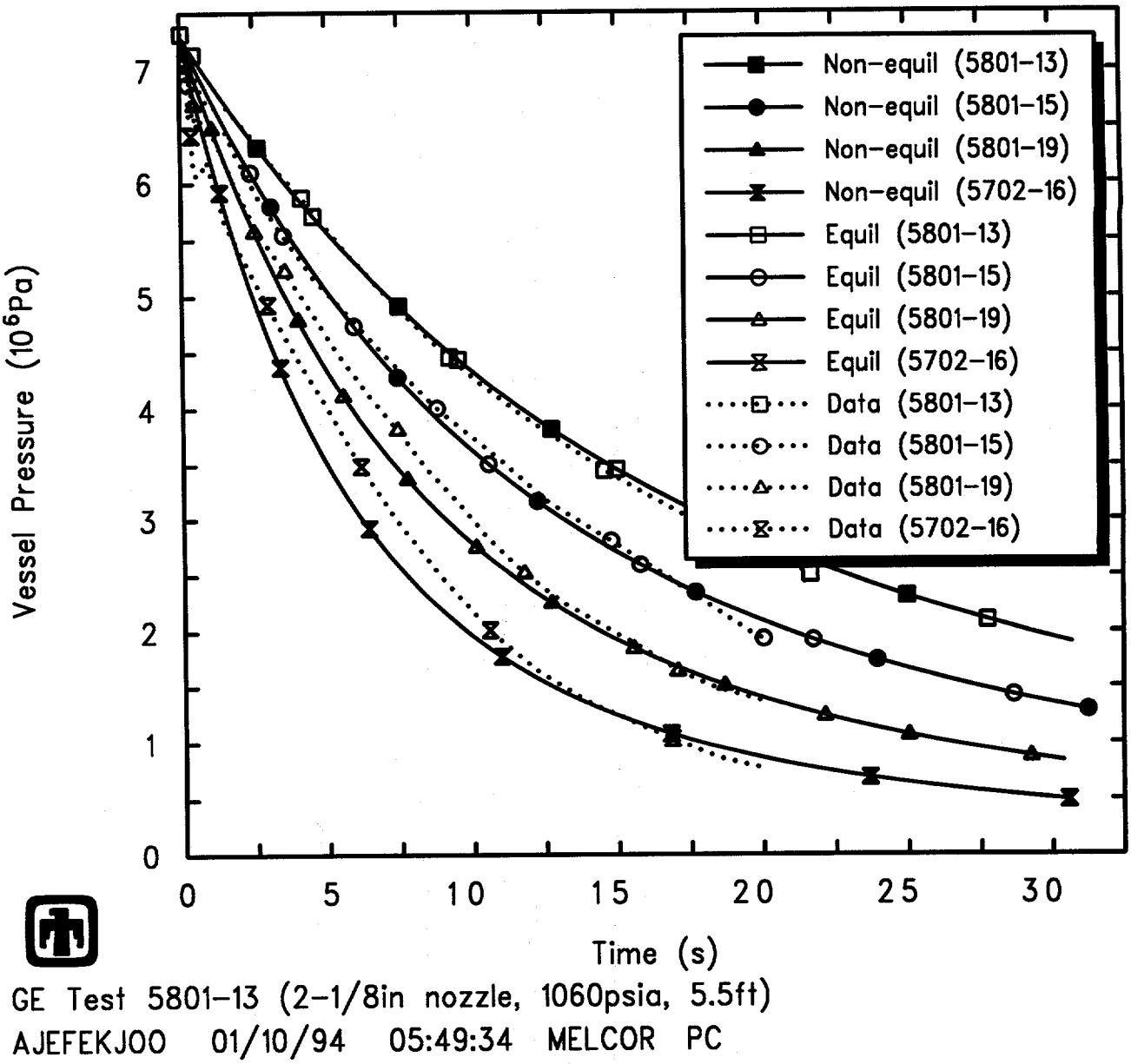

Figure 5.1.1. Vessel Pressure for GE Large Vessel Top Blowdown Tests – Equilibrium Thermodynamics Sensitivity Study

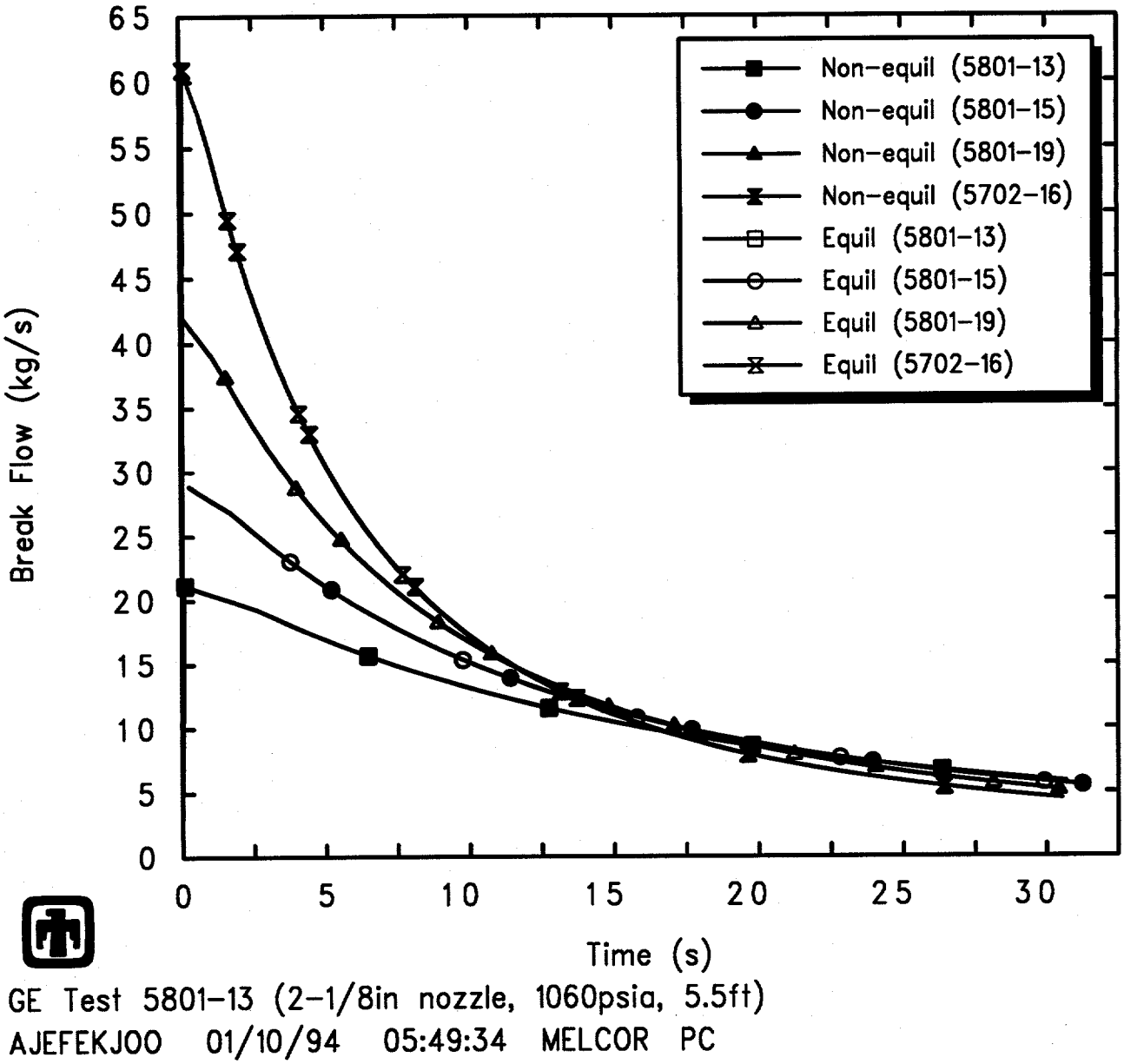

Figure 5.1.2. Blowdown Mass Flow for GE Large Vessel Top Blowdown Tests – Equilibrium Thermodynamics Sensitivity Study

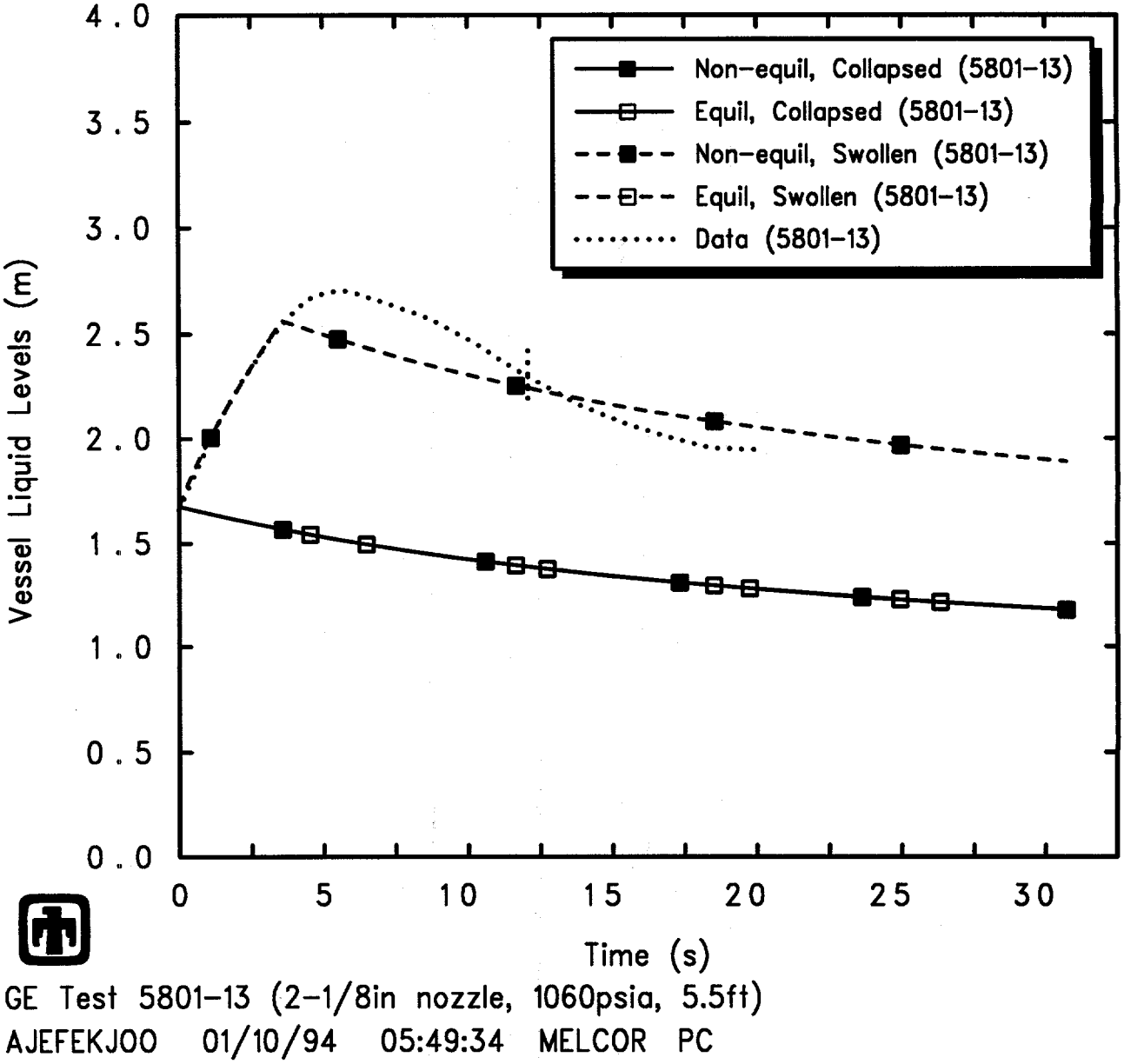

Figure 5.1.3. Vessel Liquid Levels for GE Large Vessel Top Blowdown Test 5801-13 – Equilibrium Thermodynamics Sensitivity Study

quantitative agreement with test data in every one of these top blowdown experiment analyses, even though the exact degree of level swelling may be underpredicted.

Results calculated using these different thermodynamics options for the two bottom blowdown tests are shown in Figures 5.1.4 through 5.1.6. Figure 5.1.4 shows the vessel depressurization histories calculated by MELCOR, using the equilibrium and nonequilibrium thermodynamics options, compared to experimental data. The vessel collapsed and swollen (two-phase) liquid levels predicted by MELCOR using these different thermodynamics options, also compared to experimental data, are depicted in Figure 5.1.5 for one of the bottom blowdown tests; the results for the other bottom blowdown test are the same. Figure 5.1.6 shows the break flows out the blowdown line and Venturi flow limiting nozzle causing the vessel depressurization, calculated by MELCOR for both bottom blowdown tests using these different thermodynamics options, also comparing to test data.

Unlike the behavior found in the top blowdown test analyses, changing the thermodynamics equilibrium assumption does affect the break flow rates and vessel depressurization; however, the differences appear to be generally minor. In the sensitivity study calculations with the equilibrium assumption and associated lack of any level swell, the break flow and vessel depressurization rate initially are greater than in the basecase (nonequilibrium) calculations, since the break flow is pure liquid in these cases. The break also therefore uncovers earlier in the sensitivity study calculations with the equilibrium assumption and associated lack of any level swell, and the vessel depressurization rate decreases sooner as vapor blowdown begins earlier.

5.2 Bubble Separation

In MELCOR, hydrodynamic materials in a control volume are assumed to separate under gravity to form a liquid pool beneath a vapor atmosphere. Using the nonequilibrium thermodynamics option, the separation does not have to be perfect: the pool may contain vapor bubbles and the atmosphere may contain liquid droplets. For numerical stability reasons, the maximum amount of bubbles which can exist in a pool is limited to 40%. As a sensitivity study, calculations have been done in which this maximum pool bubble fraction was reduced to 0.3, and increased to 0.5, 0.6 and 0.7, input through sensitivity coefficient SC4407(11).

The effect of varying the maximum allowed pool bubble fraction is shown in Figures 5.2.1 through 5.2.4, for the top blowdown test 5801-13. Figure 5.2.1 shows the vessel depressurization histories calculated by MELCOR using these different values for the maximum allowed pool bubble fraction, compared to experimental data, while Figure 5.2.2 shows the corresponding break flow out the blowdown line and Venturi flow limiting nozzle causing the vessel depressurization. The vessel collapsed and swollen (two-phase) liquid levels predicted by MELCOR using these different maximum allowed pool bubble fractions, also compared to experimental data, are depicted in Figure 5.2.3, while Figure 5.2.4 gives the pool bubble fractions in this set of MELCOR sensitivity study calculations.

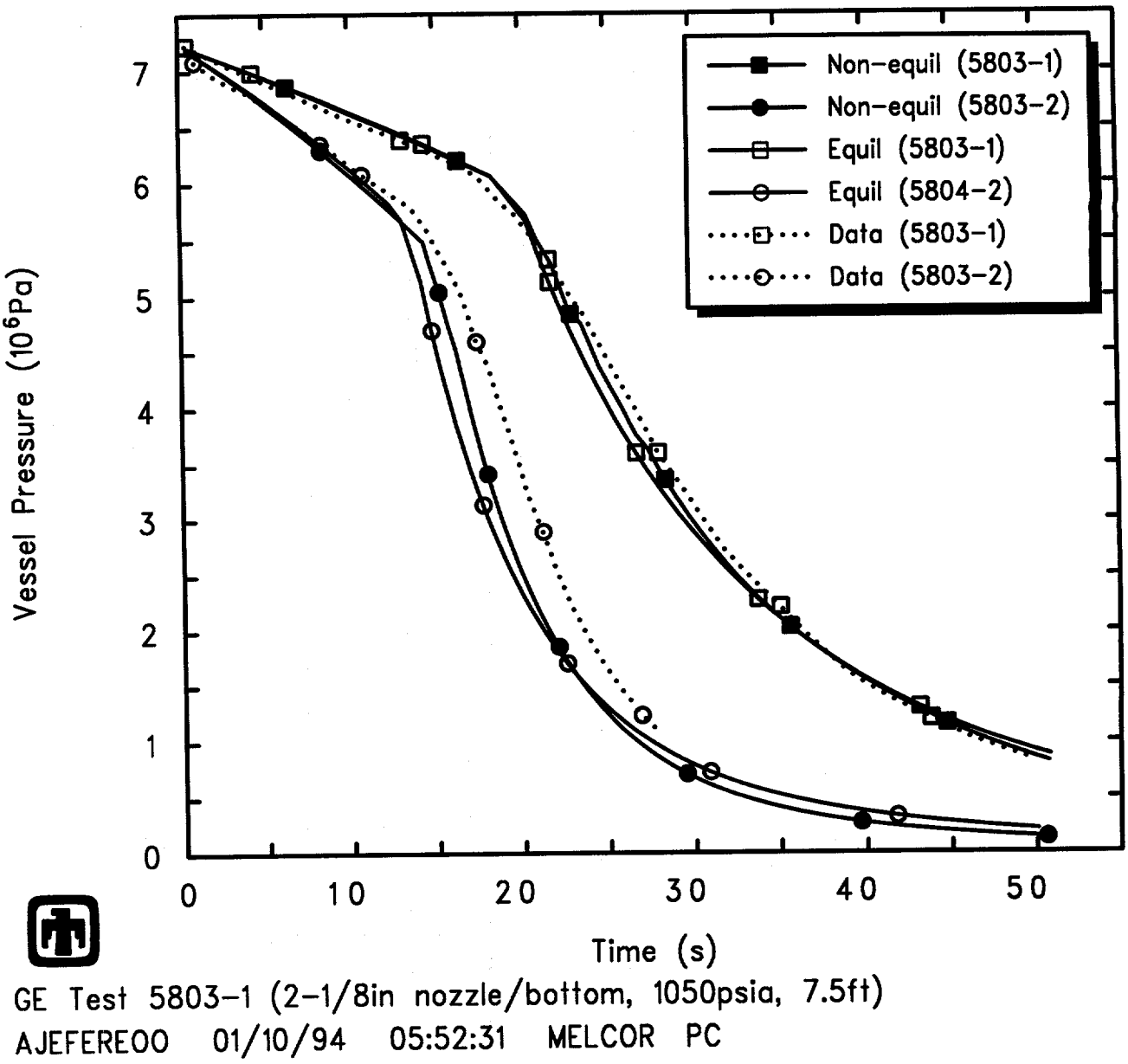

Figure 5.1.4. Vessel Pressure for GE Large Vessel Bottom Blowdown Tests – Equilibrium Thermodynamics Sensitivity Study

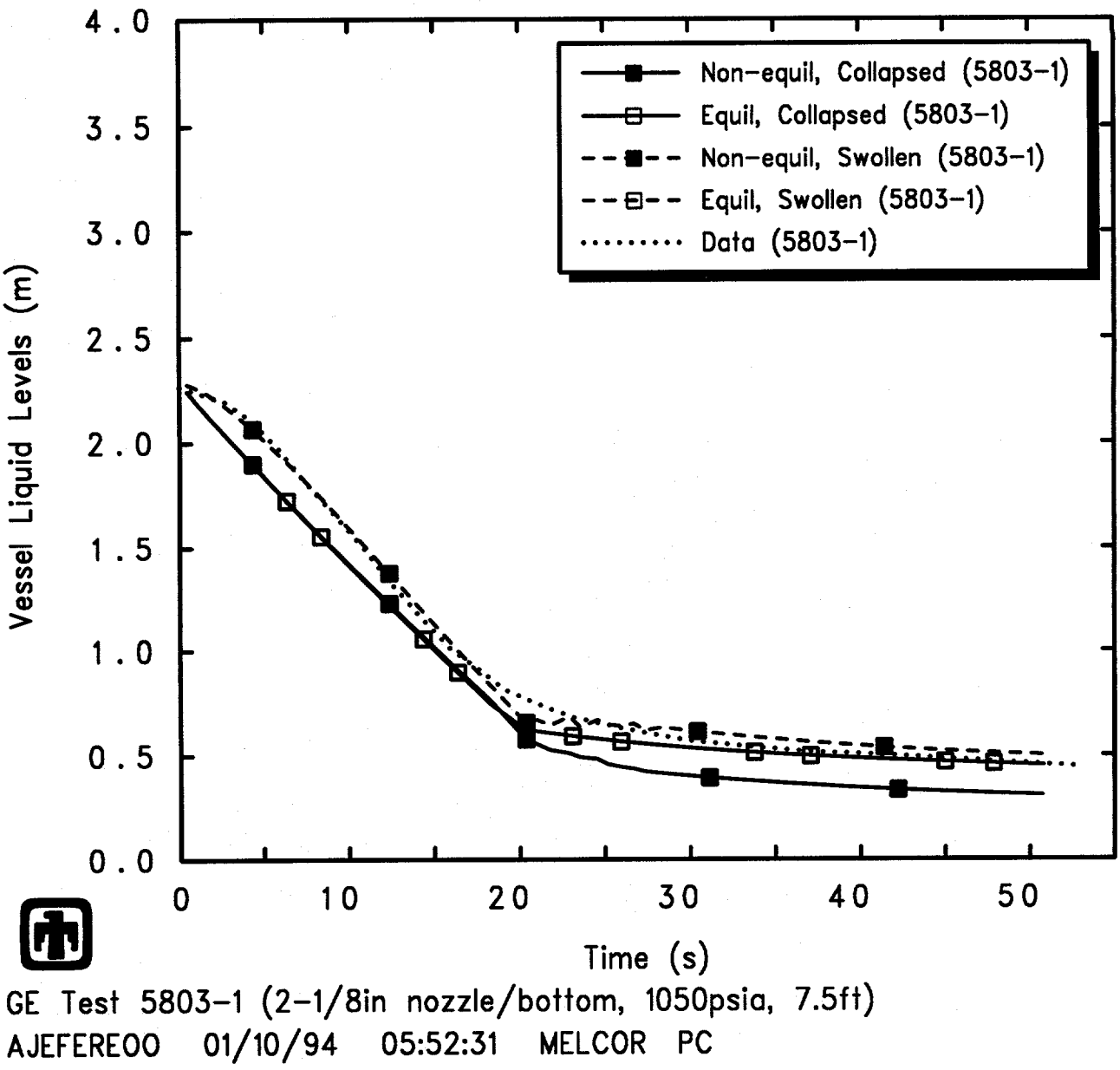

Figure 5.1.5. Vessel Liquid Levels for GÉ Large Vessel Bottom Blowdown Test 5803-1 – Equilibrium Thermodynamics Sensitivity Study

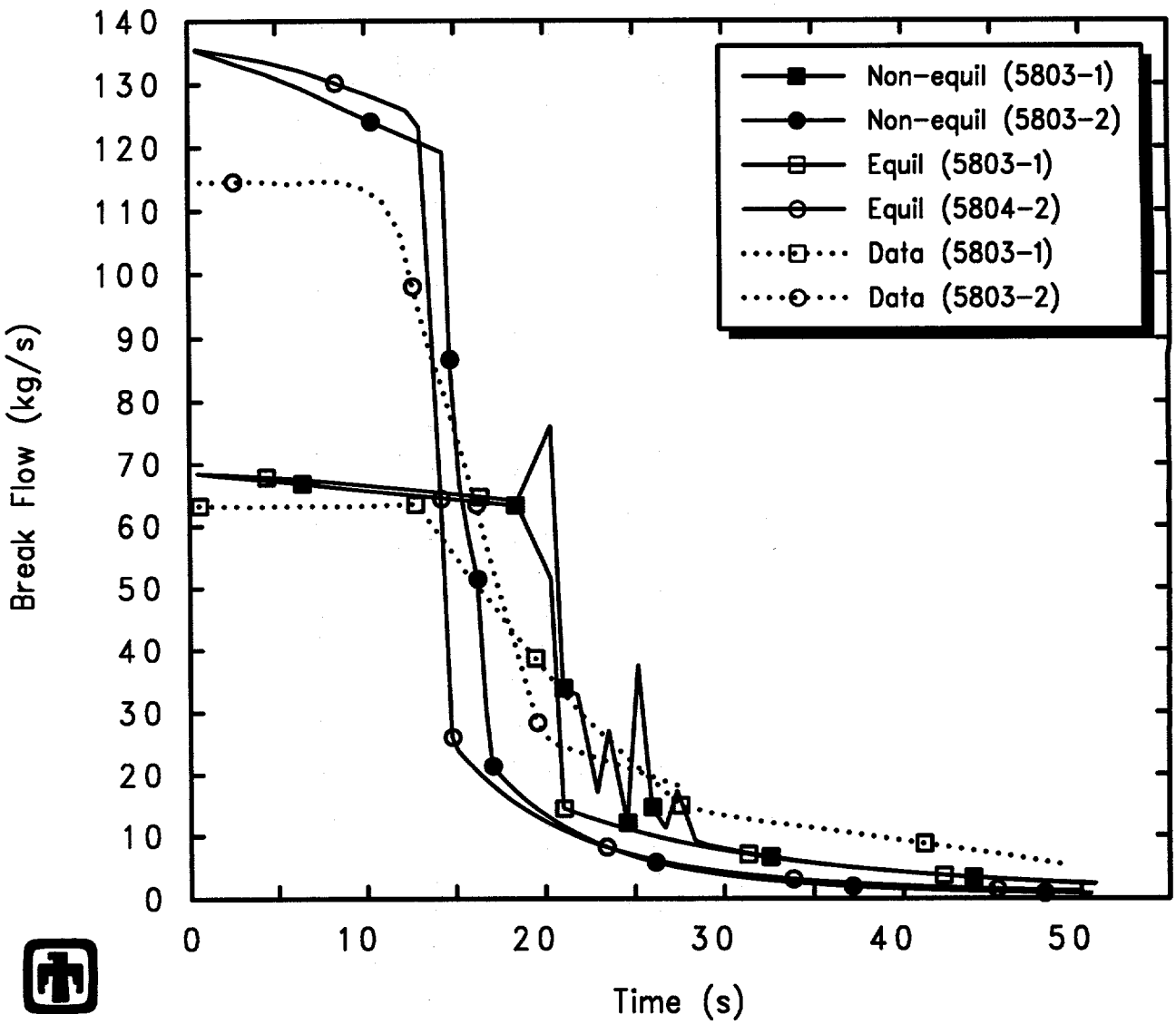

Figure 5.1.6. Blowdown Mass Flow for GE Large Vessel Bottom Blowdown Tests – Equilibrium Thermodynamics Sensitivity Study

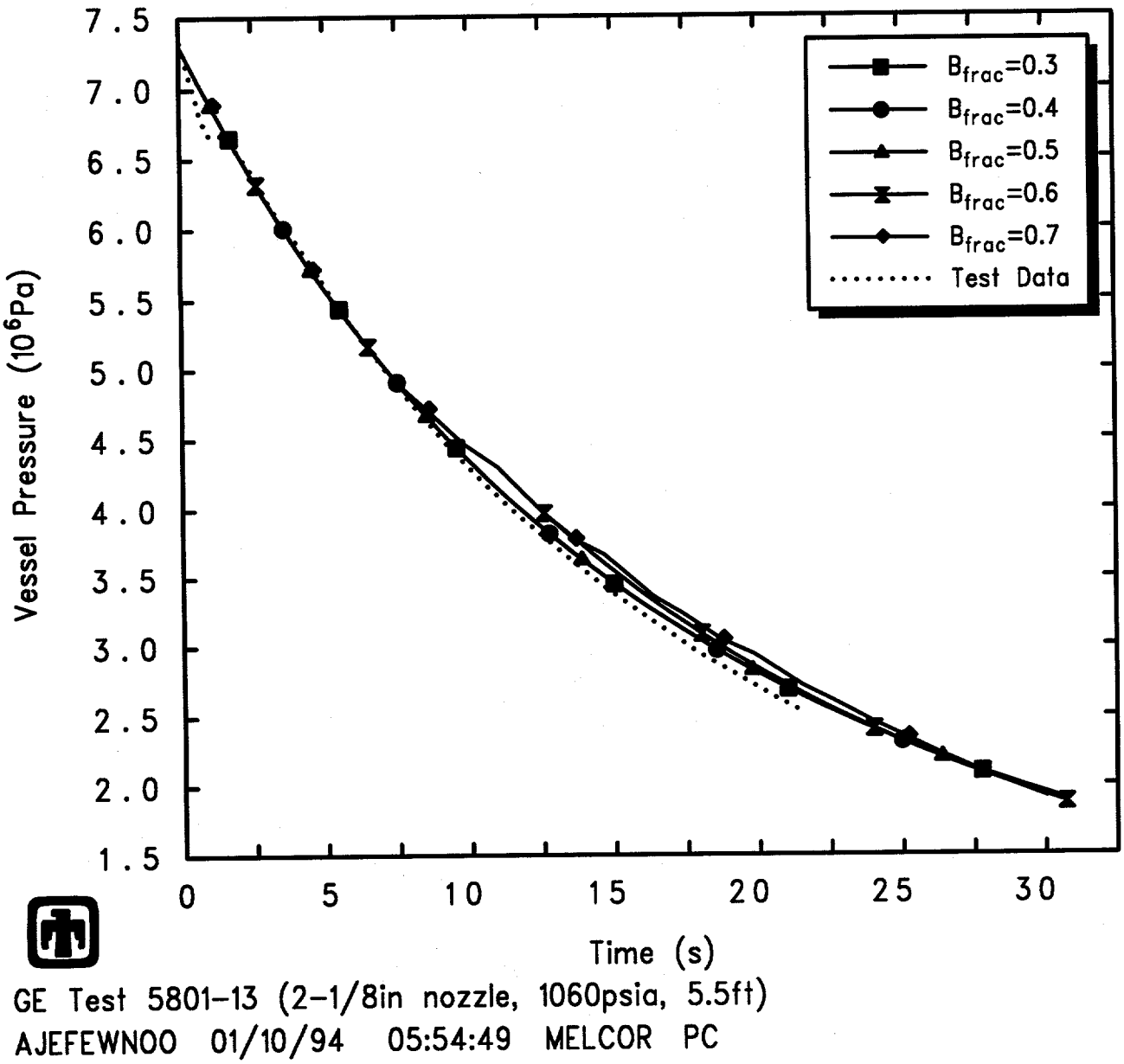

Figure 5.2.1. Vessel Pressure for GE Large Vessel Top Blowdown Test 5801-13 – Maximum Allowed Pool Bubble Fraction Sensitivity Study

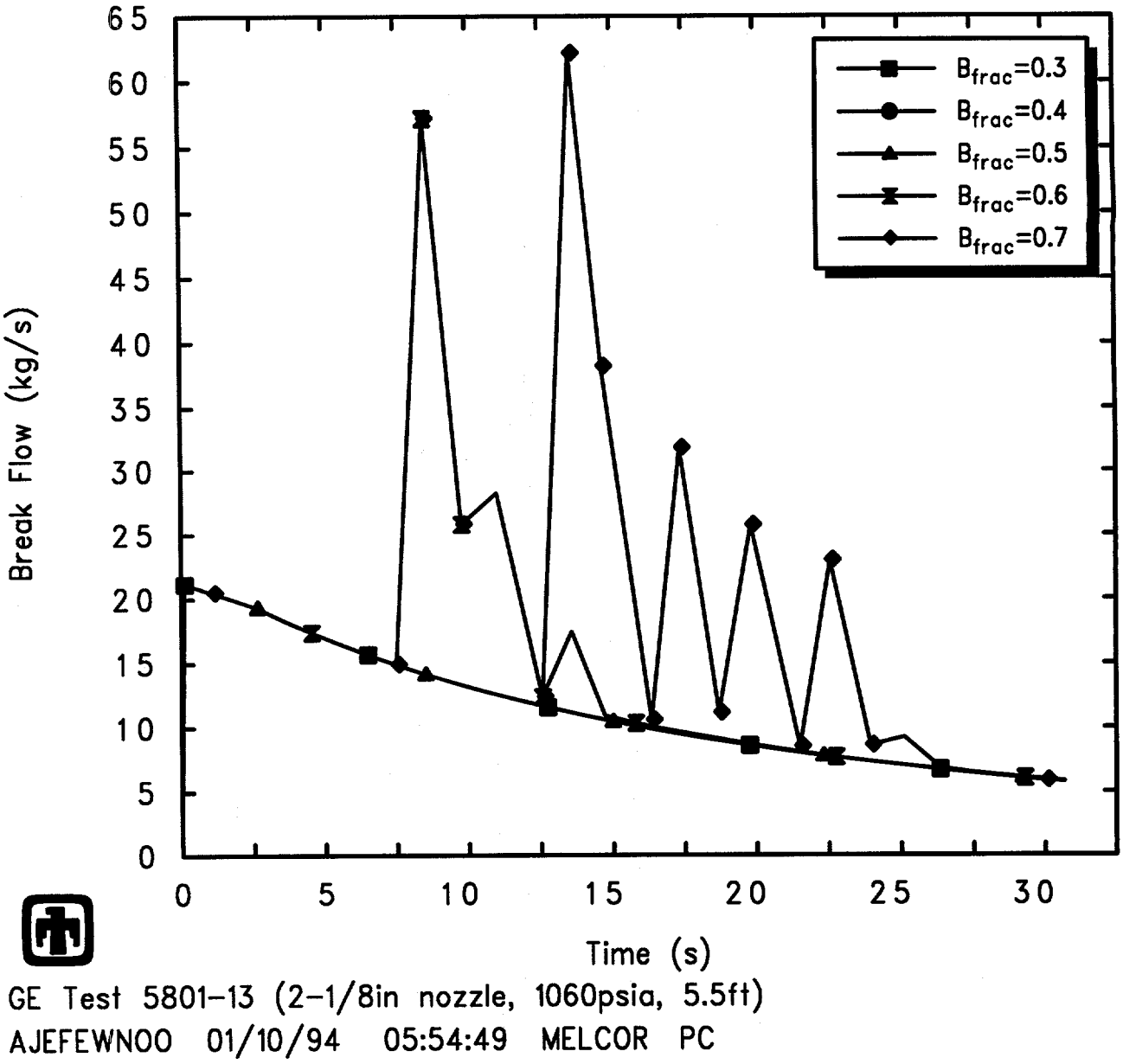

Figure 5.2.2. Blowdown Mass Flow for GE Large Vessel Top Blowdown Test 5801-13 – Maximum Allowed Pool Bubble Fraction Sensitivity Study

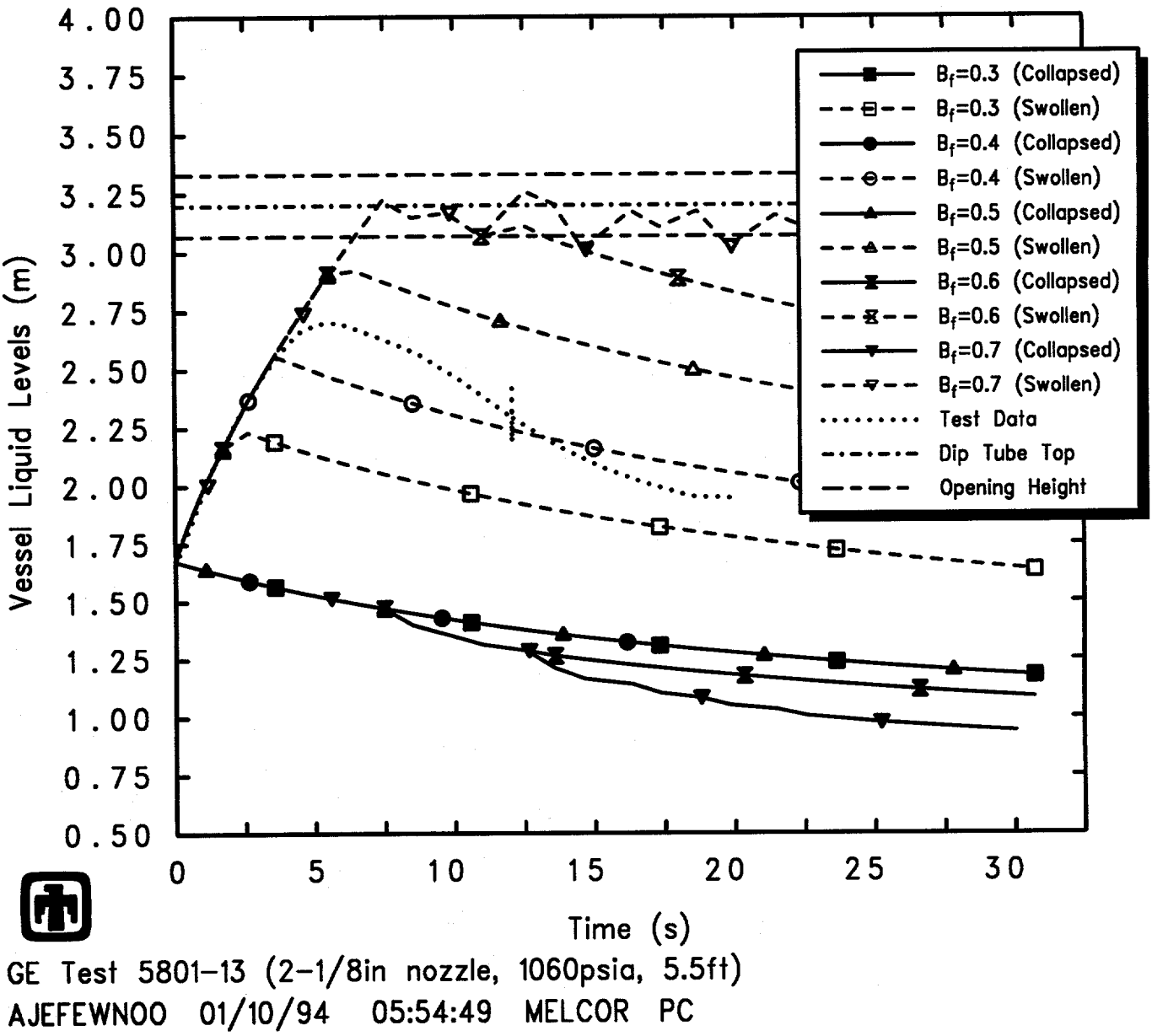

Figure 5.2.3. Vessel Liquid Levels for GE Large Vessel Top Blowdown Test 5801-13 – Maximum Allowed Pool Bubble Fraction Sensitivity Study

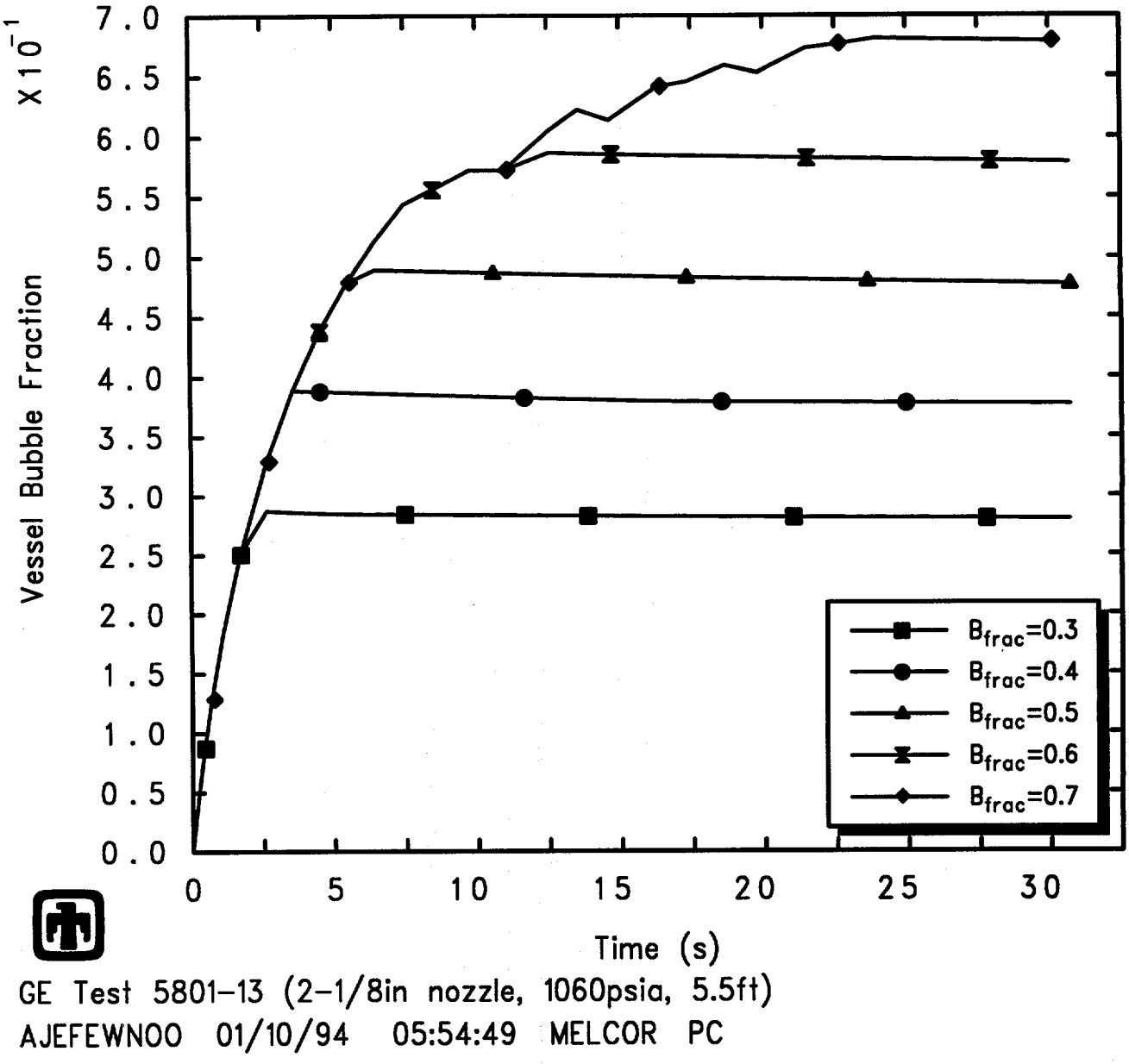

Figure 5.2.4. Vessel Two-Phase Liquid Bubble Fraction for GE Large Vessel Top Blowdown Test 5801-13 – Maximum Allowed Pool Bubble Fraction Sensitivity Study

The effect is exactly as would be expected – reducing or increasing the maximum allowed pool bubble fraction reduces or increases the calculated level swell accordingly. The bubble fraction in all cases rises to and then remains at near the maximum value allowed, as illustrated in Figure 5.2.4, although it takes longer to reach the larger maximum allowed pool bubble fraction values. (The calculations are identical until the increasing value of maximum allowed pool bubble fraction is reached, progressively later in time.) For test 5801-13, a top blowdown test with a 2-1/8in nozzle throat diameter, the best agreement with observation is found with a maximum pool bubble fraction of ~45%; agreement with data would also be improved if the pool bubble fraction slowly decreased somewhat after that maximum value had been reached. Figure 5.2.1 illustrates that there is relatively little effect found on the calculated vessel depressurization as the maximum allowed pool bubble fraction is varied, except when the two-phase liquid level rises enough (above the dip tube elevation) for liquid to flow out the blowdown line. As seen in Figure 5.2.3, this occurs intermittently in the cases with the maximum allowed pool bubble fraction is set to $\geq$60%, and whenever the two-phase liquid level swells enough for liquid to flow out the blowdown line the vessel depressurization slows down while the break flow increases sharply.

Results of similar calculations varying the maximum allowed pool bubble fraction are summarized in Figures 5.2.5 through 5.2.8 for the top blowdown test 5801-15 (which has a 2-1/2in nozzle throat diameter). Figure 5.2.5 gives the calculated vessel depressurization histories, compared to experimental data; the vessel collapsed and swollen (two-phase) liquid levels predicted by MELCOR, also compared to experimental data, are presented in Figure 5.2.6. Figures 5.2.7 and 5.2.8 show the calculated blowdown flow rates and pool bubble fractions, respectively. For test 5801-15, the best agreement with observation is found with a maximum pool bubble fraction of about 50%, again decreasing somewhat later in the blowdown.

Figure 5.2.9 shows the vessel depressurization histories with different maximum allowed blowdown pool bubble fractions used, compared to experimental data, for the top blowdown test 5801-19. The corresponding vessel collapsed and swollen (two-phase) liquid levels predicted by MELCOR are depicted in Figure 5.2.10; no test data were available for comparison for this test. Figure 5.2.11 gives the blowdown mass flows with different maximum allowed blowdown pool bubble fractions used, while the bubble fractions predicted in the vessel swollen (two-phase) pool are presented in Figure 5.2.10.

Figures 5.2.13 through 5.2.16 summarize the effect on the vessel depressurization and on the vessel liquid levels of varying the maximum allowed pool bubble fraction in the top blowdown test 5702-16, and also give blowdown flow and vessel pool bubble fraction results. For this test, the best agreement with test data is found with a maximum allowed pool bubble fraction in MELCOR of $\geq$70%.

For all these top blowdown test analyses, reducing or increasing the maximum allowed pool bubble fraction results in a corresponding reduction or increase in the calculated level swell. The bubble fraction in all cases rises to and then remains at near the maximum value allowed. There is relatively little effect on the calculated vessel depressurization as the maximum allowed pool bubble fraction is varied, except when the two-phase liquid

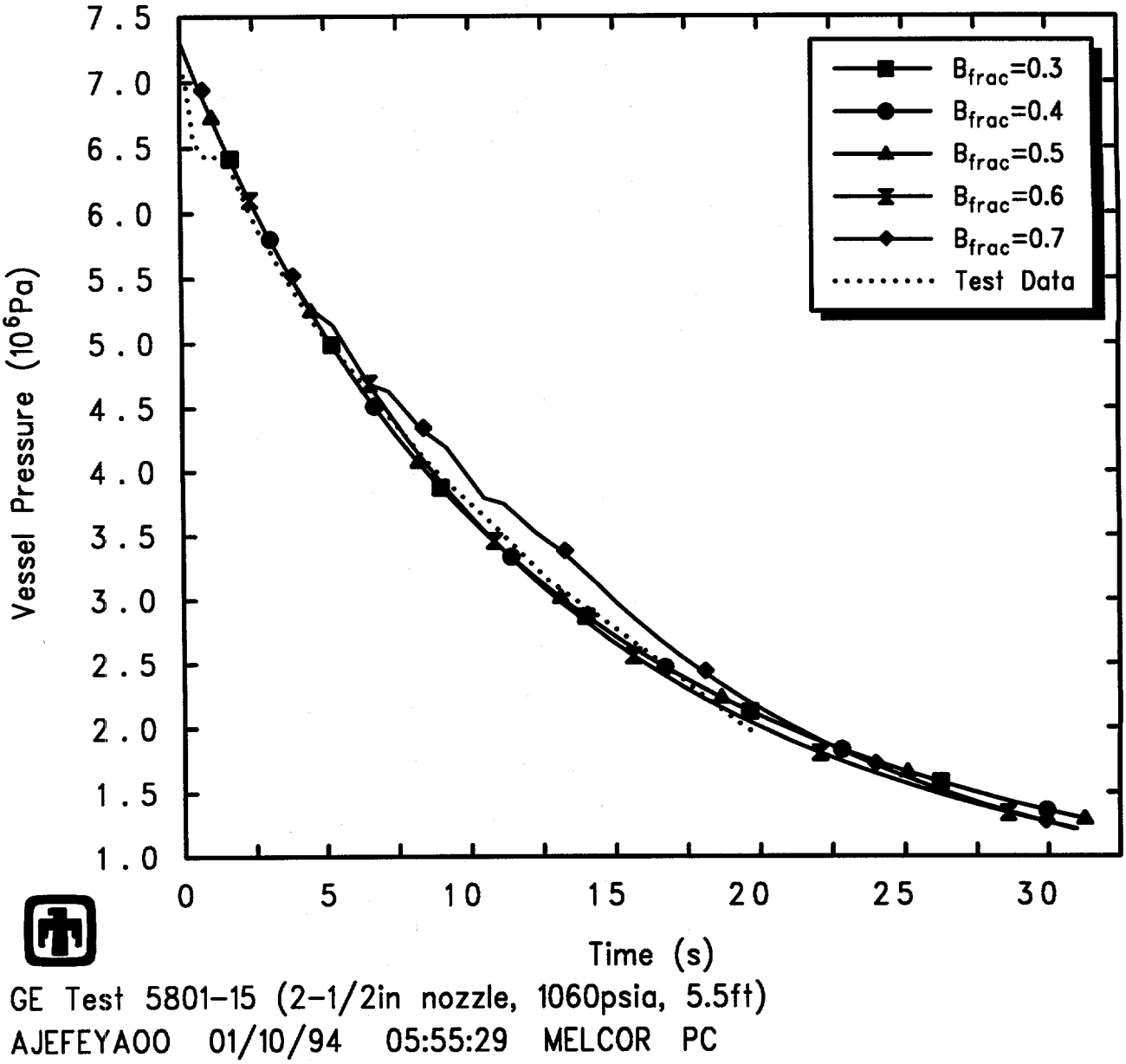

Figure 5.2.5. Vessel Pressure for GE Large Vessel Top Blowdown Test 5801-15 – Maximum Allowed Pool Bubble Fraction Sensitivity Study

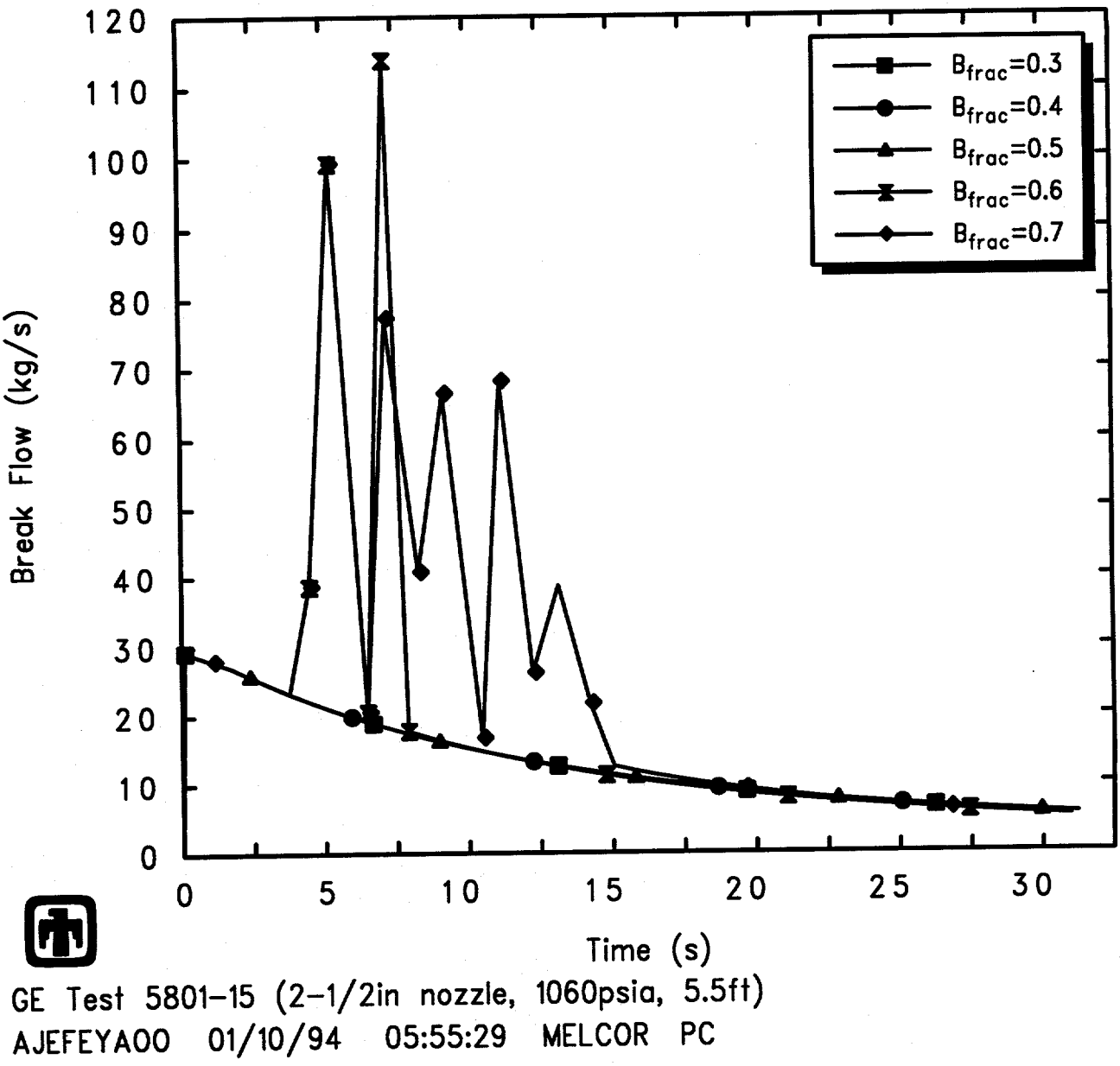

Figure 5.2.6. Vessel Liquid Levels for GE Large Vessel Top Blowdown Test 5801-15 – Maximum Allowed Pool Bubble Fraction Sensitivity Study

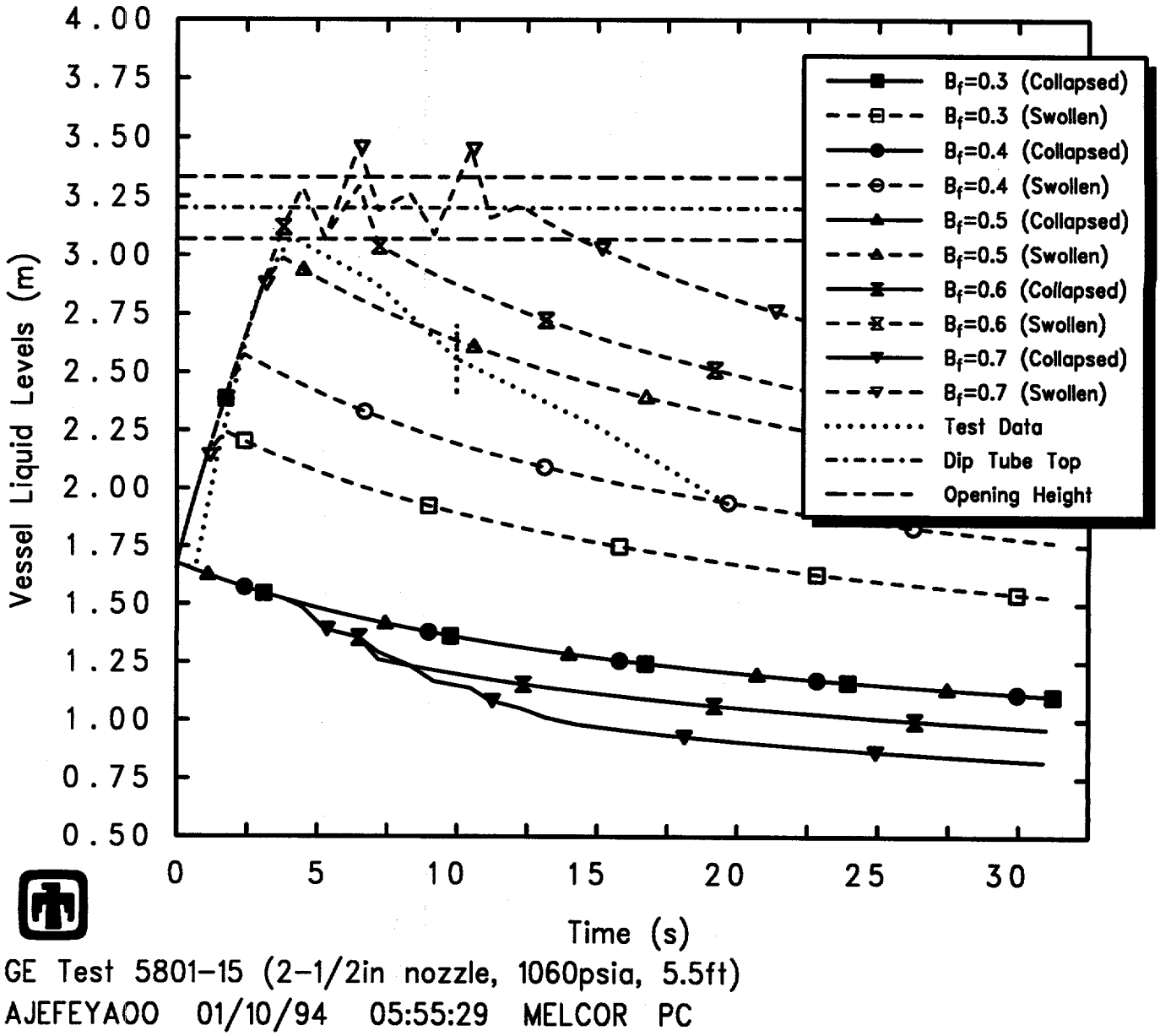

Figure 5.2.7. Blowdown Mass Flow for GE Large Vessel Top Blowdown Test 5801-15 – Maximum Allowed Pool Bubble Fraction Sensitivity Study

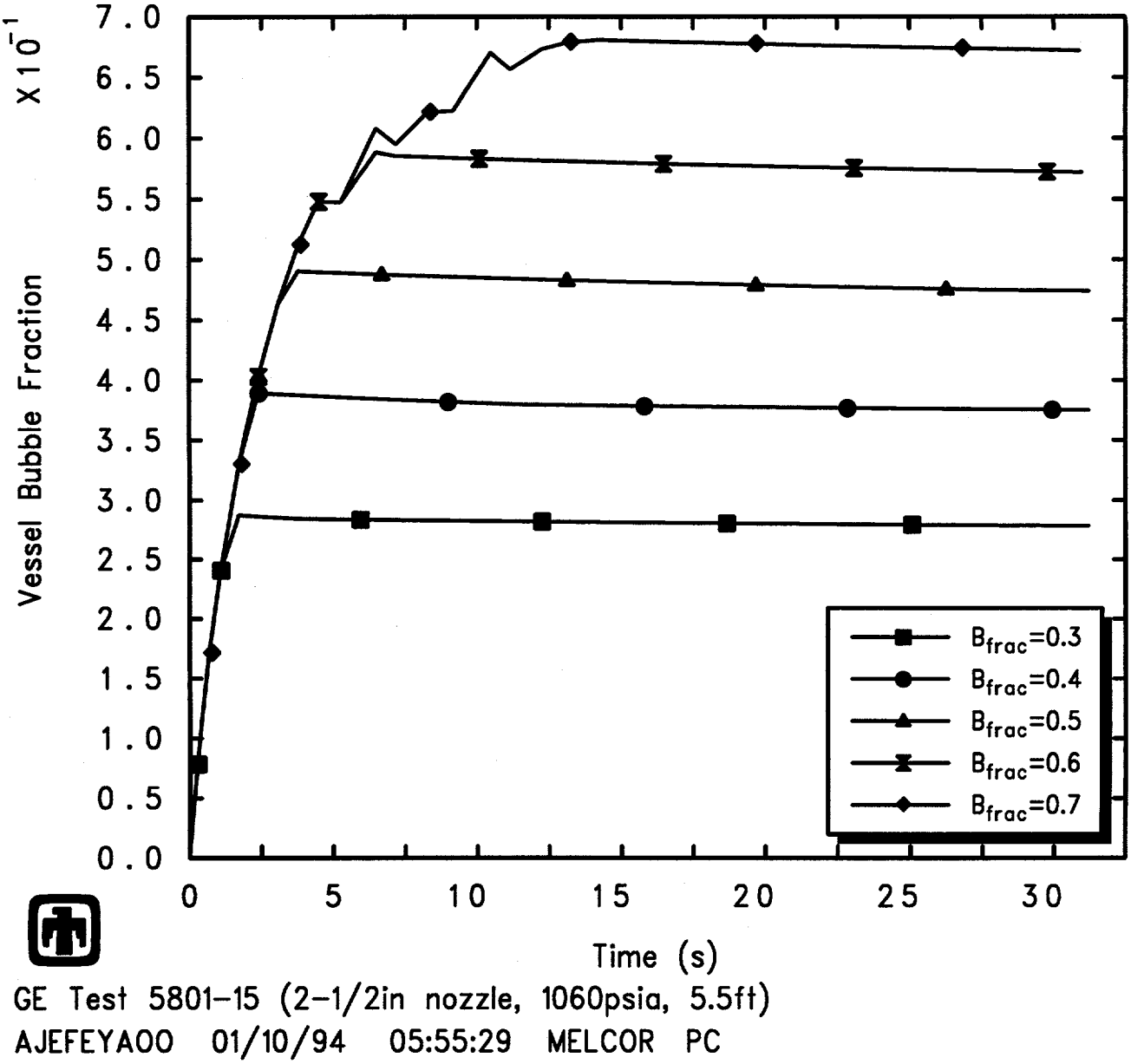

Figure 5.2.8. Vessel Two-Phase Liquid Bubble Fraction for GE Large Vessel Top Blowdown Test 5801-15 – Maximum Allowed Pool Bubble Fraction Sensitivity Study

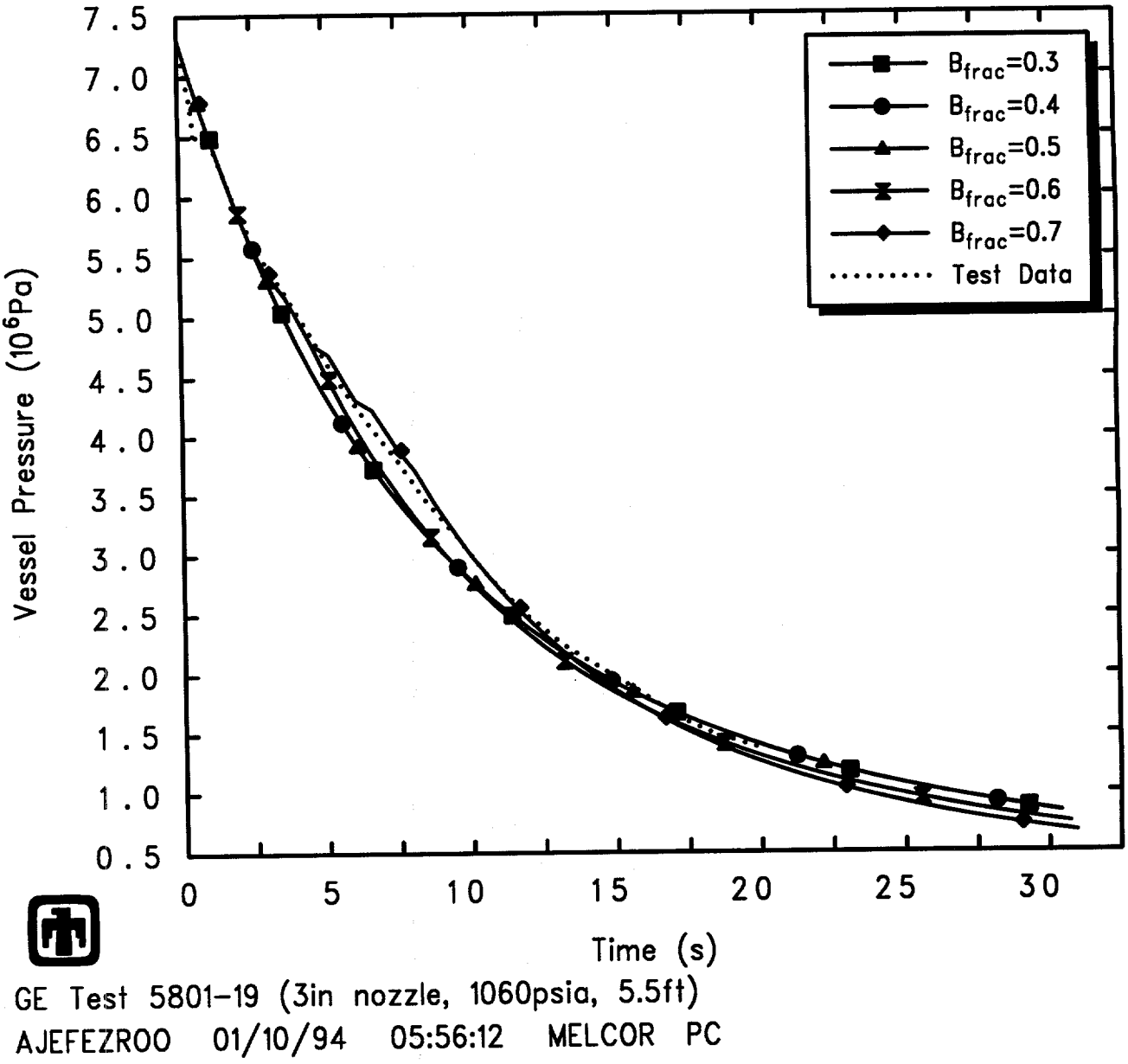

Figure 5.2.9. Vessel Pressure for GE Large Vessel Top Blowdown Test 5801-19 – Maximum Allowed Pool Bubble Fraction Sensitivity Study

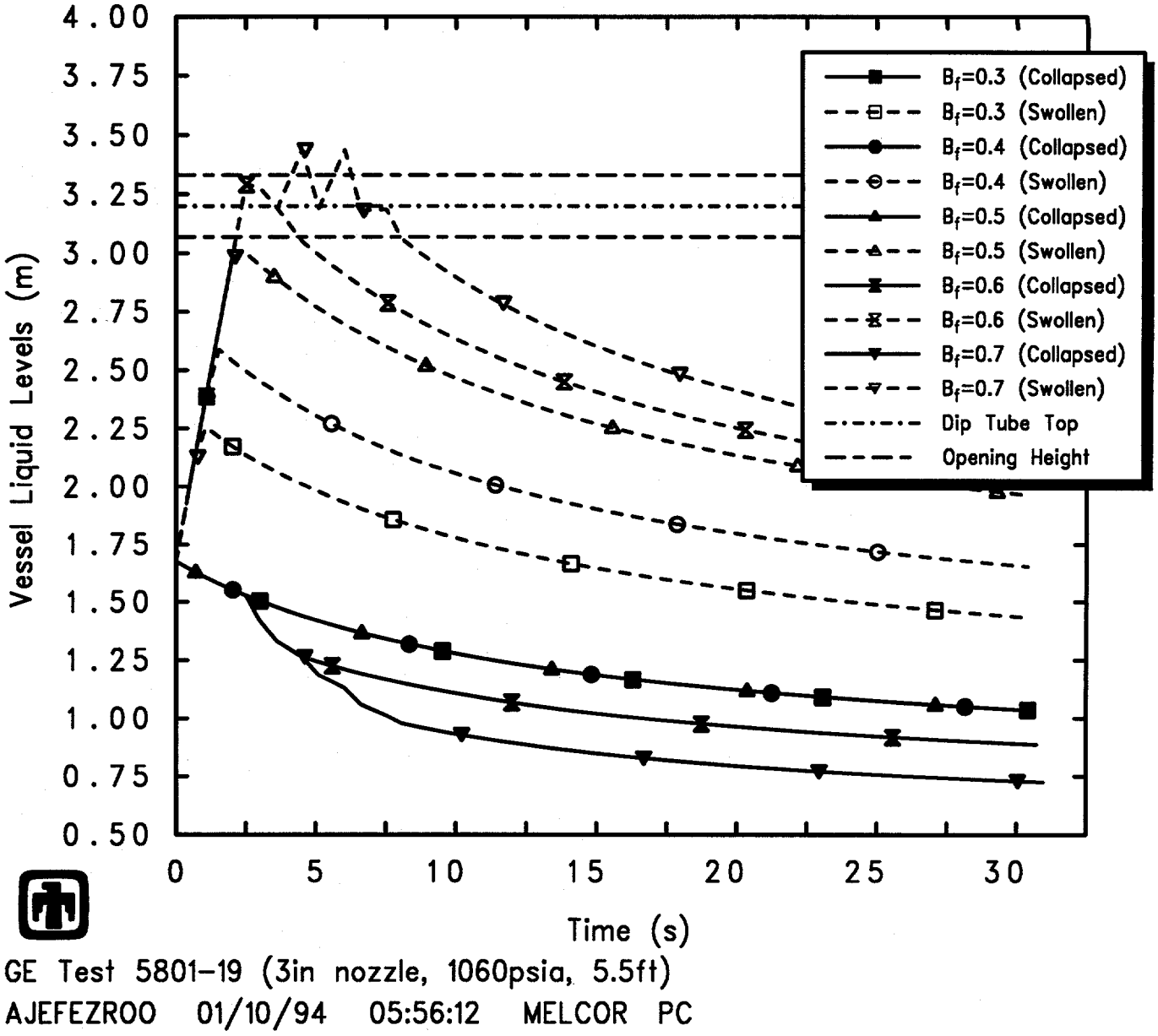

Figure 5.2.10. Vessel Liquid Levels for GE Large Vessel Top Blowdown Test 5801-19 – Maximum Allowed Pool Bubble Fraction Sensitivity Study

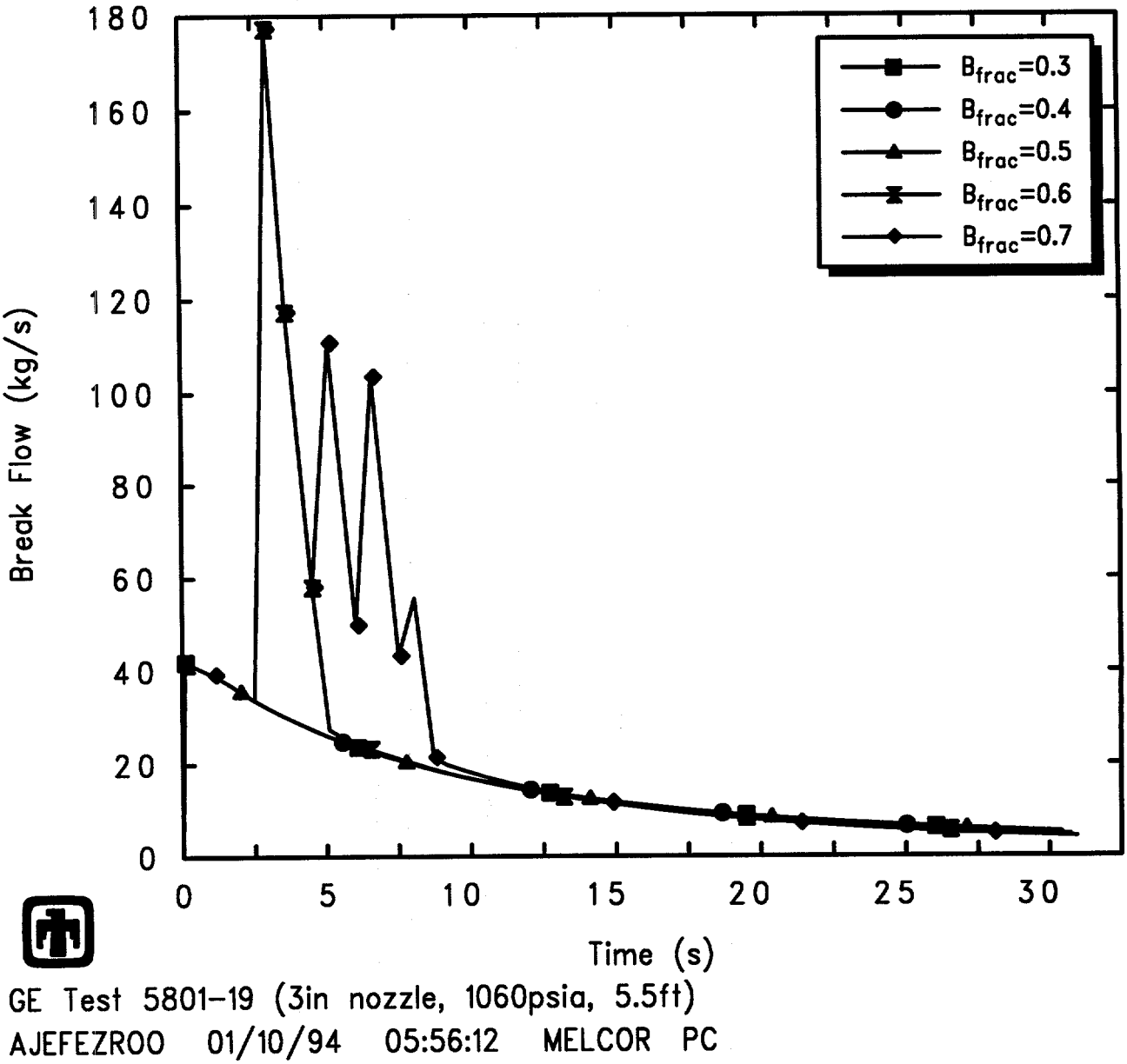

Figure 5.2.11. Blowdown Mass Flow for GE Large Vessel Top Blowdown Test 5801-19 – Maximum Allowed Pool Bubble Fraction Sensitivity Study

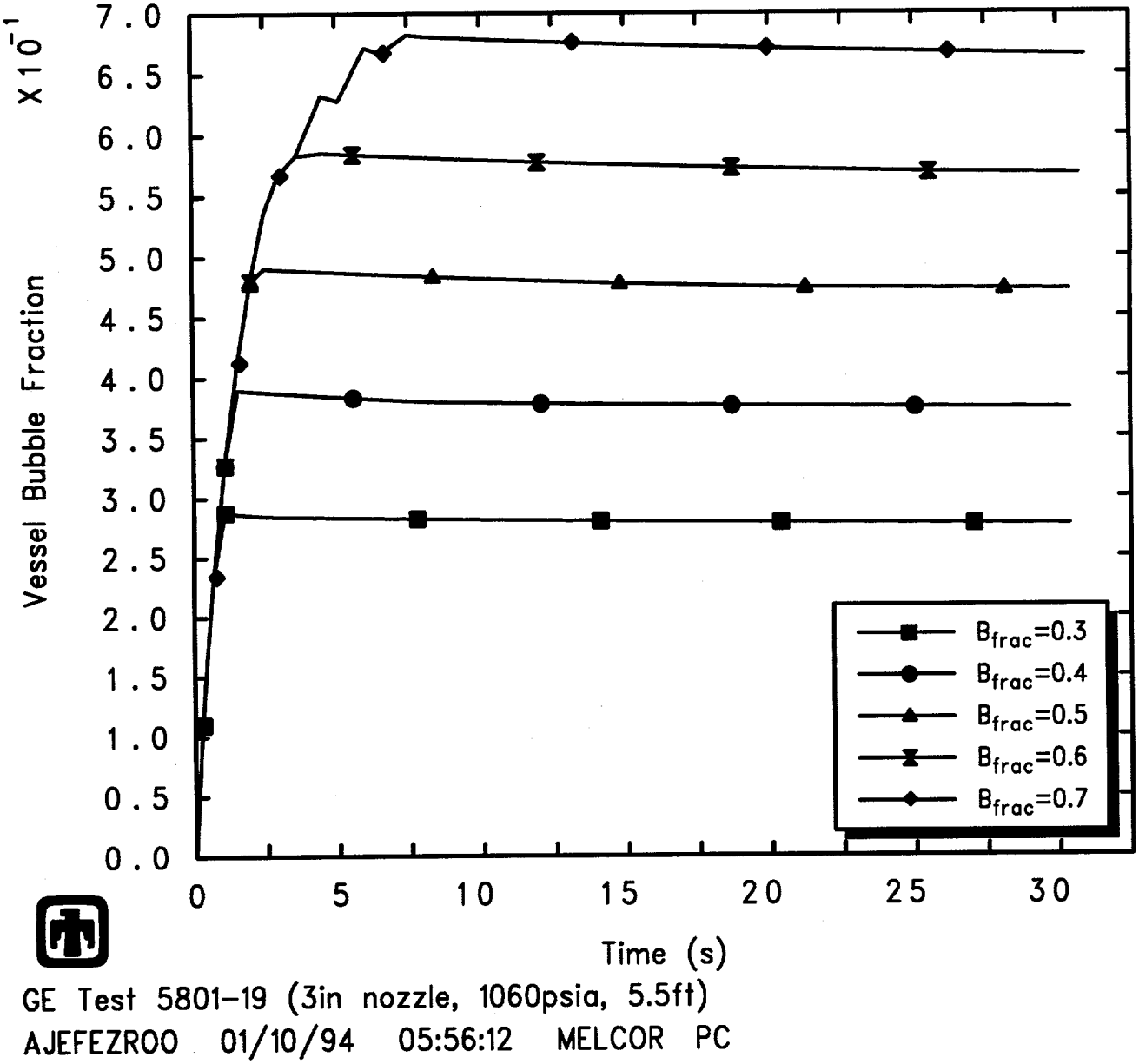

Figure 5.2.12. Vessel Two-Phase Liquid Bubble Fraction for GE Large Vessel Top Blowdown Test 5801-19 – Maximum Allowed Pool Bubble Fraction Sensitivity Study

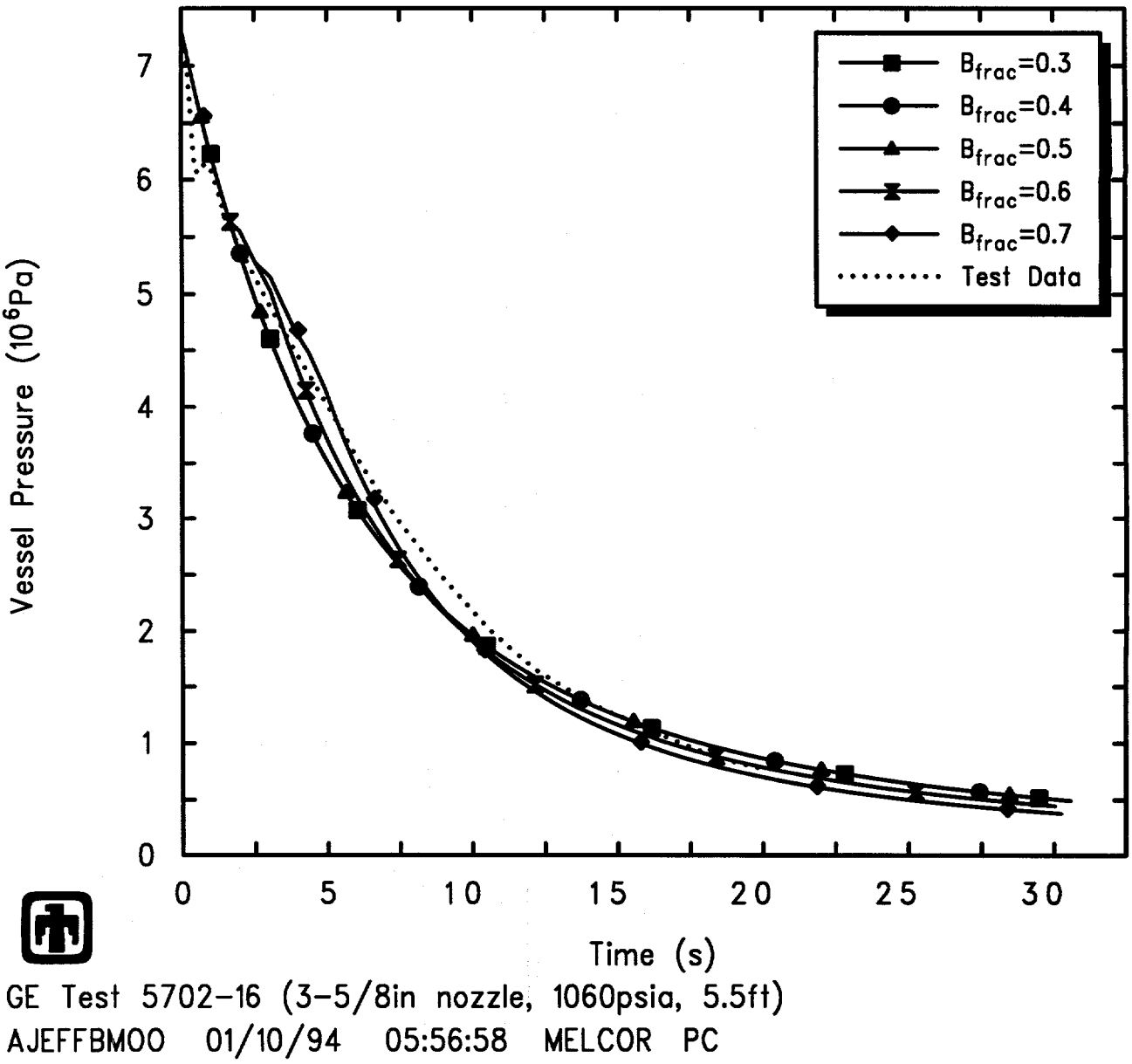

Figure 5.2.13. Vessel Pressure for GE Large Vessel Top Blowdown Test 5702-16 – Maximum Allowed Pool Bubble Fraction Sensitivity Study

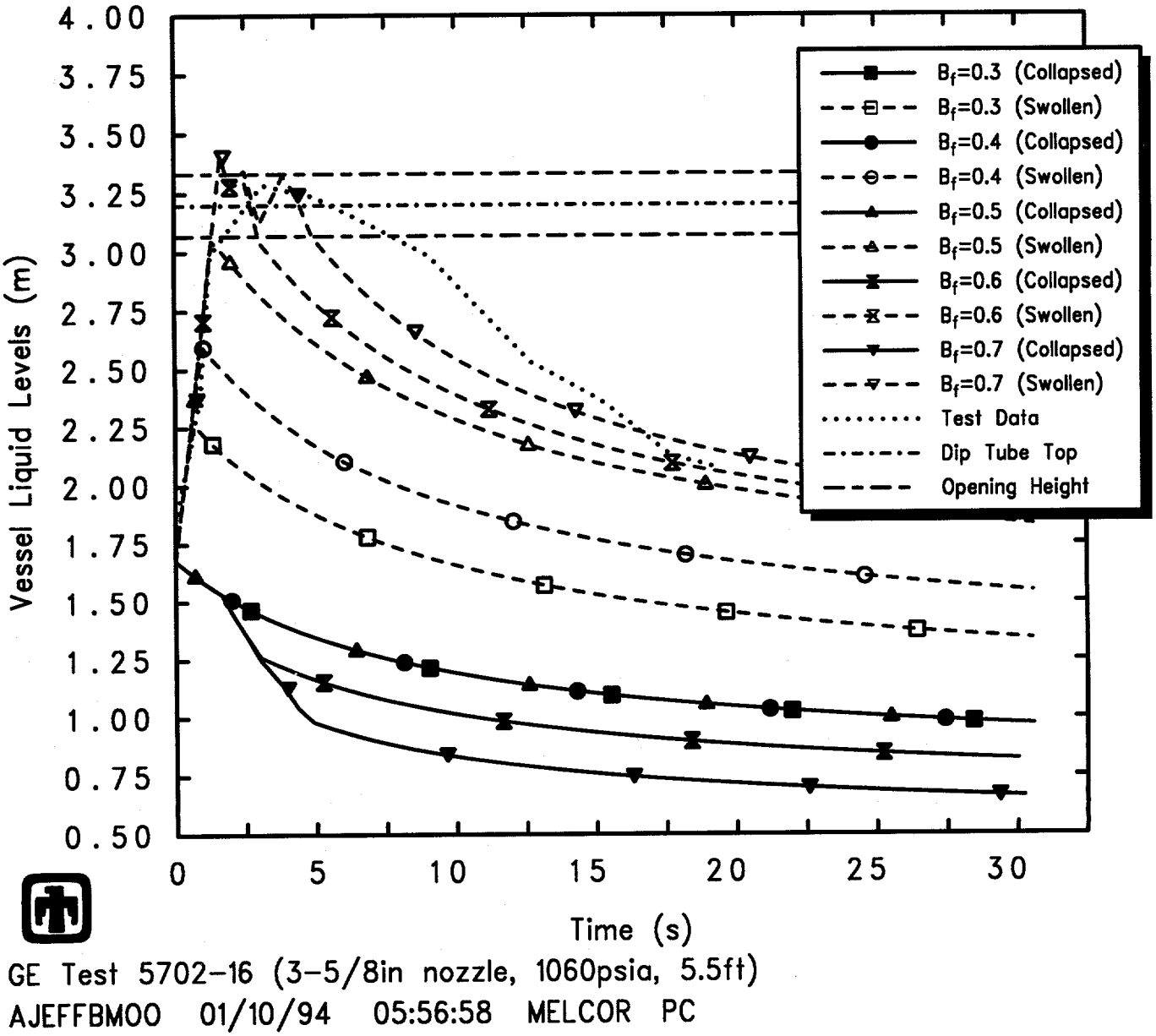

Figure 5.2.14. Vessel Liquid Levels for GE Large Vessel Top Blowdown Test 5702-16 – Maximum Allowed Pool Bubble Fraction Sensitivity Study

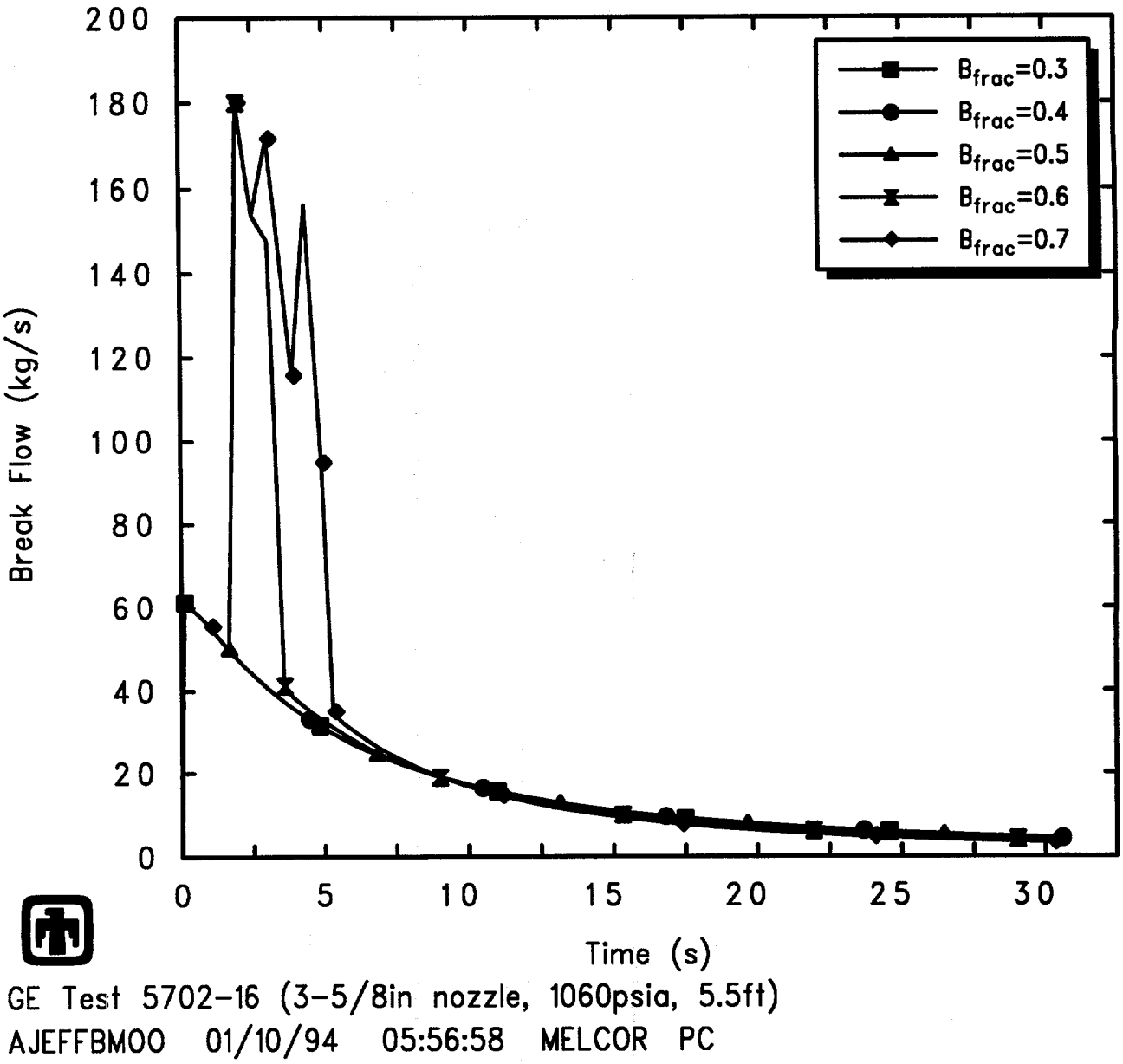

Figure 5.2.15. Blowdown Mass Flow for GE Large Vessel Top Blowdown Test 5702-16 – Maximum Allowed Pool Bubble Fraction Sensitivity Study

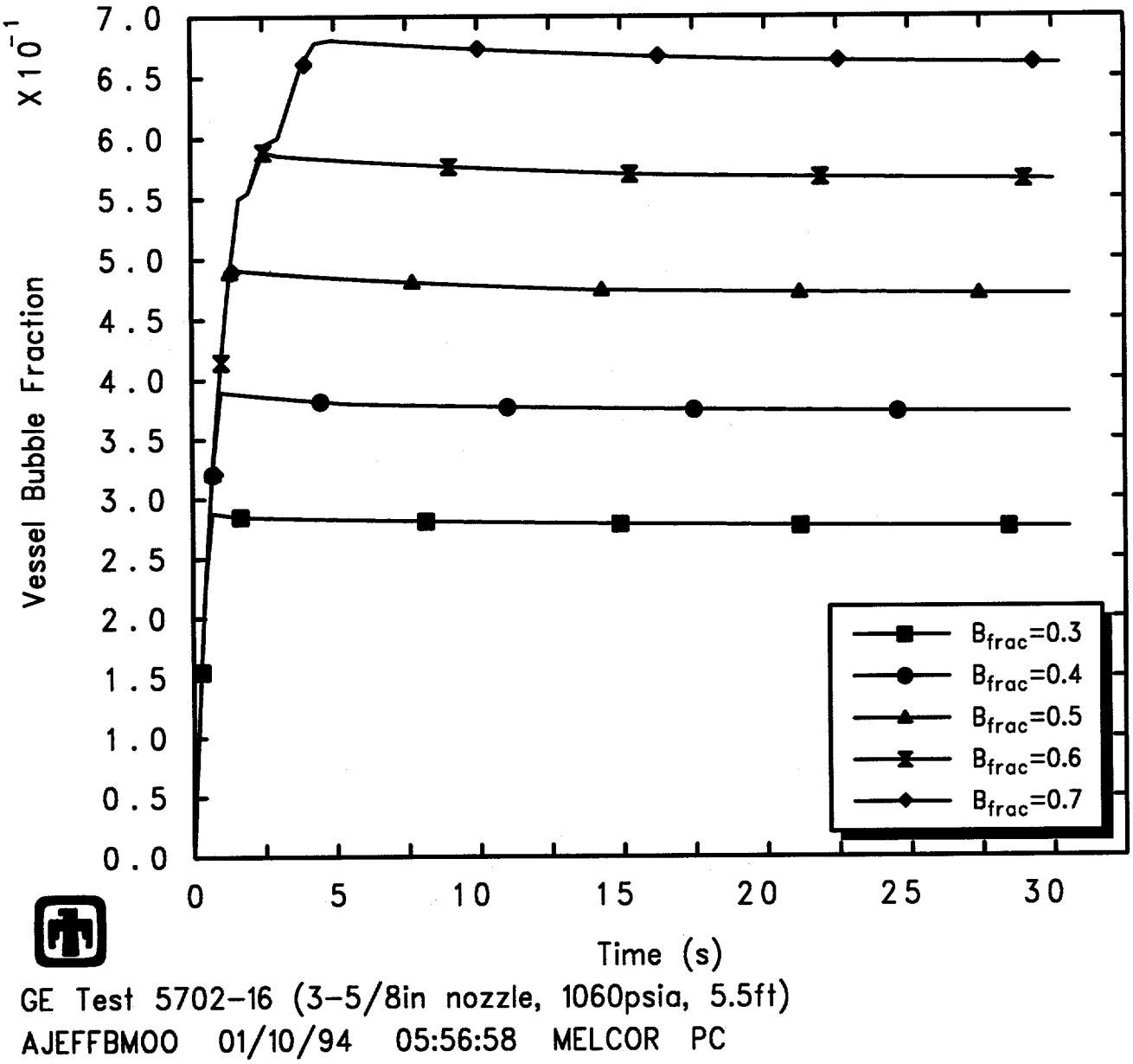

Figure 5.2.16. Vessel Two-Phase Liquid Bubble Fraction for GE Large Vessel Top Blowdown Test 5702-16 – Maximum Allowed Pool Bubble Fraction Sensitivity Study

level rises enough (above the dip tube elevation) for liquid to flow into and through the blowdown line. This occurs intermittently in all cases when the maximum allowed pool bubble fraction is set to $\geq$60%, and whenever the two-phase liquid level swells enough for liquid to flow out the blowdown line the vessel depressurization slows while the break flow increases.

The effect of changing the specified maximum allowed pool bubble fractions for the bottom blowdown test 5803-1 is summarized in Figures 5.2.17 through 5.2.20. (The results for test 5803-2 are very similar, and not shown here.) Figure 5.2.17 shows the vessel depressurization history calculated by MELCOR using these different values for the maximum allowed pool bubble fraction, compared to experimental data. The vessel collapsed and swollen (two-phase) liquid levels predicted by MELCOR using these different maximum allowed pool bubble fractions, also compared to experimental data, are depicted in Figure 5.2.18. Figure 5.2.19 shows the break flow out the blowdown line and Venturi flow limiting nozzle causing the vessel depressurization, calculated by MELCOR using different values for the maximum allowed discharge coefficients, while Figure 5.2.20 presents the calculated vessel pool bubble fractions. The effects seen are much smaller in magnitude than those noted in the top blowdown test sensitivity analyses, primarily because during most of the bottom blowdown tests the pool bubble fraction is not being controlled within MELCOR by the maximum allowed value. There is significantly less level swell in the bottom blowdown tests than in any of the top blowdown tests, and the pool bubble fraction is not affected by the maximum allowed value until very late in the transient, when little pool is left.

This set of sensitivity study calculations and the comparison to test data indicates that there is no single value for the maximum allowed pool bubble fraction which provides good agreement with measurement in all four top blowdown test analyses. The maximum pool bubble fraction matching two-phase level test data seems to increase as the nozzle dimensions and hence vessel depressurization rate is increased; also, agreement with test data could be improved further if the pool bubble fraction slowly decreased after that maximum value had been reached. The bottom blowdown test analyses show little or no sensitivity to the maximum allowed pool bubble fraction, because there is significantly less level swell in the bottom blowdown tests than in any of the top blowdown tests, and the pool bubble fraction is not affected by the maximum allowed value. Because no other single value was obviously better, we used the default maximum allowed pool bubble fraction of 40% in all other MELCOR analyses done as part of this assessment study.

5.3 Bubble Rise Velocity

In nonequilibrium calculations with MELCOR, vapor bubbles may appear in the liquid pool due to boiling (as a result of heat deposition in the pool) or flashing (in response to a reduction in pressure in the control volume). These bubbles transport mass and energy from the pool to the atmosphere as they rise to the surface. The bubble rise model in MELCOR is very simple. It assumes steady state with an upward flow

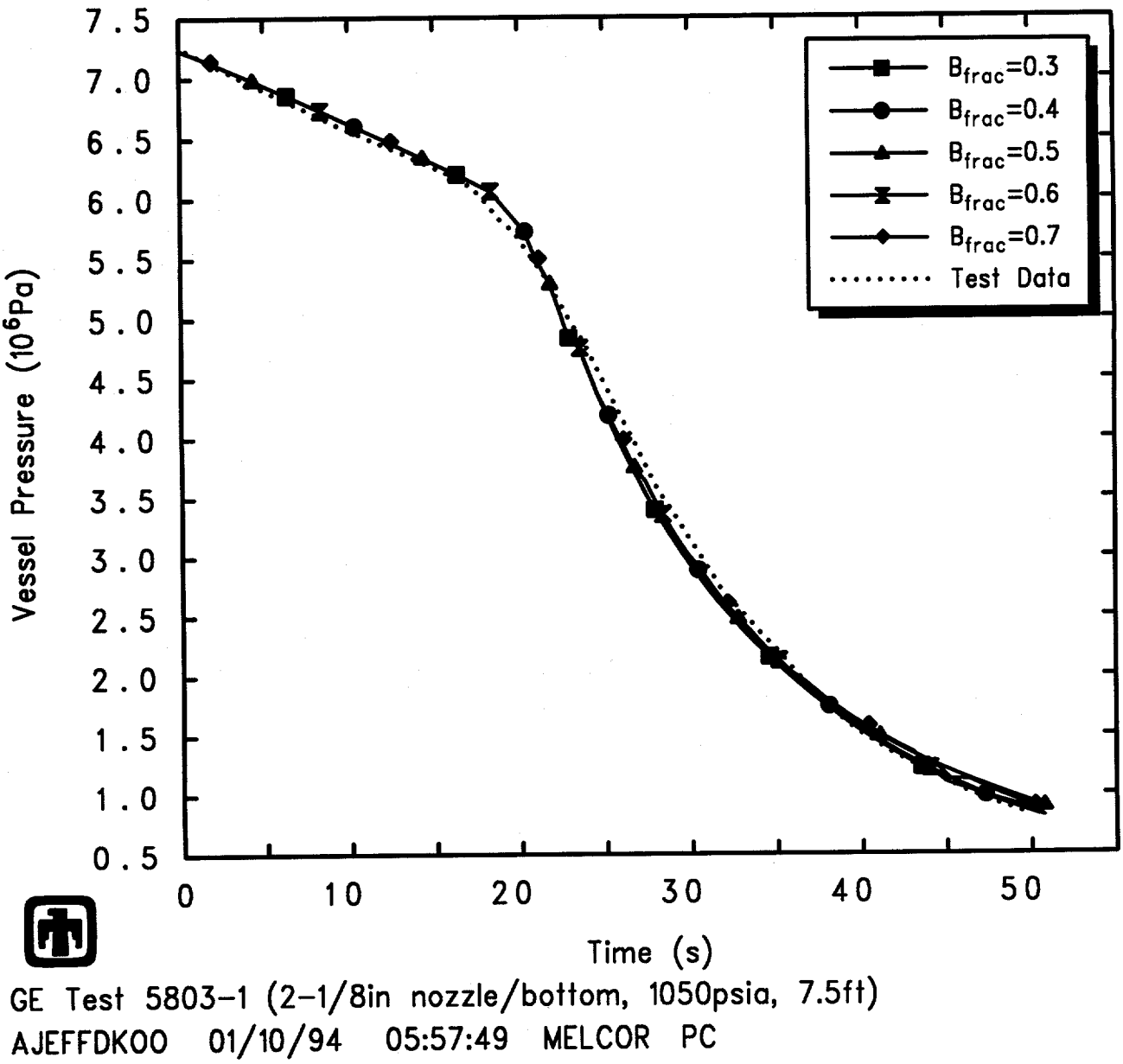

Figure 5.2.17. Vessel Pressure for GE Large Vessel Bottom Blowdown Test 5803-1 – Maximum Allowed Pool Bubble Fraction Sensitivity Study

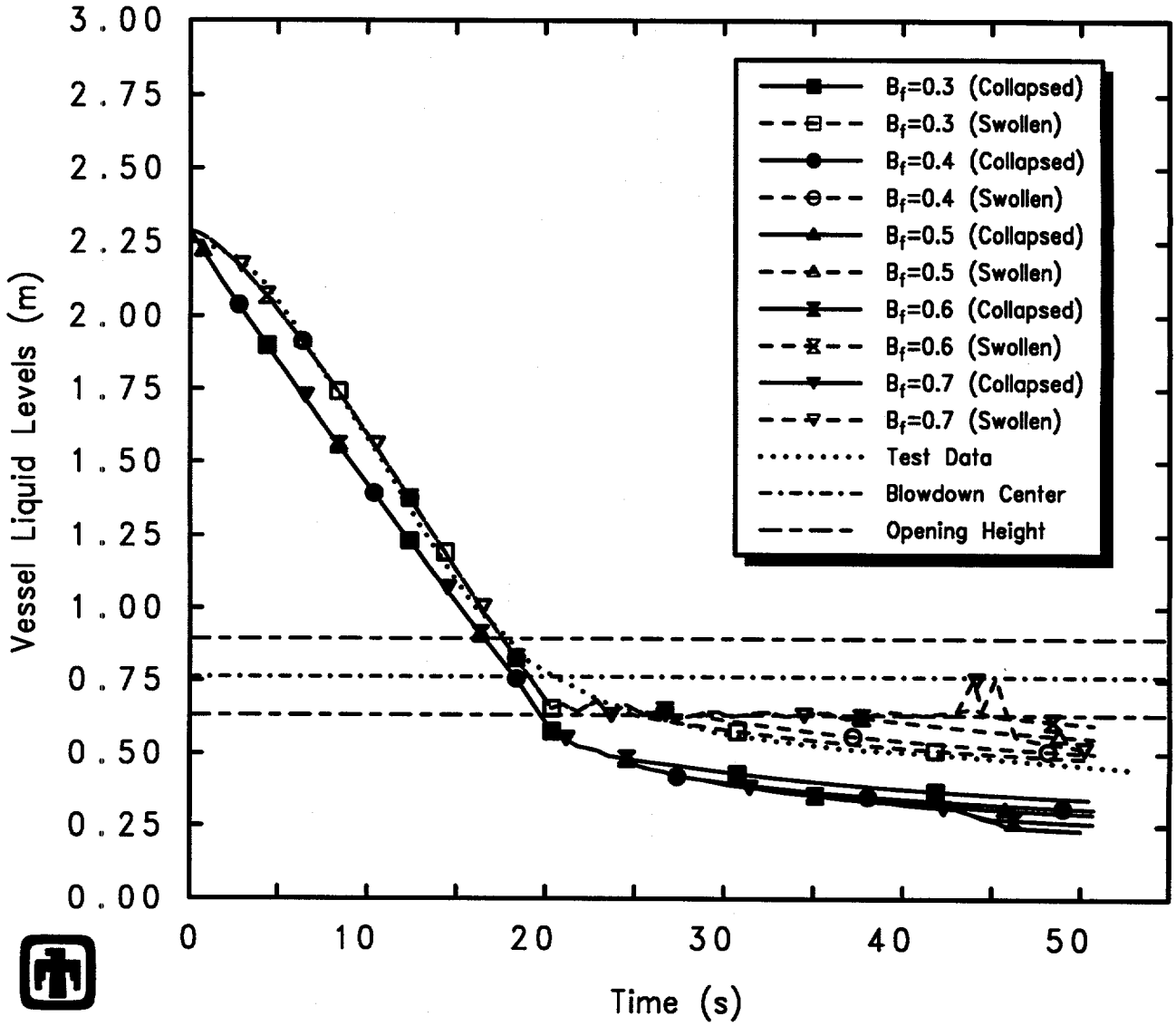

Figure 5.2.18. Vessel Liquid Levels for GE Large Vessel Bottom Blowdown Test 5803-1 – Maximum Allowed Pool Bubble Fraction Sensitivity Study

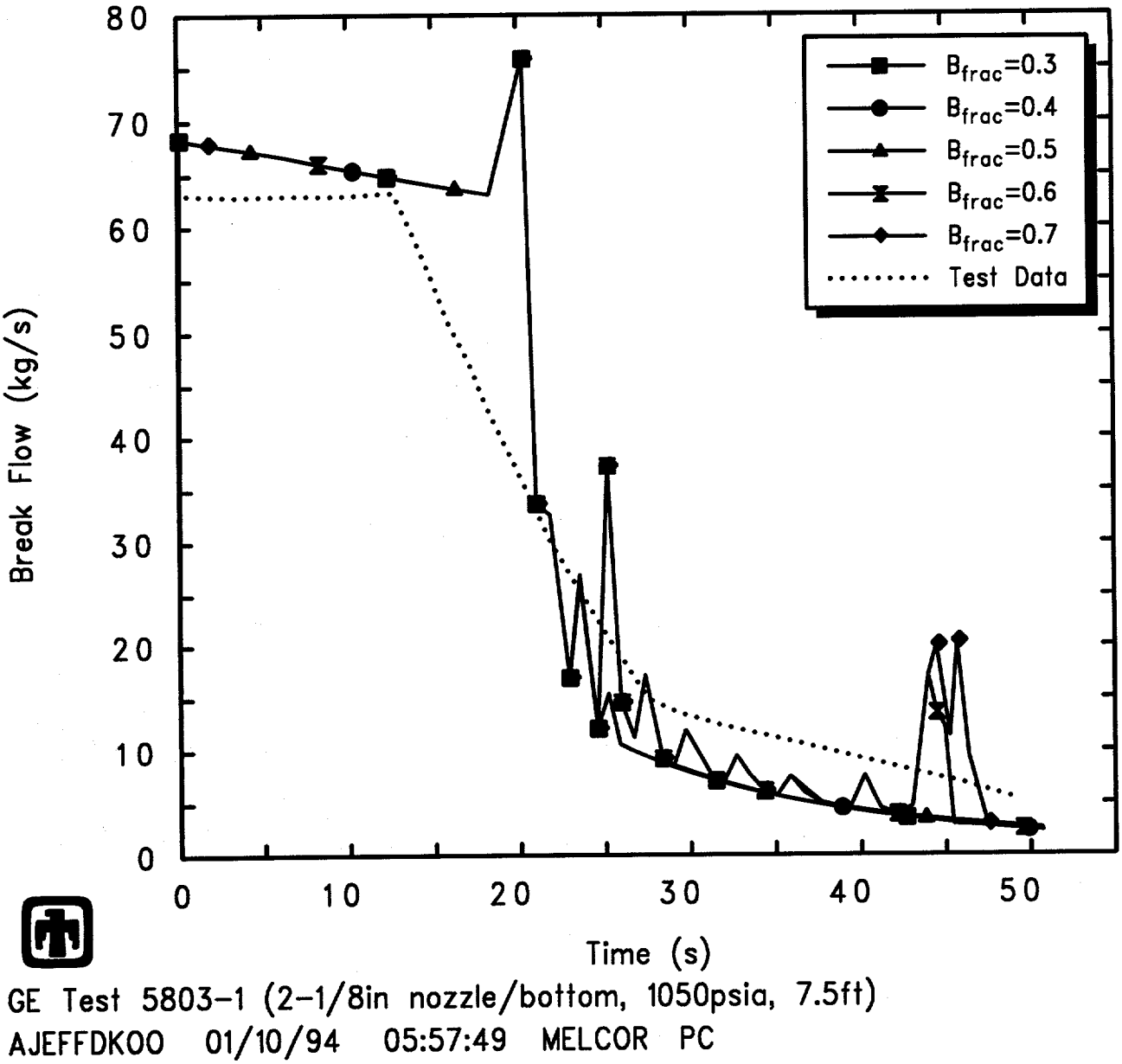

Figure 5.2.19. Blowdown Mass Flow for GE Large Vessel Bottom Blowdown Test 5803-1 – Maximum Allowed Pool Bubble Fraction Sensitivity Study

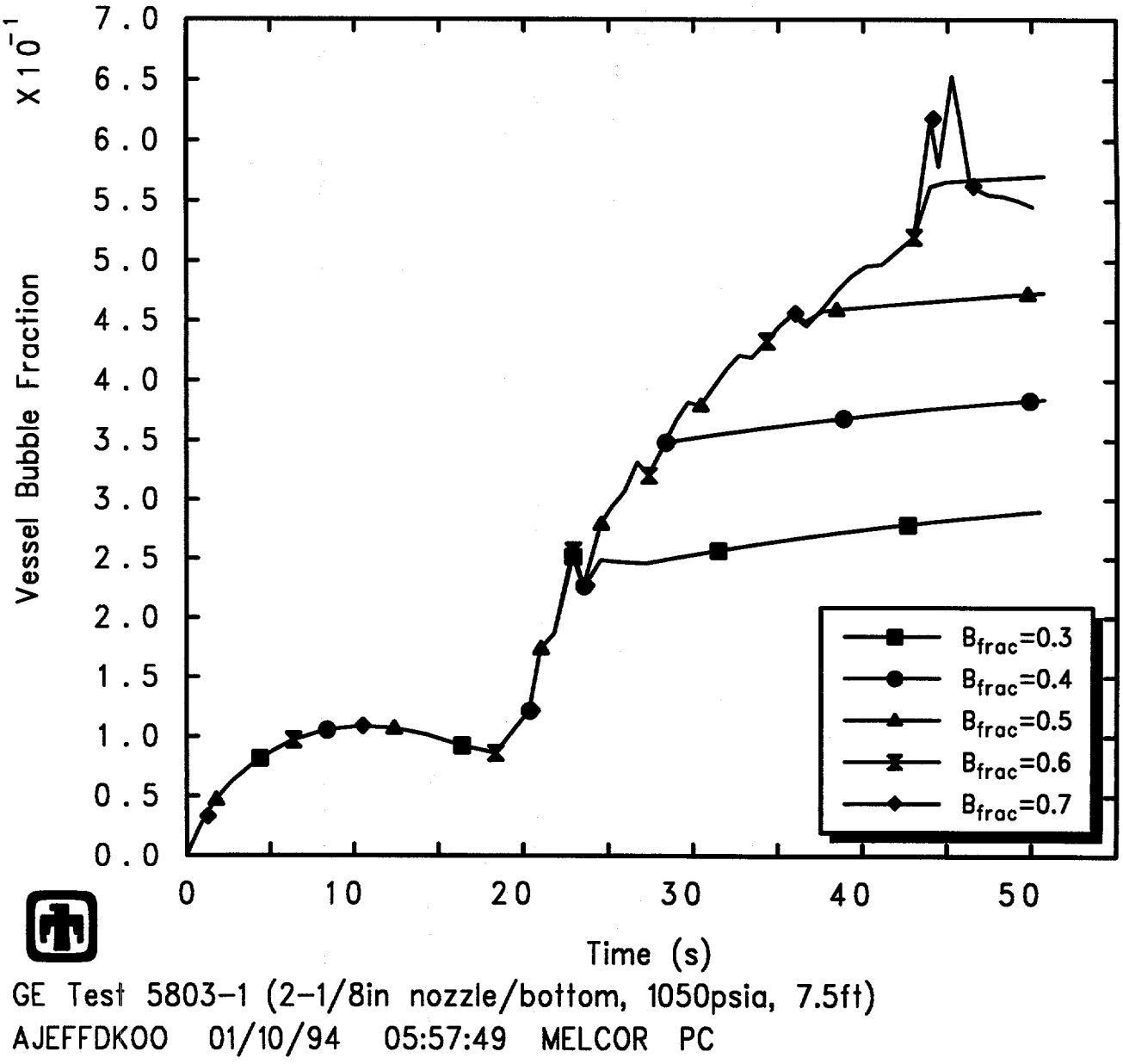

Figure 5.2.20. Vessel Two-Phase Liquid Level Bubble Fraction for GE Large Vessel Bottom Blowdown Test 5803-1 – Maximum Allowed Pool Bubble Fraction Sensitivity Study

of bubbles varying linearly in the volume and with a constant rise velocity of 0.3m/s. As a sensitivity study, calculations have been done in which this bubble rise velocity was reduced to 0.03m/s and 0.1m/s, and increased to 1m/s and 3m/s, input through sensitivity coefficient SC4407(1).

The effect of varying the pool bubble rise velocity is shown in Figures 5.3.1 through 5.3.4, for the top blowdown test 5801-13. Figure 5.3.1 presents the vessel depressurization histories calculated by MELCOR using these different pool bubble rise velocities, compared to experimental data, while Figure 5.3.2 depicts the corresponding break flow out the blowdown line and Venturi flow limiting nozzle causing the vessel depressurization. The vessel collapsed and swollen liquid levels predicted by MELCOR using these different pool bubble rise velocities, also compared to experimental data, are given in Figure 5.3.3, while Figure 5.3.4 shows the resultant pool bubble fractions in this set of MELCOR sensitivity study calculations.

The vessel pool bubble fraction rises to and then remains at near the maximum value allowed for bubble rise velocities below or at the code default ($\leq$0.3m/s), as illustrated in Figure 5.3.4, although it takes longer to reach that maximum as the pool bubble rise velocity increases; for faster bubble rise velocities ($\geq$1m/s), the vessel pool bubble fraction equilibrates at progressively lower values. Figure 5.3.3 suggests that, for test 5801-13, the best agreement with the measured rate of level swell and the observed timing of the two-phase level peak is found with the pool bubble rise velocity at the default code value of 0.3m/s. Figures 5.3.1 and 5.3.2 demonstrate that there is relatively little effect found on the calculated vessel depressurization or blowdown outflow as the pool bubble rise velocity is varied, because the two-phase liquid level never rises enough (above the dip tube elevation, shown in Figure 5.3.3 for reference) for liquid to flow out the blowdown line.

Results of similar calculations varying the pool bubble rise velocity are summarized in Figures 5.3.5 through 5.3.7 for the top blowdown test 5801-15 (which has a slightly larger nozzle throat diameter than used in test 5801-13). For test 5801-15, the best agreement with observation is found with a pool bubble rise velocity of $\geq$0.3m/s, the code default.

The results for test 5803-19 in this bubble rise velocity sensitivity study are qualitatively the same as those just presented for tests 5801-13 and 5801-15, and are not shown because no two-phase level data are available for comparison for evaluation of which value of bubble rise velocity to use.

Figures 5.3.8 through 5.3.11 summarize the effect on the vessel depressurization and on the vessel liquid levels of varying the pool bubble rise velocity in the top blowdown test 5702-16, and also give blowdown flow and vessel pool bubble fraction results. For this test (as for test 5801-19), the best agreement with test data is found with a pool bubble rise velocity in MELCOR of $\leq$0.3m/s, the code default.

The effect of changing the pool bubble rise velocities for the bottom blowdown test 5803-1 is illustrated in Figures 5.3.12 through 5.3.15. Figure 5.3.12 shows the vessel depressurization history calculated by MELCOR using these different values for the pool bubble rise velocity, compared to experimental data. The vessel collapsed and swollen

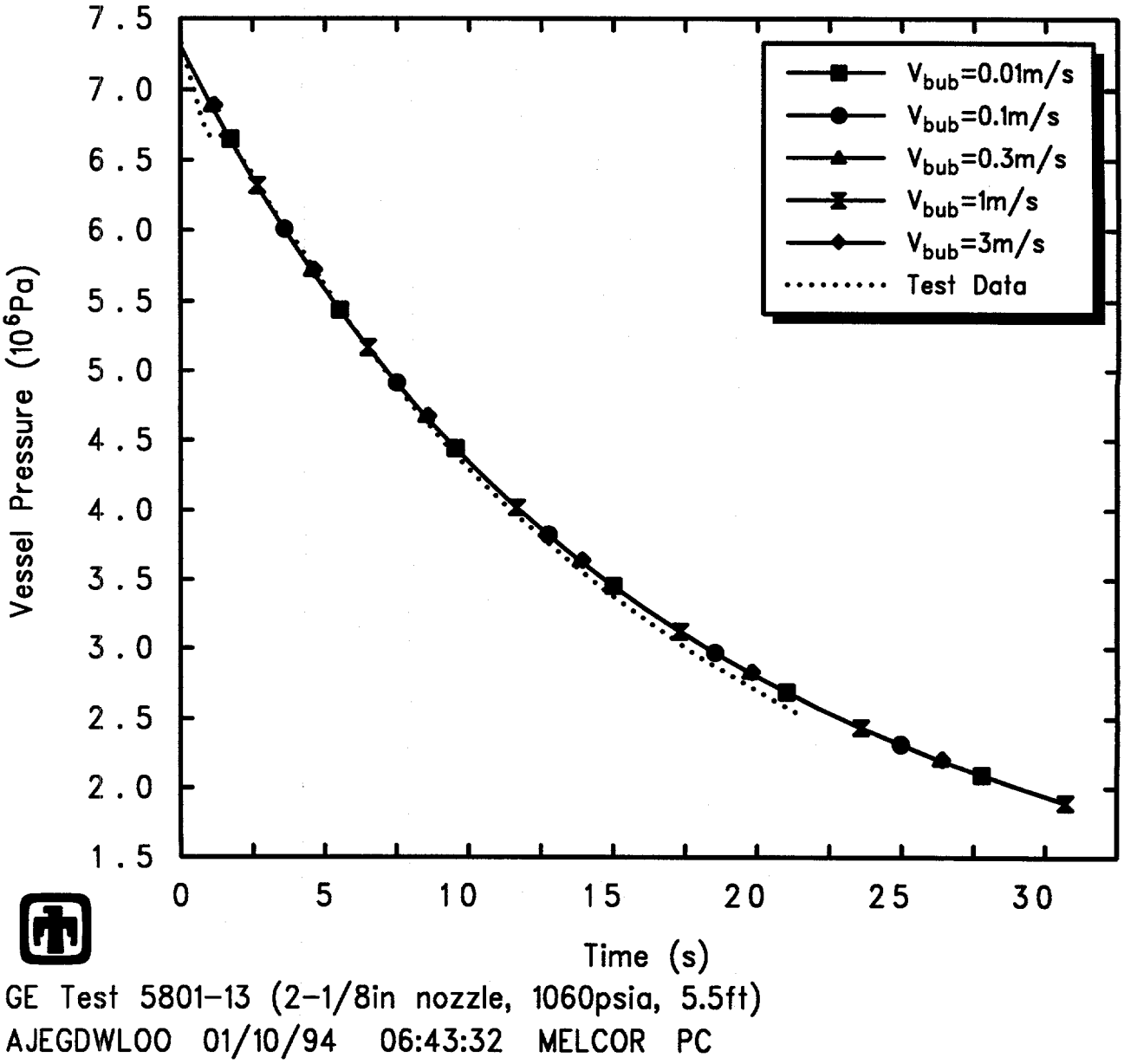

Figure 5.3.1. Vessel Pressure for GE Large Vessel Top Blowdown Test 5801-13 – Pool Bubble Rise Velocity Sensitivity Study

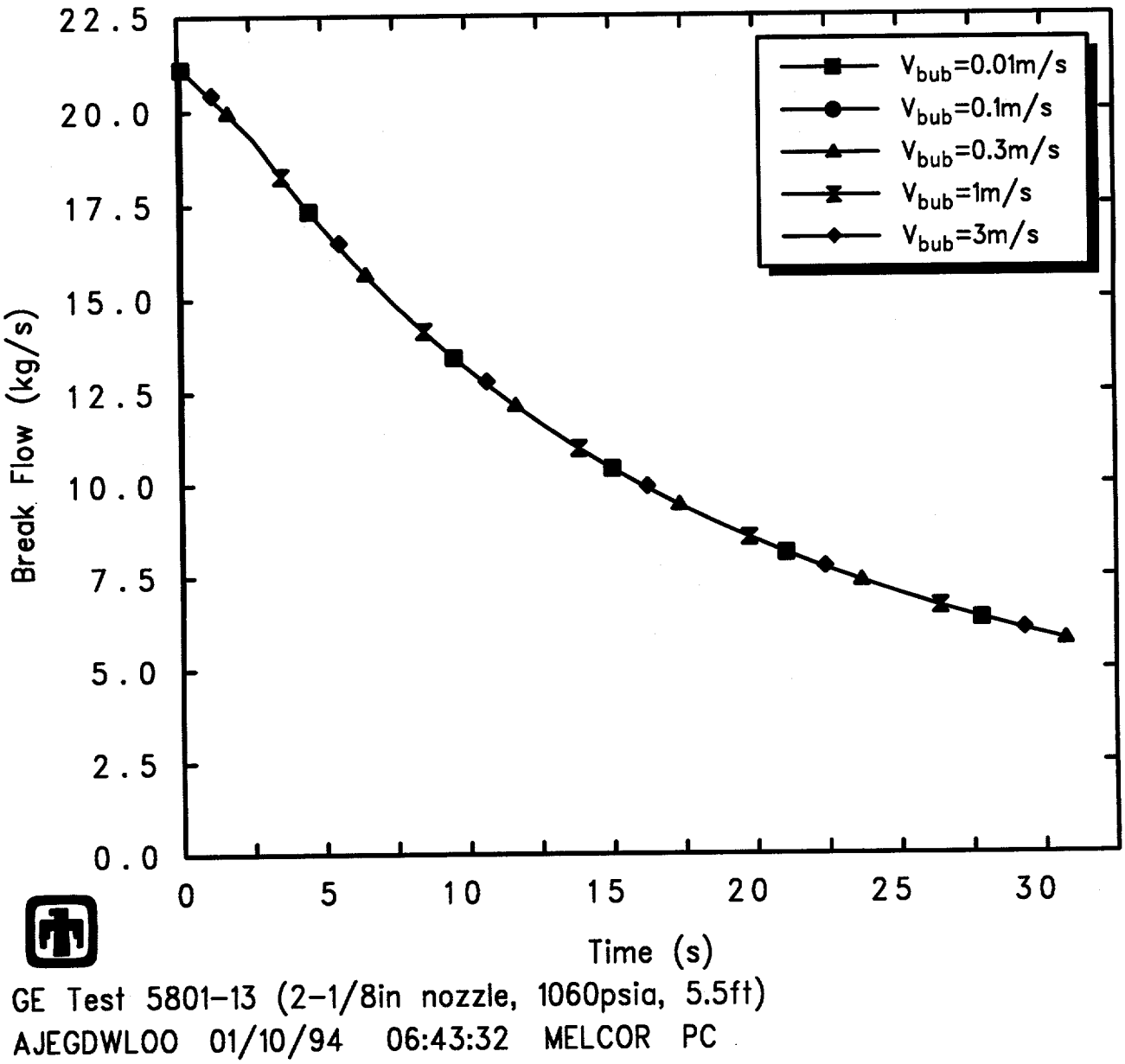

Figure 5.3.2. Blowdown Mass Flow for GE Large Vessel Top Blowdown Test 5801-13 – Pool Bubble Rise Velocity Sensitivity Study

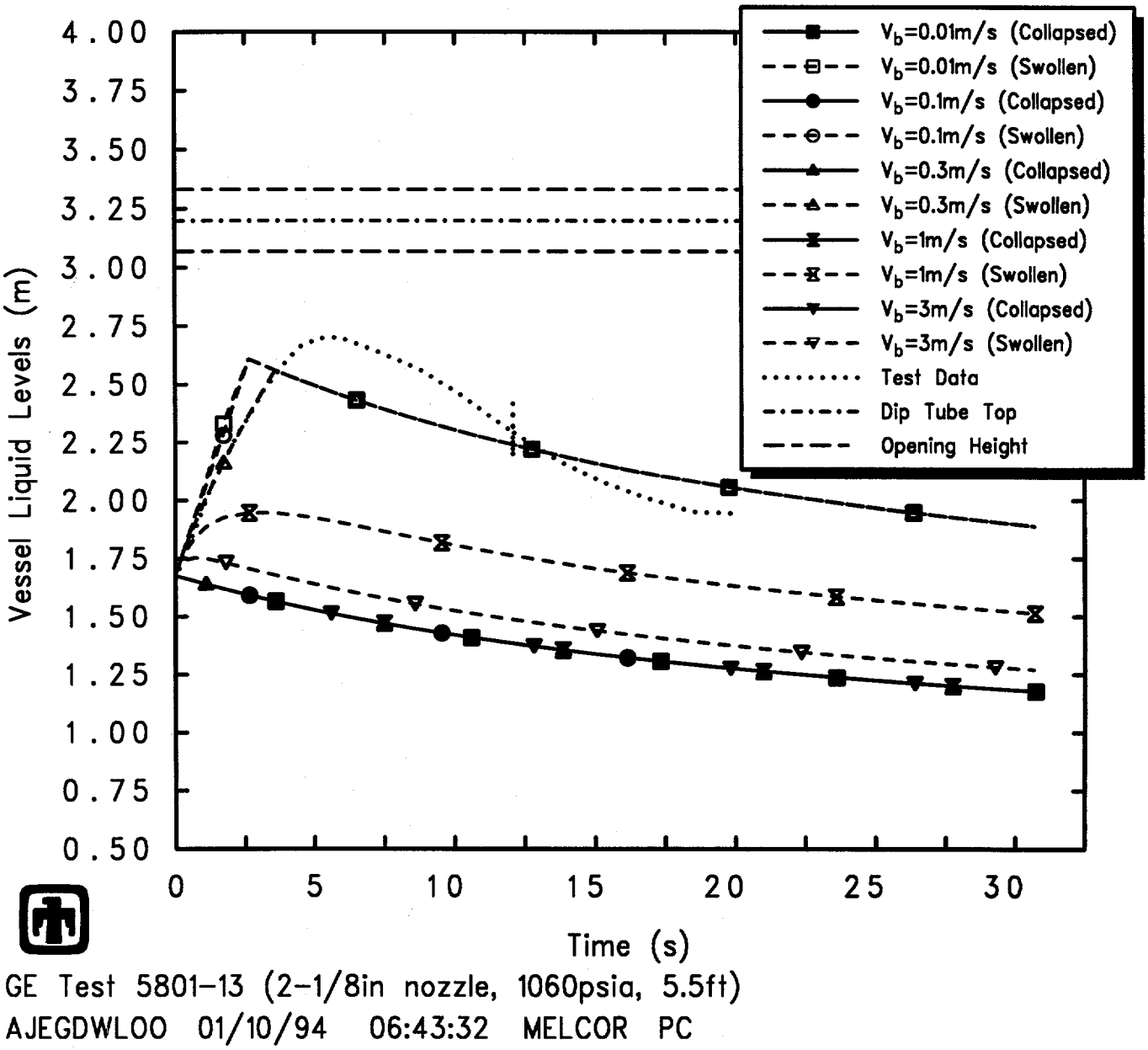

Figure 5.3.3. Vessel Liquid Levels for GE Large Vessel Top Blowdown Test 5801-13 – Pool Bubble Rise Velocity Sensitivity Study

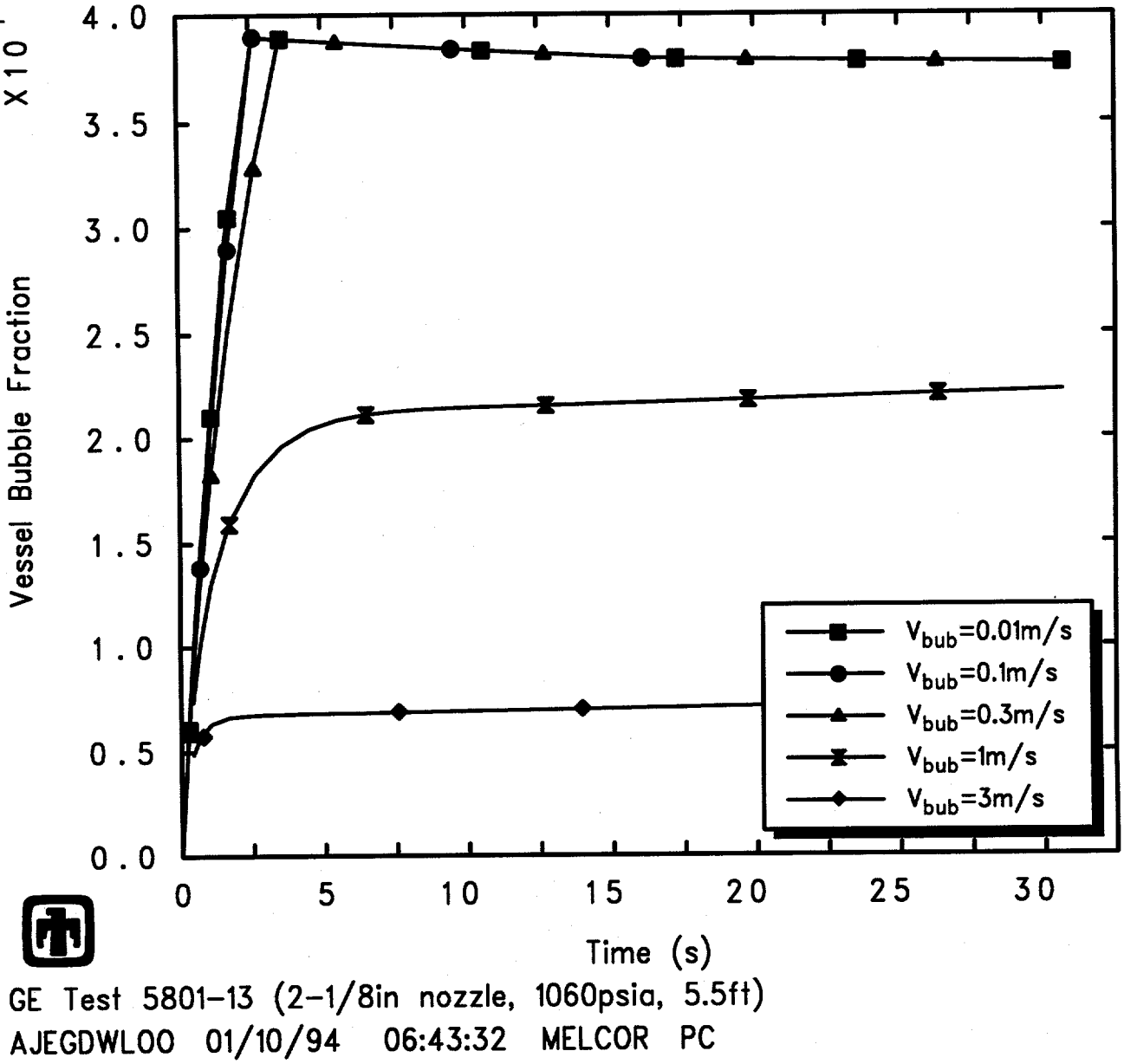

Figure 5.3.4. Vessel Two-Phase Liquid Bubble Fraction for GE Large Vessel Top Blowdown Test 5801-13 – Pool Bubble Rise Velocity Sensitivity Study

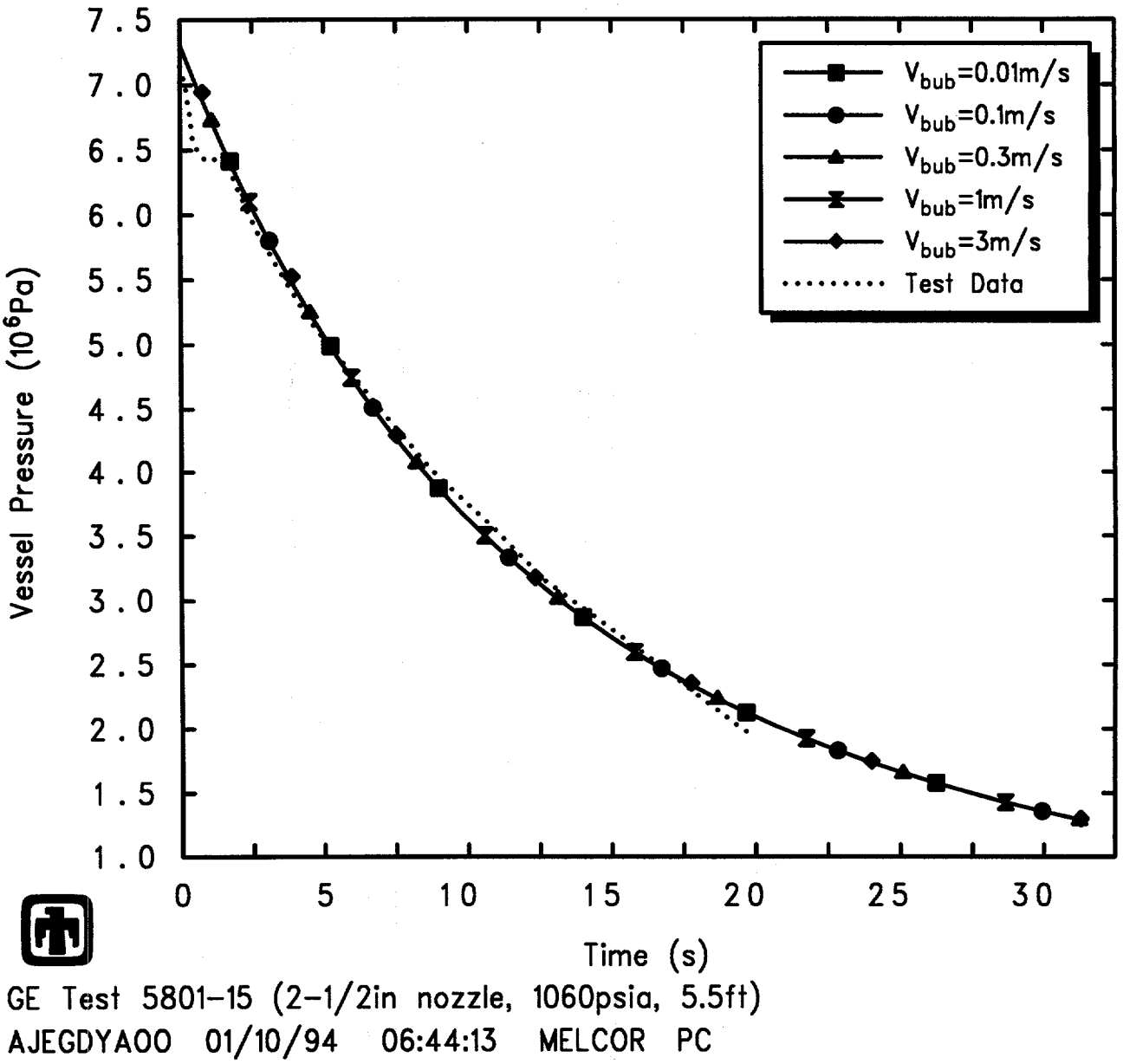

Figure 5.3.5. Vessel Pressure for GE Large Vessel Top Blowdown Test 5801-15 – Pool Bubble Rise Velocity Sensitivity Study

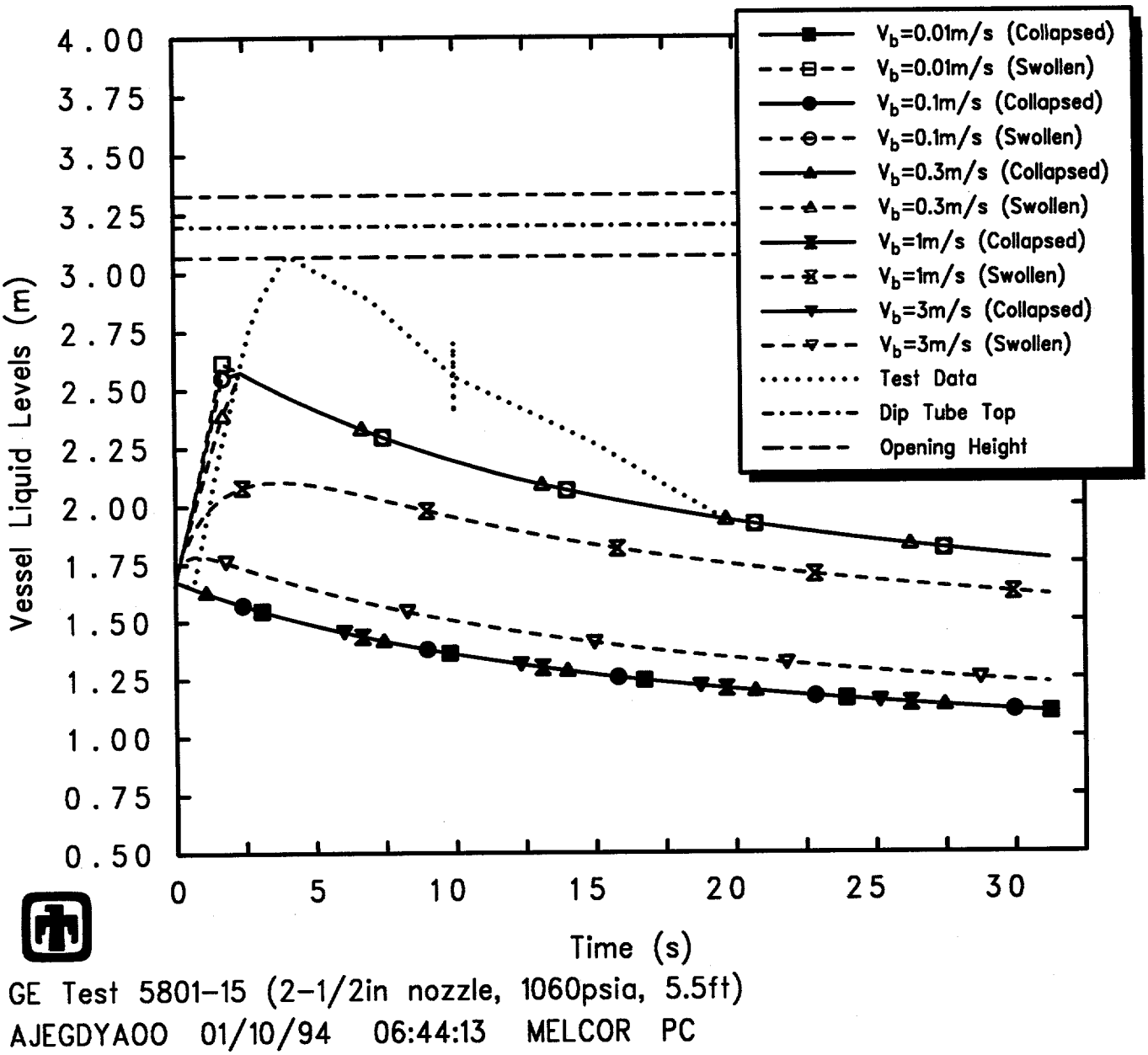

Figure 5.3.6. Vessel Liquid Levels for GE Large Vessel Top Blowdown Test 5801-15 – Pool Bubble Rise Velocity Sensitivity Study

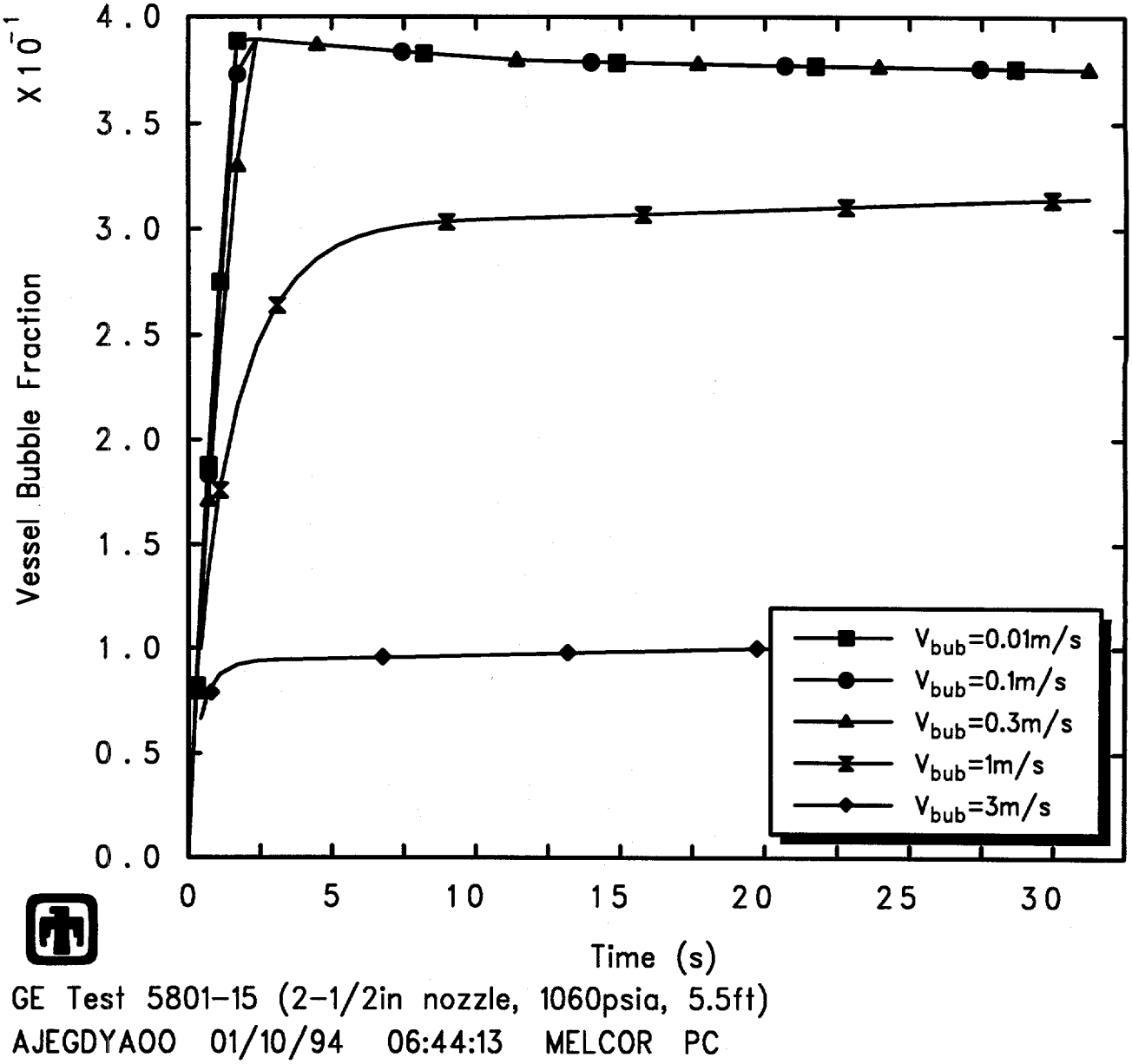

Figure 5.3.7. Vessel Two-Phase Liquid Bubble Fraction for GE Large Vessel Top Blowdown Test 5801-15 – Pool Bubble Rise Velocity Sensitivity Study

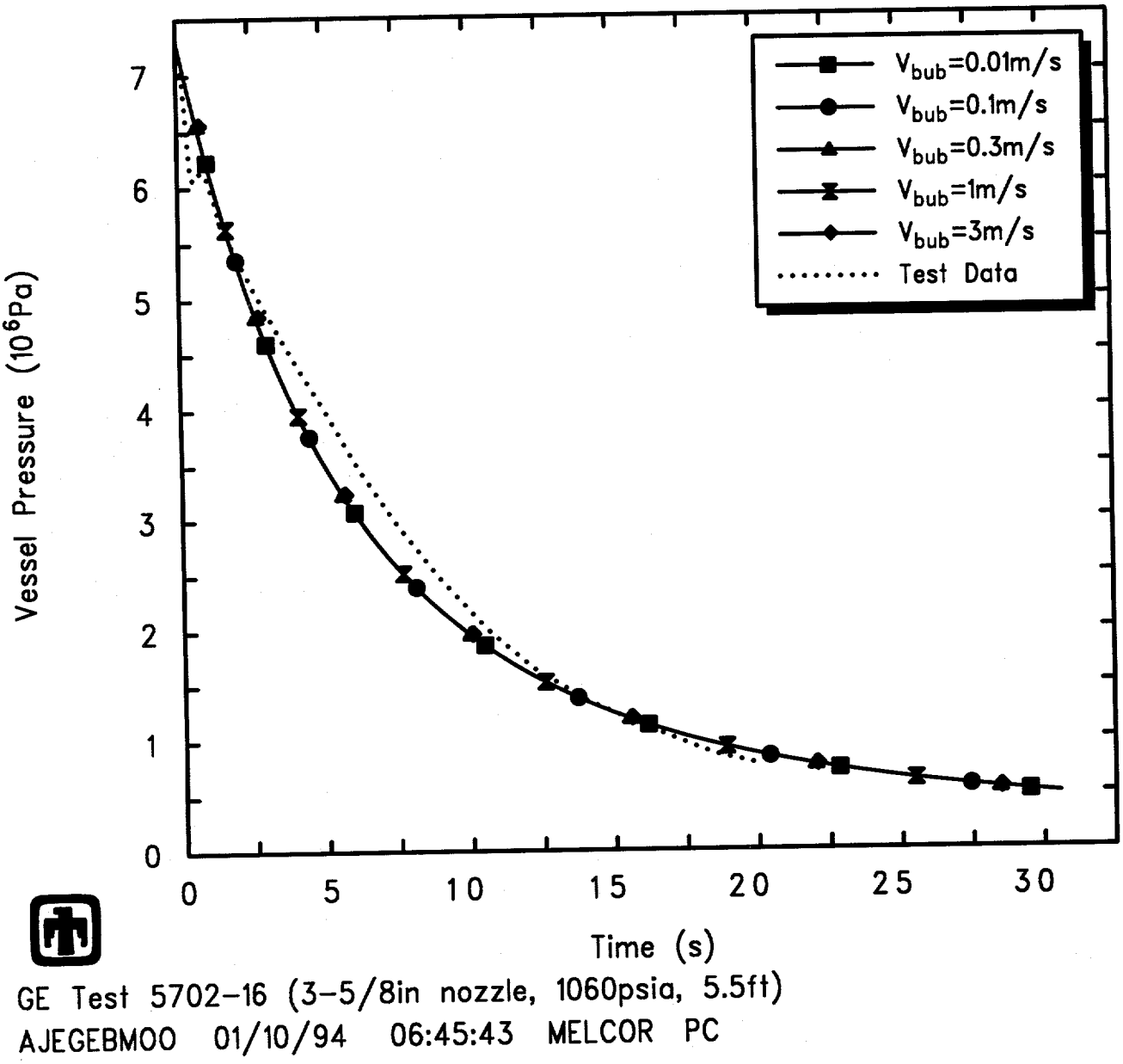

Figure 5.3.8. Vessel Pressure for GE Large Vessel Top Blowdown Test 5702-16 – Pool Bubble Rise Velocity Sensitivity Study

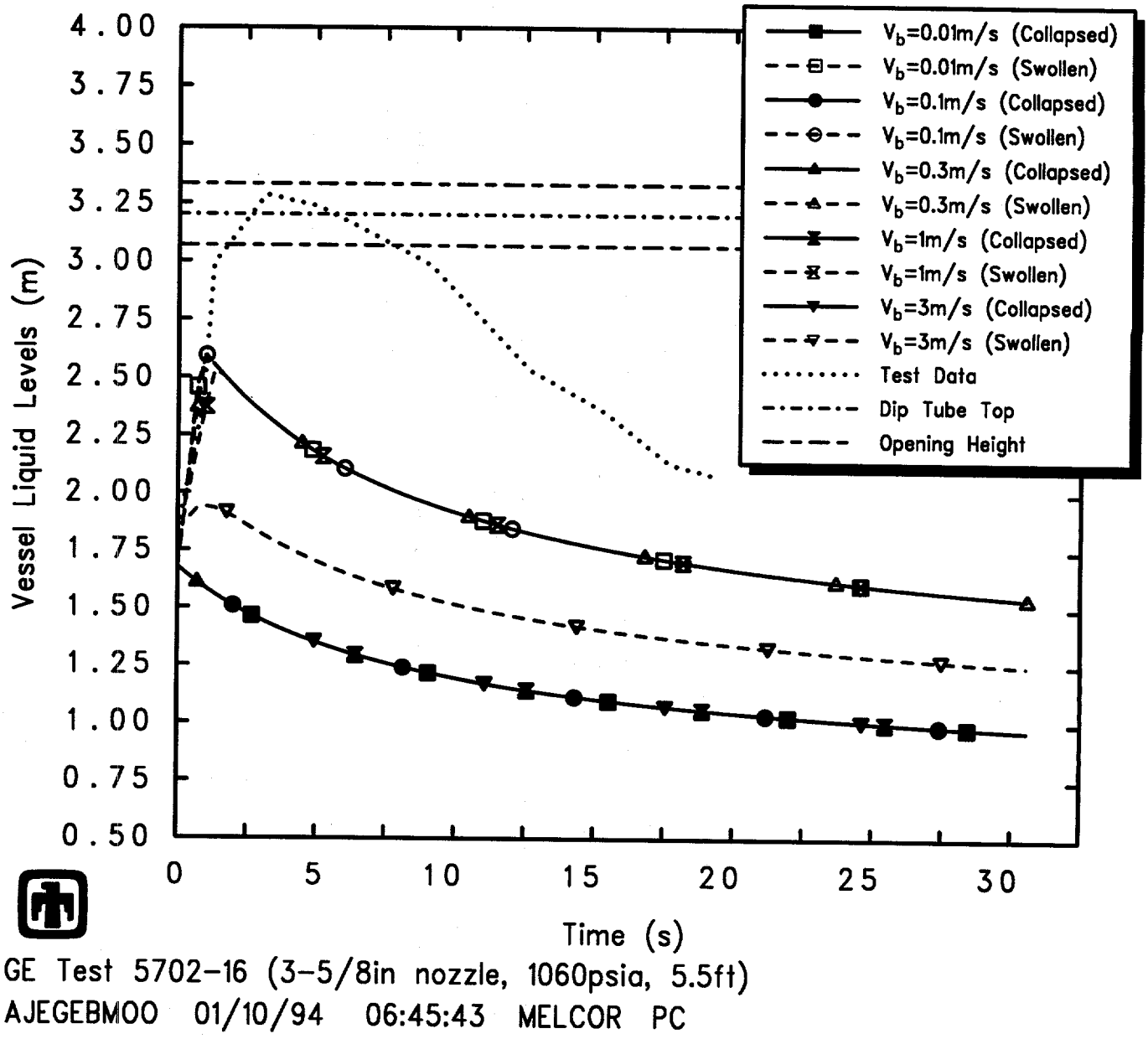

Figure 5.3.9. Vessel Liquid Levels for GE Large Vessel Top Blowdown Test 5702-16 – Pool Bubble Rise Velocity Sensitivity Study

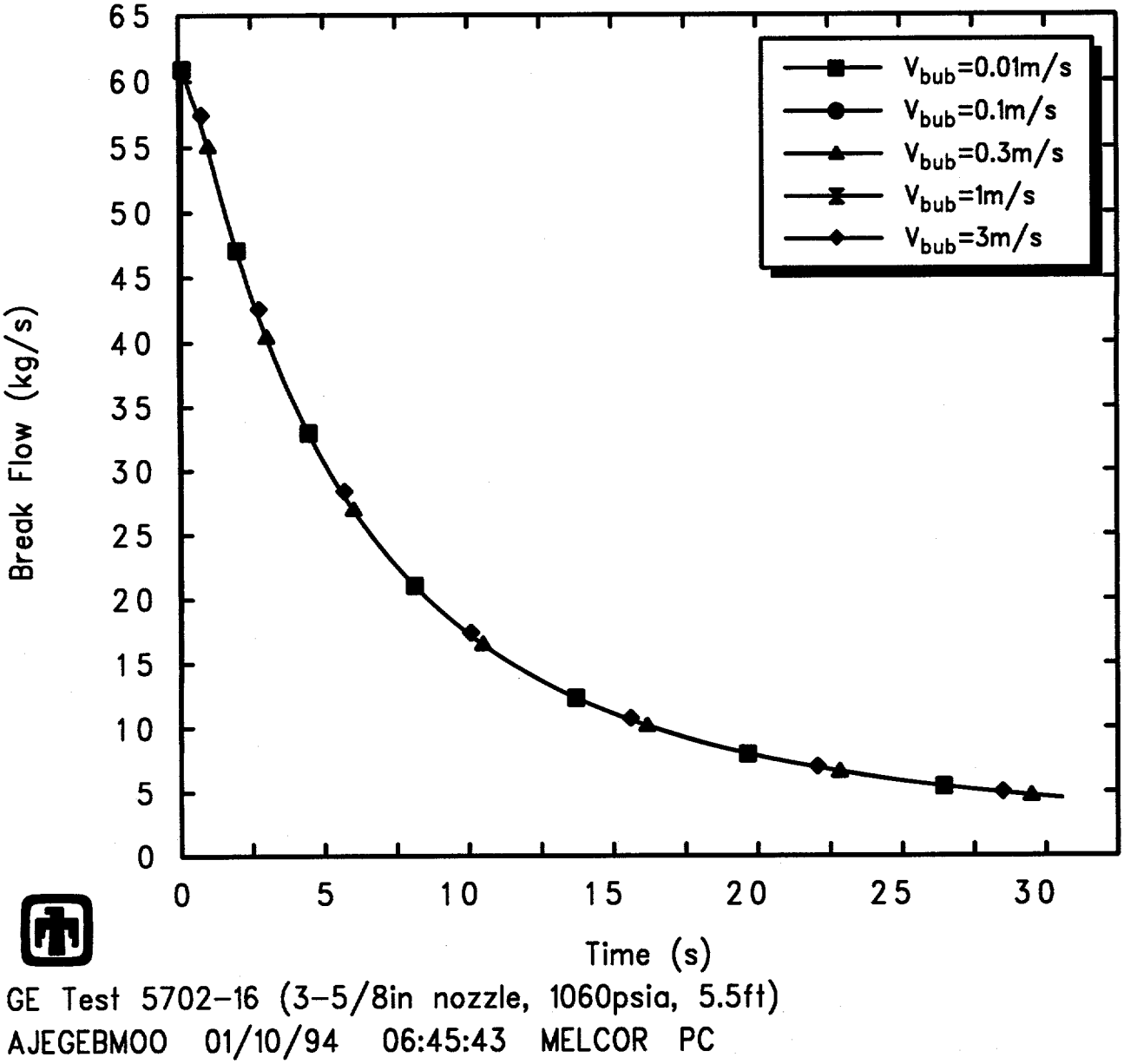

Figure 5.3.10. Blowdown Mass Flow for GE Large Vessel Top Blowdown Test 5702-16 – Pool Bubble Rise Velocity Sensitivity Study

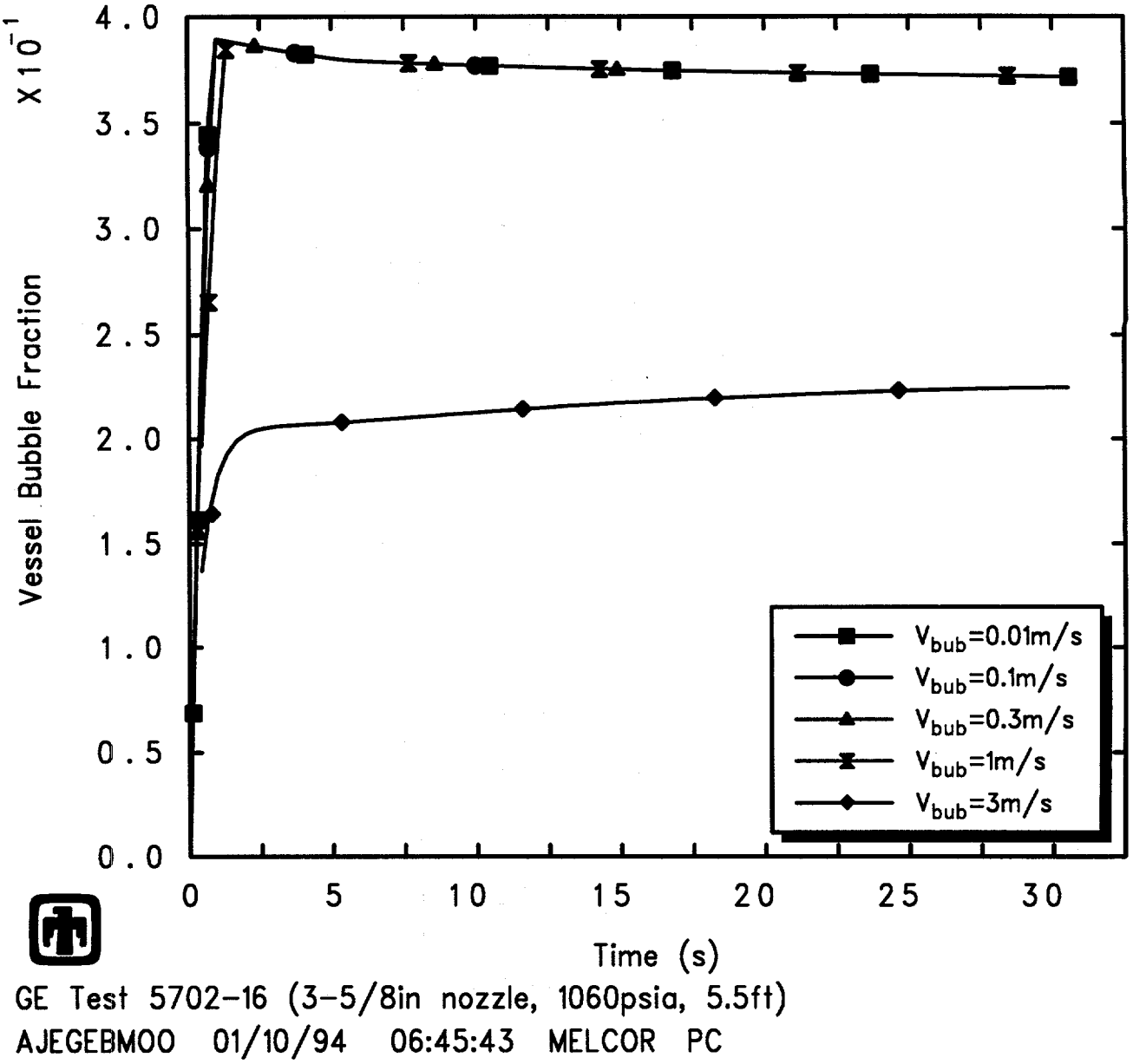

Figure 5.3.11. Vessel Two-Phase Liquid Bubble Fraction for GE Large Vessel Top Blowdown Test 5702-16 – Pool Bubble Rise Velocity Sensitivity Study

(two-phase) liquid levels predicted by MELCOR are depicted in Figure 5.3.13, while Figure 5.3.14 shows the break flow out the blowdown line and Venturi flow limiting nozzle causing the vessel depressurization, together with experimental data. Figure 5.3.15 presents the corresponding vessel pool bubble fractions.

Unlike the results for the top blowdown test analysis in this sensitivity study, there are visible changes in both vessel depressurization in Figure 5.3.12 and blowdown flow in Figure 5.3.14 as the bubble rise velocity is varied, because the time for the blowdown line to uncover and the transition in break flow from liquid to vapor varies. Decreasing the bubble rise velocity causes more apparent level swell, as shown in Figure 5.3.13 because the time to reach the maximum allowed pool bubble fraction is reduced, as indicated in Figure 5.3.15. The results with the default bubble rise velocity, 0.3m/s, appear to agree best with the measured two-phase level.

The effect of changing the pool bubble rise velocities for the bottom blowdown test 5803-2 (with a larger blowdown nozzle and higher initial liquid level than test 5803-1) is illustrated in Figures 5.3.16 through 5.3.19. Like the results for the other bottom blowdown test analysis in this sensitivity study, there are visible changes in both vessel depressurization in Figure 5.3.16 and blowdown flow in Figure 5.3.18 as the bubble rise velocity is varied, because the time for the blowdown line to uncover and the transition in break flow from liquid to vapor varies. Also as observed in the test 5803-1 analysis, decreasing the bubble rise velocity causes more apparent level swell, as shown in Figure 5.3.17 because the time to reach the maximum allowed pool bubble fraction is reduced, as indicated in Figure 5.3.19. However, for this test also the results with the default bubble rise velocity agree best with the measured two-phase level.

This set of sensitivity study calculations and the comparison to test data indicates that there is no obvious single value for the pool bubble rise velocity other than the current code default (0.3m/s) which provides improved agreement with measurement in all GE large vessel blowdown and level swell test analyses. Because no other single value was obviously better, we used the default pool bubble rise velocity of 0.3m/s in all other MELCOR analyses done as part of this assessment study.

5.4 Noding Resolution

The basecase MELCOR input model for these GE large vessel blowdown and level swell experiments used a single control volume for the test vessel. This is standard modelling in MELCOR, where multiple control volumes are used to subdivide regions only if there is some obvious change in geometry or flow pattern. Unlike best-estimate codes such as TRAC or RELAP, MELCOR does not necessarily give better results if components or volumes are subdivided; most MELCOR models assume large, lumped component volumes.

A sensitivity study was done in which the single vessel control volume was subdivided into a stack of control volumes, 11 for the cylindrical section, each 0.3048m (1ft) high, and one each for the hemispherical ends, as illustrated in Figure 3.2 for a bottom

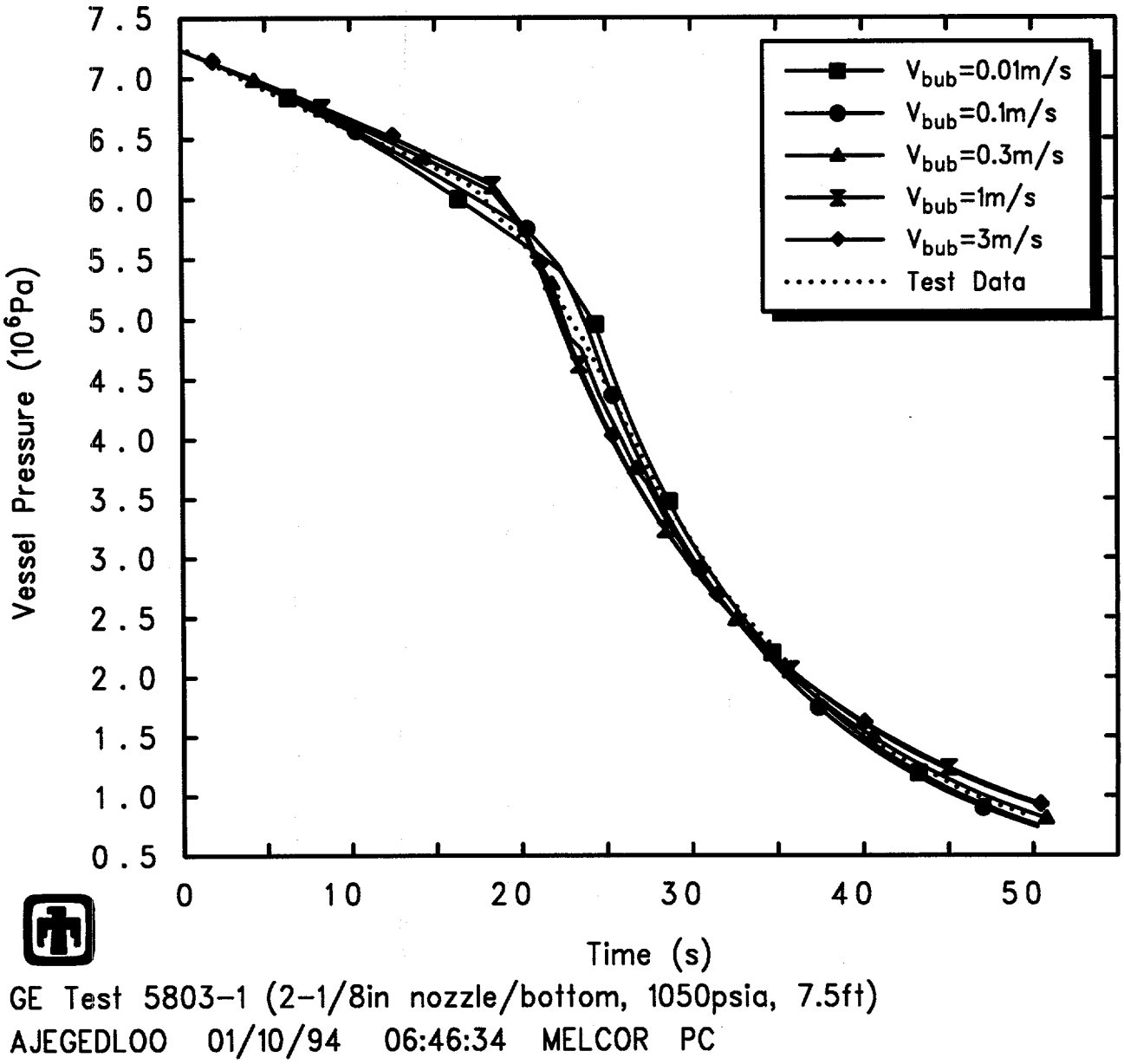

Figure 5.3.12. Vessel Pressure for GE Large Vessel Bottom Blowdown Test 5803-1 – Pool Bubble Rise Velocity Sensitivity Study

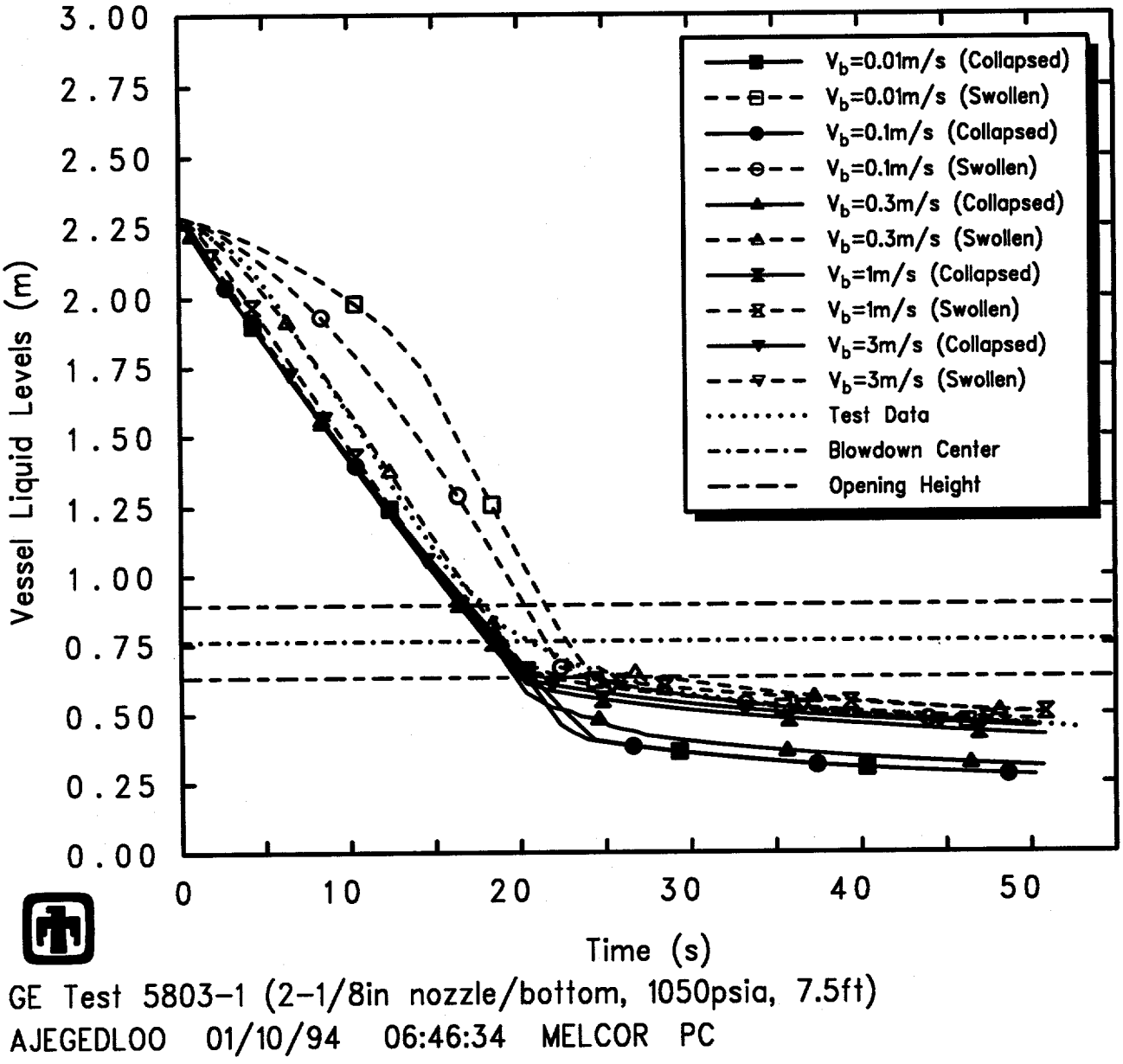

Figure 5.3.13. Vessel Liquid Levels for GE Large Vessel Bottom Blowdown Test 5803-1 – Pool Bubble Rise Velocity Sensitivity Study

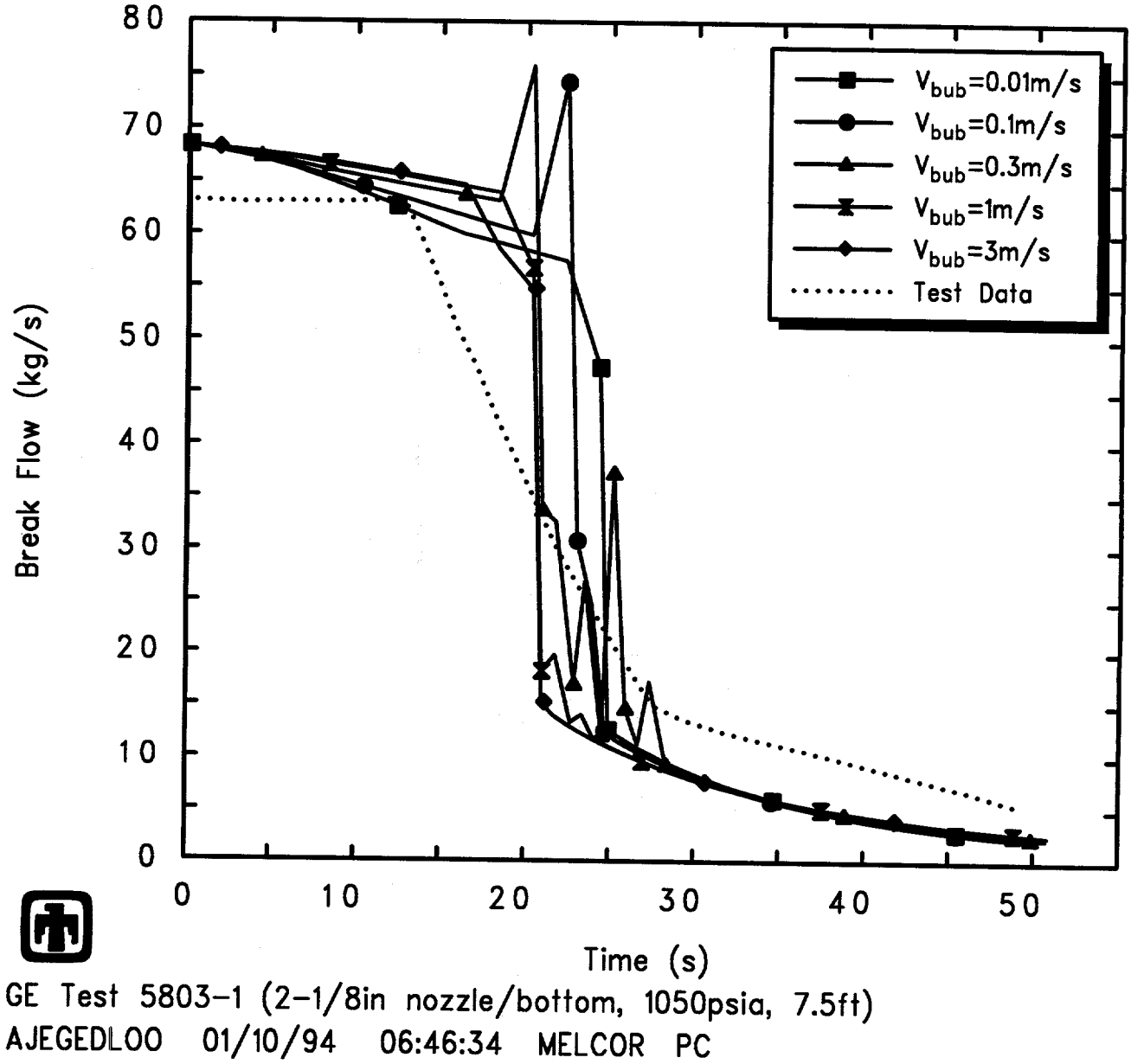

Figure 5.3.14. Blowdown Mass Flow for GE Large Vessel Bottom Blowdown Test 5803-1 – Pool Bubble Rise Velocity Sensitivity Study

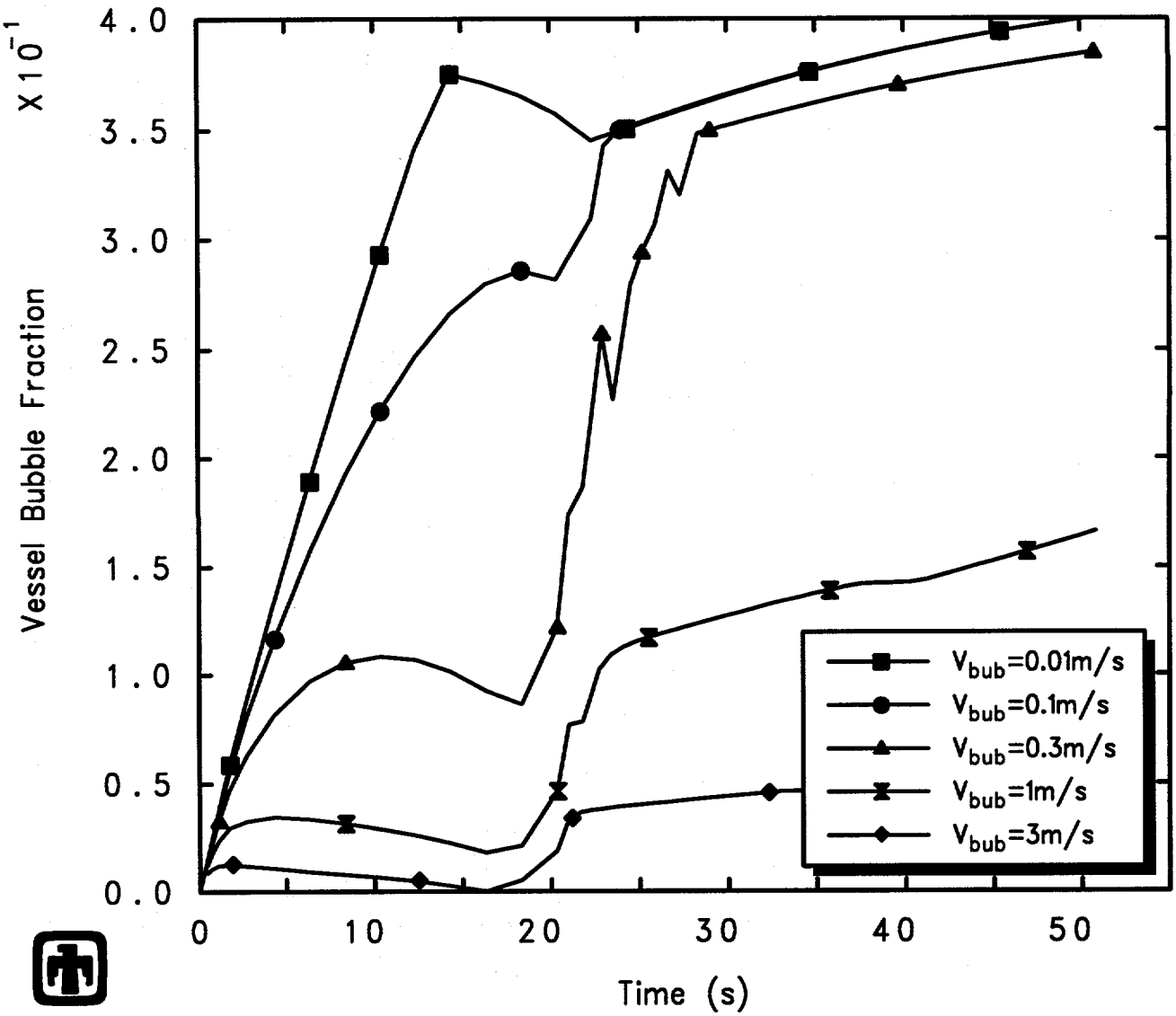

Figure 5.3.15. Vessel Two-Phase Liquid Level Bubble Fraction for GE Large Vessel Bottom Blowdown Test 5803-1 – Pool Bubble Rise Velocity Sensitivity Study

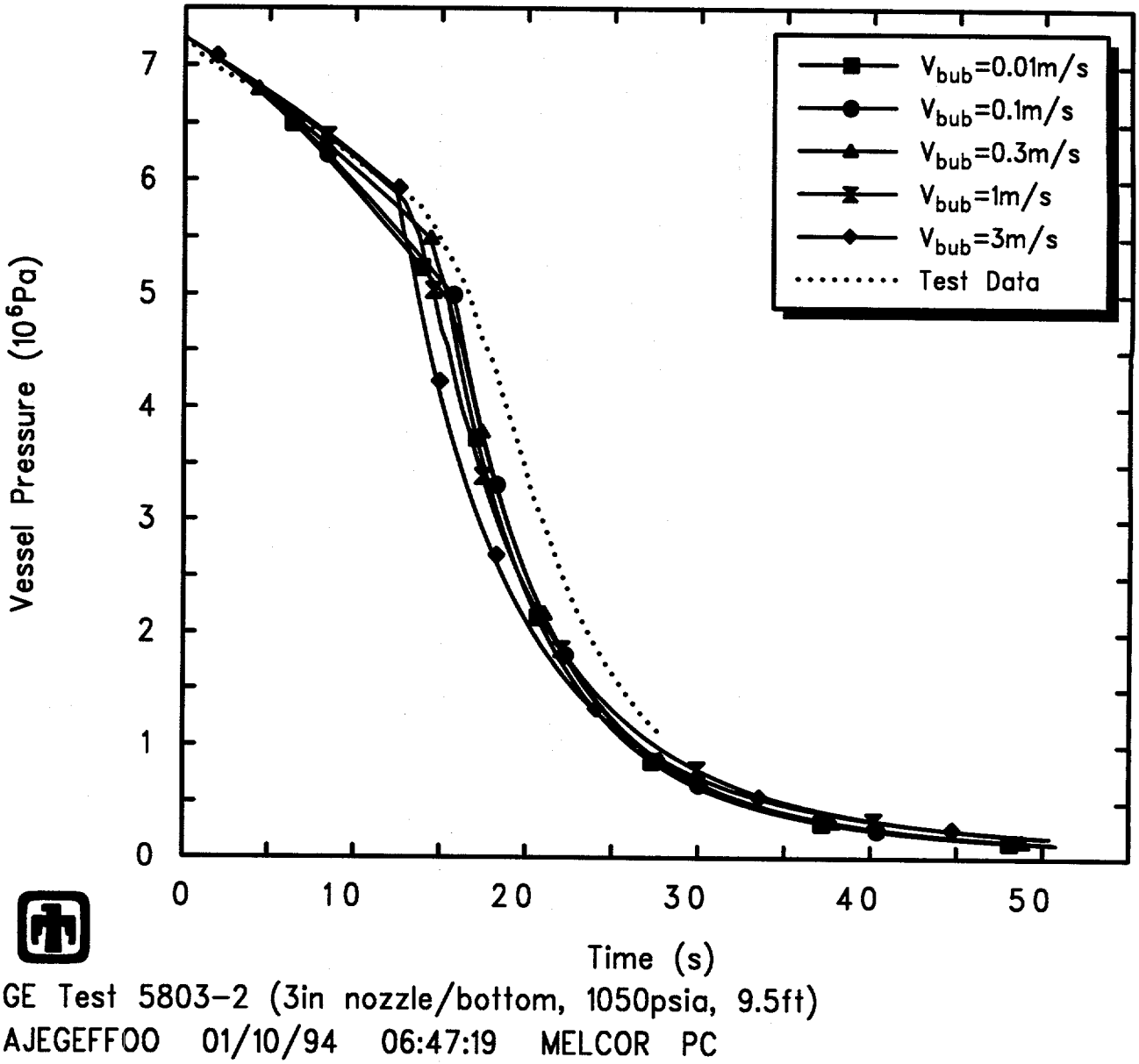

Figure 5.3.16. Vessel Pressure for GE Large Vessel Bottom Blowdown Test 5803-2 – Pool Bubble Rise Velocity Sensitivity Study

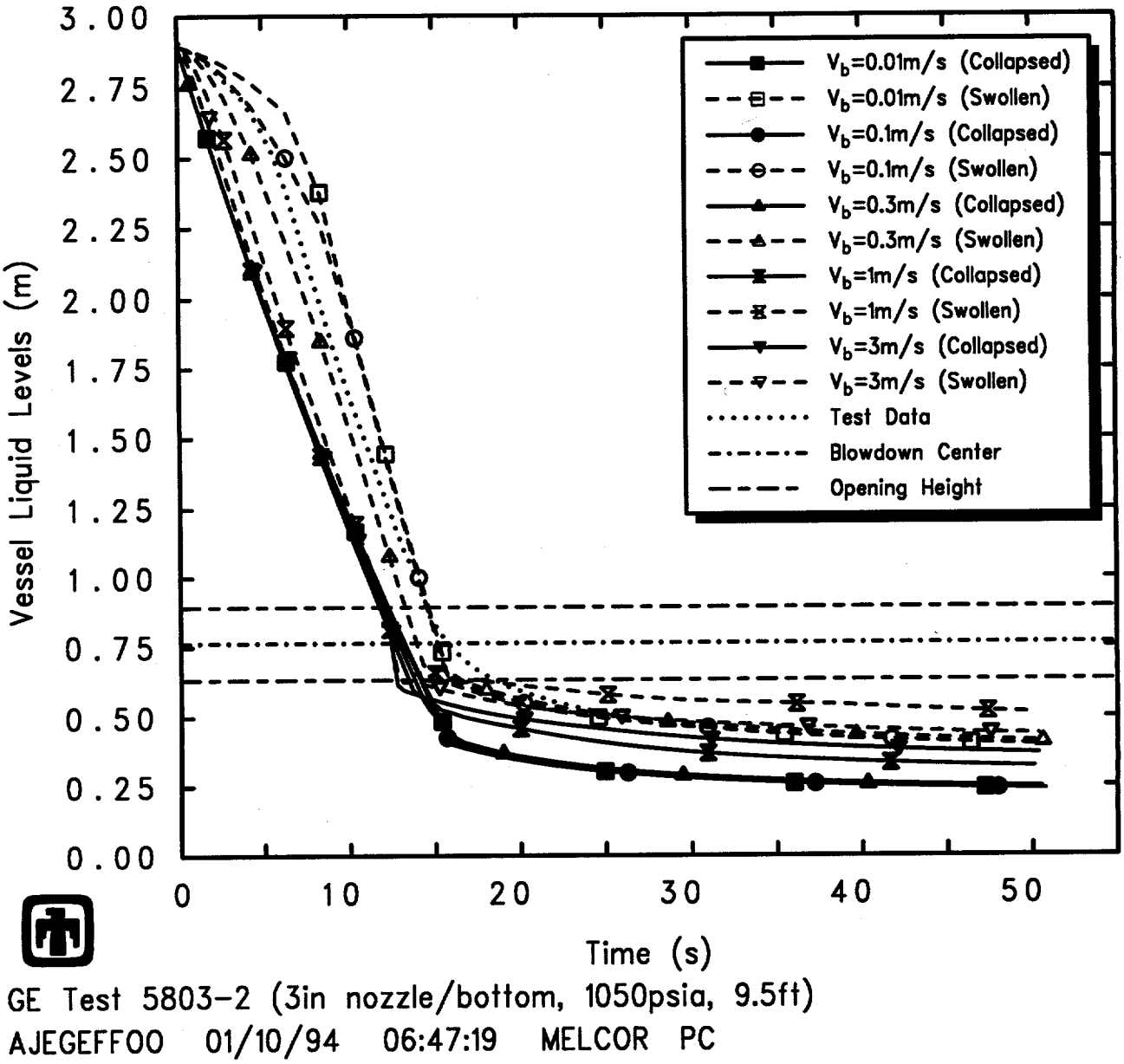

Figure 5.3.17. Vessel Liquid Levels for GE Large Vessel Bottom Blowdown Test 5803-2 – Pool Bubble Rise Velocity Sensitivity Study

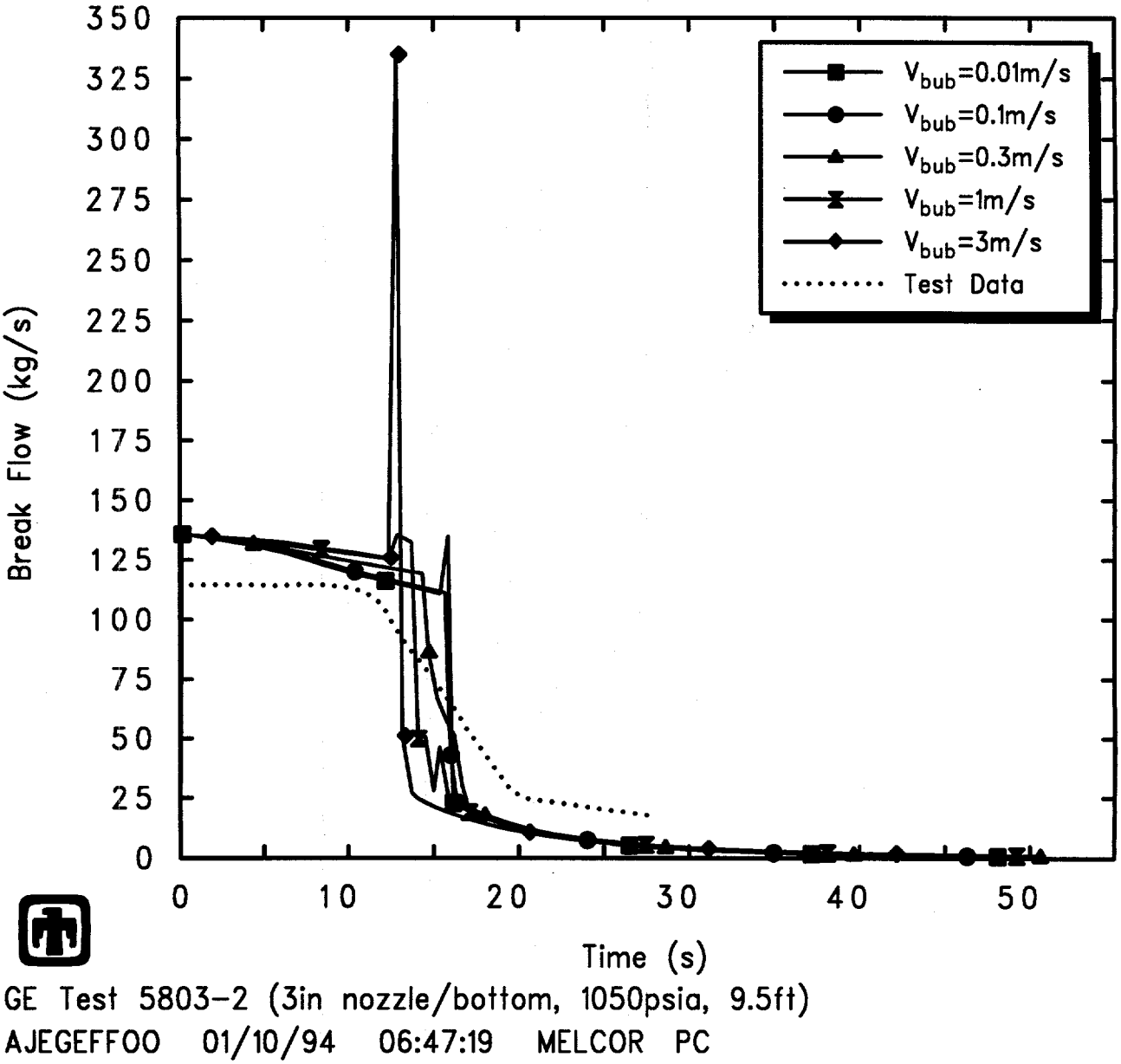

Figure 5.3.18. Blowdown Mass Flow for GE Large Vessel Bottom Blowdown Test 5803-2 – Pool Bubble Rise Velocity Sensitivity Study

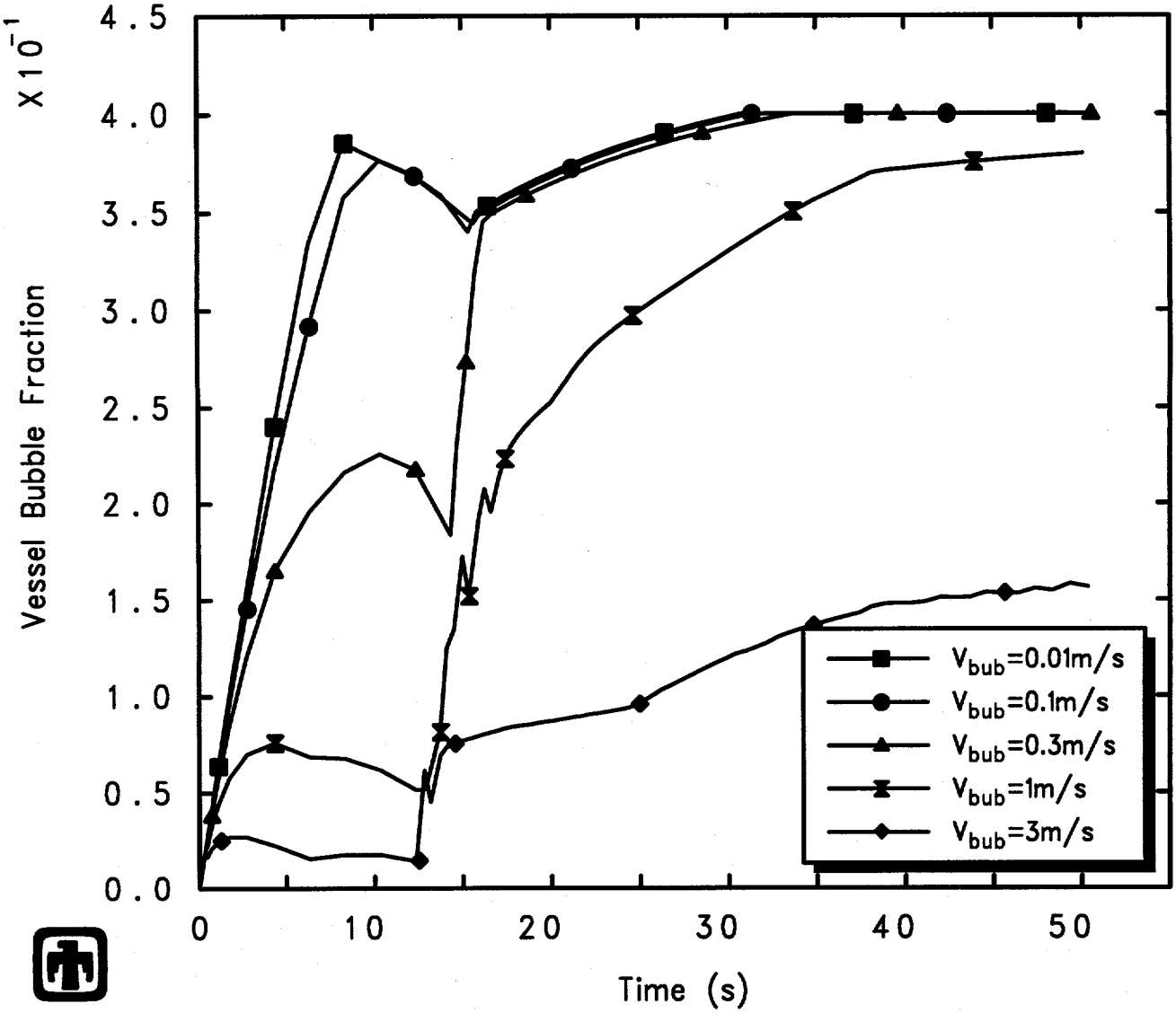

Figure 5.3.19. Vessel Two-Phase Liquid Level Bubble Fraction for GE Large Vessel Bottom Blowdown Test 5803-2 – Pool Bubble Rise Velocity Sensitivity Study

blowdown experiment configuration. Vertical flow paths were added as needed to connect the stacked volumes, with flow areas equal to the vessel cylinder area, and lengths set to 0.3048m (1ft). The heat structure modelling the vessel cylinder was subdivided correspondingly, also. This is a noding more typical of TRAC and/or RELAP than for MELCOR analyses. Since there is no obvious geometrically "correct" value for junction opening heights in flow paths connecting such a stack of volumes in MELCOR, both large (1ft) and small (1cm) junction opening heights were tried.

The vessel pressures predicted by MELCOR using the 1-volume basecase noding and the 13-volume finer noding (with the large junction opening heights) are compared with each other and with test data in Figure 5.4.1, for the top blowdown experiment 5801-13; Figure 5.4.2 compares the corresponding calculated break flows. The pressure histories predicted by MELCOR using either noding for this top blowdown test appear identical, while small differences are found in the break flows predicted by MELCOR using either noding.

Figure 5.4.3 gives the swollen and collapsed liquid levels in the vessel control volumes predicted by MELCOR using the 1-volume basecase noding and the 13-volume finer noding (with the large junction opening heights) for the top blowdown test 5801-13, together with the blowdown tube entrance centerline and opening elevations and test data on the two-phase mixture level; dotted lines show the division between volumes in the finer noding, for reference. The corresponding vessel pool bubble fractions are presented in Figure 5.4.4.

The calculation for test 5801-13 with subdivided, stacked volumes shows voiding and swelling in all volumes below ~2.5m, with a "layer-cake" of alternating liquid and vapor regions. All volumes in the finer noding model remain at saturation, with no stratification or subcooling visible. Volumes below the initial pool level (1.6764m) show a sustained drop in both collapsed and swollen levels from blowdown start, while a few volumes above the initial pool level (1.6764m) show an early-time increase in both collapsed and swollen levels followed by a gradual dropoff. The "top-most" swollen level in the finer noding analysis (*i.e.*, the swollen level in the uppermost volume containing some liquid) remains below the swollen level in the single vessel volume in the basecase calculation, and the results for two-phase level calculated using the single-volume basecase noding are in better quantitative agreement with test data in this top blowdown experiment analyze, even though the exact degree of level swelling is underpredicted due to limiting by the maximum allowed pool bubble fraction of 40%. Unlike the single volume basecase analysis, the finer noding calculation with subdivided, stacked volumes predicts pool bubble fractions substantially below the maximum allowed pool bubble fraction value in all volumes containing liquid, with the largest pool bubble fraction in the lowest control volume and progressively smaller pool bubble fractions going up the stack of volumes. Physically, we would expect the opposite behavior – the smallest pool bubble fraction in the lowest control volume and progressively increasing pool bubble fractions with increasing elevation.

There are no significant differences in vessel depressurization or break flow in the calculations for test 5801-13 using the finer noding with large or with small junction

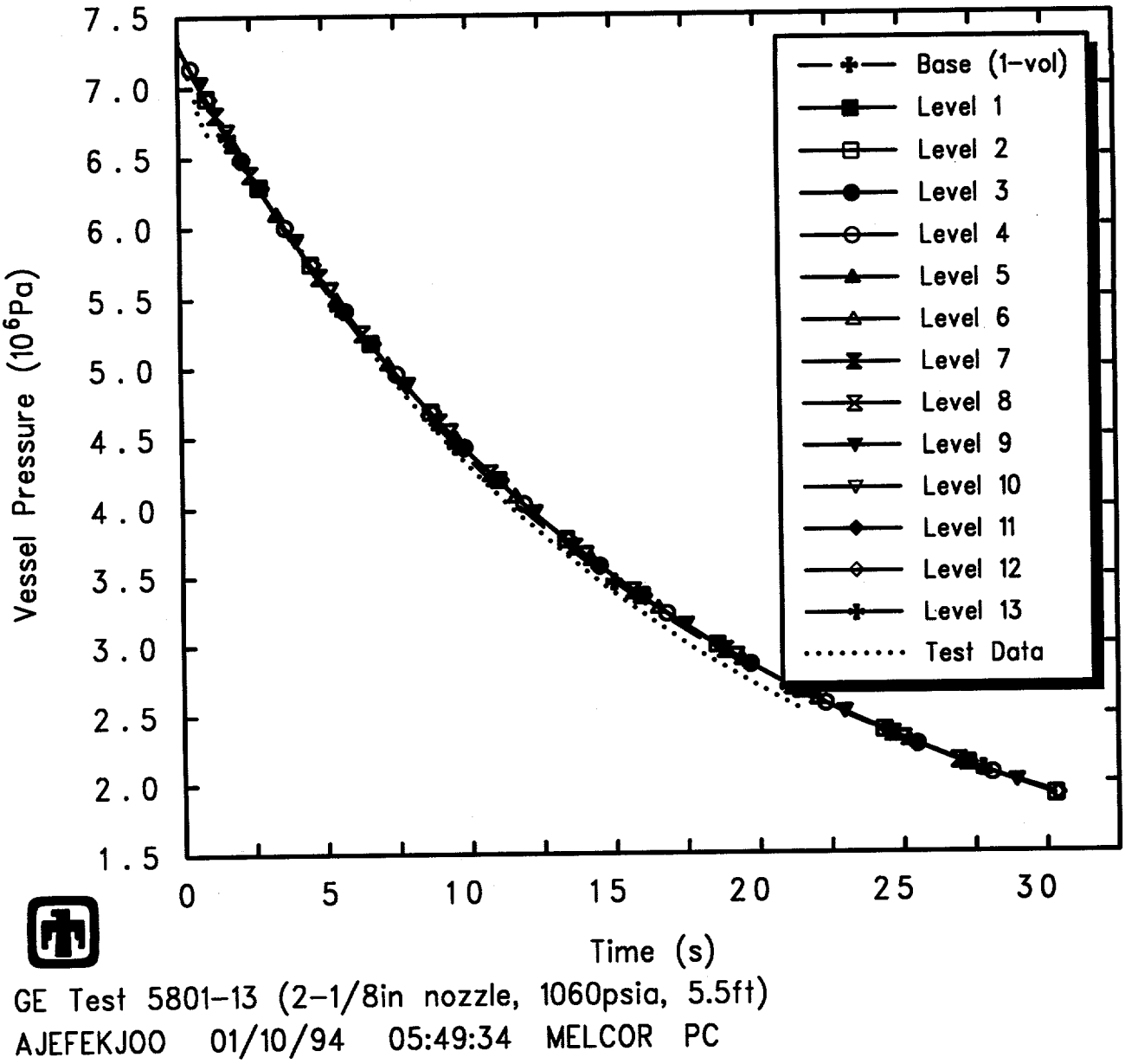

Figure 5.4.1. Vessel Pressure for GE Large Vessel Top Blowdown Test 5801-13 – Noding Resolution Sensitivity Study (with Large Junction Opening Heights in Finer Noding Model)

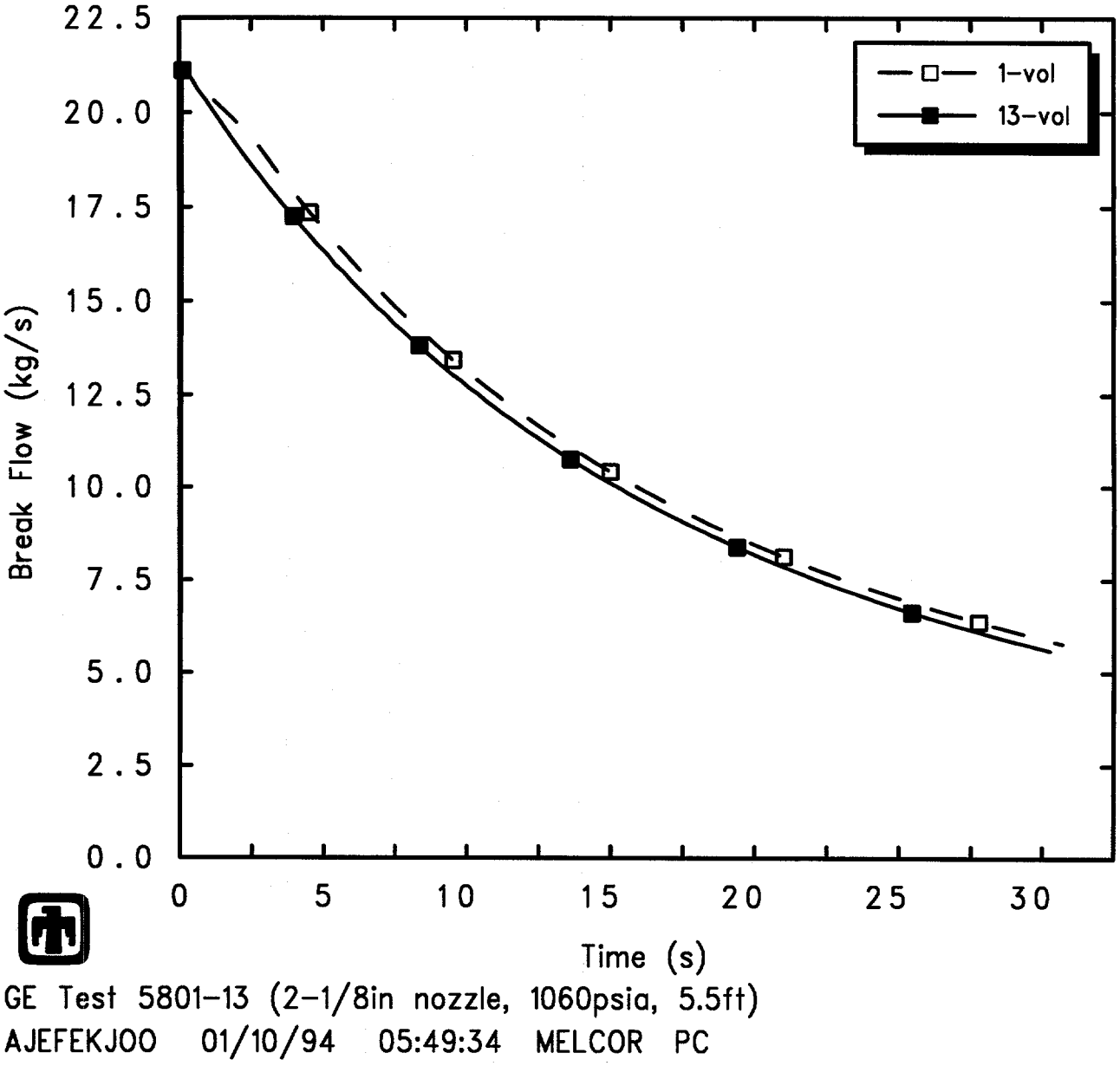

Figure 5.4.2. Blowdown Mass Flow for GE Large Vessel Top Blowdown 5801-13 – Noding Resolution Sensitivity Study (with Large Junction Opening Heights in Finer Noding Model)

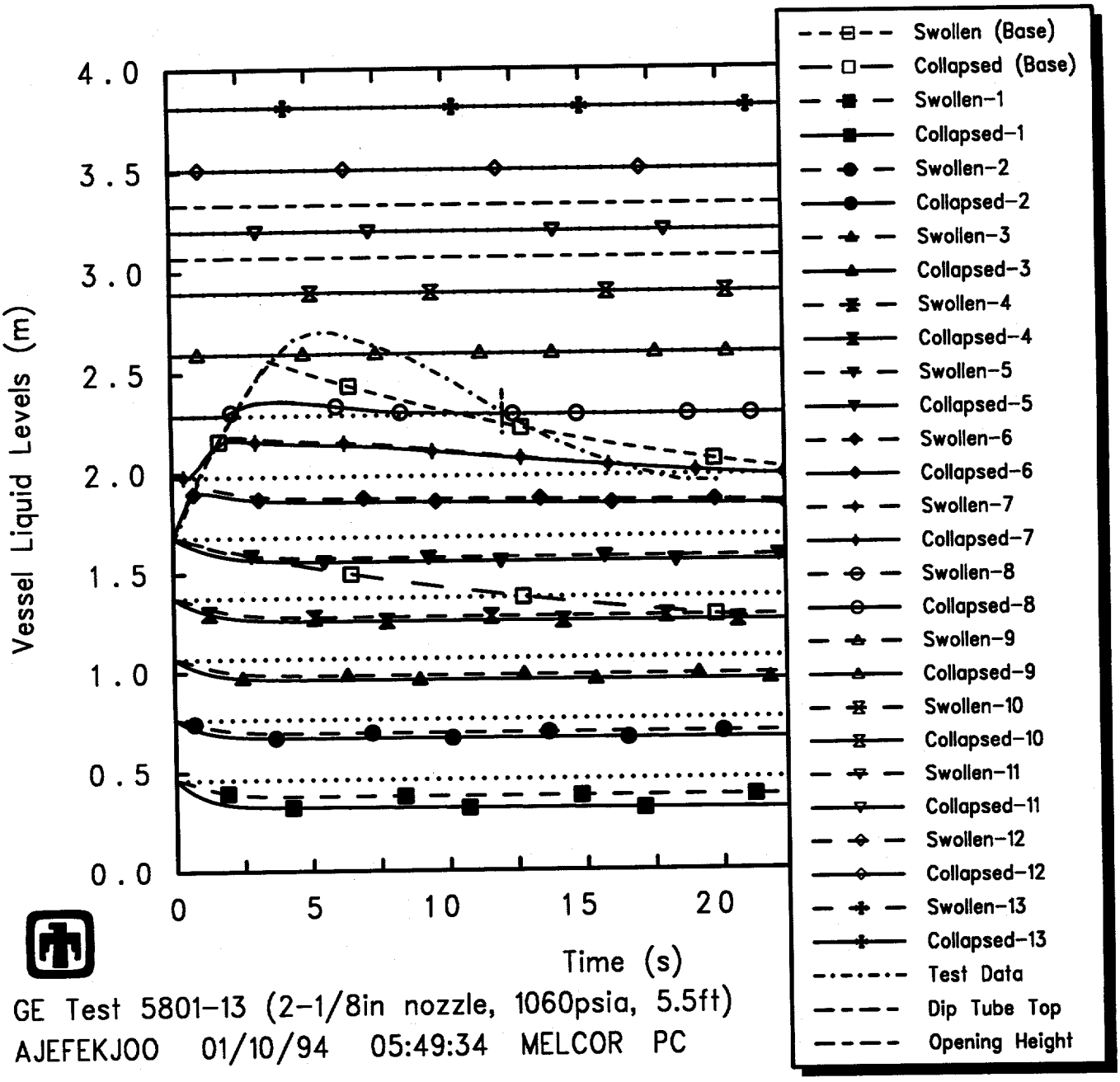

Figure 5.4.3. Vessel Liquid Levels for GE Large Vessel Top Blowdown Test 5801-13 – Noding Resolution Sensitivity Study (with Large Junction Opening Heights in Finer Noding Model)

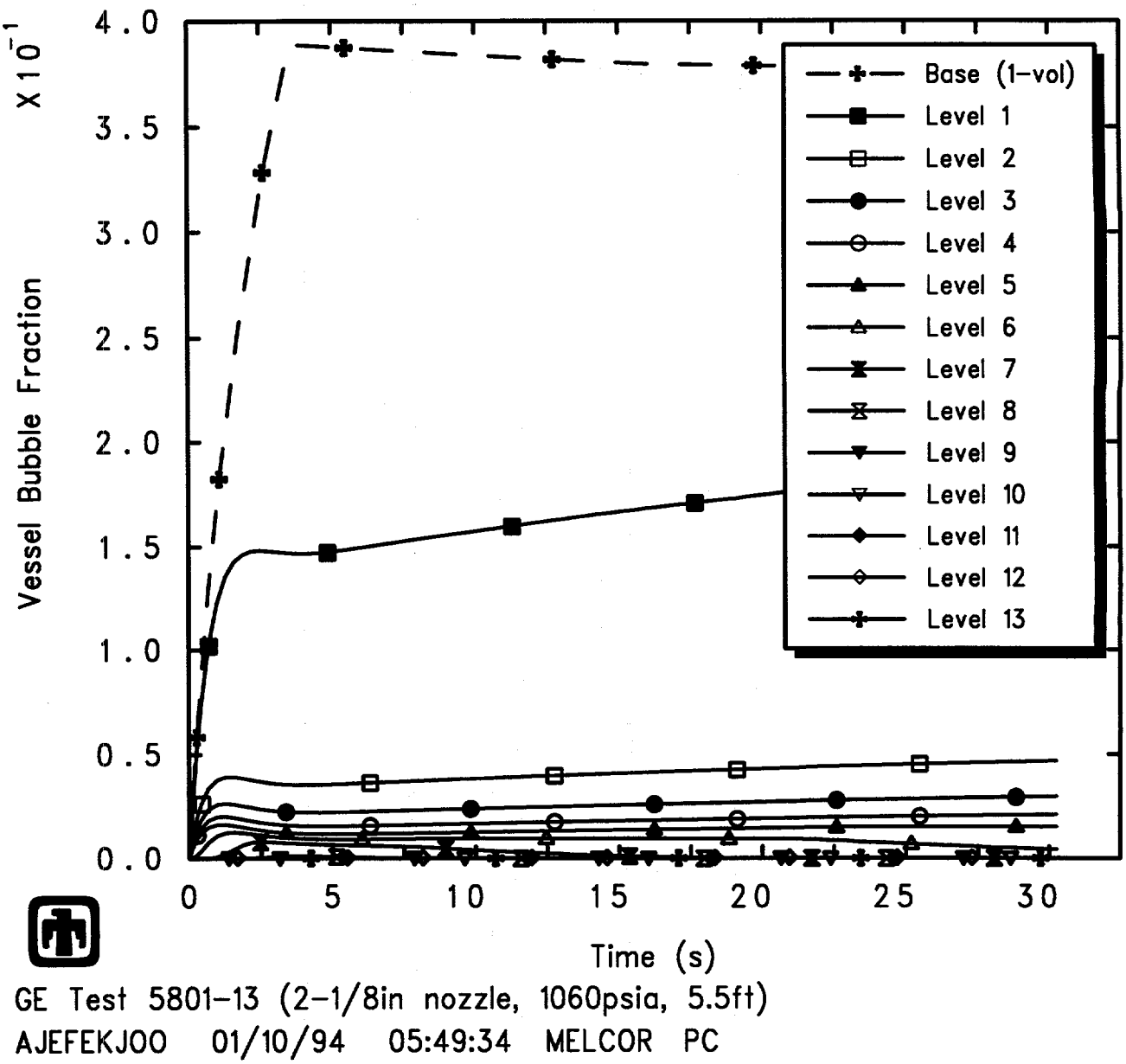

Figure 5.4.4. Vessel Two-Phase Liquid Bubble Fraction for GE Large Vessel Top Blowdown Test 5801-13 – Noding Resolution Sensitivity Study (with Large Junction Opening Heights in Finer Noding Model)

opening heights, as illustrated by comparing the results in Figures 5.4.1 and 5.4.2 with the corresponding results in Figures 5.4.5 and 5.4.6. There is, however, much less overall level swell in the calculation for test 5801-13 using the finer noding with small junction opening heights, as illustrated by comparing the results in Figure 5.4.7 with those given in Figure 5.4.3. Figure 5.4.8 also indicates lower bubble fractions in the mid-vessel control volumes (particularly in levels 6 and 7) in the calculation for test 5801-13 using the finer noding with small junction opening heights, as compared to corresponding results in the calculation using the finer noding with large junction opening heights, shown in Figure 5.4.4.

(The results and conclusions for the calculated pressures, break flows, vessel levels and pool bubble fractions in the other three top blowdown test analyses are very similar to the behavior noted for these test 5801-13 analyses, and are not shown here.)

Results calculated using these different vessel nodings for the bottom blowdown test 5803-1 are shown in Figures 5.4.9 through 5.4.12, in the case where large junction opening heights are used in the finer noding.

Figure 5.4.9 shows the vessel depressurization histories calculated by MELCOR, using the 1-volume basecase model and the 13-volume finer noding, compared to experimental data, and indicates a small difference in vessel depressurization histories predicted in the 1-volume basecase calculation and in the 13-volume finer noding analysis using large junction opening heights. Figure 5.4.10 shows the break flows out the blowdown line and Venturi flow limiting nozzle causing the vessel depressurization, calculated by MELCOR using these different noding schemes, together with test data; the break flow calculated using the finer noding is clearly smoother and less oscillatory than the blowdown flow calculated in the basecase calculation during the transition from liquid through two-phase to vapor blowdown in mid-transient.

The vessel collapsed and swollen (two-phase) liquid levels predicted by MELCOR using these different vessel nodings (for a finer noding using big junction opening heights), also compared to experimental data, are depicted in Figure 5.4.11, and the corresponding pool bubble fractions in the vessel volumes are illustrated in Figure 5.4.12. There are some minor differences visible in the overall level swell calculated by MELCOR using the 1-volume basecase model and the 13-volume finer noding, but these appear generally quite small. There is little or no voiding or level swell predicted in the bottom blowdown test configuration with either the basecase or the finer noding analyses. As in the top blowdown test analyses, using a finer noding consisting of subdivided, stacked control volumes yields smaller pool bubble fractions than using a single equivalent volume, with more level swell calculated in the lower vessel than in control volumes higher up.

There are no significant differences in vessel depressurization or break flow in the calculations for test 5803-1 using the finer noding with large or with small junction opening heights, as illustrated by comparing the results in Figures 5.4.9 and 5.4.10 with the corresponding results in Figures 5.4.13 and 5.4.14. There is, however, much more overall level swell in the calculation for test 5803-1 using the finer noding with small junction opening heights, as illustrated by comparing the results in Figure 5.4.15 with

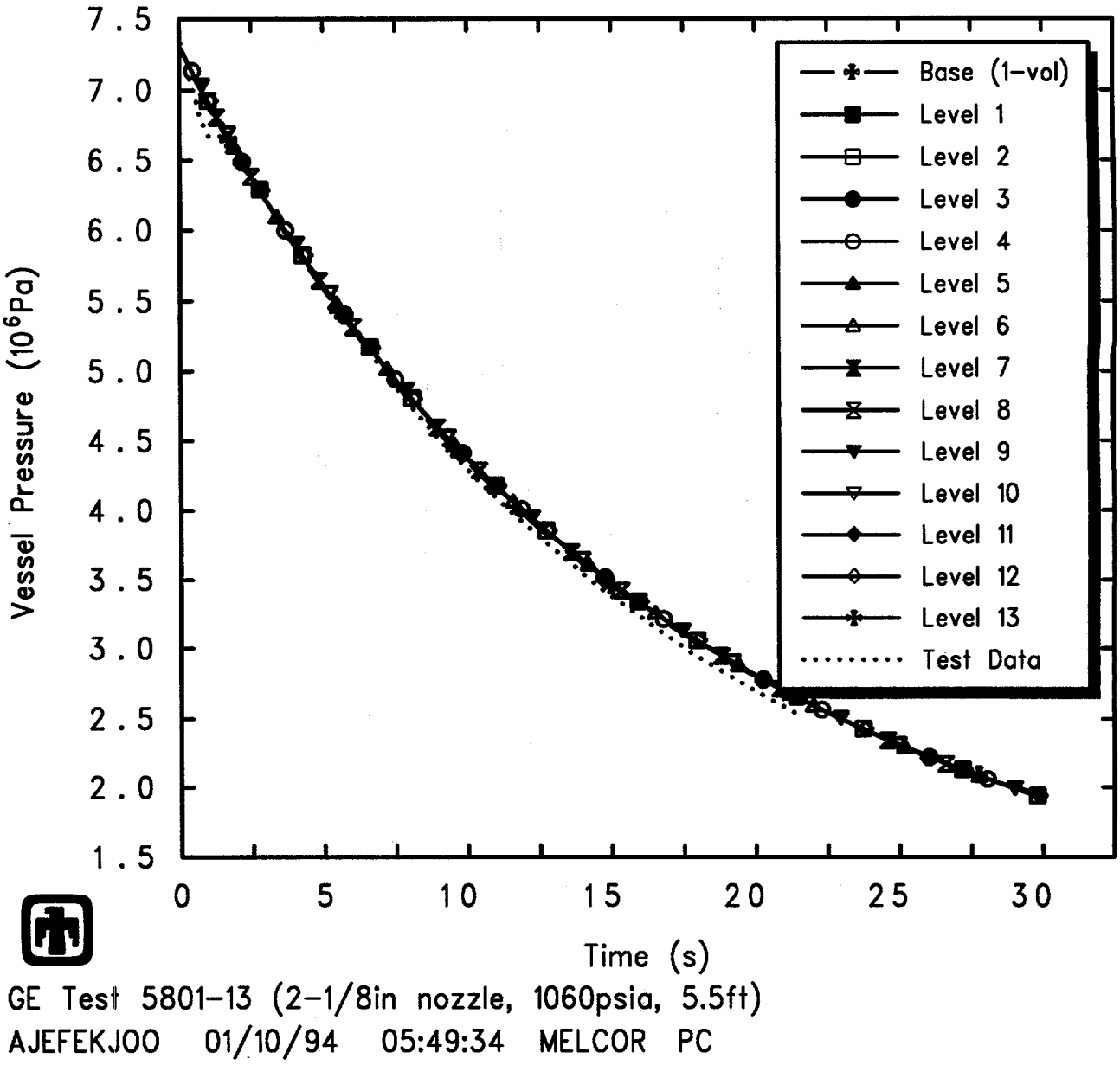

Figure 5.4.5. Vessel Pressure for GE Small Vessel Top Blowdown Test 5801-13 – Noding Resolution Sensitivity Study (with Small Junction Opening Heights in Finer Noding Model)

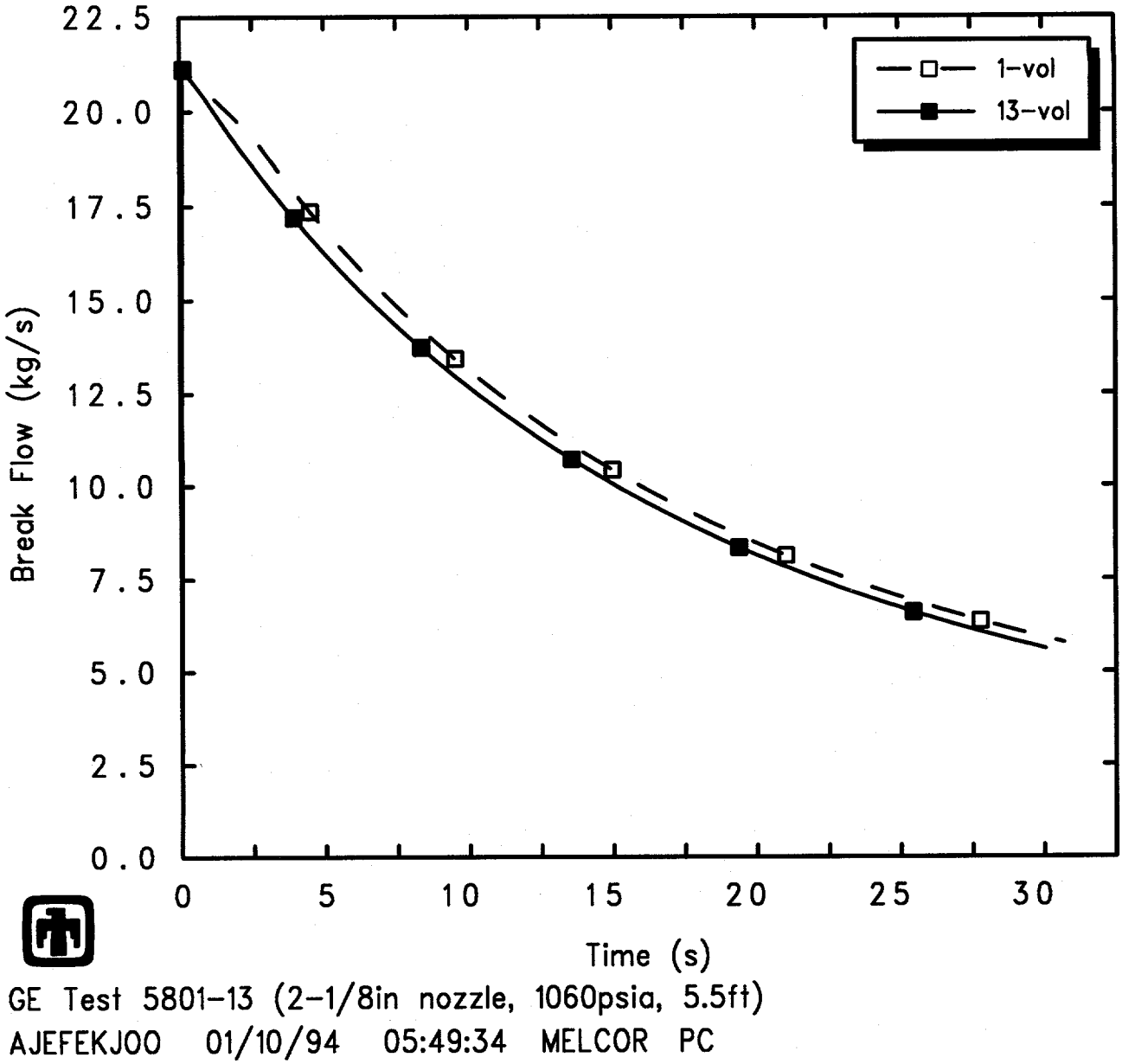

Figure 5.4.6. Blowdown Mass Flow for GE Small Vessel Top Blowdown Test 5801-13 – Noding Resolution Sensitivity Study (with Small Junction Opening Heights in Finer Noding Model)

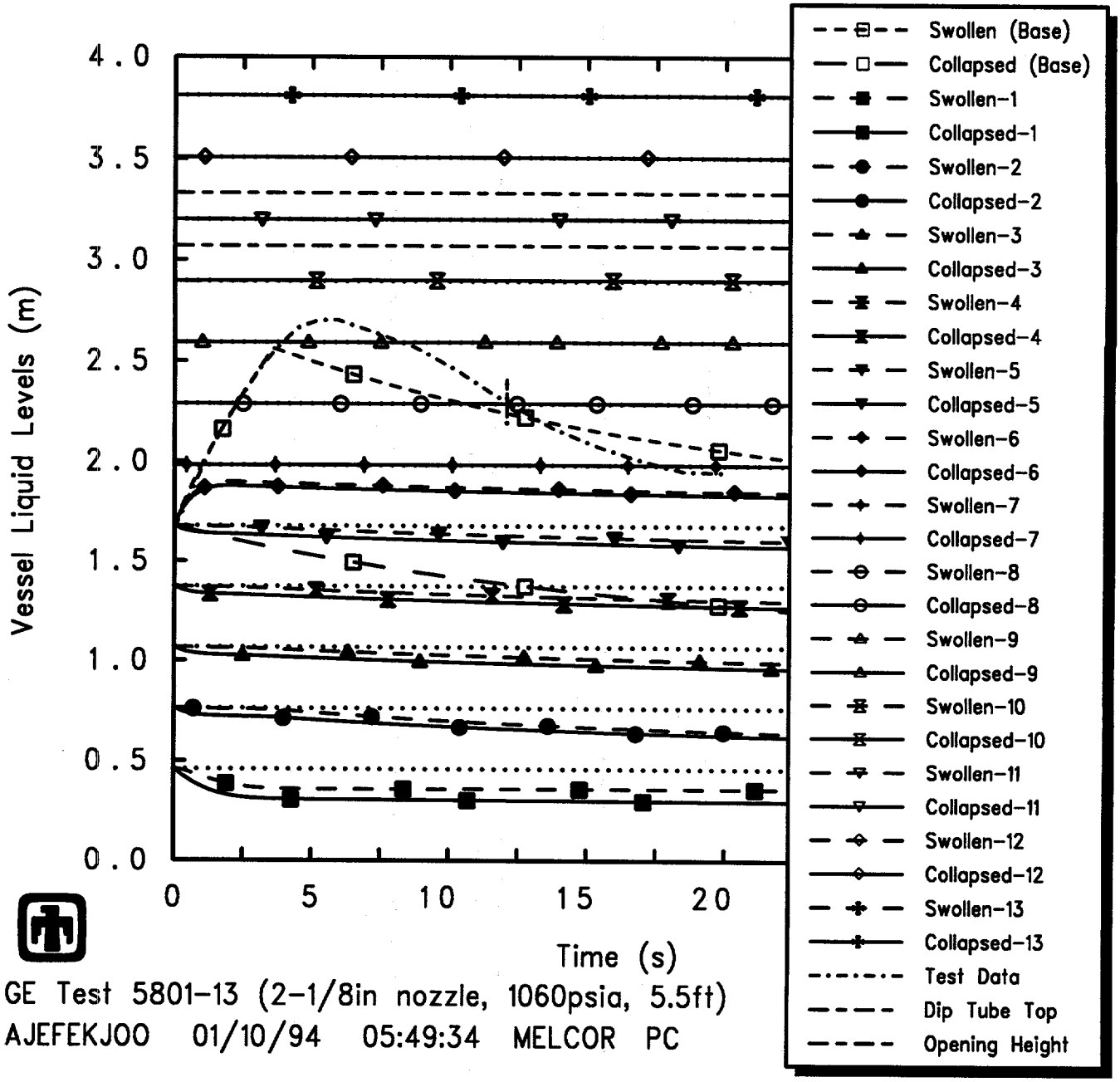

Figure 5.4.7. Vessel Liquid Levels for GE Small Vessel Top Blowdown Test 5801-13 – Noding Resolution Sensitivity Study (with Small Junction Opening Heights in Finer Noding Model)

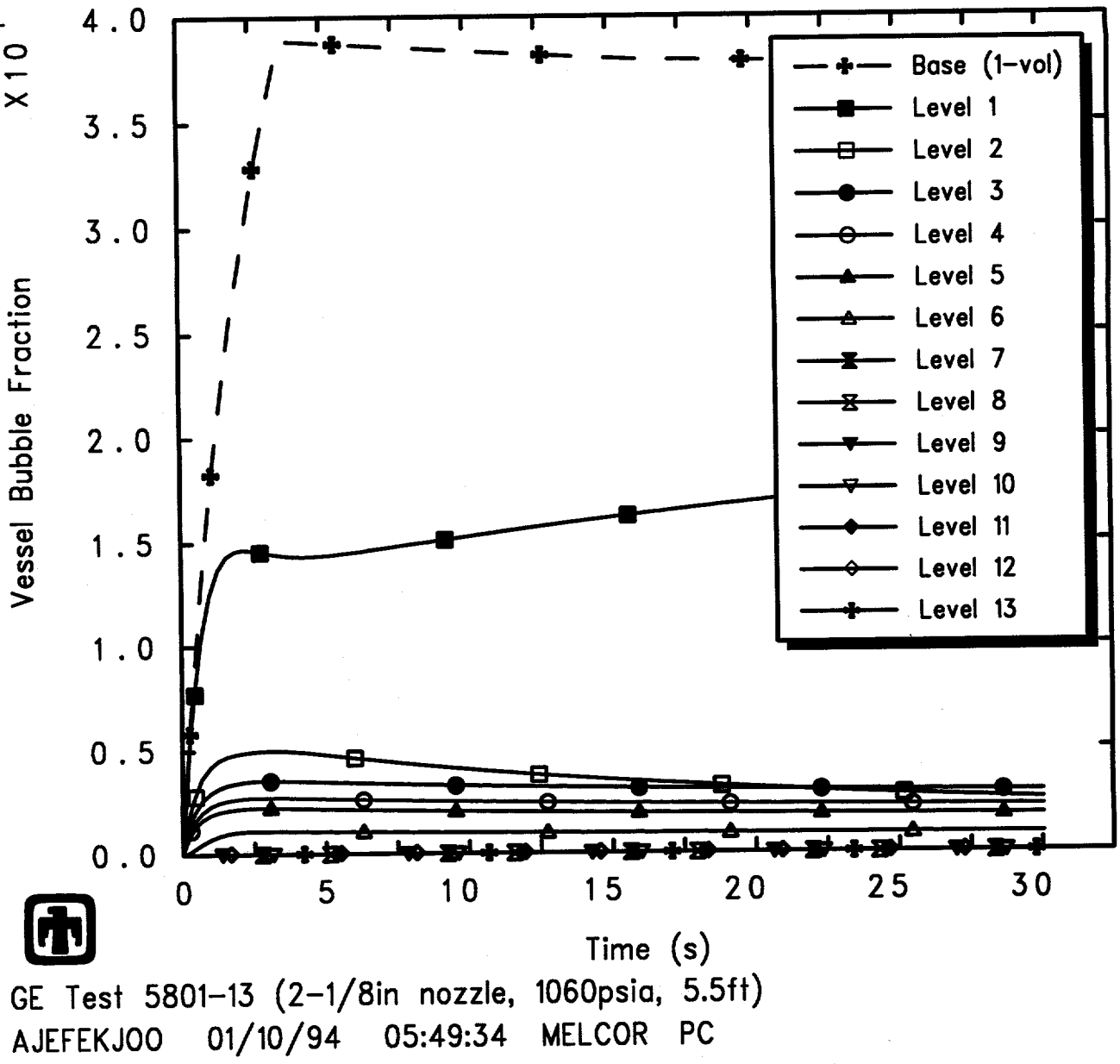

Figure 5.4.8. Vessel Two-Phase Liquid Bubble Fraction for GE Small Vessel Top Blowdown Test 5801-13 – Noding Resolution Sensitivity Study (with Small Junction Opening Heights in Finer Noding Model)

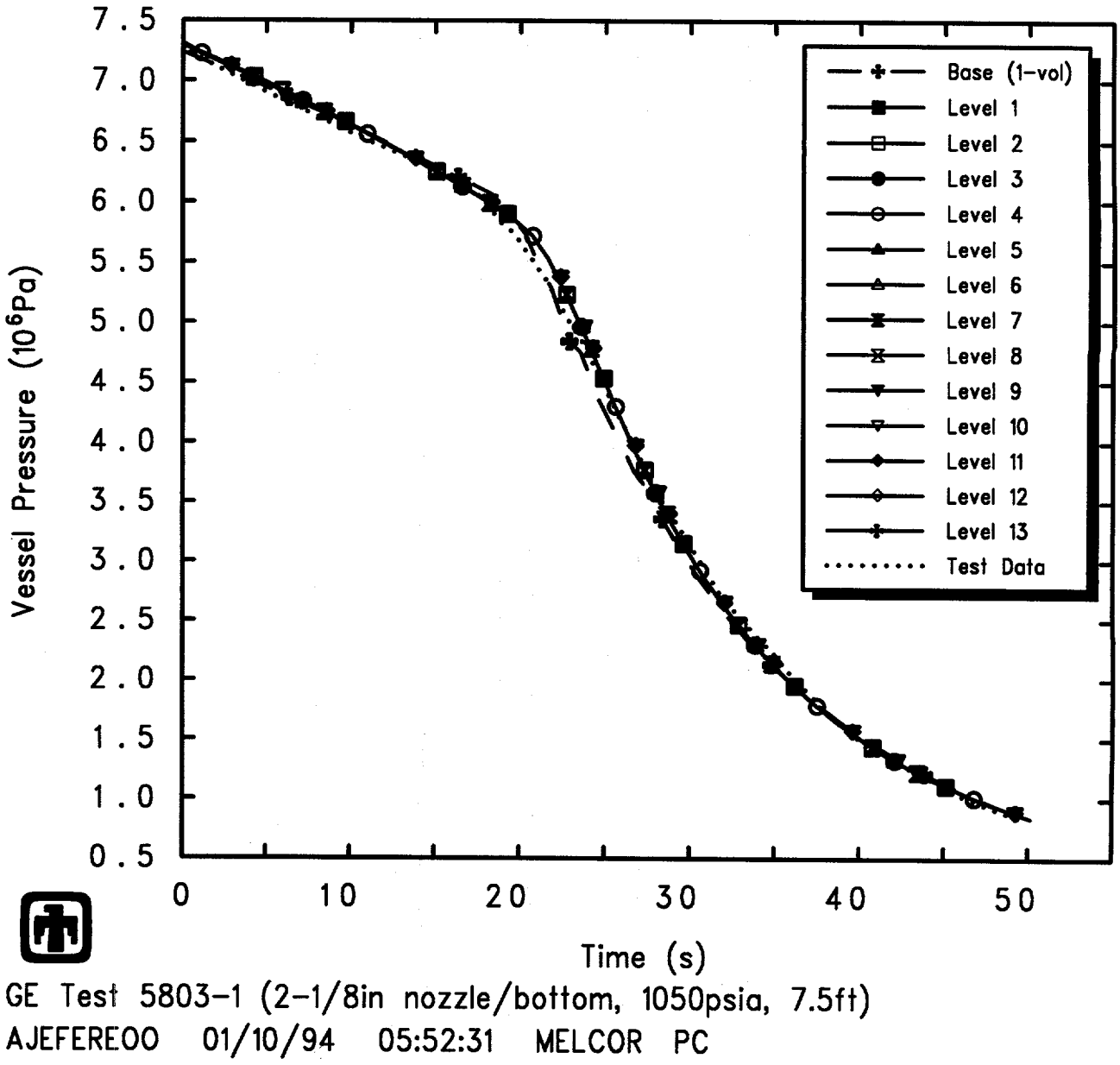

Figure 5.4.9. Vessel Pressure for GE Large Vessel Bottom Blowdown Test 5803-1 – Noding Resolution Sensitivity Study (with Large Junction Opening Heights in Finer Noding Model)

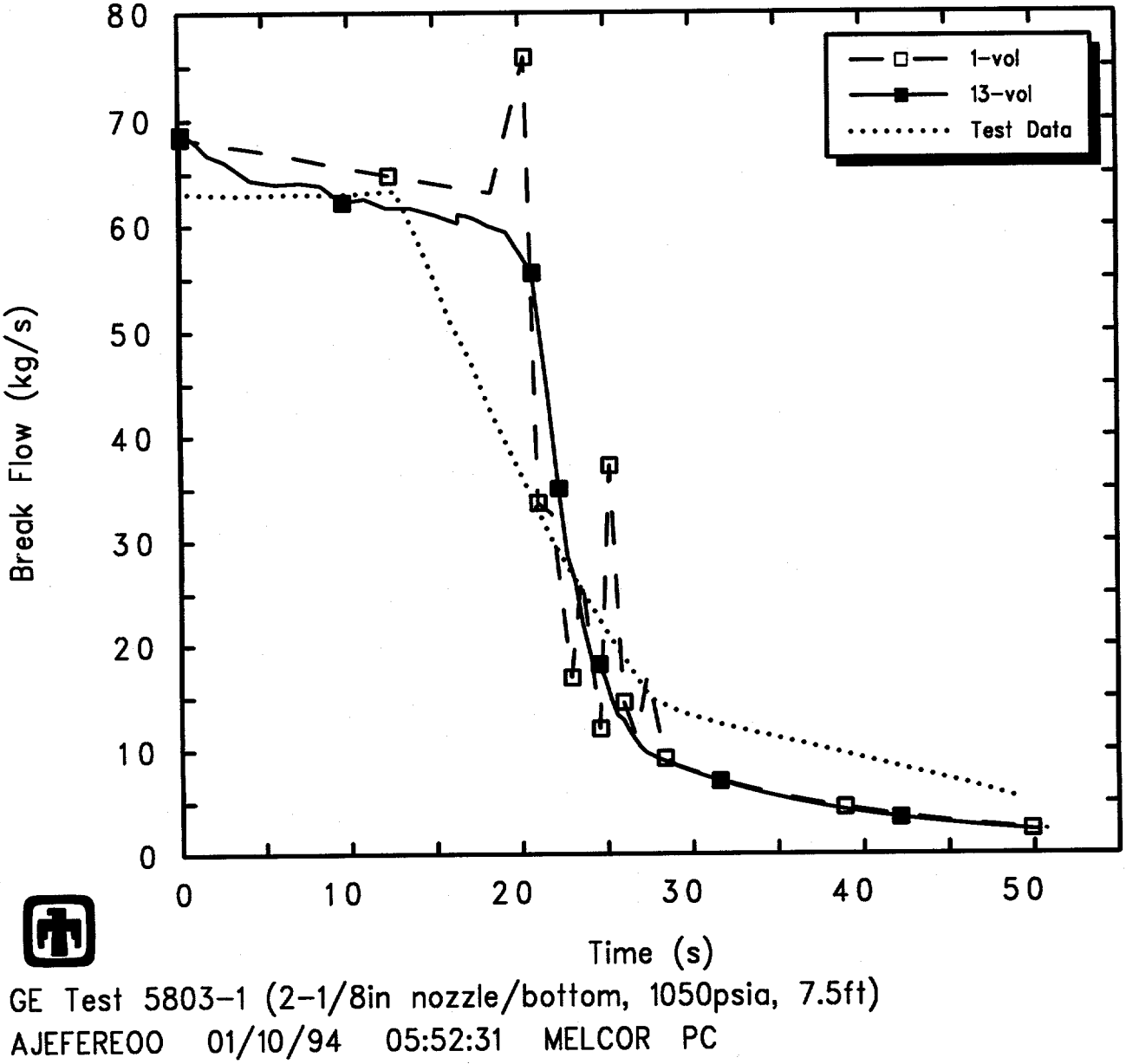

Figure 5.4.10. Blowdown Mass Flow for GE Large Vessel Bottom Blowdown Test 5803-1 – Noding Resolution Sensitivity Study (with Large Junction Opening Heights in Finer Noding Model)

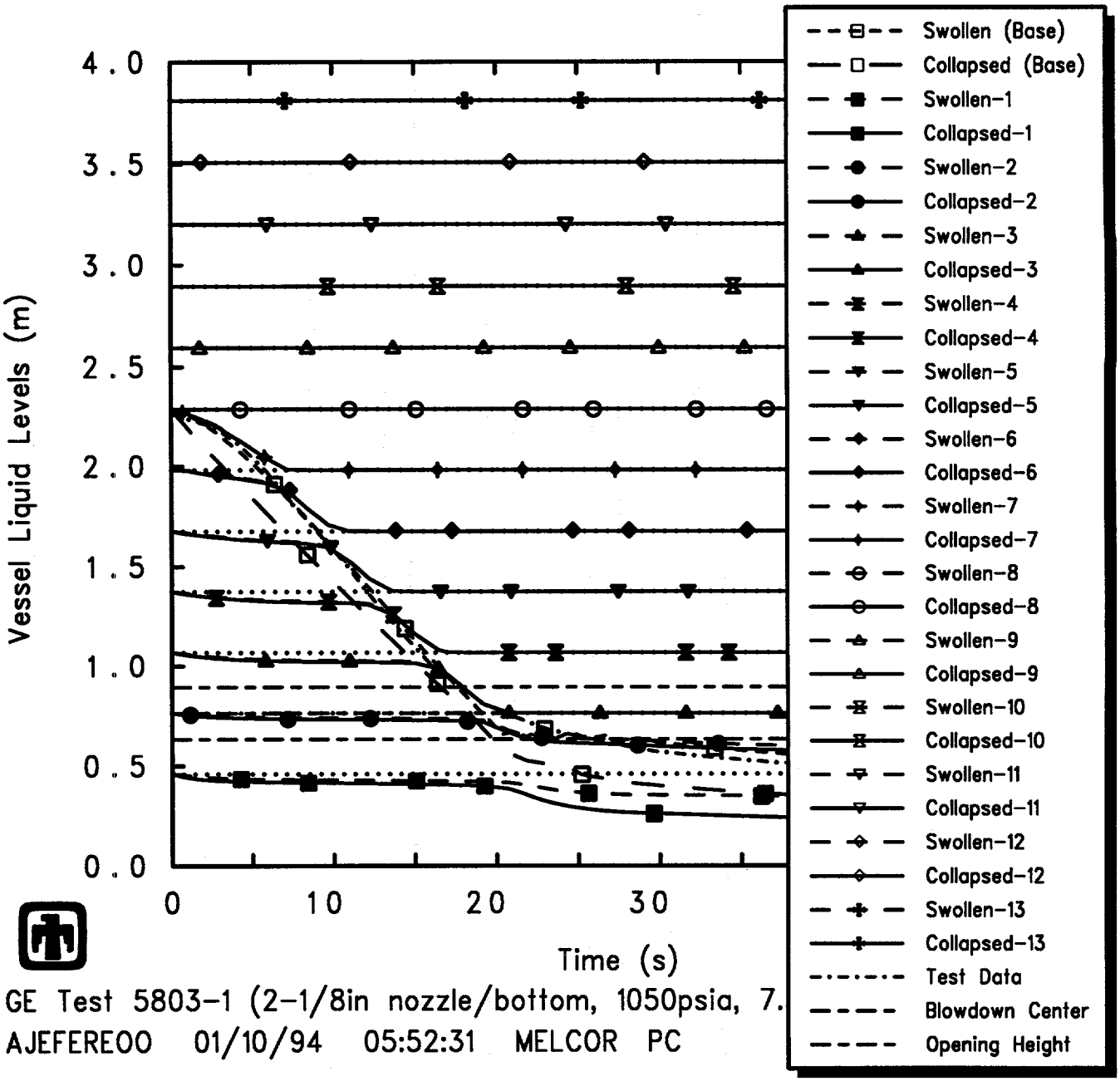

Figure 5.4.11. Vessel Liquid Levels for GE Large Vessel Bottom Blowdown Test 5803-1 – Noding Resolution Sensitivity Study (with Large Junction Opening Heights in Finer Noding Model)

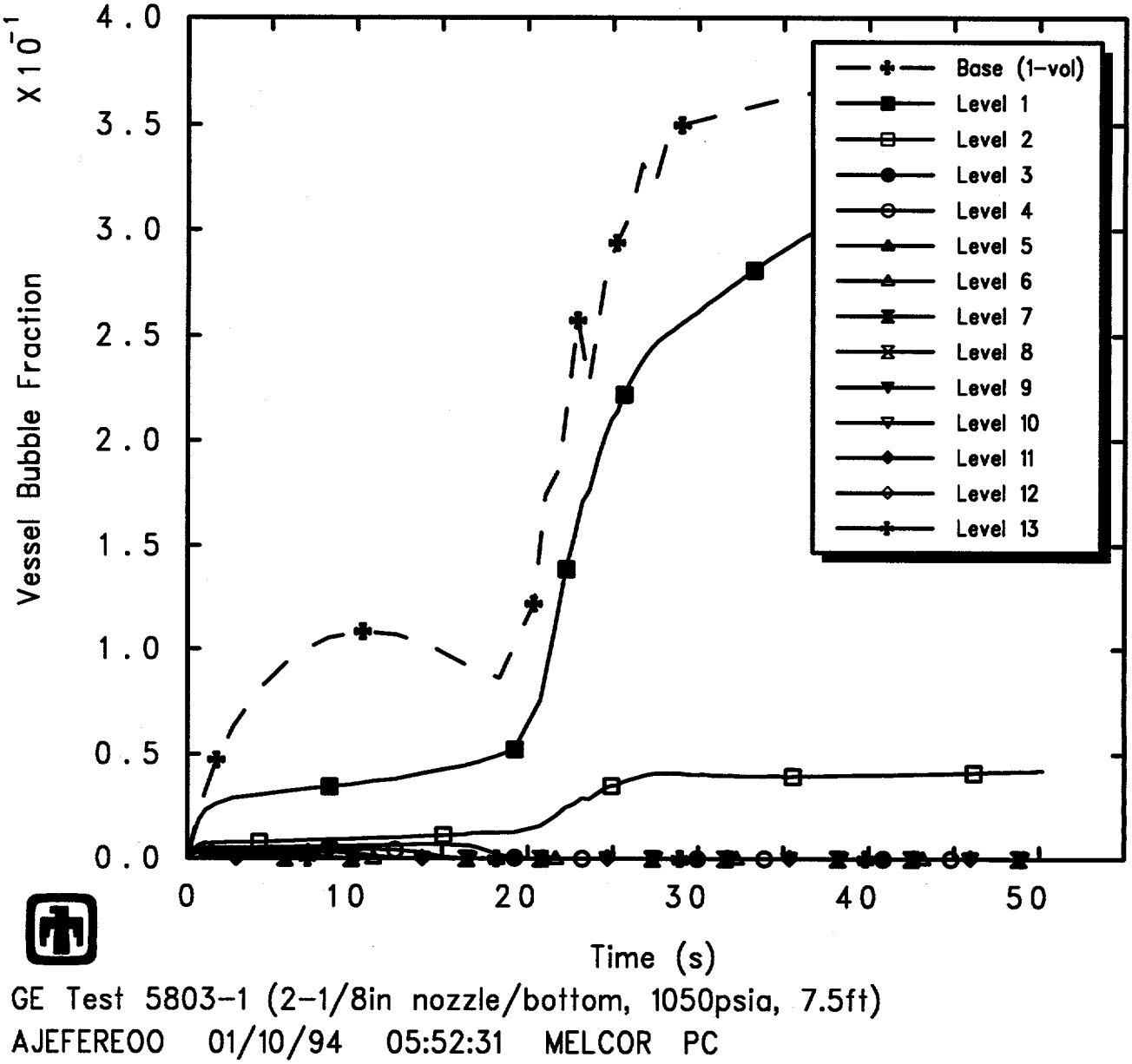

Figure 5.4.12. Vessel Two-Phase Liquid Bubble Fraction for GE Large Vessel Bottom Blowdown Test 5803-1 – Noding Resolution Sensitivity Study (with Large Junction Opening Heights in Finer Noding Model)

those given in Figure 5.4.11. Figure 5.4.16 also indicates lower bubble fractions in some vessel control volumes (particularly in levels 3 and 4) in the calculation for test 5803-1 using the finer noding with small junction opening heights, as compared to corresponding results in the calculation using the finer noding with large junction opening heights, shown in Figure 5.4.12.

(The results obtained for a noding study on the bottom blowdown test 5803-2 analysis are similar to the results presented for test 5803-1, and are not shown here.)

Figures 5.4.17 and 5.4.18 show that there is a substantial run time increase associated with using the finer noding for both the top and bottom blowdown test analyses. This is partly due to reduced time steps but primarily due to the multiplicity of volumes, flow paths and heat structures. (The run times for the single-volume basecase calculations may be hard to see in these figures because they lie so near the abcissa; the total run times for the single-volume basecase calculations are also shown in several plots in Sections 7.1 and 7.2.)

Subdividing the blowdown vessel into a stack of multiple control volumes has no significant effect on the vessel depressurization in the top blowdown test analyses. The results for two-phase level calculated using the single-volume basecase noding are in better quantitative agreement with test data in all of these top blowdown experiment analyses than the swollen levels calculated using a subdivided, stacked, multiple control volume model, even though the exact degree of level swelling is underpredicted with the basecase model. For bottom blowdown tests, using a subdivided noding yields small differences in depressurization history, a smoother break flow, and little or no difference in overall vessel level swell compared to test data or to basecase results when large junction opening heights are used. For both the top and bottom blowdown test analyses, using large junction opening heights (equal to the volume heights) in the flow paths connecting the subdivided, stacked control volumes in the finer noding produced much better agreement with both test data and with the 1-volume basecase results than did using small junction opening heights. However, the results of this sensitivity study demonstrate no significant improvement in agreement with test data using a subdivided, stacked, multiple control volume vessel model rather than a single large volume. The results with the subdivided finer noding show more level swell at the bottom of the stack than further up, which seems counterintuitive. There appear to be no benefits found in subdividing the vessel into multiple, stacked control volumes, especially given the increased run times required.

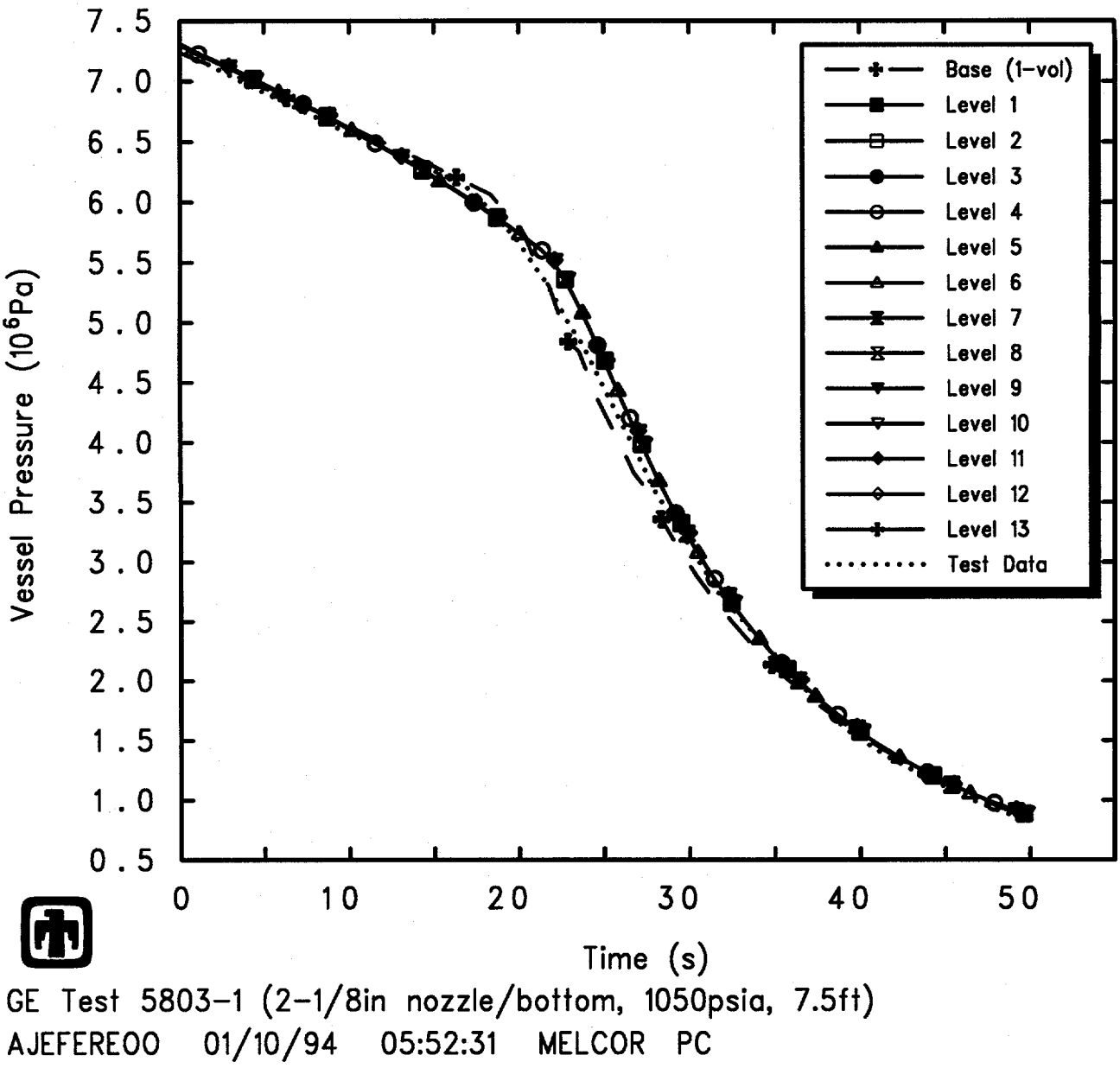

Figure 5.4.13. Vessel Pressure for GE Small Vessel Bottom Blowdown Test 5803-1 – Noding Resolution Sensitivity Study (with Small Junction Opening Heights in Finer Noding Model)

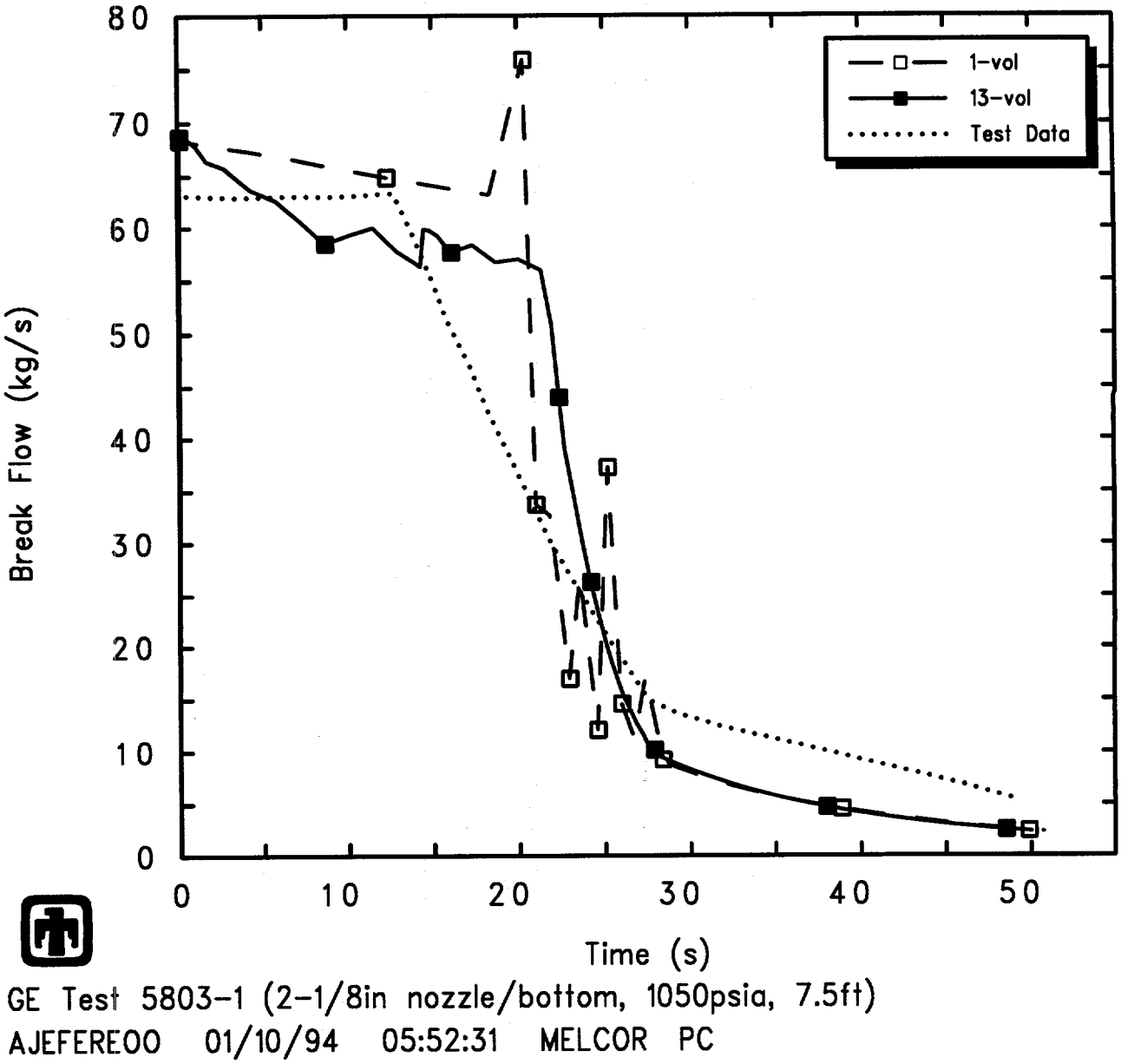

Figure 5.4.14. Blowdown Mass Flow for GE Small Vessel Bottom Blowdown Test 5803-1 – Noding Resolution Sensitivity Study (with Small Junction Opening Heights in Finer Noding Model)

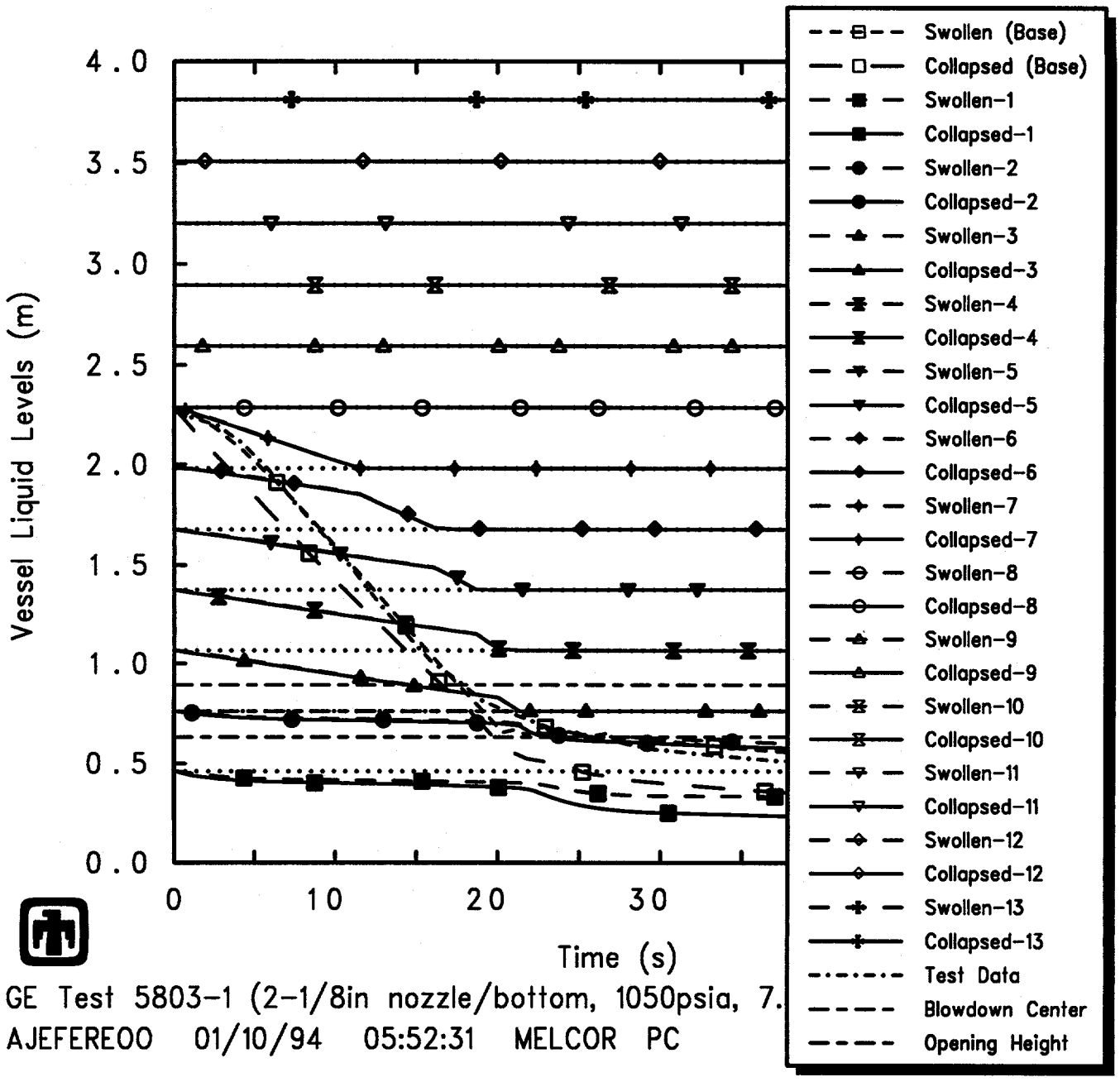

Figure 5.4.15. Vessel Liquid Levels for GE Small Vessel Bottom Blowdown Test 5803-1 – Noding Resolution Sensitivity Study (with Small Junction Opening Heights in Finer Noding Model)

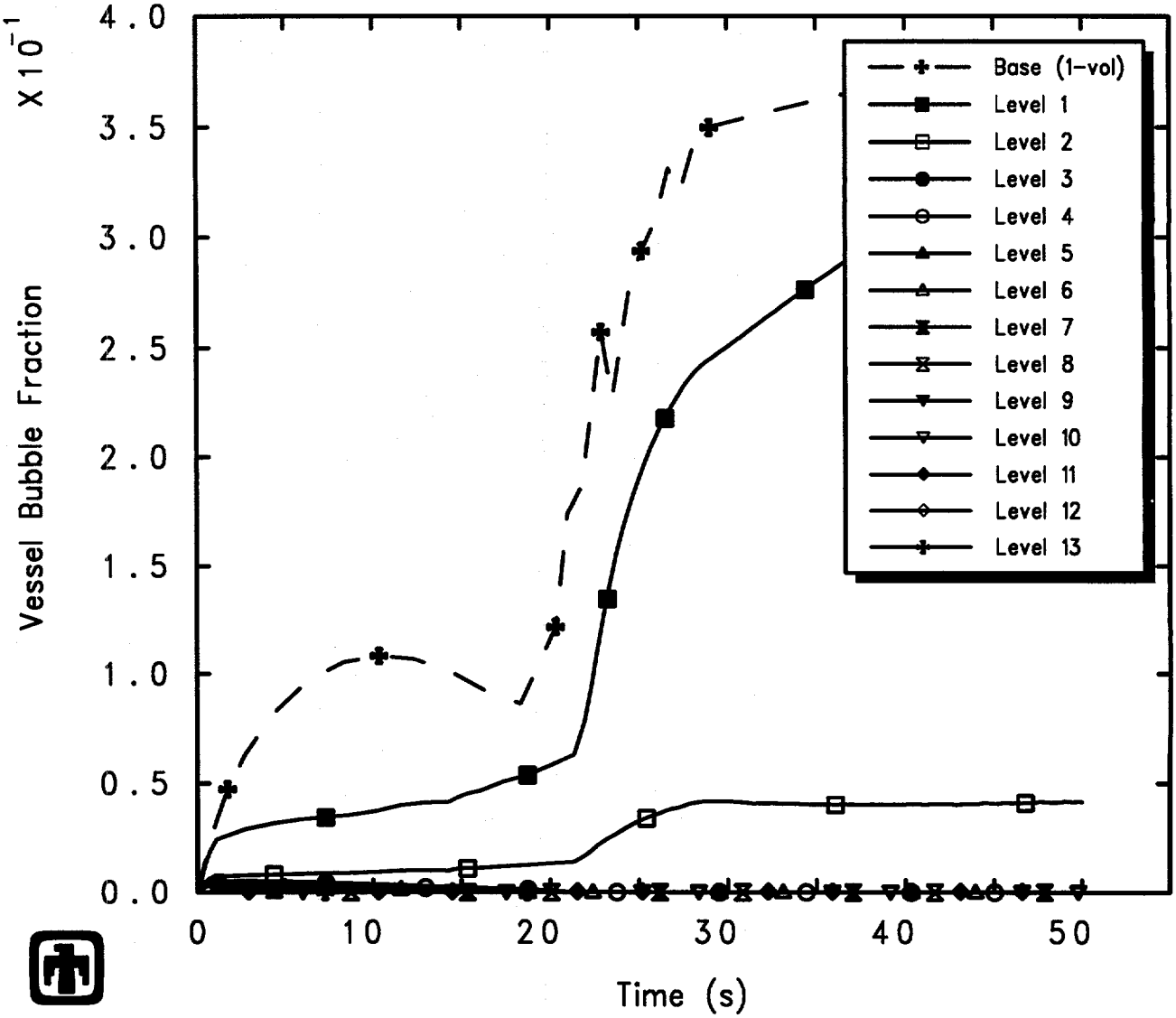

Figure 5.4.16. Vessel Two-Phase Liquid Bubble Fraction for GE Small Vessel Bottom Blowdown Test 5803-1 – Noding Resolution Sensitivity Study (with Small Junction Opening Heights in Finer Noding Model)

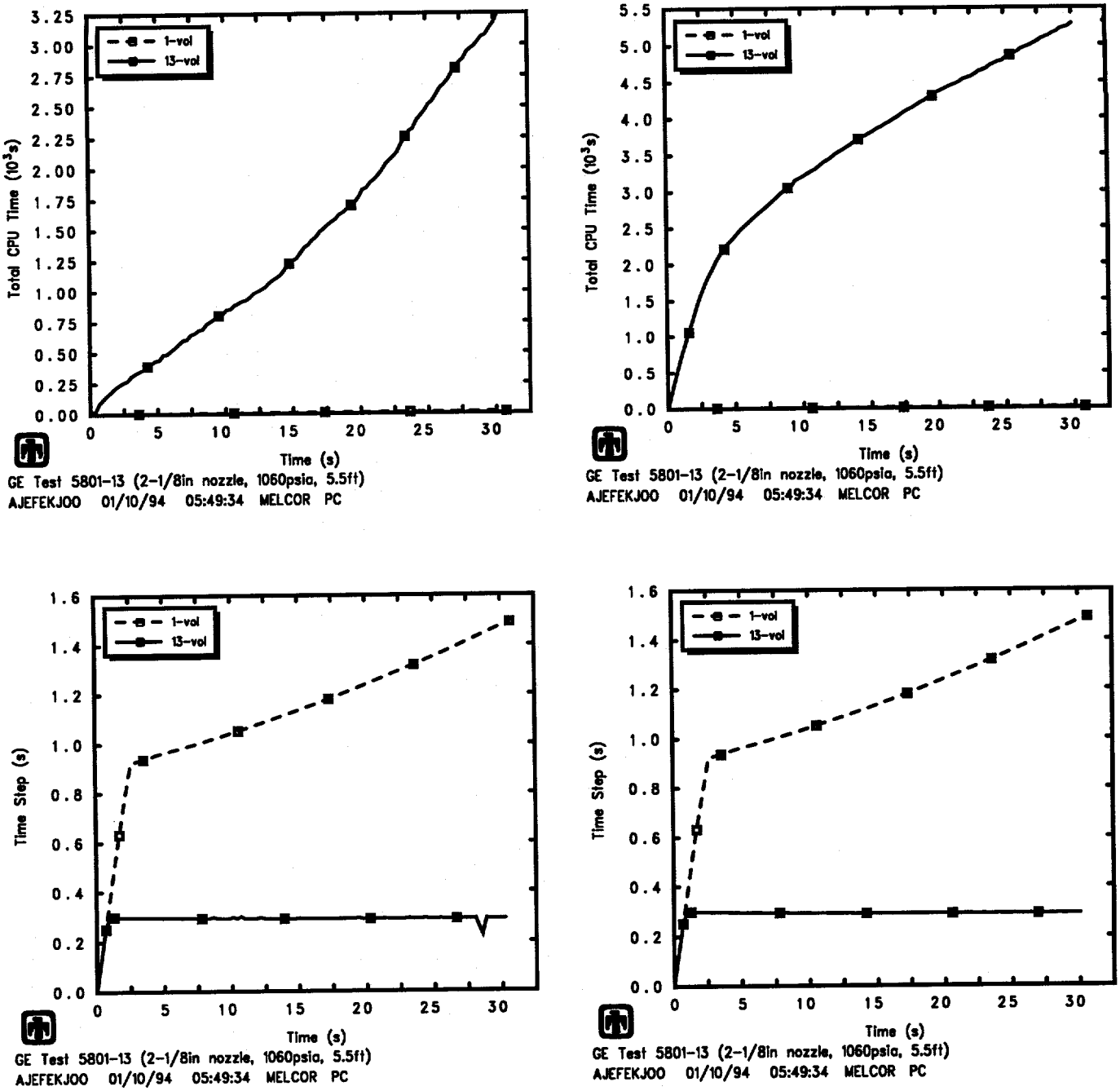

Figure 5.4.17. Total Run Time (top) and Time Step (bottom) for GE Large Vessel Top Blowdown Test 5801-13 – Noding Resolution Sensitivity Study with Large (left) and Small (right) Junction Opening Heights in Finer Noding Model

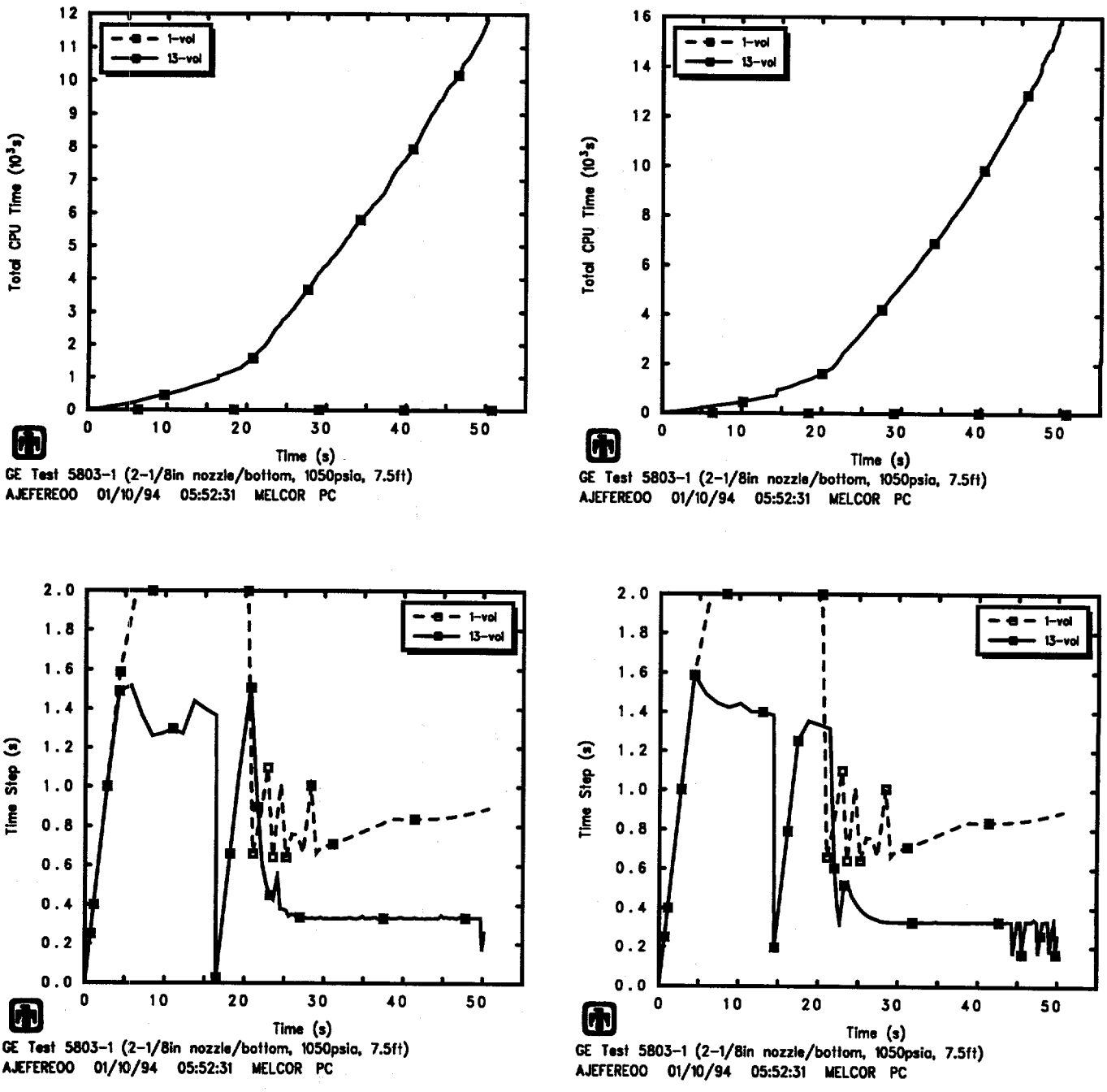

Figure 5.4.18. Total Run Time (top) and Time Step (bottom) for GE Large Vessel Bottom Blowdown Test 5803-1 – Noding Resolution Sensitivity Study with Large (left) and Small (right) Junction Opening Heights in Finer Noding Model

6 FL Sensitivity Studies

There are options and uncertainties for some MELCOR input values and in the modelling approach taken to represent test conditions. As described in this and the previous section, a set of sensitivity studies has been done varying some of these parameters to determine how the results could be affected by such modelling variations and uncertainties. This section investigates modelling variations affecting the flow path (FL) package, while the preceding section presents results varying modelling parameter and options affecting the CVH package.

6.1 Blowdown Discharge Coefficient

The computed flow in a flow path in MELCOR is limited by a calculated critical flow, which it is not allowed to exceed. User-input discharge coefficients are available as multipliers on the critical flow values calculated by the MELCOR choked flow models. MELCOR uses the same choked flow discharge coefficients for both subcooled and saturated flow; however, the allowed input distinguishes between forward and reverse flow. The default MELCOR values are 1.0 in each direction. As a sensitivity study, calculations were done in which the discharge coefficients were reduced to 0.9, 0.8, 0.7 and 0.6.

The effect of varying the choked flow discharge coefficients is shown in Figures 6.1.1 through 6.1.4, for the top blowdown test 5801-13 (which has a 2-1/8in nozzle throat diameter). Figure 6.1.1 shows the vessel depressurization history calculated by MELCOR using these different values for the choked flow discharge coefficients, compared to experimental data. The vessel collapsed and swollen (two-phase) liquid levels predicted by MELCOR using these different choked flow discharge coefficients, also compared to experimental data, are depicted in Figure 6.1.2. Figure 6.1.3 shows the break flow out the blowdown line and Venturi flow limiting nozzle causing the vessel depressurization, calculated by MELCOR using these different values for the choked flow discharge coefficients. The effect is exactly as expected – reducing the discharge coefficients reduces the break flow rates and resultant overall inventory loss, and causes less rapid depressurization. There is relatively little effect found on the calculated degree of level swelling as the break discharge coefficient is varied, with the bubble fractions in all cases rising and remaining at near the maximum value allowed (0.40), as illustrated in Figure 6.1.4, although reducing the discharge coefficient and hence decreasing the vessel depressurization rate does result in reaching that limiting bubble fraction slightly later in time. For test 5801-13, a top blowdown test with a 2-1/8in nozzle throat diameter, the best agreement with observation is found with a discharge coefficient beginning at $\sim$0.80 and increased to $\sim$0.90 late in the blowdown.

Results of similar calculations varying the choked flow discharge coefficient are shown in Figures 6.1.5 and 6.1.6 for the top blowdown test 5801-15 (which has a 2-1/2in nozzle throat diameter). Figure 6.1.5 gives the calculated vessel depressurization histories,

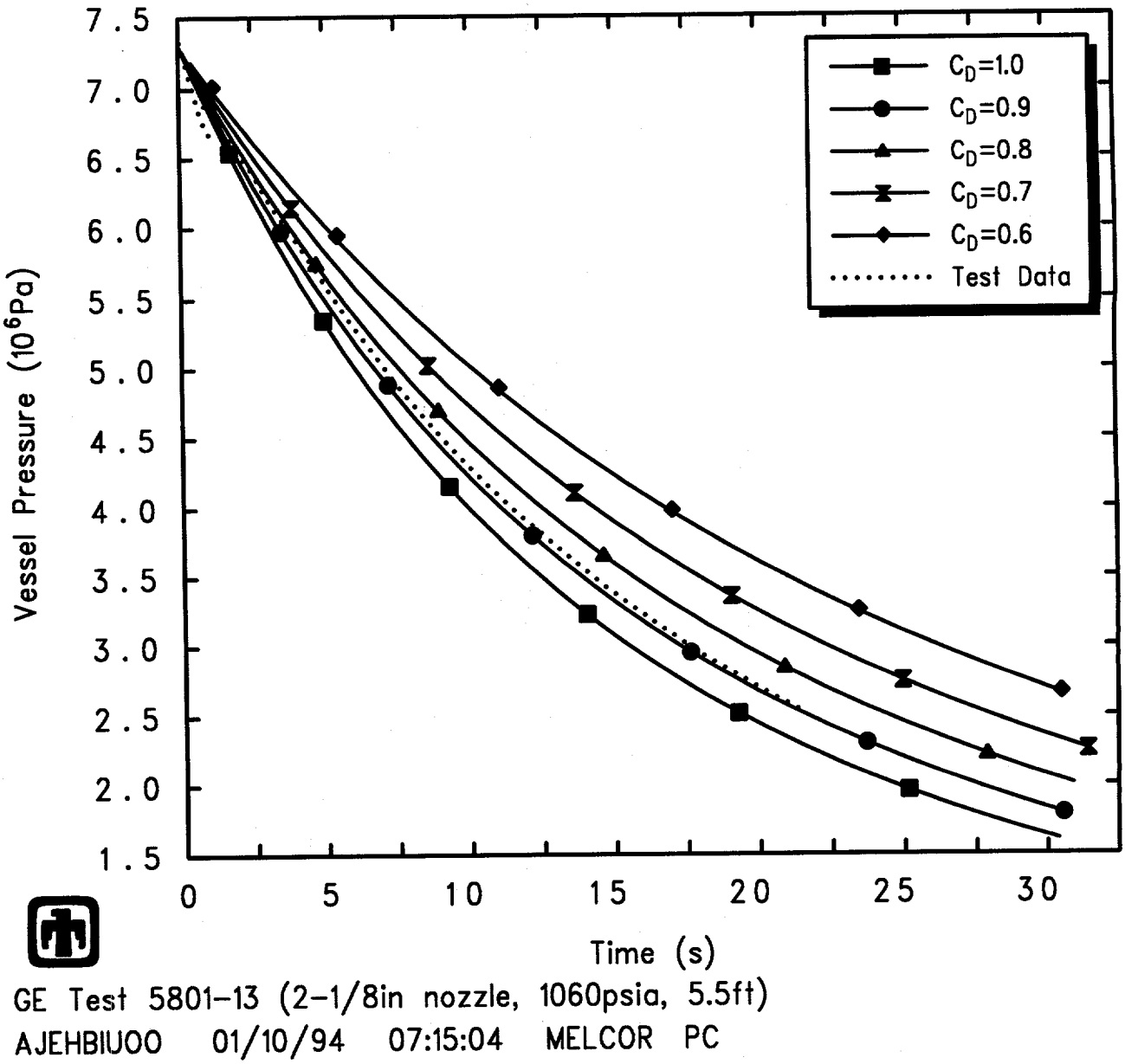

Figure 6.1.1. Vessel Pressure for GE Large Vessel Top Blowdown Test 5801-13 – Break Discharge Coefficient Sensitivity Study

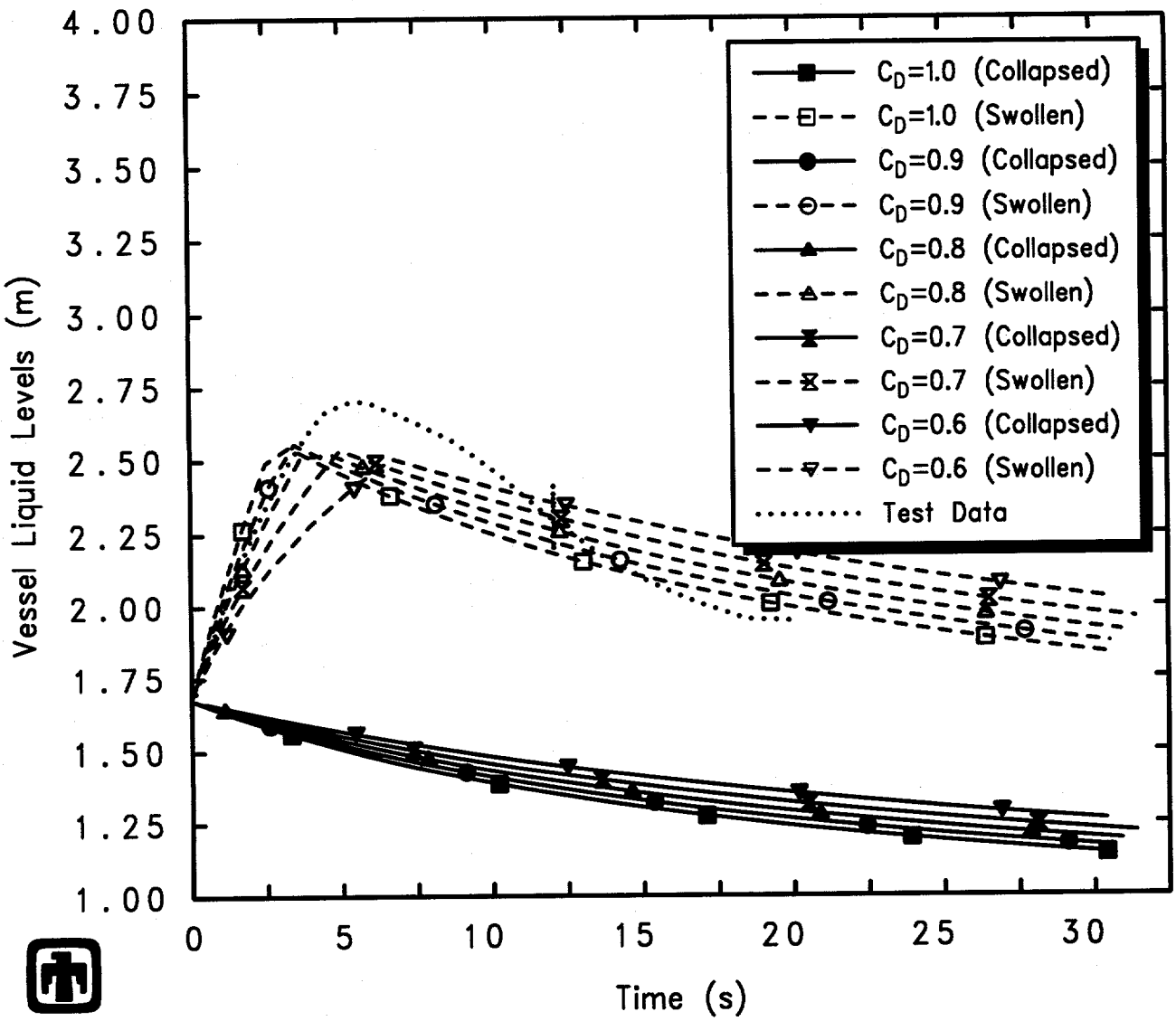

Figure 6.1.2. Vessel Liquid Levels for GE Large Vessel Top Blowdown Test 5801-13 – Break Discharge Coefficient Sensitivity Study

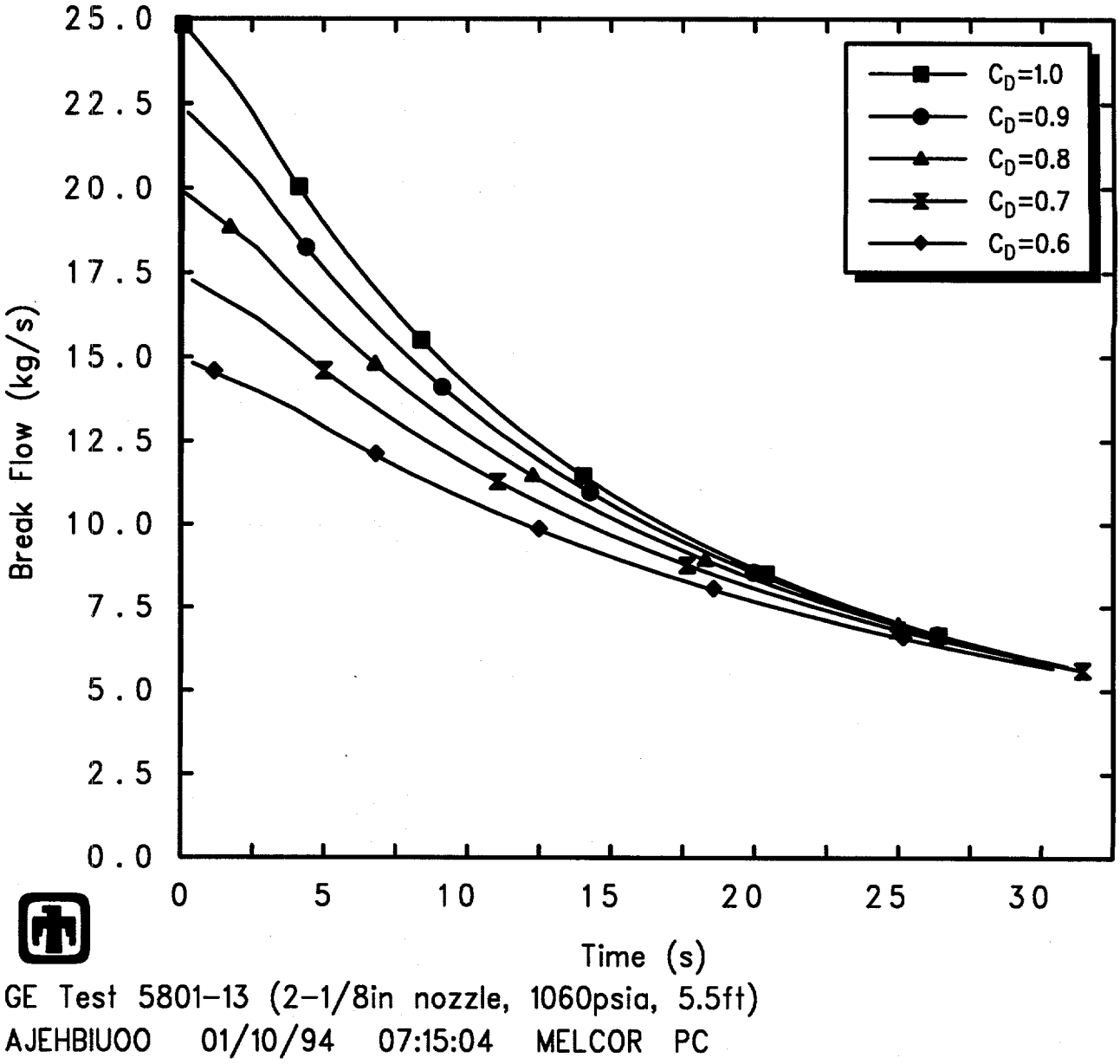

Figure 6.1.3. Blowdown Mass Flow for GE Large Vessel Top Blowdown Test 5801-13 – Break Discharge Coefficient Sensitivity Study

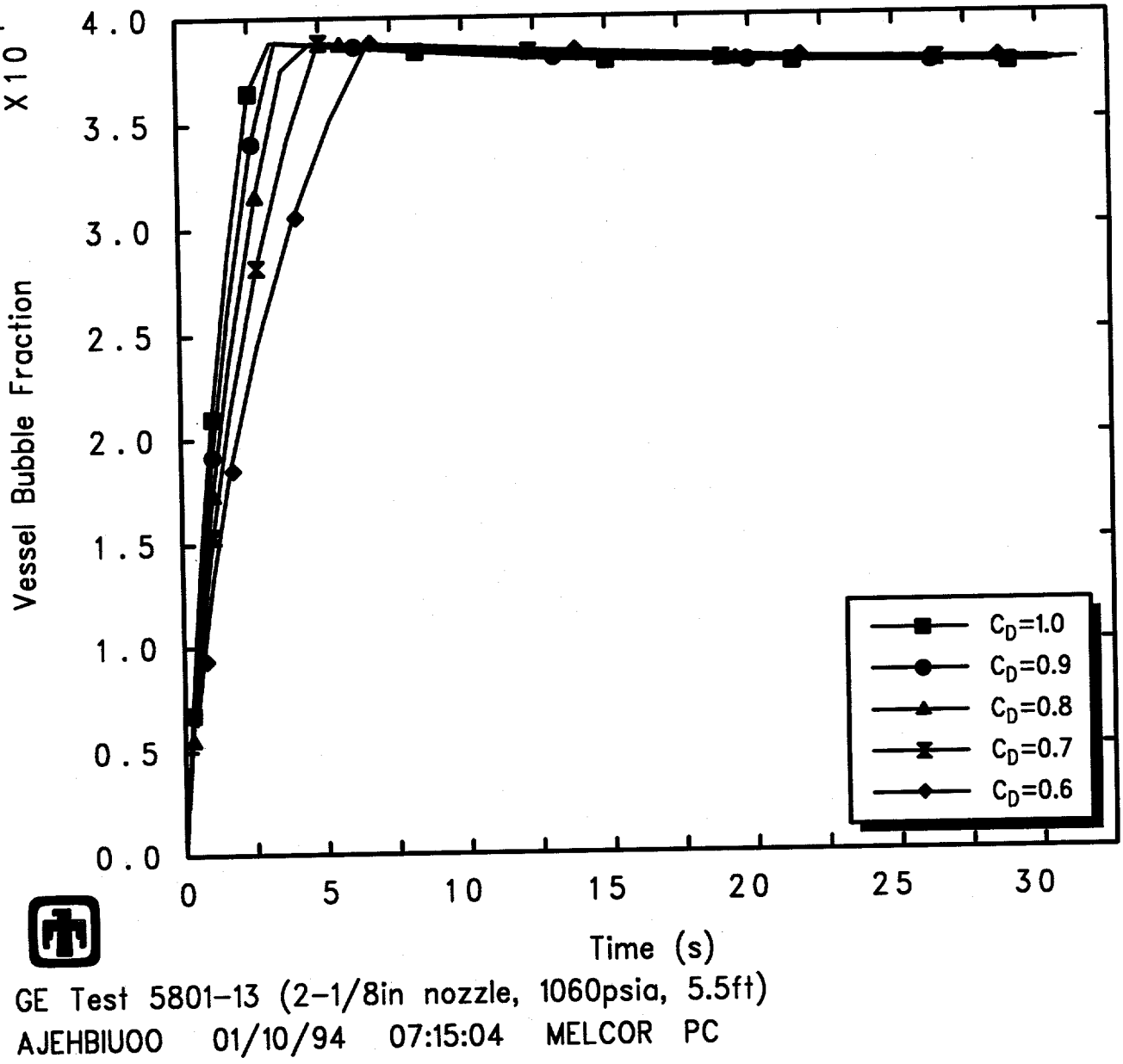

Figure 6.1.4. Vessel Two-Phase Liquid Bubble Fraction for GE Large Vessel Top Blowdown Test 5801-13 – Break Discharge Coefficient Sensitivity Study

compared to experimental data; the vessel collapsed and swollen (two-phase) liquid levels predicted by MELCOR, also compared to experimental data, are presented in Figure 6.1.6. For test 5801-15, the best agreement with observation is found with a discharge coefficient somewhere between 0.80 (in mid-blowdown) and 0.90 (early and late in the blowdown).

Figure 6.1.7 shows the vessel depressurization histories with different blowdown discharge coefficients used, compared to experimental data, for the top blowdown test 5801-19. The corresponding vessel collapsed and swollen (two-phase) liquid levels predicted by MELCOR are depicted in Figure 6.1.8. For this test, a top blowdown test with a 3in nozzle throat diameter, the best agreement with observation is found with a discharge coefficient between $\geq$0.70 midway through the transient and $\leq$0.90 both earlier and later in the blowdown.

Figures 6.1.9 and 6.1.10 summarize the effect on the vessel depressurization and on the vessel liquid levels, respectively, of varying the choked flow discharge coefficients in the top blowdown test 5702-16 (which has a 3-5/8in nozzle throat diameter). For test 5702-16, the best agreement with test data is found with a discharge coefficient somewhere between 0.70 (in mid-blowdown) and 0.90 (early and late in the blowdown).

Changing the specified choked flow discharge coefficients for the bottom blowdown test 5803-1 (which has a 2-1/8in nozzle throat diameter) is shown in Figures 6.1.11 through 6.1.14. Figure 6.1.11 shows the vessel depressurization history calculated by MELCOR using these different values for the choked flow discharge coefficients, compared to experimental data. The vessel collapsed and swollen (two-phase) liquid levels predicted by MELCOR using these different choked flow discharge coefficients, also compared to experimental data, are depicted in Figure 6.1.12. Figure 6.1.13 shows the break flow out the blowdown line and Venturi flow limiting nozzle causing the vessel depressurization, calculated by MELCOR using different values for the choked flow discharge coefficients. As with the top blowdown test analyses, reducing the discharge coefficients reduces the break flow rates and resultant overall inventory loss, and causes less rapid depressurization. There is relatively little effect found on the calculated degree of level swelling as the break discharge coefficient is varied, with the bubble fractions reduced as the discharge coefficients are reduced, in all cases, but rising to about the maximum value allowed (0.40) by the end of the blowdown period calculated, as indicated in Figure 6.1.14. For test 5803-1, a bottom blowdown test with a 2-1/8in nozzle throat diameter, the best agreement with observation is found with a discharge coefficient between $\sim$0.80 and $\sim$0.70.

Results of similar calculations varying the choked flow discharge coefficient for the other bottom blowdown test (5803-2, which has a 3in nozzle throat diameter) are shown in Figures 6.1.15 through 6.1.17. Figure 6.1.15 gives the calculated vessel depressurization histories, compared to experimental data; the vessel collapsed and swollen (two-phase) liquid levels predicted by MELCOR, also compared to experimental data, are presented in Figure 6.1.16, while Figure 6.1.17 shows the break flow out the blowdown line and Venturi flow limiting nozzle causing the vessel depressurization. For test 5803-2, the best

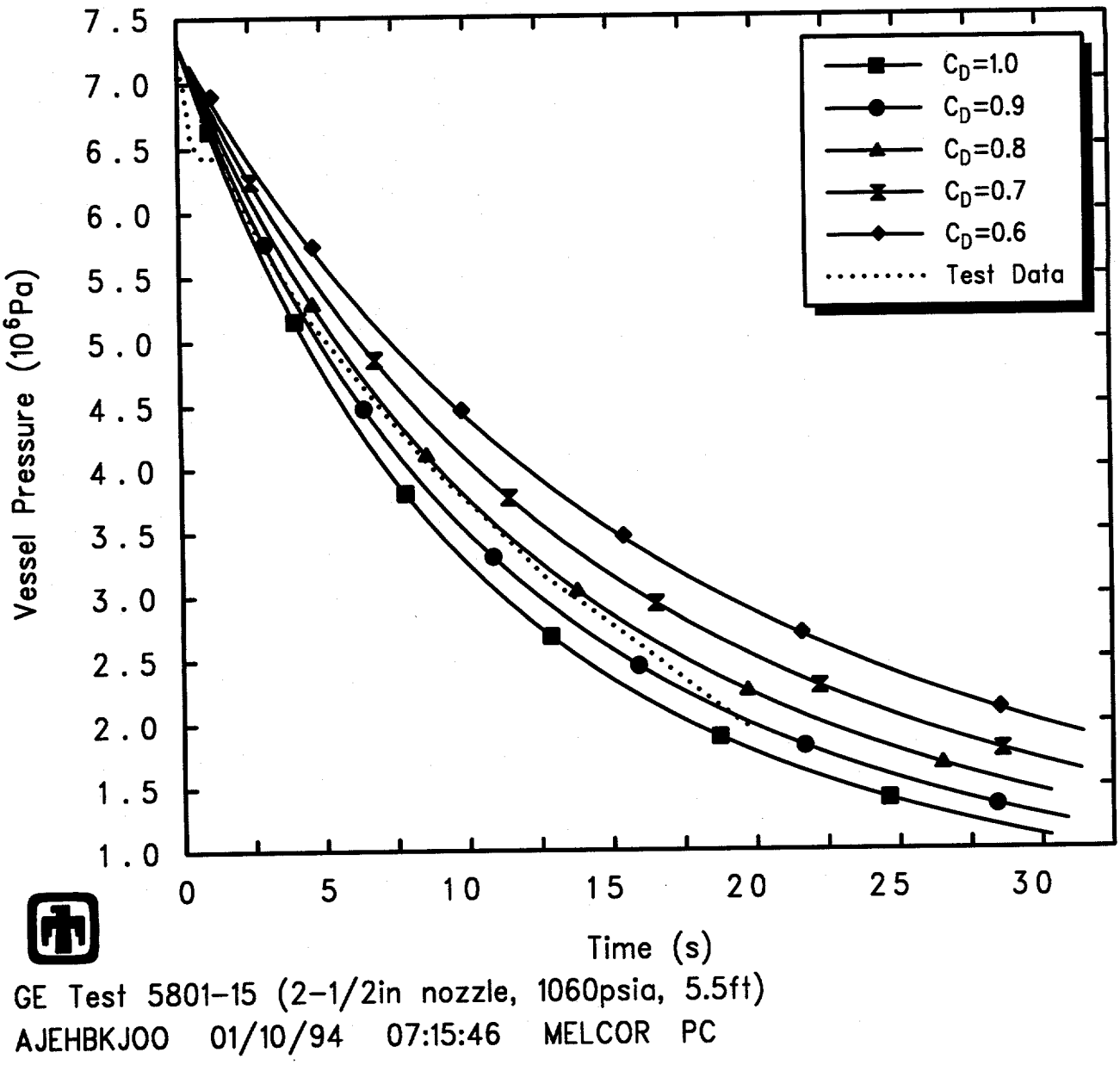

Figure 6.1.5. Vessel Pressure for GE Large Vessel Top Blowdown Test 5801-15 – Break Discharge Coefficient Sensitivity Study

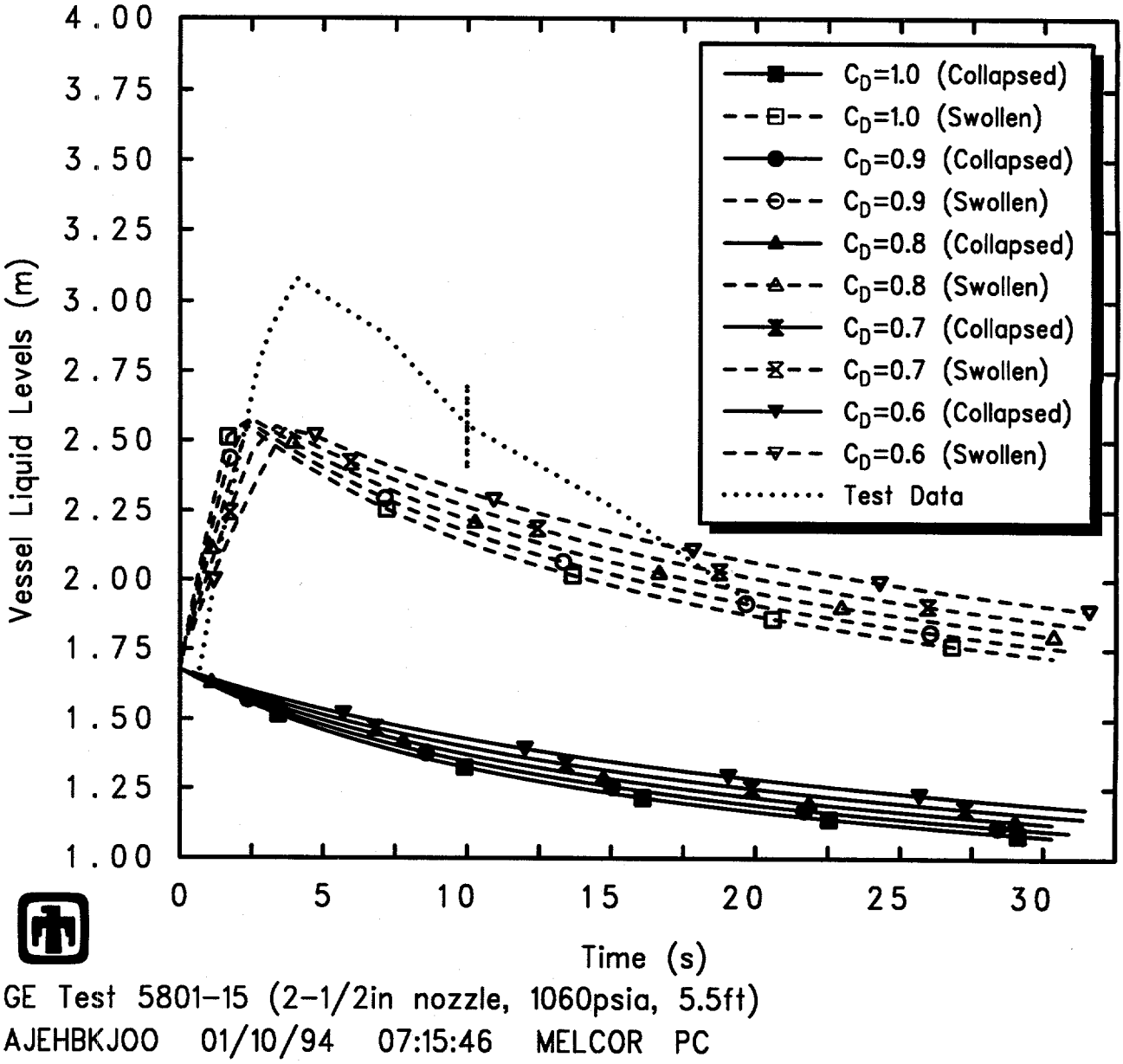

Figure 6.1.6. Vessel Liquid Levels for GE Large Vessel Top Blowdown Test 5801-15 – Break Discharge Coefficient Sensitivity Study

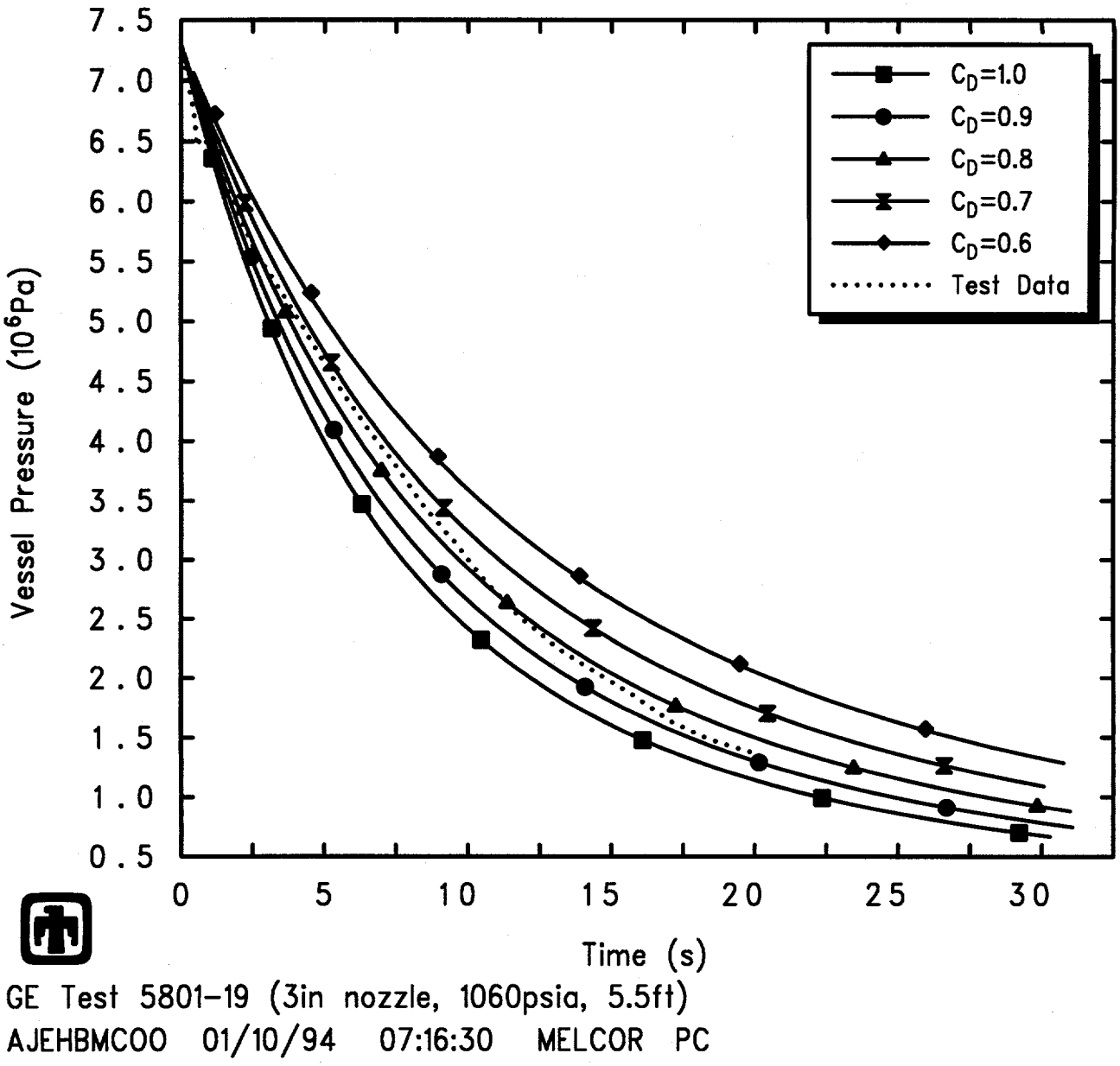

Figure 6.1.7. Vessel Pressure for GE Large Vessel Top Blowdown Test 5801-19 – Break Discharge Coefficient Sensitivity Study

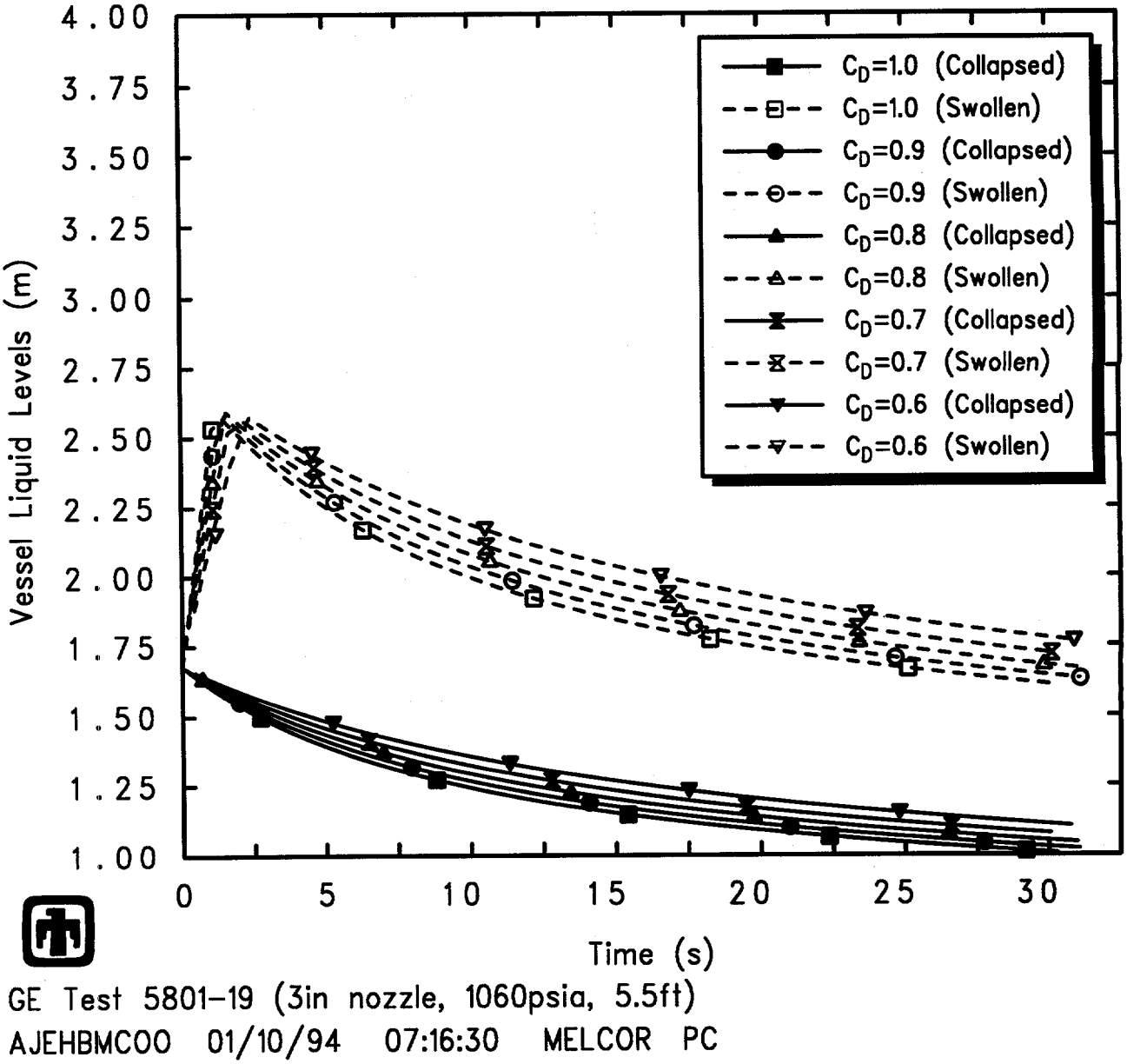

Figure 6.1.8. Vessel Liquid Levels for GE Large Vessel Top Blowdown Test 5801-19 – Break Discharge Coefficient Sensitivity Study

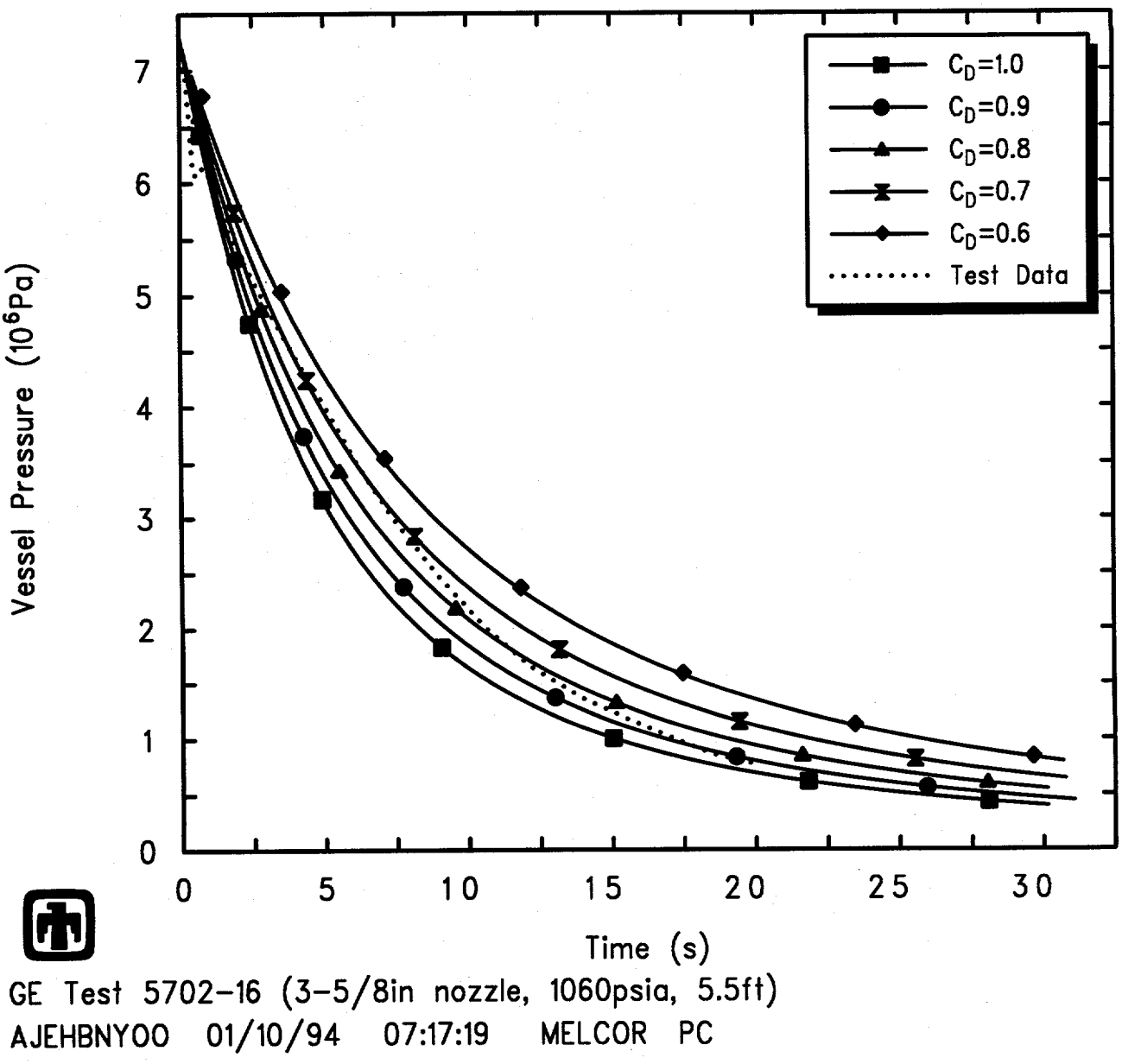

Figure 6.1.9. Vessel Pressure for GE Large Vessel Top Blowdown Test 5702-16 – Break Discharge Coefficient Sensitivity Study

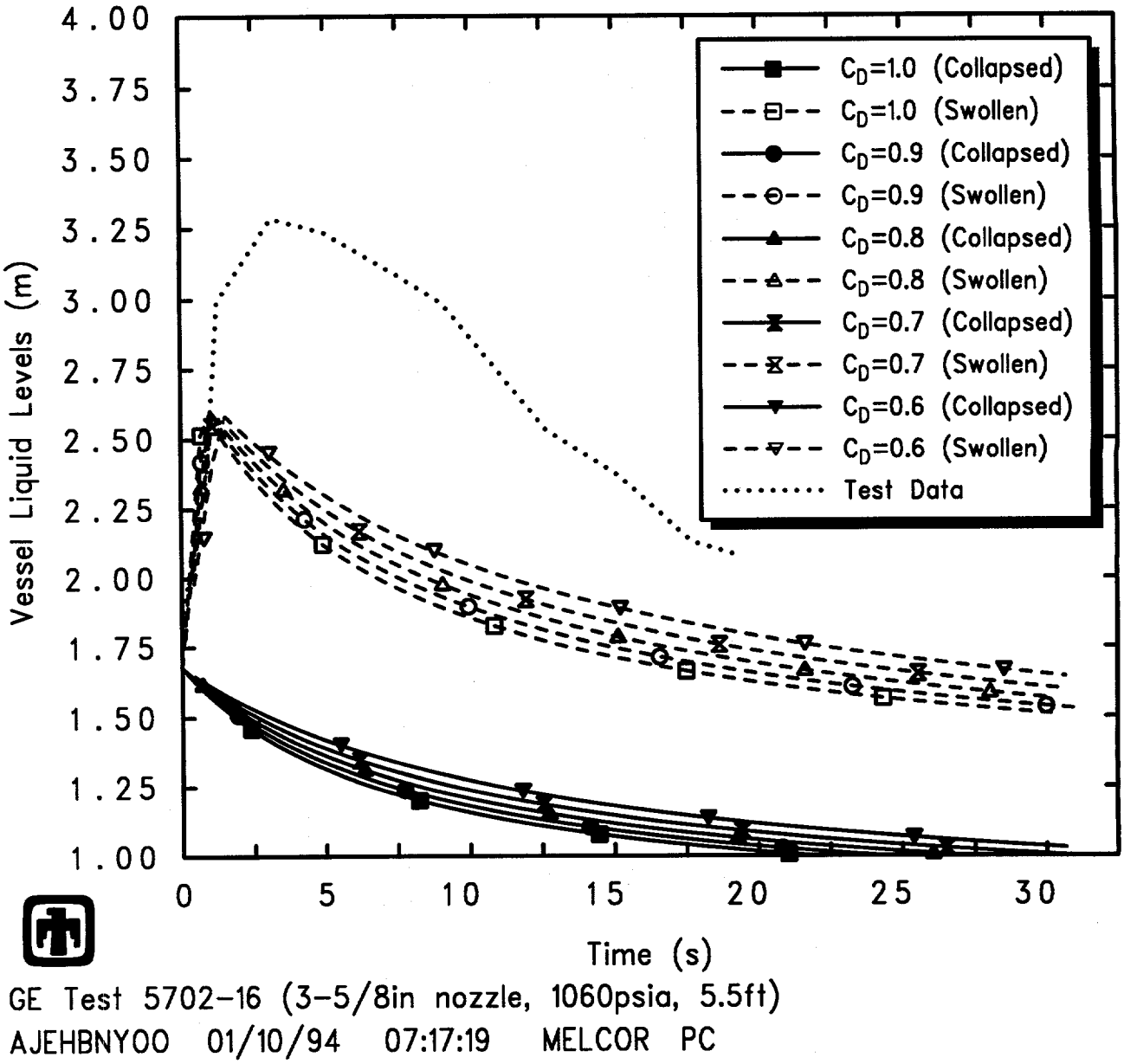

Figure 6.1.10. Vessel Liquid Levels for GE Large Vessel Top Blowdown Test 5702-16 – Break Discharge Coefficient Sensitivity Study

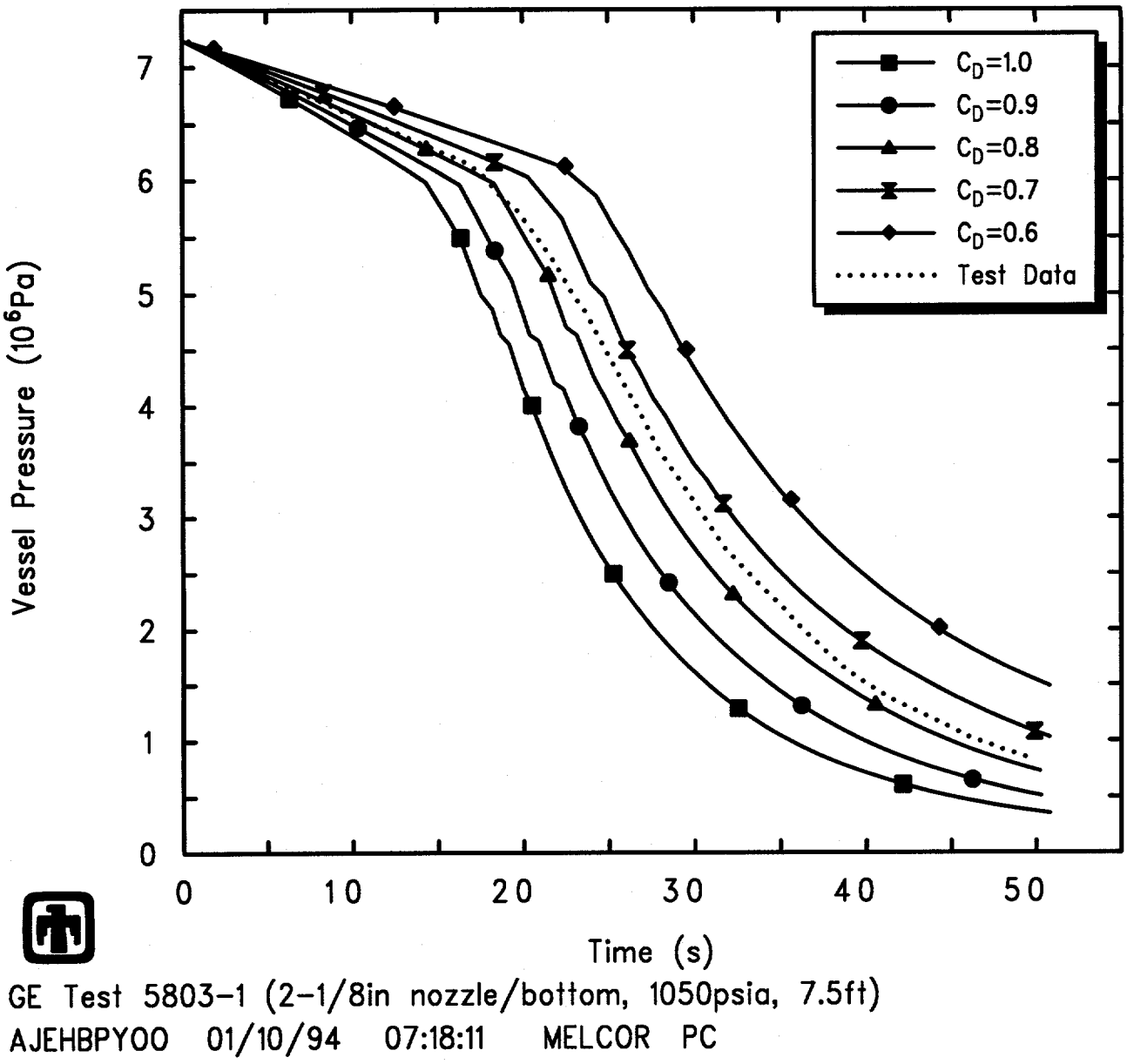

Figure 6.1.11. Vessel Pressure for GE Large Vessel Bottom Blowdown Test 5803-1 – Break Discharge Coefficient Sensitivity Study

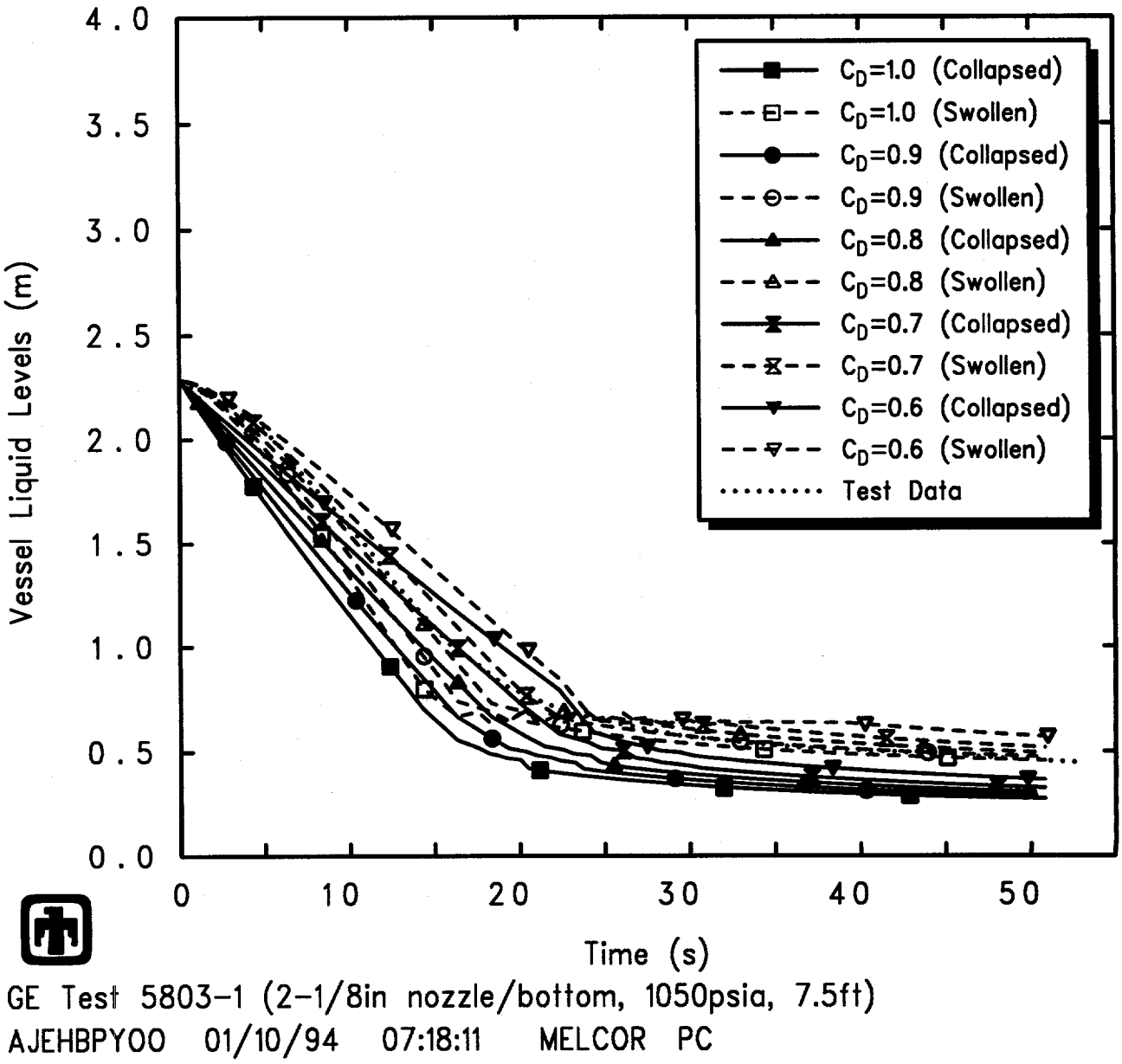

Figure 6.1.12. Vessel Liquid Levels for GE Large Vessel Bottom Blowdown Test 5803-1 – Break Discharge Coefficient Sensitivity Study

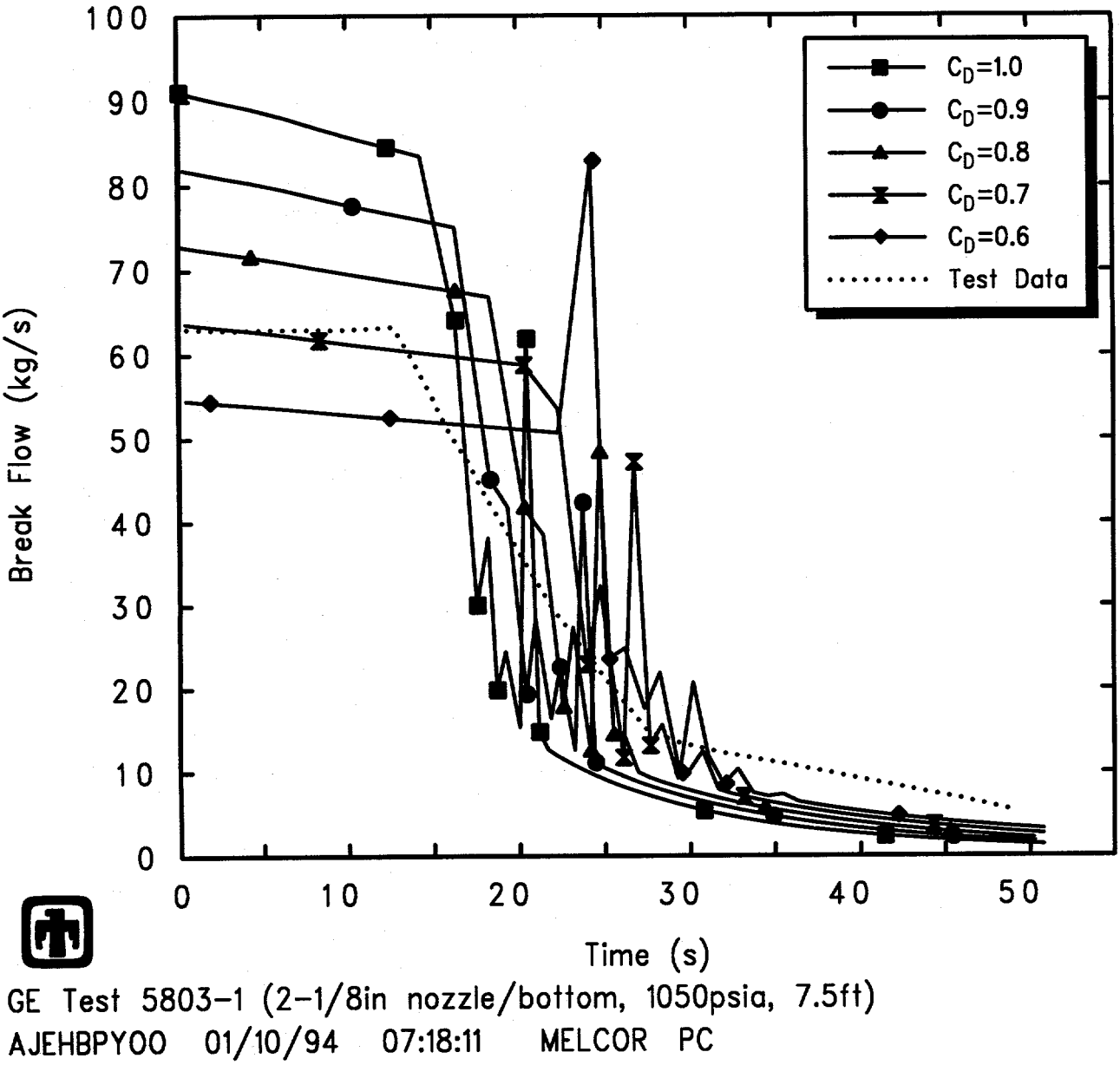

Figure 6.1.13. Blowdown Mass Flow for GE Large Vessel Bottom Blowdown Test 5803-1 – Break Discharge Coefficient Sensitivity Study

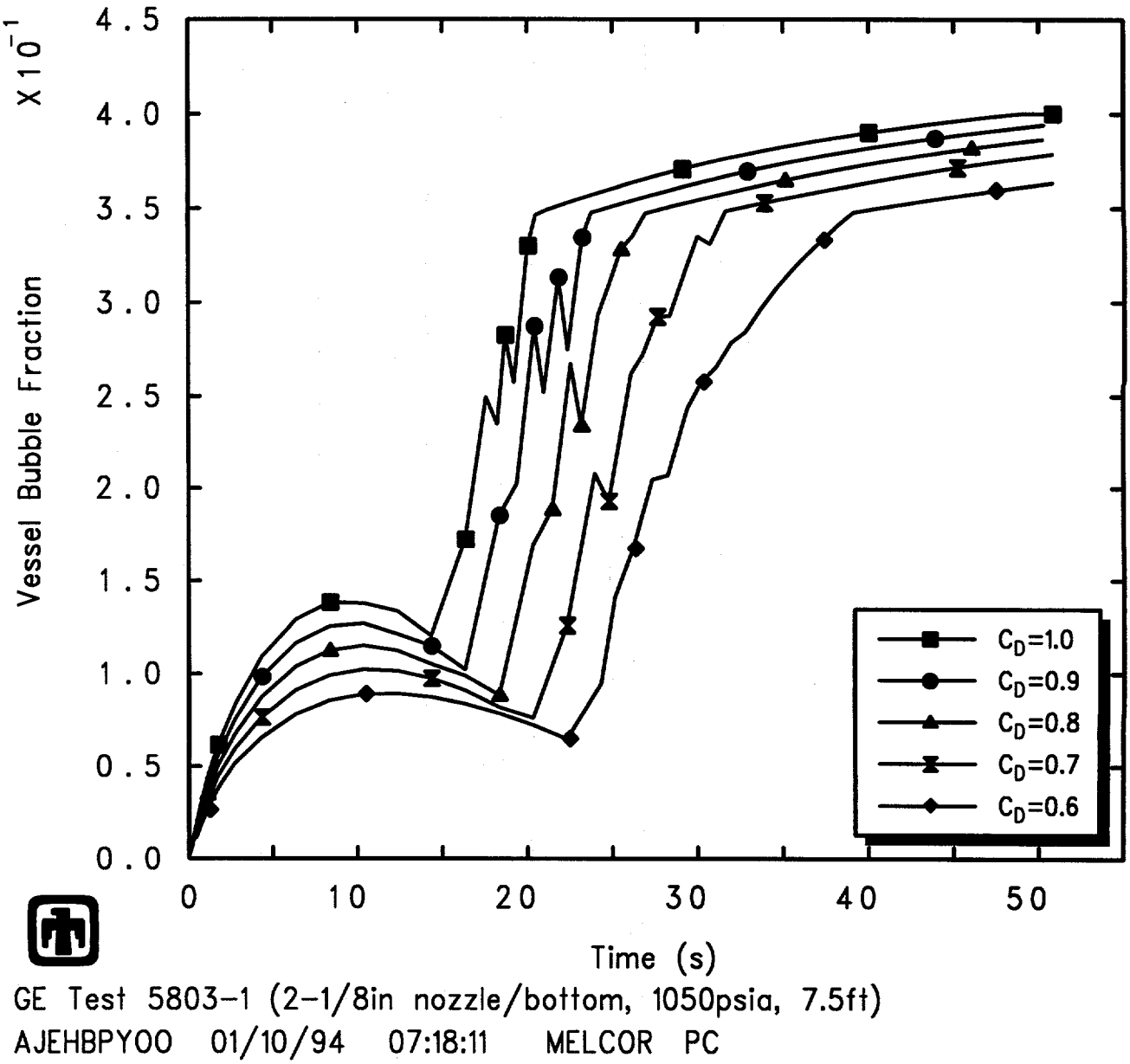

Figure 6.1.14. Vessel Two-Phase Liquid Level Bubble Fraction for GE Large Vessel Bottom Blowdown Test 5803-1 – Break Discharge Coefficient Sensitivity Study

agreement with test data is found with a discharge coefficient of ≤ 0.70 throughout the blowdown.

The results of this study demonstrate that no single value of choked flow discharge coefficient gives best agreement with test data for all tests analyzed and through the entire experiment period analyzed. However, the results indicate that values of 0.7-0.9 give better agreement with test data than either lower (0.6) or higher (1.0) values. This is a very encouraging result, since this closely resembles typical discharge coefficient values used in best-estimate thermal/hydraulic codes. The results of this sensitivity study also indicate that better agreement with data is obtained using somewhat larger discharge coefficients for the top blowdown tests (dominated by steam outflow) than for the bottom blowdown tests (dominated mostly by liquid and two-phase outflow). Thus, we used discharge coefficients of 0.85 for the top blowdown tests and 0.75 for the bottom blowdown tests in all other MELCOR analyses done as part of this assessment study.

6.2 Flow Loss Coefficient

Frictional pressure drops resulting from material flows include contributions from both form loss and wall friction. In MELCOR, the form loss term is determined by user input form loss coefficients, while the wall friction terms are computed based upon flow path segment lengths and roughnesses also input by the user. The form loss coefficients represent pressure drops associated with sudden area changes and/or bends.

In addition to the discharge-coefficient break flow sensitivity study described above in Section 6.1, another set of sensitivity study calculations have been done in which the loss coefficients on the blowdown flow path were varied from 0.0 to 0.5, 1.0, 1.5 and 2.0. Both the discharge coefficients and the loss coefficients specified in the blowdown flow path affect the blowdown flow, but in different ways; the discharge coefficients act only when the blowdown flow is choked, as simple multipliers on the maximum allowed velocity, while the loss coefficients act any time there is blowdown flow, choked or not, and indirectly as a loss proportional to the square of the flow velocity within the overall momentum equation.

The effect of varying the blowdown flow path loss coefficients is shown in Figures 6.2.1 and 6.2.2, for the top blowdown test 5801-13 (which has a 2-1/8in nozzle throat diameter). Figure 6.2.1 shows the vessel depressurization history calculated by MELCOR using these different values for the flow path form loss coefficients, compared to experimental data. The vessel collapsed and swollen (two-phase) liquid levels predicted by MELCOR using these different flow path form loss coefficients, also compared to experimental data, are depicted in Figure 6.2.2. The effect on vessel depressurization of varying the blowdown flow path loss coefficient is hardly visible, and there is virtually no effect found on the calculated degree of level swelling.

Results of similar sensitivity study calculations for the other three top blowdown tests are virtually identical to the results shown for test 5801-13: varying the blowdown

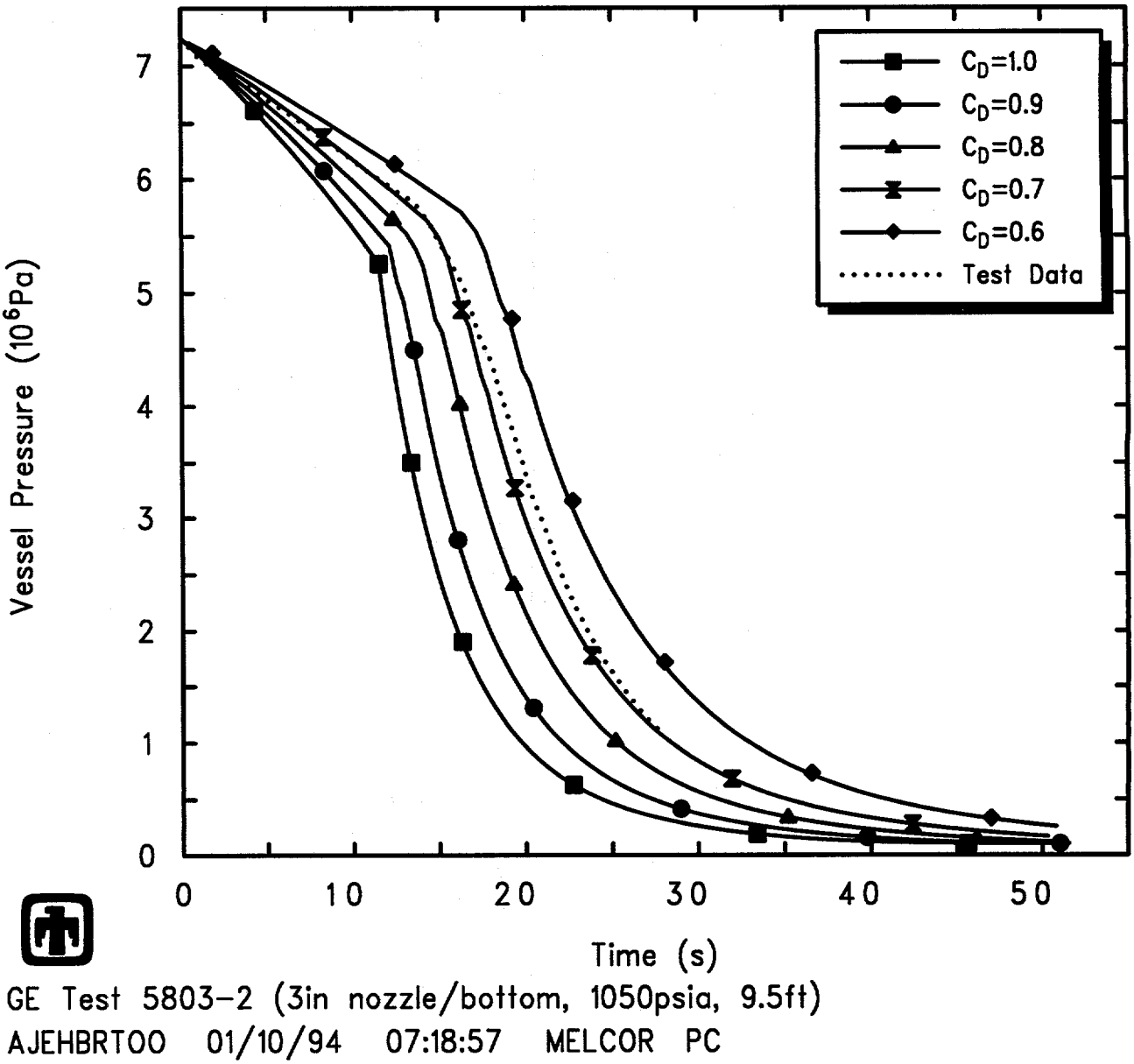

Figure 6.1.15. Vessel Pressure for GE Large Vessel Bottom Blowdown Test 5803-2 – Break Discharge Coefficient Sensitivity Study

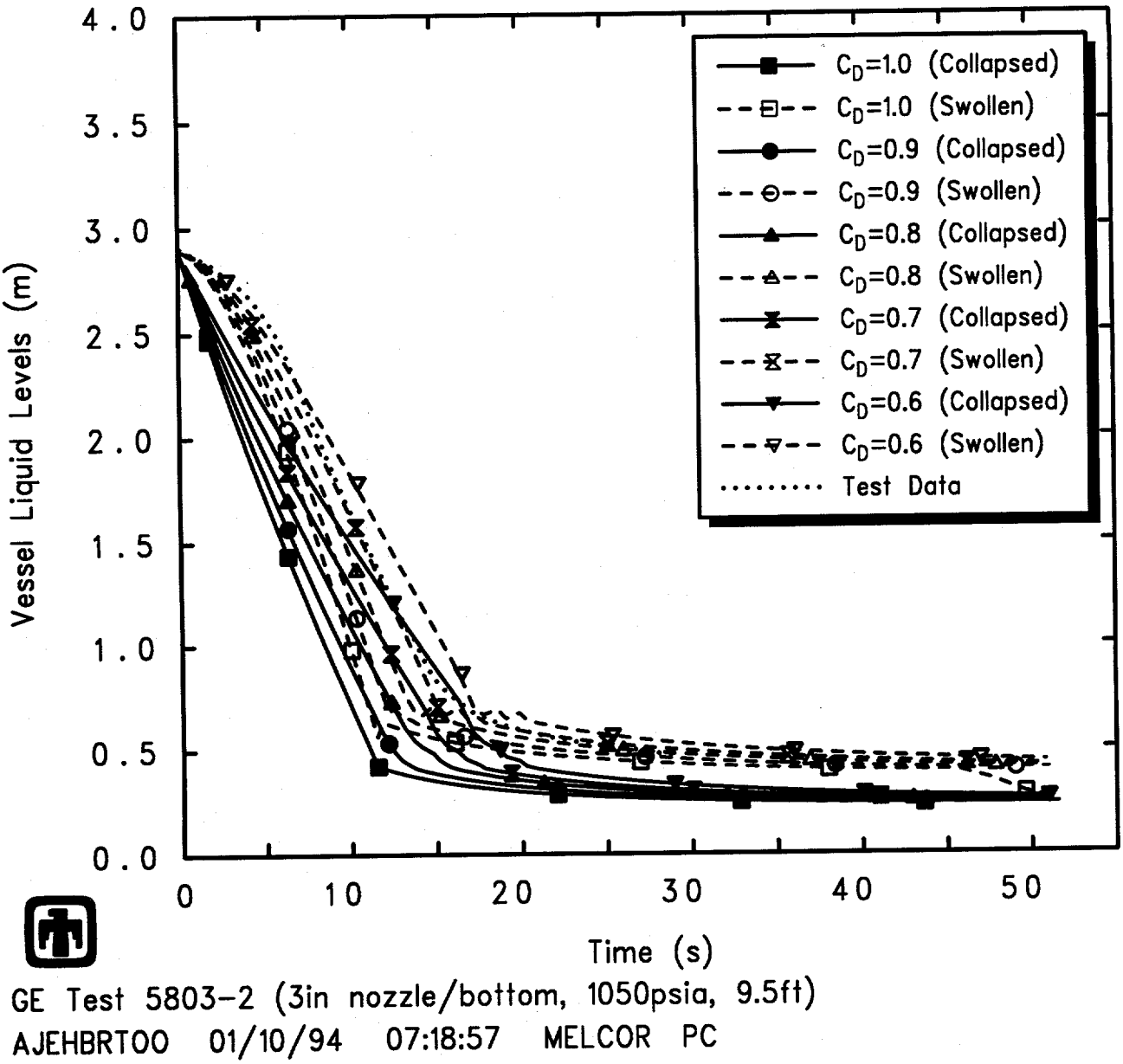

Figure 6.1.16. Vessel Liquid Levels for GE Large Vessel Bottom Blowdown Test 5803-2 – Break Discharge Coefficient Sensitivity Study

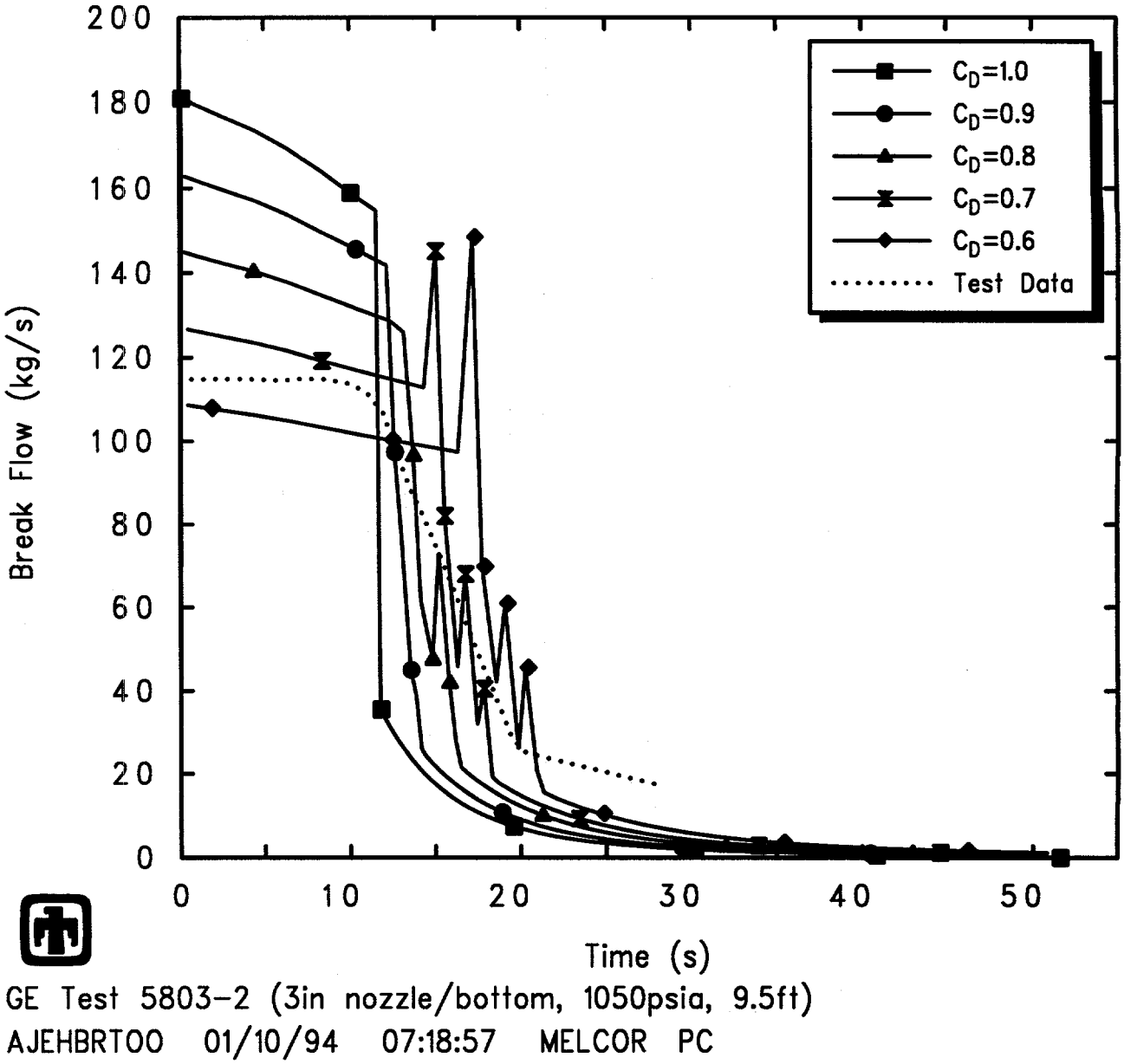

Figure 6.1.17. Blowdown Mass Flow for GE Large Vessel Bottom Blowdown Test 5803-2 – Break Discharge Coefficient Sensitivity Study

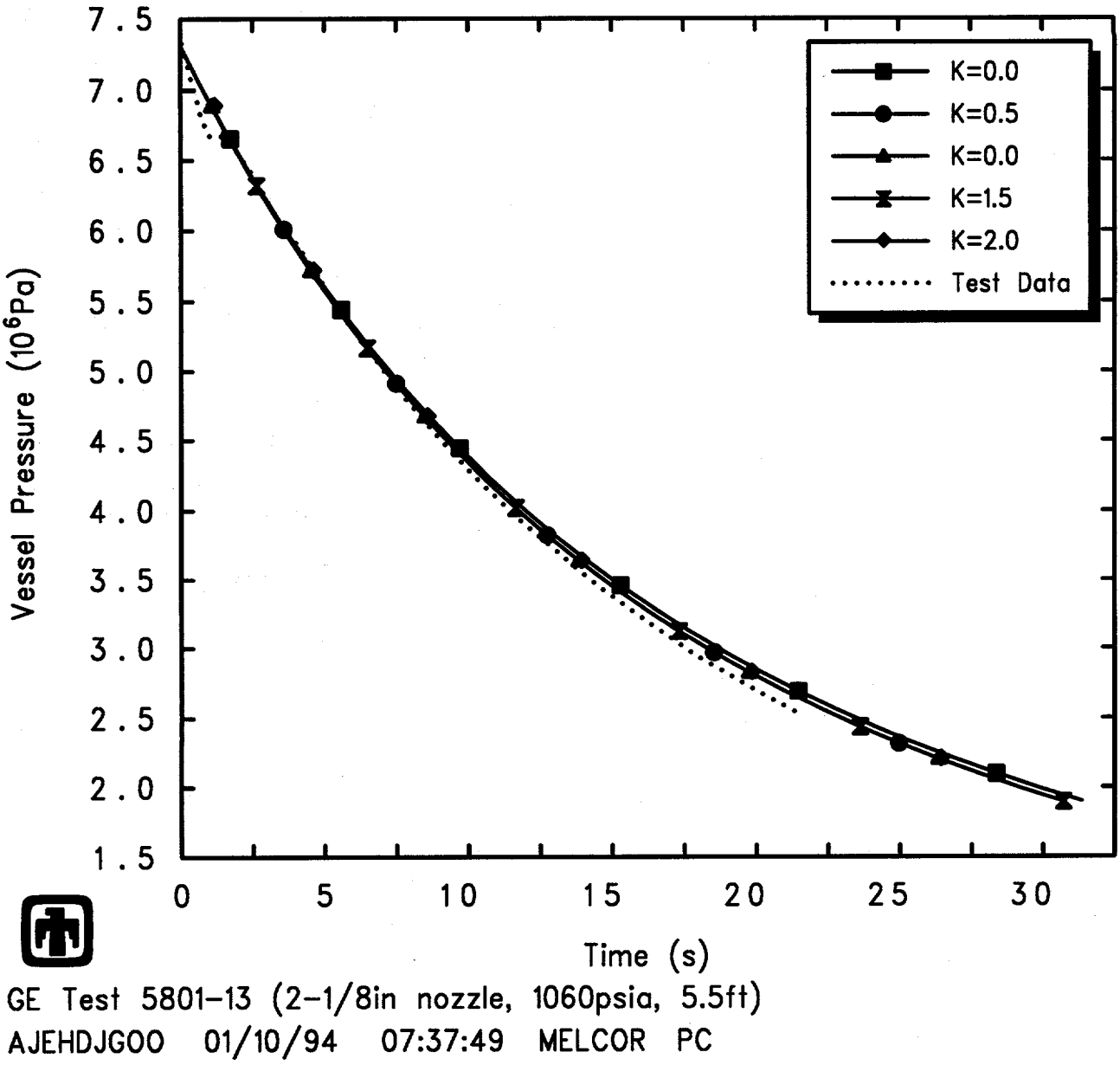

Figure 6.2.1. Vessel Pressure for GE Large Vessel Top Blowdown Test 5801-13 – Blowdown Loss Coefficient Sensitivity Study

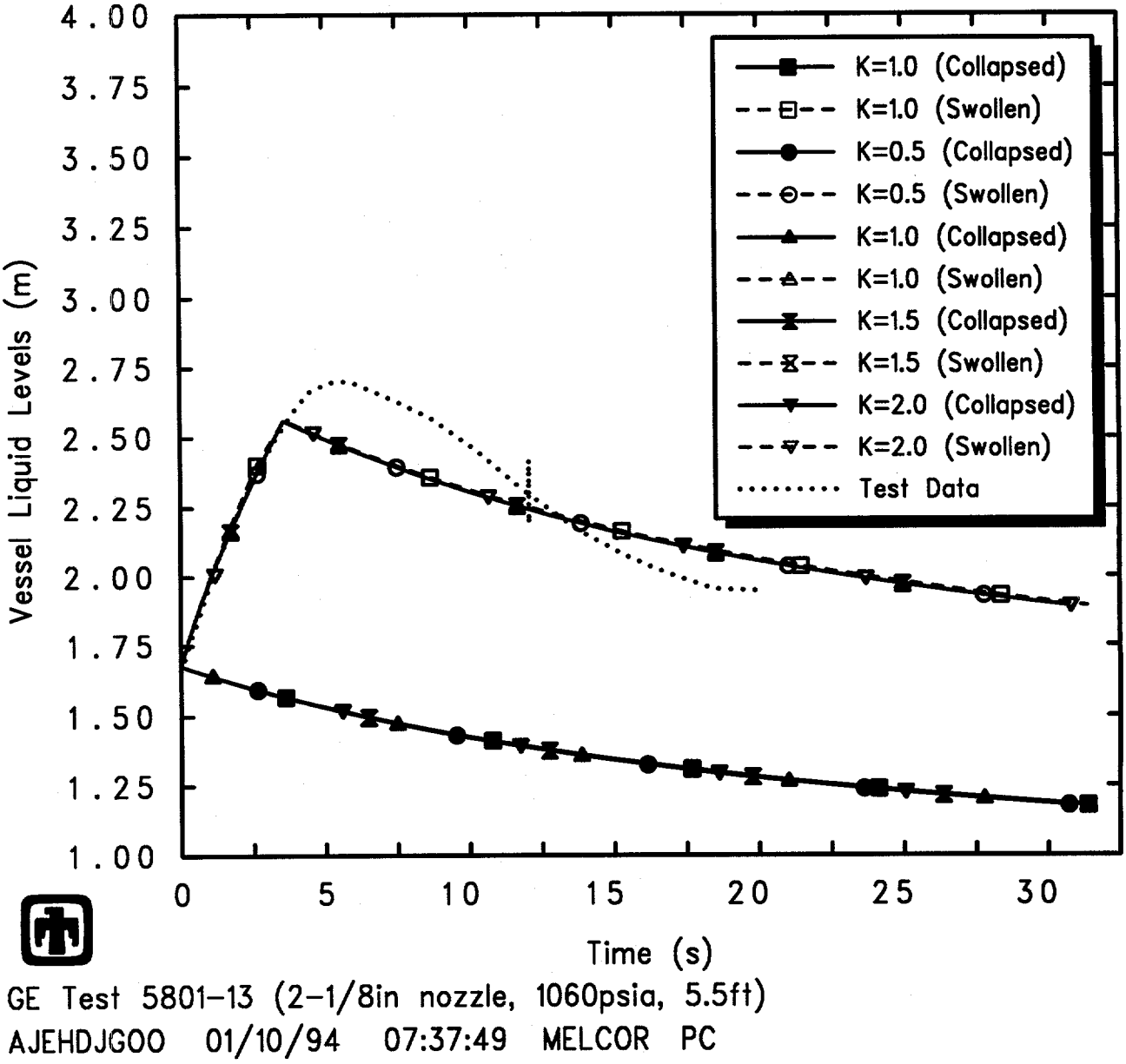

Figure 6.2.2. Vessel Liquid Levels for GE Large Vessel Top Blowdown Test 5801-13 – Blowdown Loss Coefficient Sensitivity Study

flow path form loss coefficients has virtually no visible effect on the predicted vessel depressurization or the two-phase level swell calculated during the depressurization.

Changing the specified blowdown flow path loss coefficients for the bottom blowdown test 5803-1 (with a 2-1/8in nozzle throat diameter) is shown in Figures 6.2.3 through 6.2.6. (Results and conclusions for the other bottom blowdown test, 5803-2, are similar.) Figure 6.2.3 shows the vessel depressurization history calculated by MELCOR, compared to experimental data. The vessel collapsed and swollen (two-phase) liquid levels predicted by MELCOR using these different flow path form loss coefficients, also compared to experimental data, are depicted in Figure 6.2.4. Figure 6.2.5 shows the break flow out the blowdown line and Venturi flow limiting nozzle causing the vessel depressurization, calculated by MELCOR using these different values for the loss coefficients, also comparing to test data, while Figure 6.2.6 presents the calculated bubble fraction within the two-phase mixture in the vessel. Unlike the behavior found in the top blowdown test analyses, reducing the loss coefficients to zero noticeably increases the break flow rates and resultant overall inventory loss, and causes more rapid depressurization, especially in the first part of the transient while the blowdown flow is liquid or a two-phase mixture. There is less level swelling predicted during the liquid and two-phase portions of the blowdown with the flow path loss coefficient set to zero, although the bubble fractions in all cases rises and remains at near the maximum value allowed (0.40) late in the transient, during steam blowdown. The differences, however, are generally minor, and the best agreement with observation is found with the blowdown flow path loss coefficient set to $\geq$1.0.

The insensitivity to form loss coefficient in the top blowdown experiment analyses is primarily because the top of the dip tube remains uncovered in those blowdown transients (in the MELCOR calculations) and thus the blowdown flow is generally steam, with little or no liquid. Due to its low density, the form loss associated with steam (or other vapor) flow is a small term in the overall momentum equation. The greater sensitivity to form loss coefficient found in the bottom blowdown experiment analyses is seen when the blowdown flow is liquid or two-phase, and the results converge after the blowdown flow is generally steam, with little or no liquid.

The results of this study demonstrate that no single value of blowdown flow path form loss coefficient gives visibly agreement with test data, the results indicate that a loss coefficient of 1.0-2.0 gives generally generally agreement with test data through the entire experiment period analyzed. Thus, we used blowdown flow path form loss coefficients of 1.5 in all other MELCOR analyses done as part of this assessment study. This value corresponds to the form loss for an abrupt contraction followed by an abrupt expansion. While the Venturi nozzle used in the blowdown line provides a more gradual contraction and expansion, the results of this study indicate that any differences are minor.

There are also form losses associated with the blowdown pipe entrance (contraction) and exit (expansion) in all these tests, and with the bend in the dip tube in the top blowdown tests. These are negligible relative to the nozzle loss coefficient because they are referenced to the full blowdown line area, rather than to the nozzle minimum area.

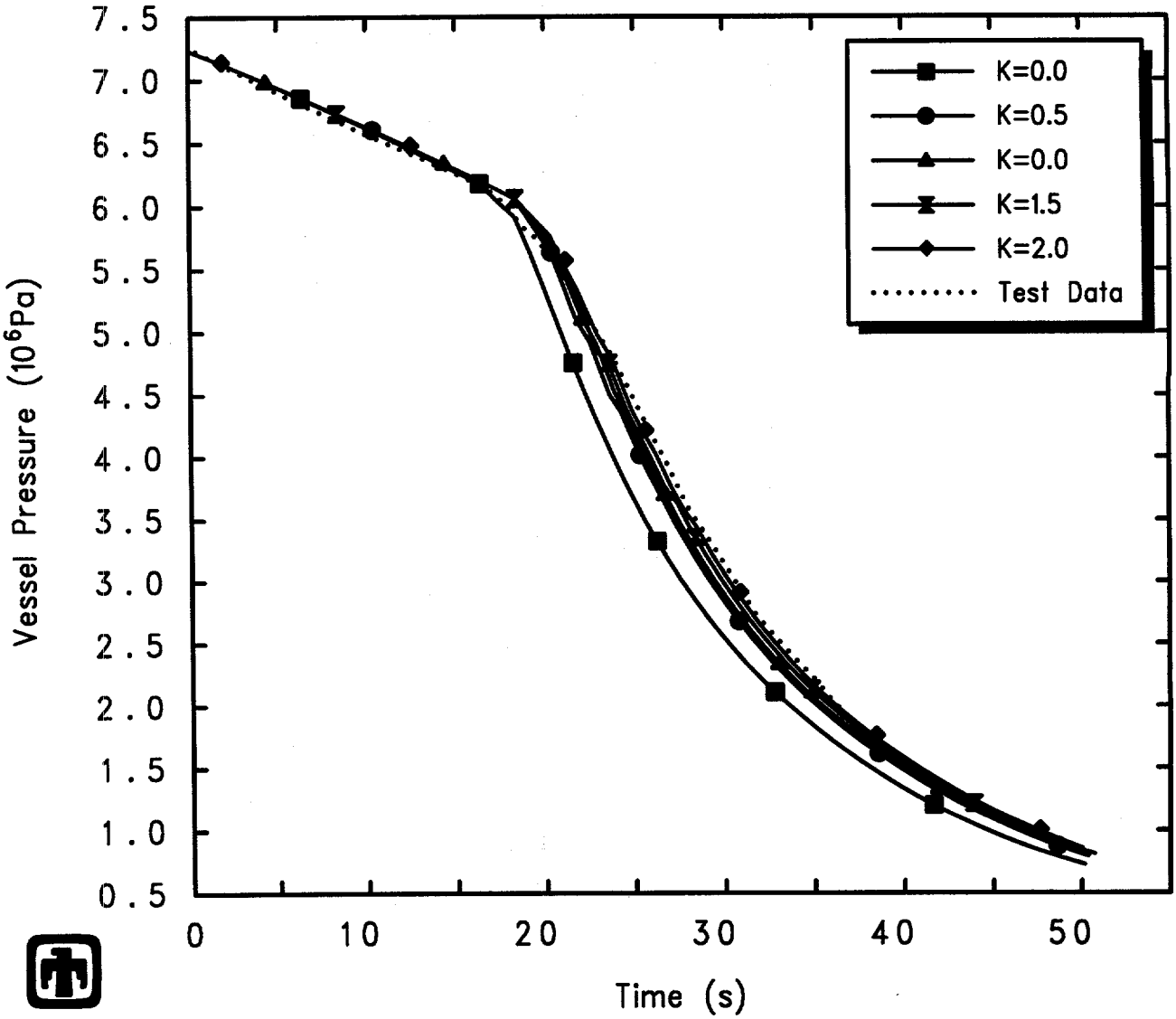

Figure 6.2.3. Vessel Pressure for GE Large Vessel Bottom Blowdown Test 5803-1 – Blowdown Loss Coefficient Sensitivity Study

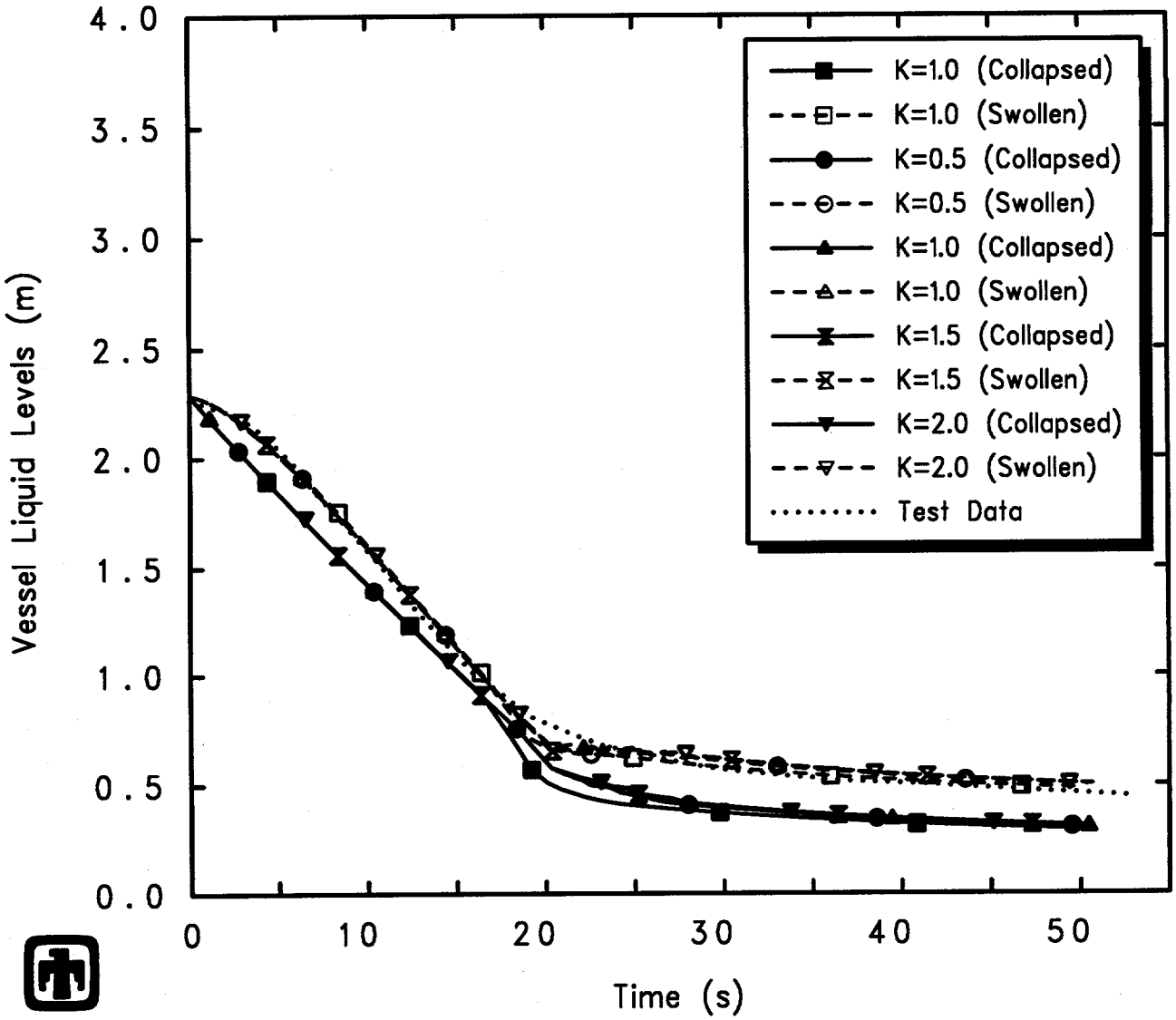

Figure 6.2.4. Vessel Liquid Levels for GE Large Vessel Bottom Blowdown Test 5803-1 – Blowdown Loss Coefficient Sensitivity Study

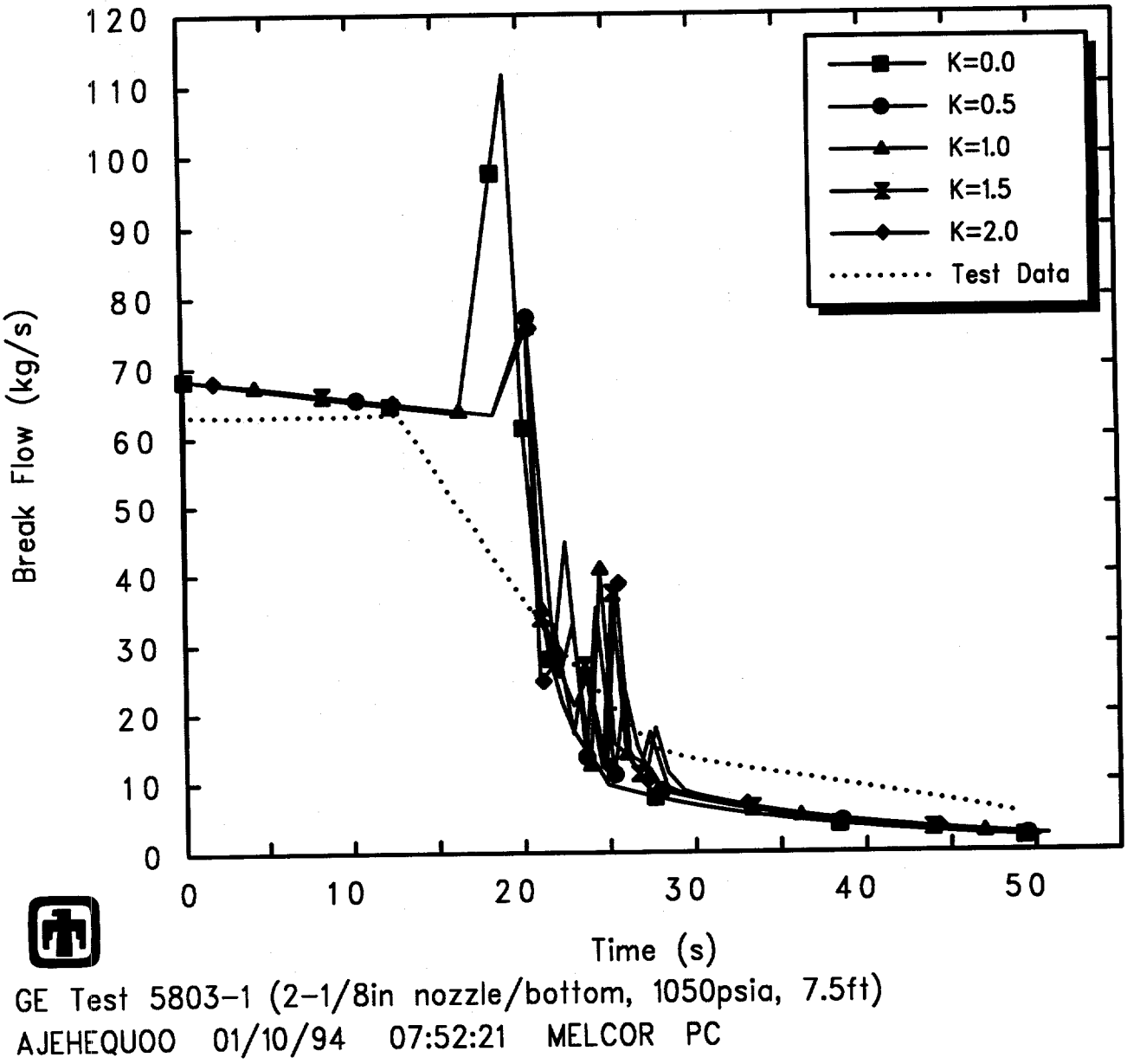

Figure 6.2.5. Blowdown Mass Flow for GE Large Vessel Bottom Blowdown Test 5803-1 – Blowdown Loss Coefficient Sensitivity Study

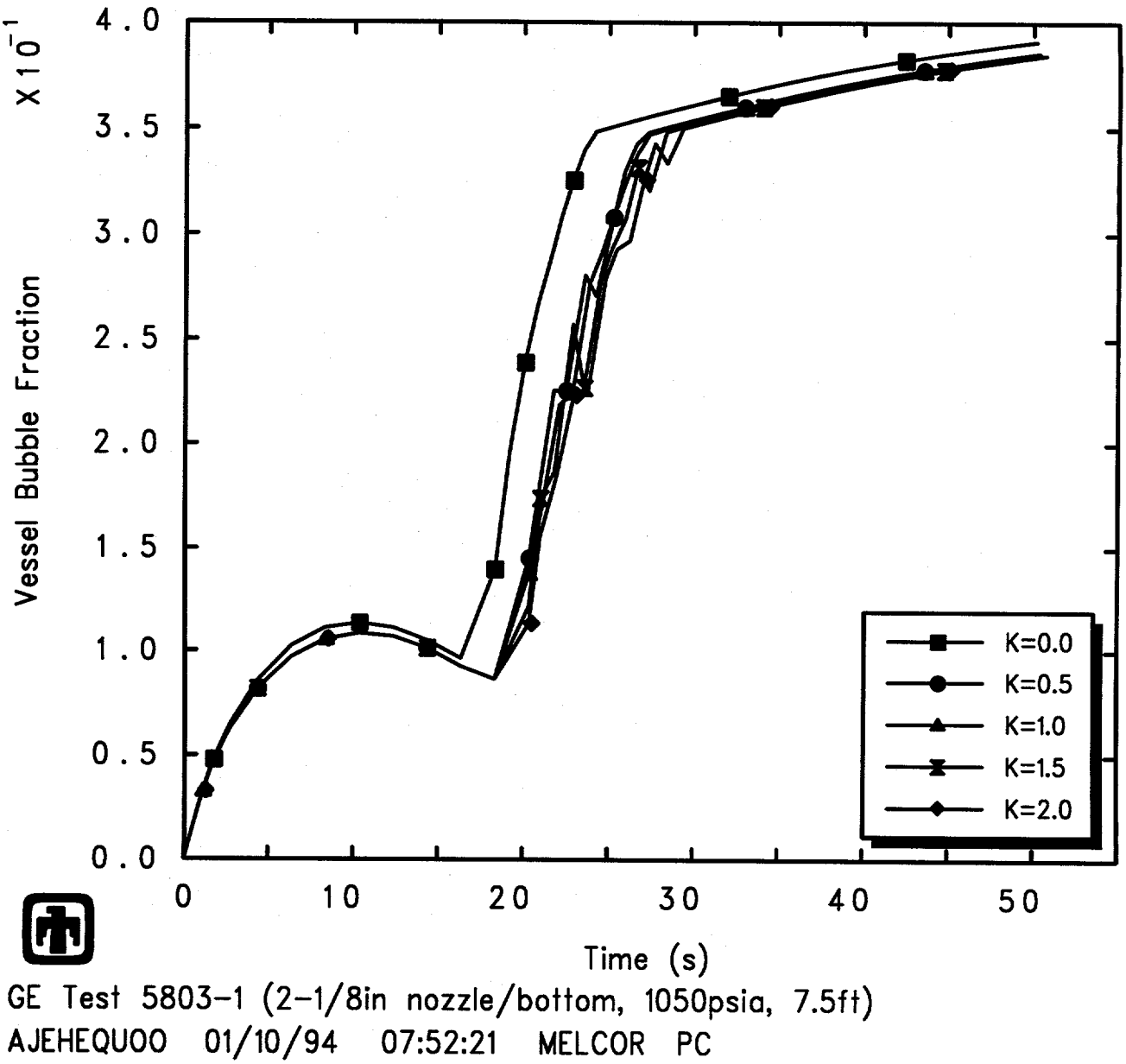

Figure 6.2.6. Vessel Two-Phase Liquid Level Bubble Fraction for GE Large Vessel Bottom Blowdown Test 5803-1 – Blowdown Loss Coefficient Sensitivity Study

6.3 SPARC Bubble Rise Physics

The default code logic in MELCOR is to simply transport any steam and/or non-condensables flowing through a junction directly to the downstream-volume atmosphere. The optional SPARC bubble rise physics model is provided to account for interaction with any intervening water pool in the downstream volume.

Otherwise identical calculations were done for the GE large vessel blowdown and level swell experiments in which the SPARC physics model was turned either on or off in the blowdown flow path, in the inlet (*i.e.*, vessel-side), in the outlet (*i.e.*, environment-side), and in neither or in both sides of the flow path. There were no significant differences in the calculated response in any of the tests analyzed, as illustrated by the sample results for the top blowdown test 5801-13 presented in Figures 6.3.1 through 6.3.4. This bubble rise model does not contribute to the behavior response being predicted by MELCOR for these blowdown and level swell experiment analyses, even though two-phase conditions exist for significant periods in the test vessel, because the model only affects vapor flowing out of a flow path into a two-phase pool region; in the GE large vessel blowdown and level swell experiments, the two-phase conditions are on the upstream, inlet side of the flow path and the downstream sink volume consists of only atmosphere.

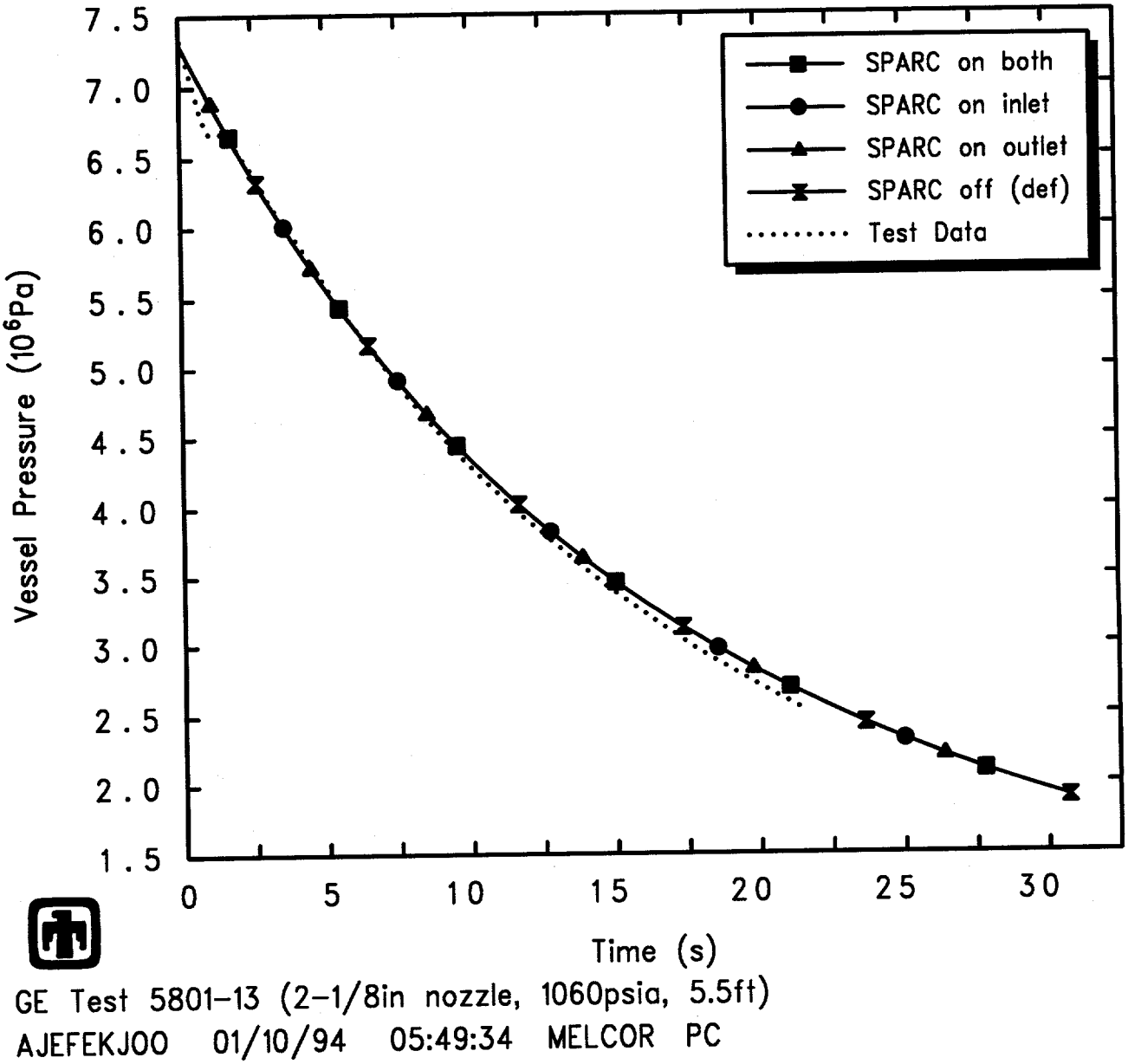

Figure 6.3.1. Vessel Pressure for GE Large Vessel Top Blowdown Test 5801-13 – SPARC Physics Sensitivity Study

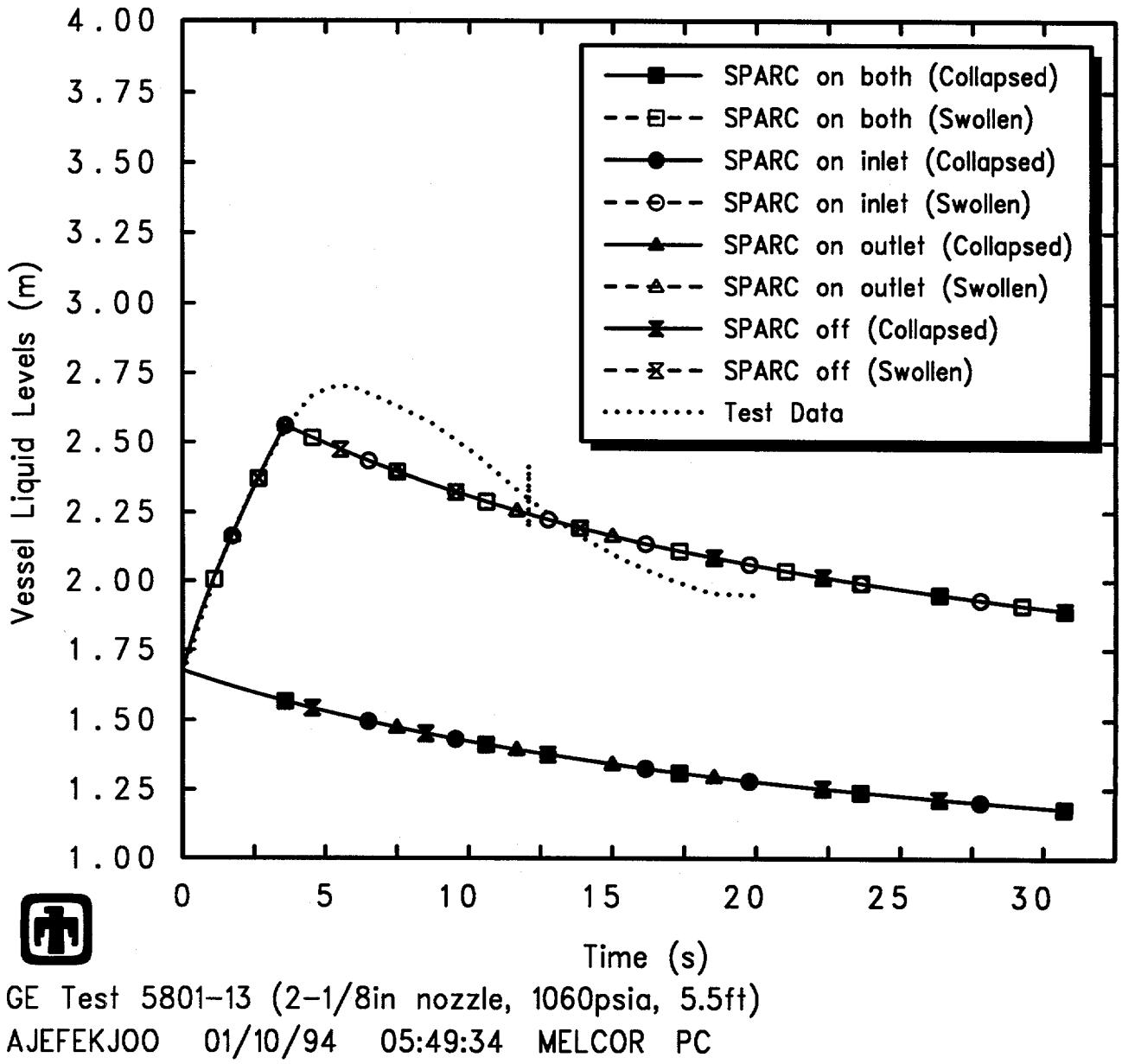

Figure 6.3.2. Vessel Liquid Levels for GE Large Vessel Top Blowdown Test 5801-13 – SPARC Physics Sensitivity Study

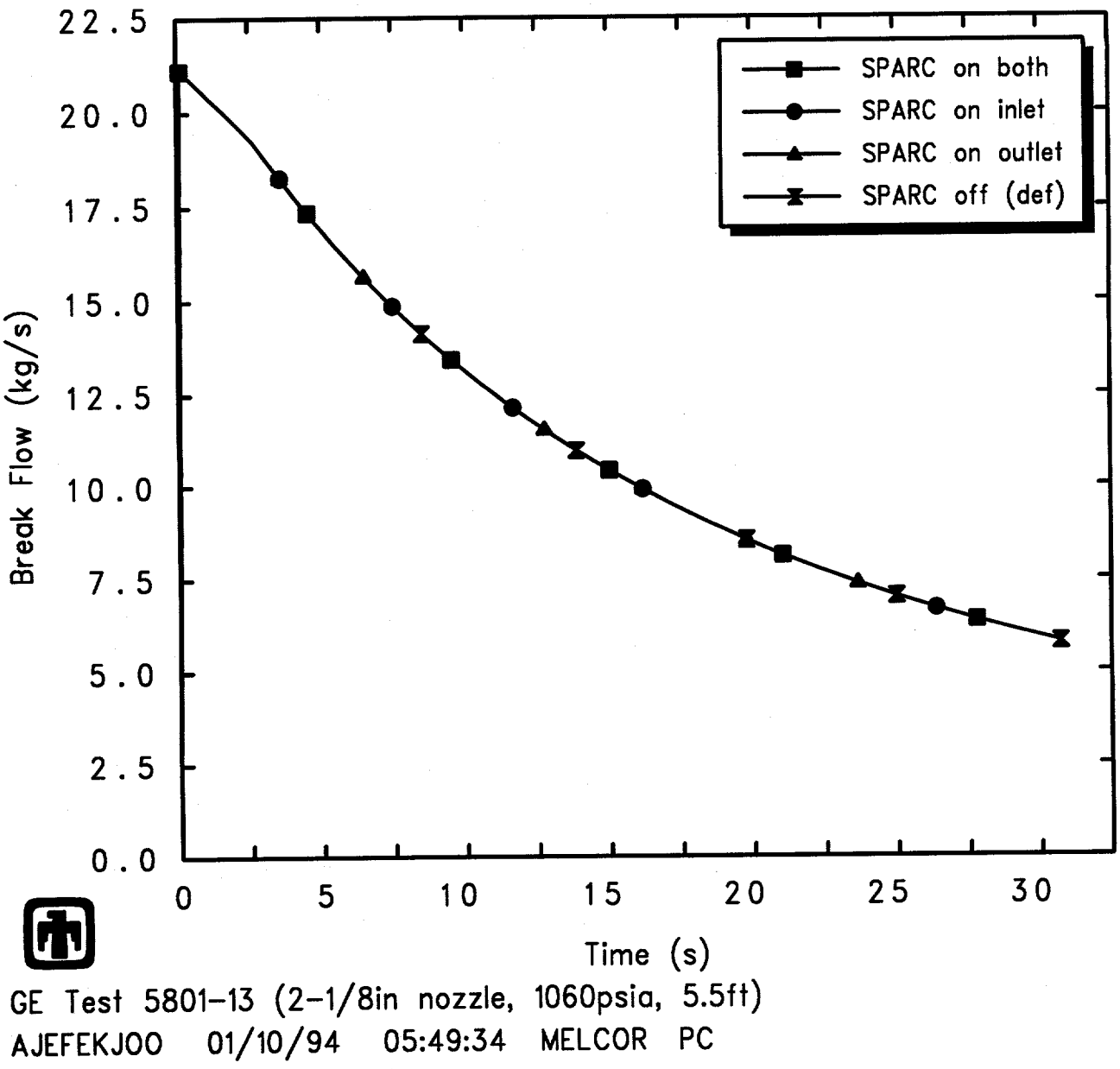

Figure 6.3.3. Blowdown Mass Flow for GE Large Vessel Top Blowdown Test 5801-13 – SPARC Physics Sensitivity Study

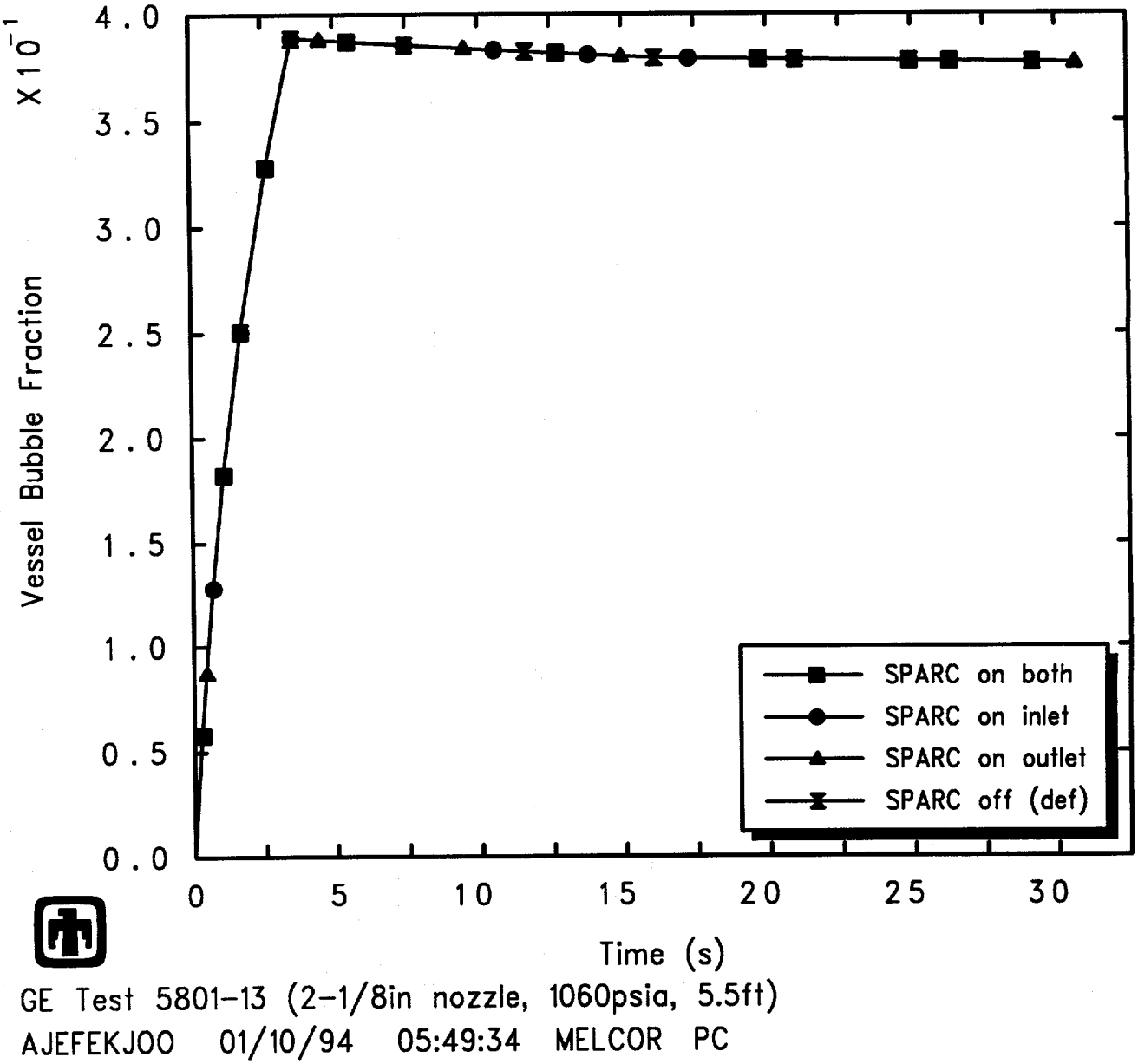

Figure 6.3.4. Vessel Two-Phase Liquid Level Bubble Fraction for GE Large Vessel Top Blowdown Test 5801-13 – SPARC Physics Sensitivity Study

7 Time Step Effects and Machine Dependency

There has been a lot of concern in the past about numeric effects seen in various MELCOR calculations [17], producing either differences in results for the same input on different machines or differences in results when the time step used is varied. Several calculations have been done to identify whether any such effects existed in our GE large vessel blowdown and level swell assessment analyses. This section also compares results obtained with a recent code version (1.8OO) which includes a new implicit bubble separation algorithm with results obtained using the release version of MELCOR 1.8.2, 1.8NM (in which the bubble rise calculation is explicitly coupled to the rest of the thermal/hydraulics analysis).

7.1 Machine Dependencies

The calculations discussed in detail in Section 4, and the majority of our sensitivity study analyses, were run on a 50MHz 486PC (IBM clone). The GE large vessel basecase calculations were rerun, using the same code version (1.8OO), on an IBM RISC-6000 Model 550 workstation, on an HP 755 workstation, on a SUN Sparc2 workstation and on a CRAY Y-MP8/864.

The predicted vessel pressures for the SUN, IBM and HP workstation, and Cray and PC, calculation sets are presented for the top blowdown test 5801-13 in Figure 7.1.1, while the collapsed and swollen vessel liquid levels calculated on these various platforms are compared in Figure 7.1.2. In both figures, experimental data are included for reference. Figure 7.1.3 gives the corresponding blowdown flow rates predicted, and Figure 7.1.4 shows the vessel pool bubble fractions calculated for this test analysis using these various machines. There is very little or no difference found in the results obtained on any of these hardware platforms, and the results seen for this test are characteristic of the behavior found for the other three top blowdown test analyses (not shown here).

Figure 7.1.5 presents total run times required for this top blowdown test 5801-13 analysis on the various platforms; this result is typical of the comparison seen for the other three top blowdown tests. The SUN and PC are always slowest in run time required; the IBM, HP and Cray are all significantly faster with the Cray the fastest by a small fraction for these analyses.

Figure 7.1.6 gives the predicted vessel pressures from the SUN, IBM and HP workstation, and Cray and PC, calculation sets for the bottom blowdown test 5803-1 in Figure 7.1.6. Figure 7.1.7 presents the collapsed and swollen vessel liquid levels calculated on these various platforms, and Figure 7.1.8 compares the corresponding blowdown flow rates predicted. Experimental data are included for reference in all three plots. The vessel pool bubble fractions calculated for this bottom blowdown test analysis on these various machines are illustrated in Figure 7.1.9. There is very little or no difference found in the results obtained on any of these hardware platforms, and the results seen for this test are characteristic of the behavior found for the other bottom blowdown test (5803-2).

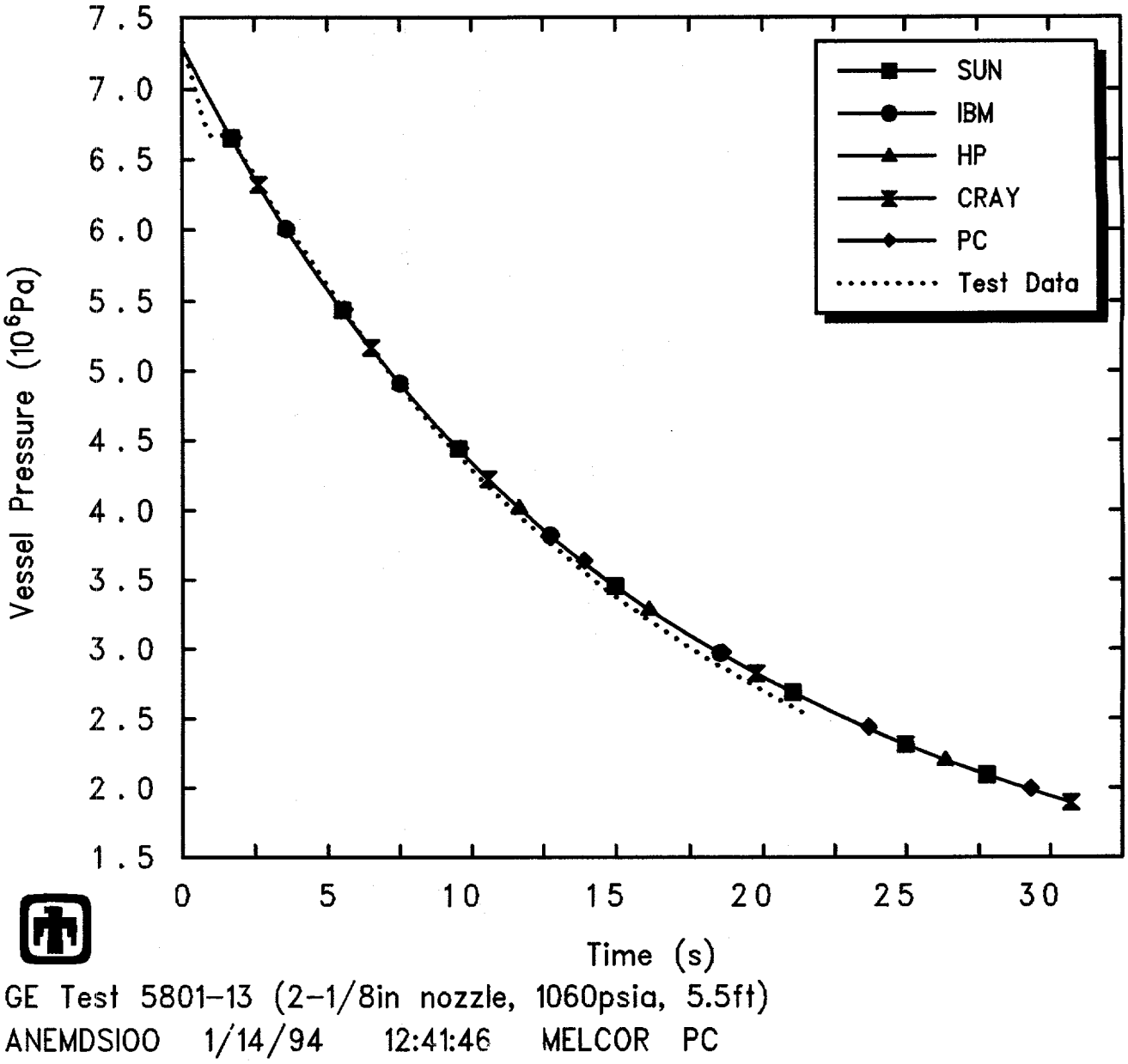

Figure 7.1.1. Vessel Pressure for GE Large Vessel Top Blowdown Test 5801-13 – Machine Dependency Sensitivity Study

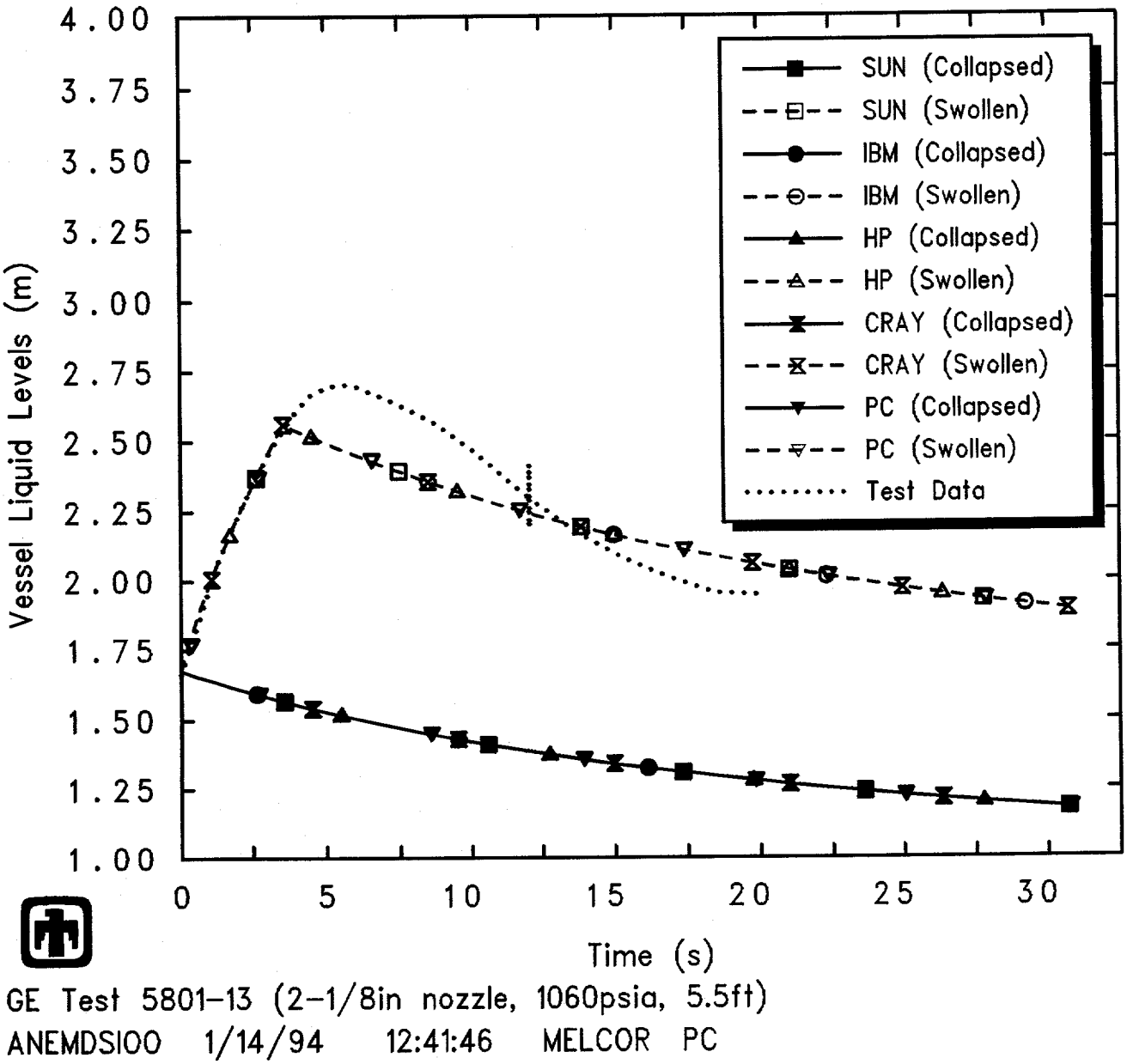

Figure 7.1.2. Vessel Liquid Levels for GE Large Vessel Top Blowdown Test 5801-13 – Machine Dependency Sensitivity Study

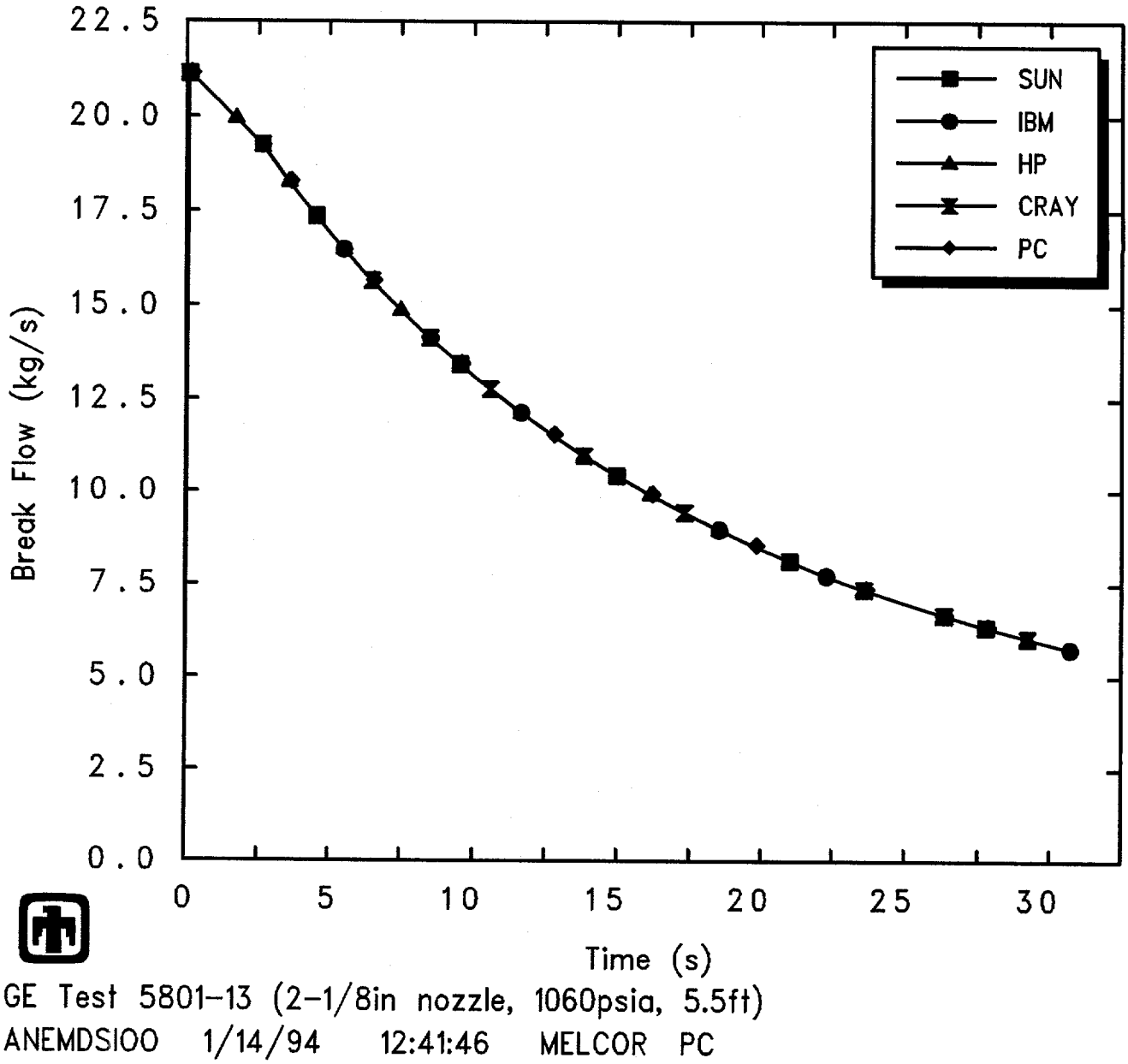

Figure 7.1.3. Blowdown Mass Flow for GE Large Vessel Top Blowdown Test 5801-13 – Machine Dependency Sensitivity Study

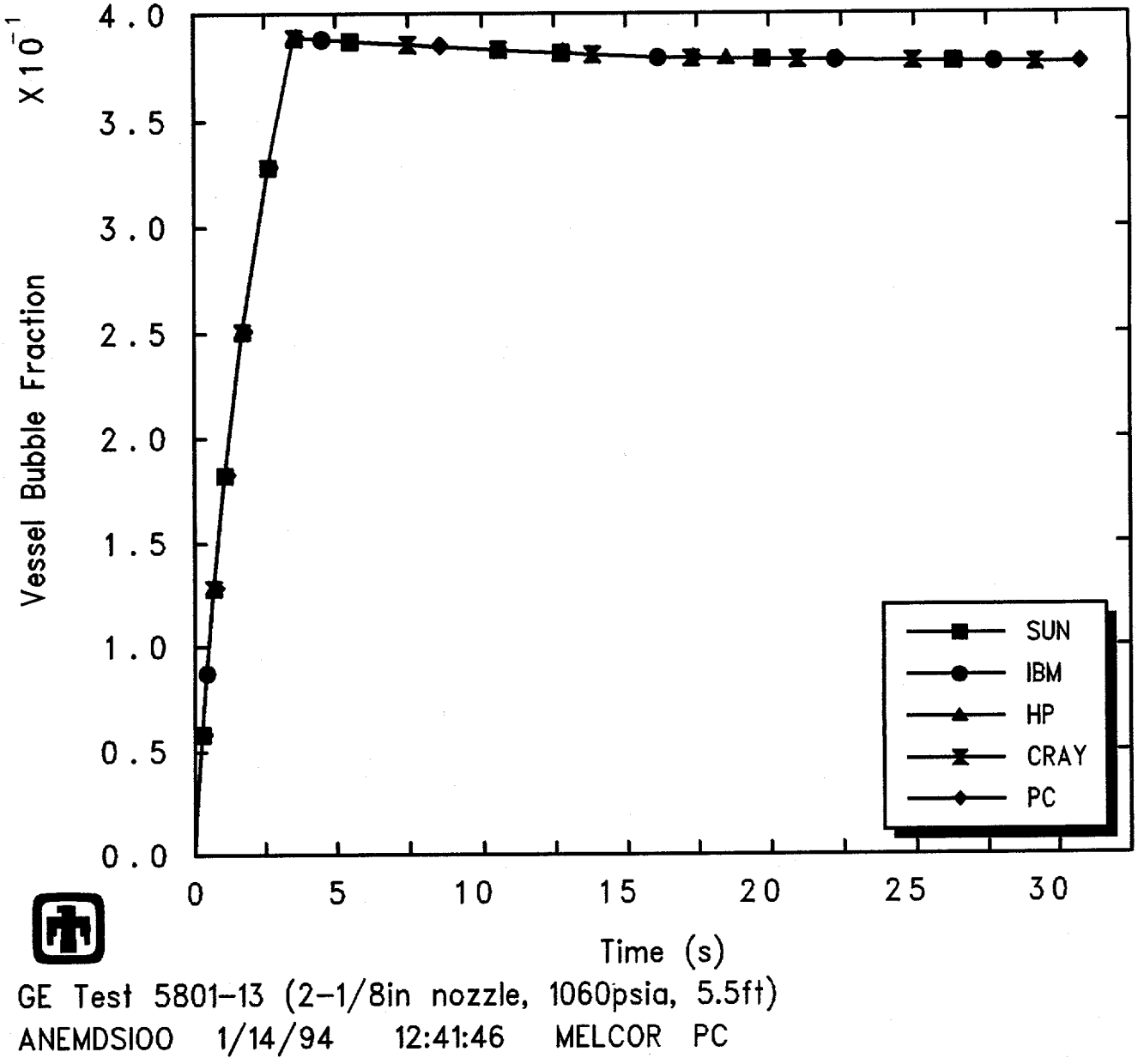

Figure 7.1.4. Vessel Two-Phase Liquid Bubble Fraction for GE Large Vessel Top Blowdown Test 5801-13 – Machine Dependency Sensitivity Study

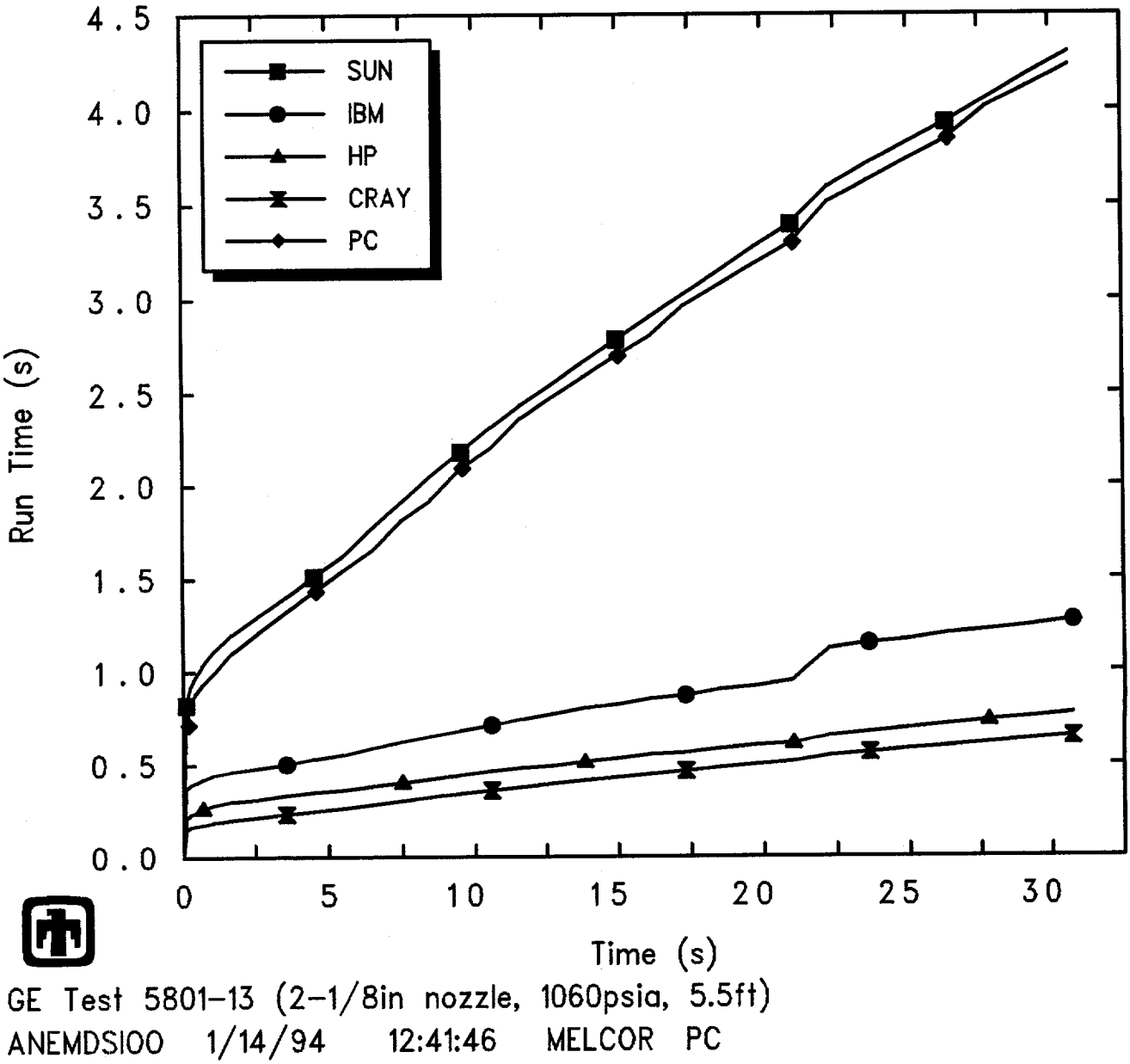

Figure 7.1.5. Total Run Time for GE Large Vessel Top Blowdown Test 5801-13 – Machine Dependency Sensitivity Study

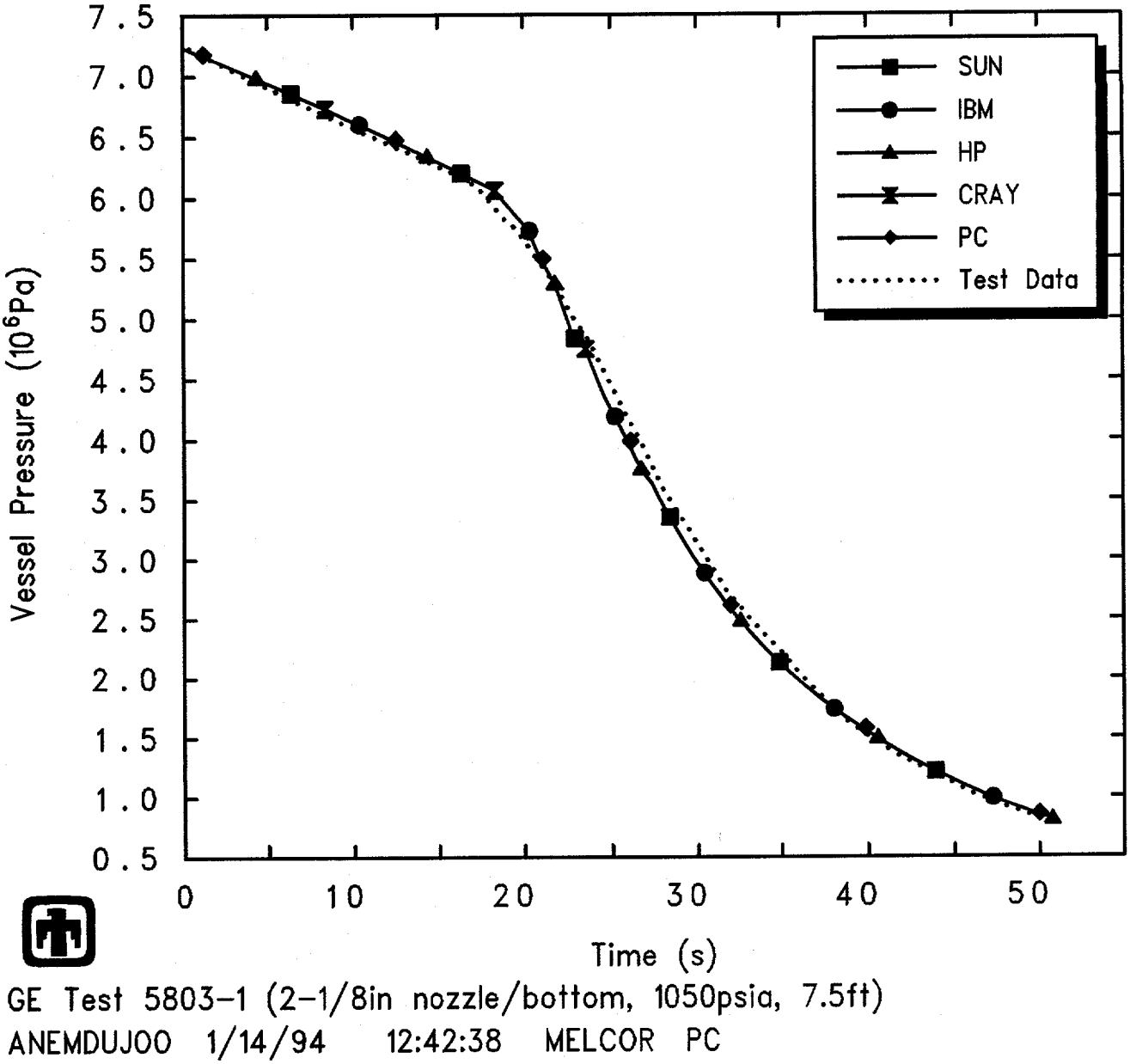

Figure 7.1.6. Vessel Pressure for GE Large Vessel Bottom Blowdown Test 5803-1 – Machine Dependency Sensitivity Study

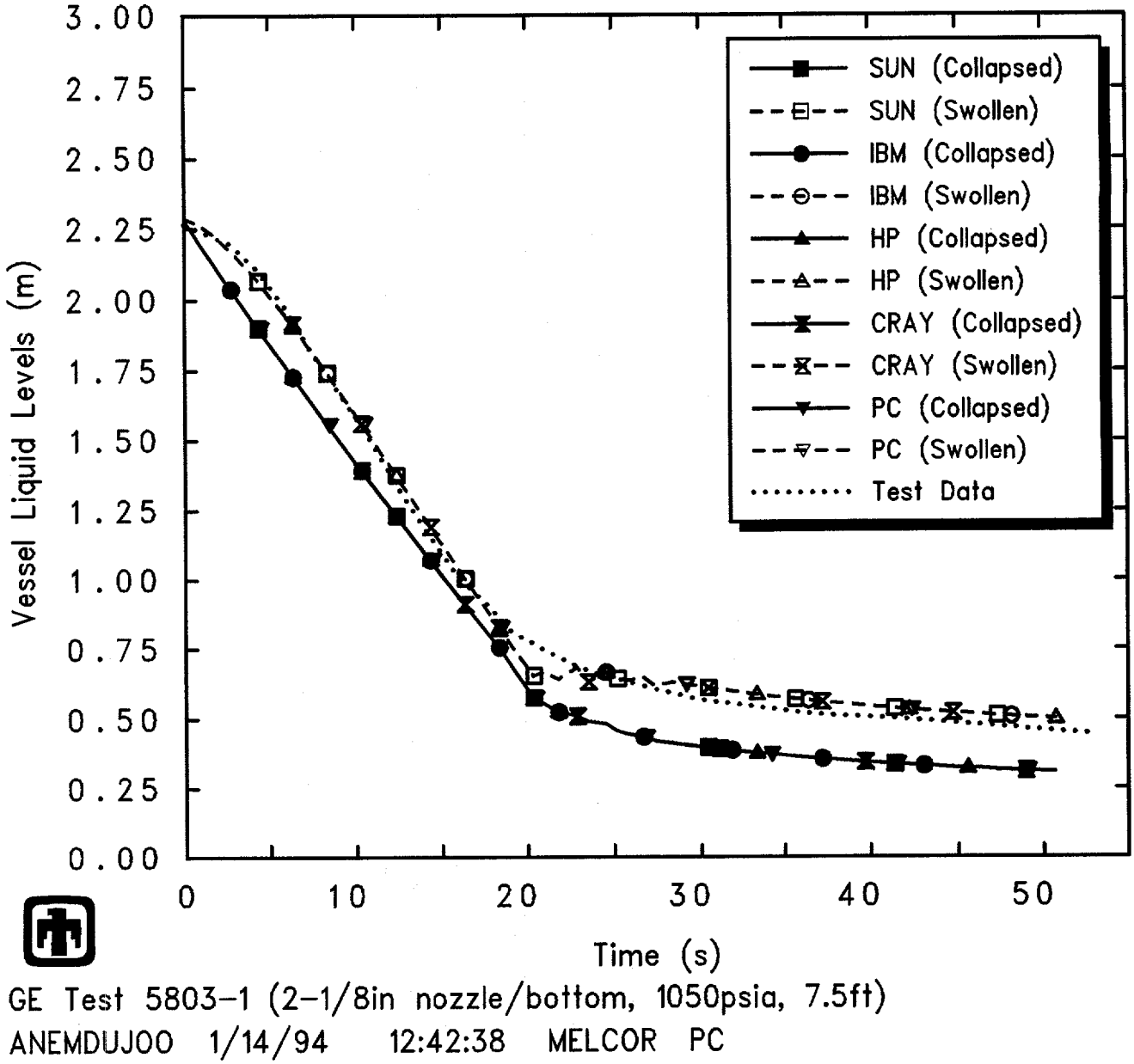

Figure 7.1.7. Vessel Liquid Levels for GE Large Vessel Bottom Blowdown Test 5803-1 – Machine Dependency Sensitivity Study

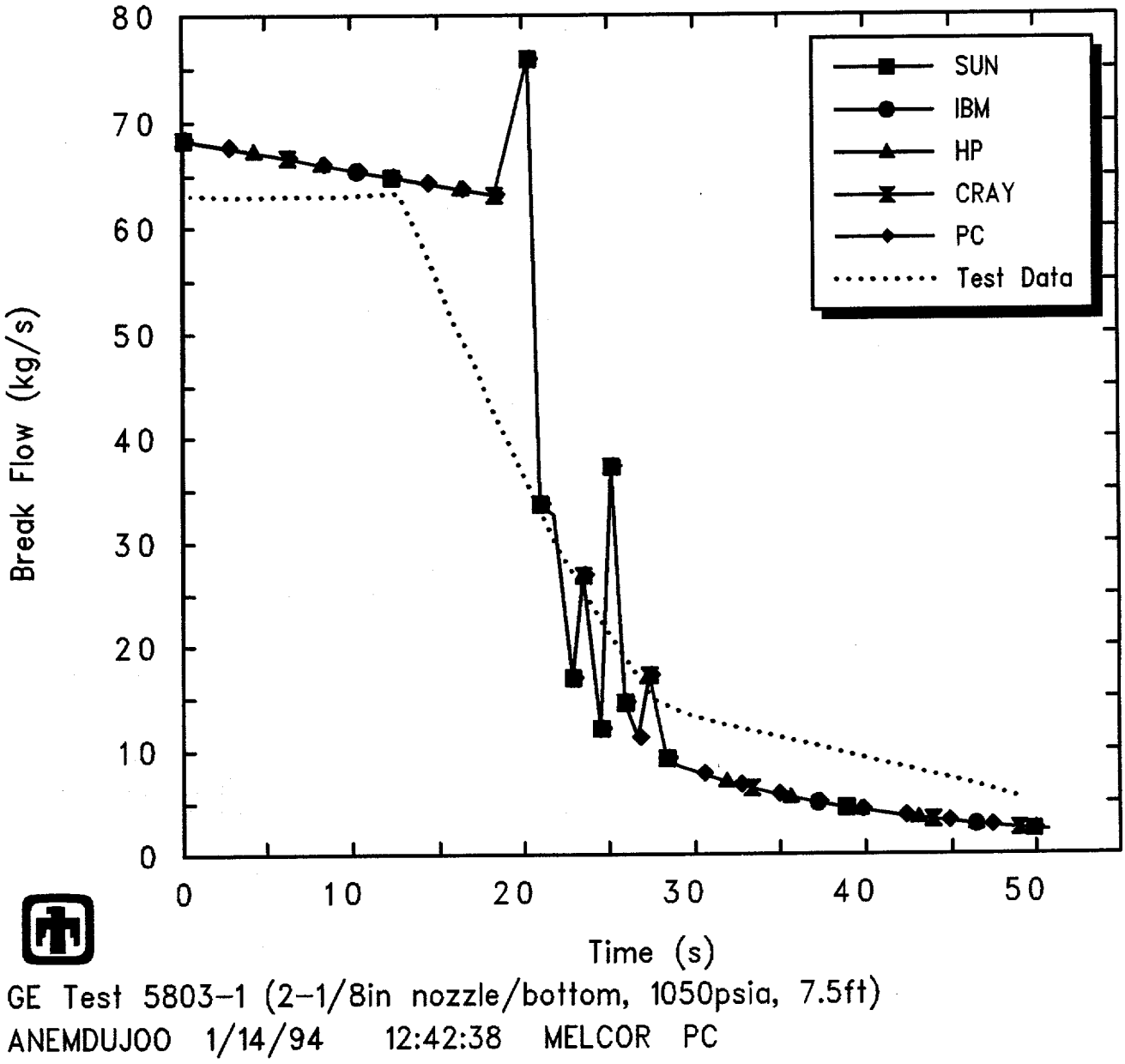

Figure 7.1.8. Blowdown Mass Flow for GE Large Vessel Bottom Blowdown Test 5803-1 – Machine Dependency Sensitivity Study

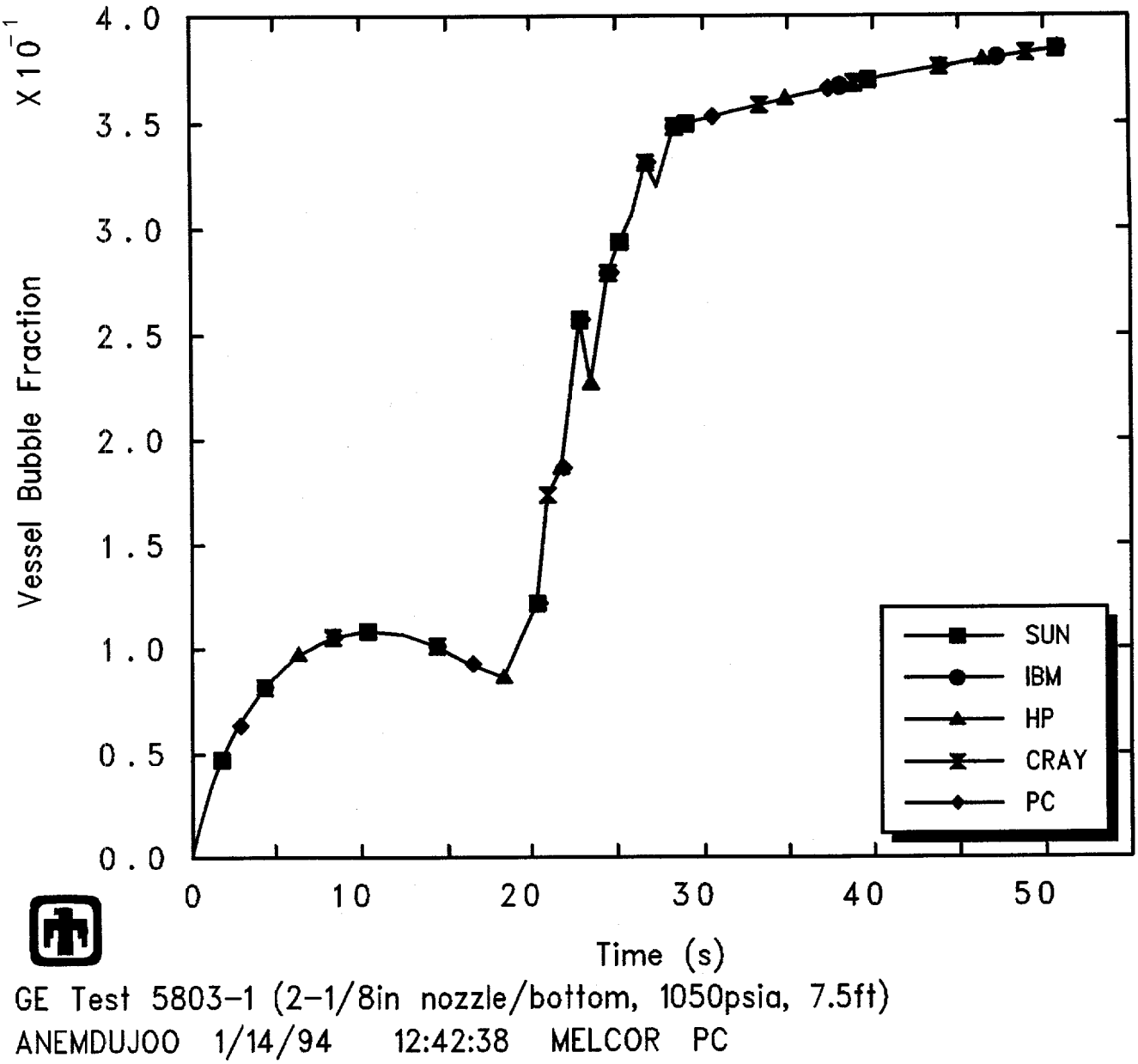

Figure 7.1.9. Vessel Two-Phase Liquid Bubble Fraction for GE Large Vessel Bottom Blowdown Test 5803-1 – Machine Dependency Sensitivity Study

Total run times required for this top blowdown test 5803-1 analysis on the various platforms are compared in Figure 7.1.10, and are typical of the comparison seen for the other bottom blowdown test. As for the top blowdown test analyses, The SUN and PC are always slowest in run time required for these GE large vessel blowdown and level swell experiment analyses; the IBM, HP and Cray are all significantly faster with the Cray the fastest by a small fraction for these analyses.

7.2 Time Step Effects

The user-specified maximum allowed time step in the basecase calculations discussed in Section 4 was set to 2s. As a time step sensitivity study, otherwise identical MELCOR GE large vessel blowdown and level swell assessment calculations were run on a 50MHz 486PC with the user-input maximum allowed time step progressively reduced to 1s, 0.5s, 0.25s and 0.1s. The initial time step in all cases was set to 1ms.

Figure 7.2.1 illustrates for our test 5801-13 analysis that the time step always began increasing smoothly from its initial value of 1ms at the maximum rate of increase allowed until reaching the user-specified maximum allowed Δt. In the basecase calculation, the code internally limited the time step to $\geq$1s before reaching the user-specified maximum allowed value of 2s; setting the user-specified maximum allowed value to >2s would therefore have no effect.

The vessel pressures calculated using these various values of user-specified maximum time steps are presented for the top blowdown test 5801-13 in Figure 7.2.2, while the corresponding collapsed and swollen vessel liquid levels are compared in Figure 7.2.3. In both figures, experimental data are included for reference. Figure 7.2.4 gives the blowdown flow rates predicted in these time step sensitivity study calculations, and Figure 7.2.5 shows the vessel pool bubble fractions calculated for this test analysis using these various maximum allowed time steps. There is very little or no difference found in the results obtained; a small spread in calculated blowdown flow rates is visible in Figure 7.2.4, but with no apparent effect on the predicted vessel depressurization rates.

Figure 7.2.6 presents total run times required for this top blowdown test 5801-13 analysis with the time step histories shown in Figure 7.2.1. As would be expected, reducing the time step and thus increasing the number of cycles required correspondingly increases the run times required.

The results seen for test 5801-13 are typical of the behavior found for the other three top blowdown test analyses which are, therefore, not shown here.

The response found varying the time step in the bottom blowdown test analyses was generally similar to that seen in the top blowdown test calculations. Also, the results presented here for the bottom blowdown test 5803-1 analyses are characteristic of the behavior found for the other bottom blowdown test (5803-2), which also are not shown.

Figure 7.2.7 presents the actual time step histories in calculations varying the user-specified maximum allowed time steps. As shown in Figure 7.2.1 for the top blowdown

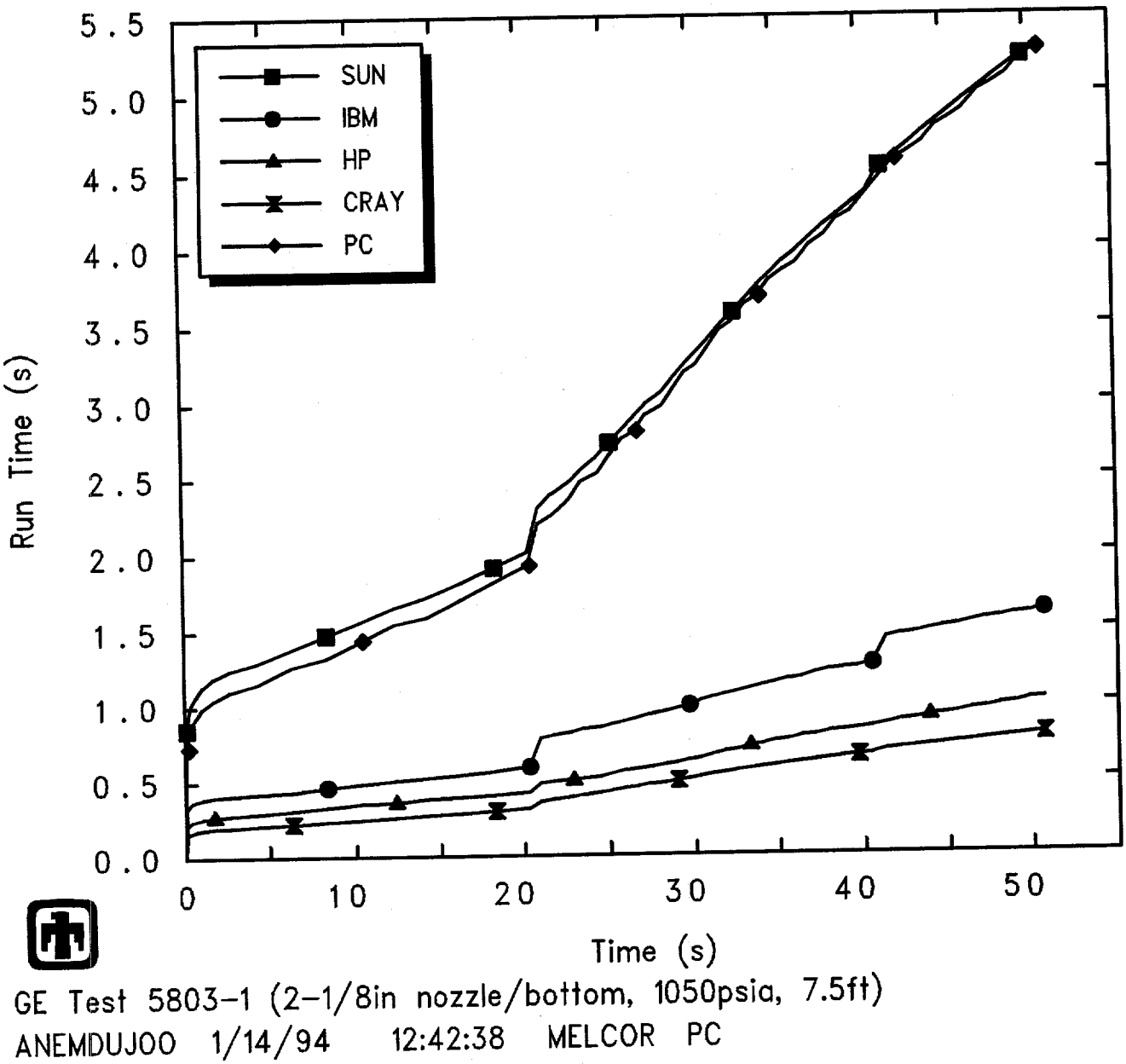

Figure 7.1.10. Total Run Time for GE Large Vessel Bottom Blowdown Test 5803-1 – Machine Dependency Sensitivity Study

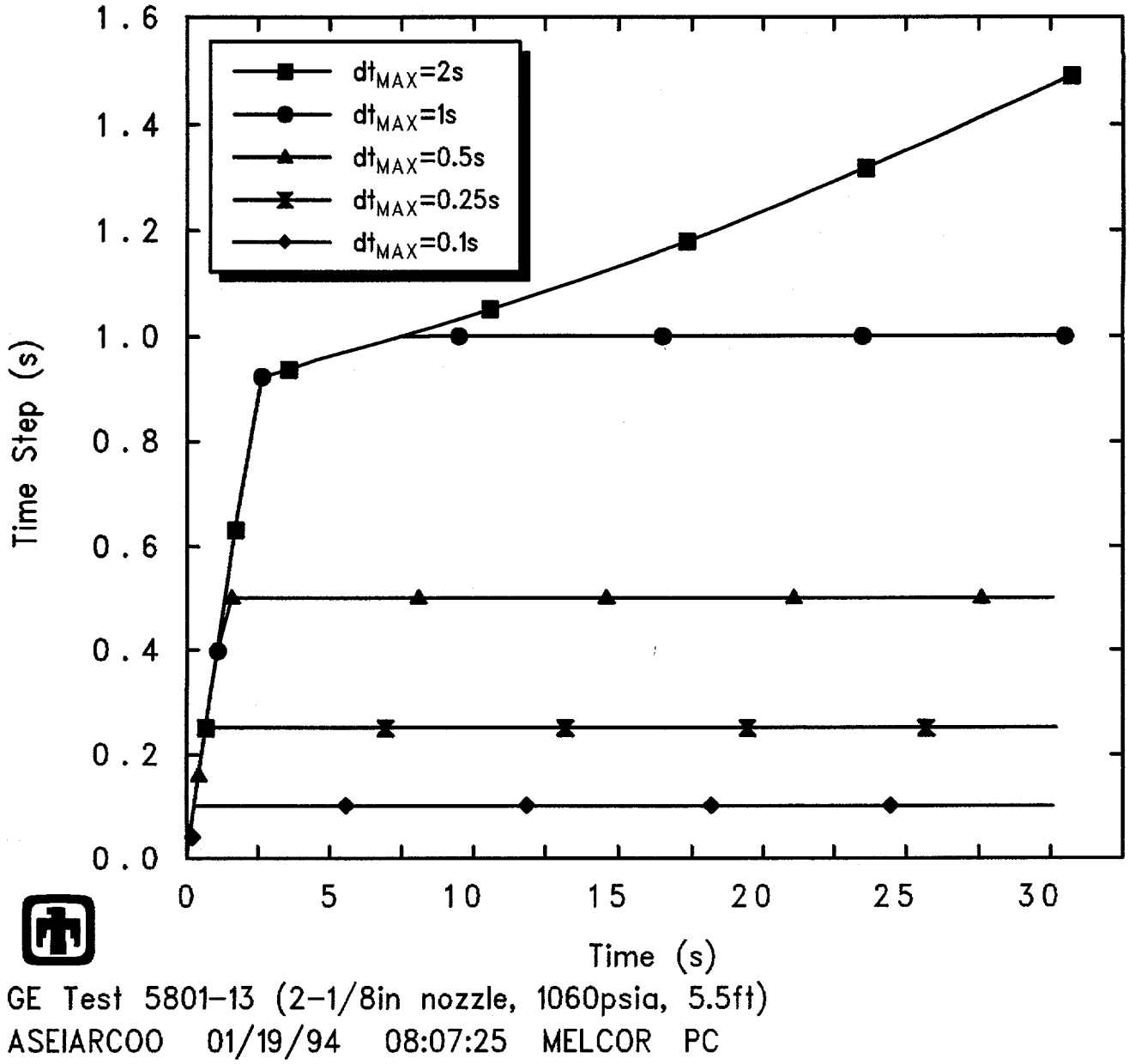

Figure 7.2.1. Time Steps for GE Large Vessel Top Blowdown Test 5801-13 – Time Step Sensitivity Study

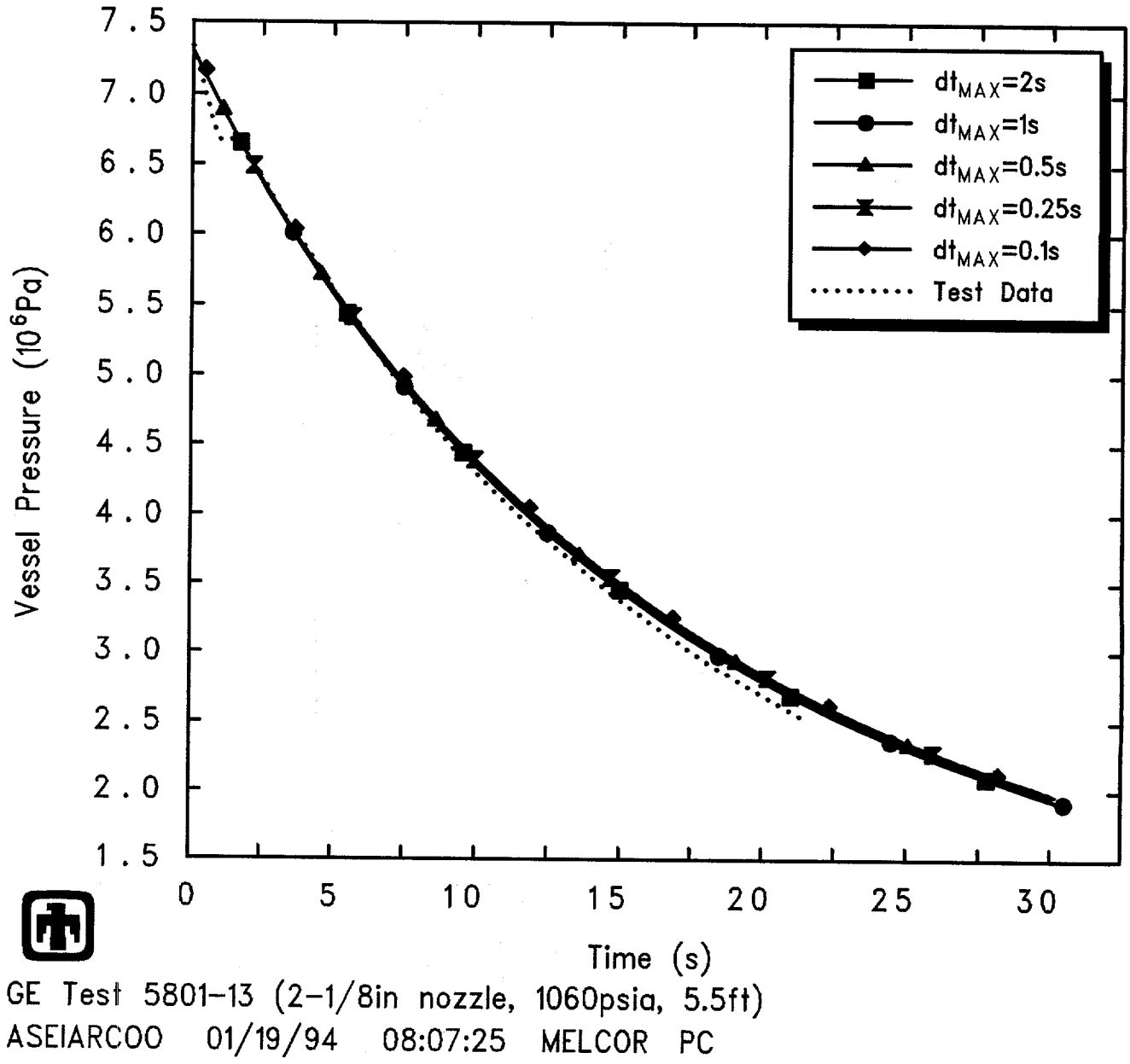

Figure 7.2.2. Vessel Pressure for GE Large Vessel Top Blowdown Test 5801-13 – Time Step Sensitivity Study

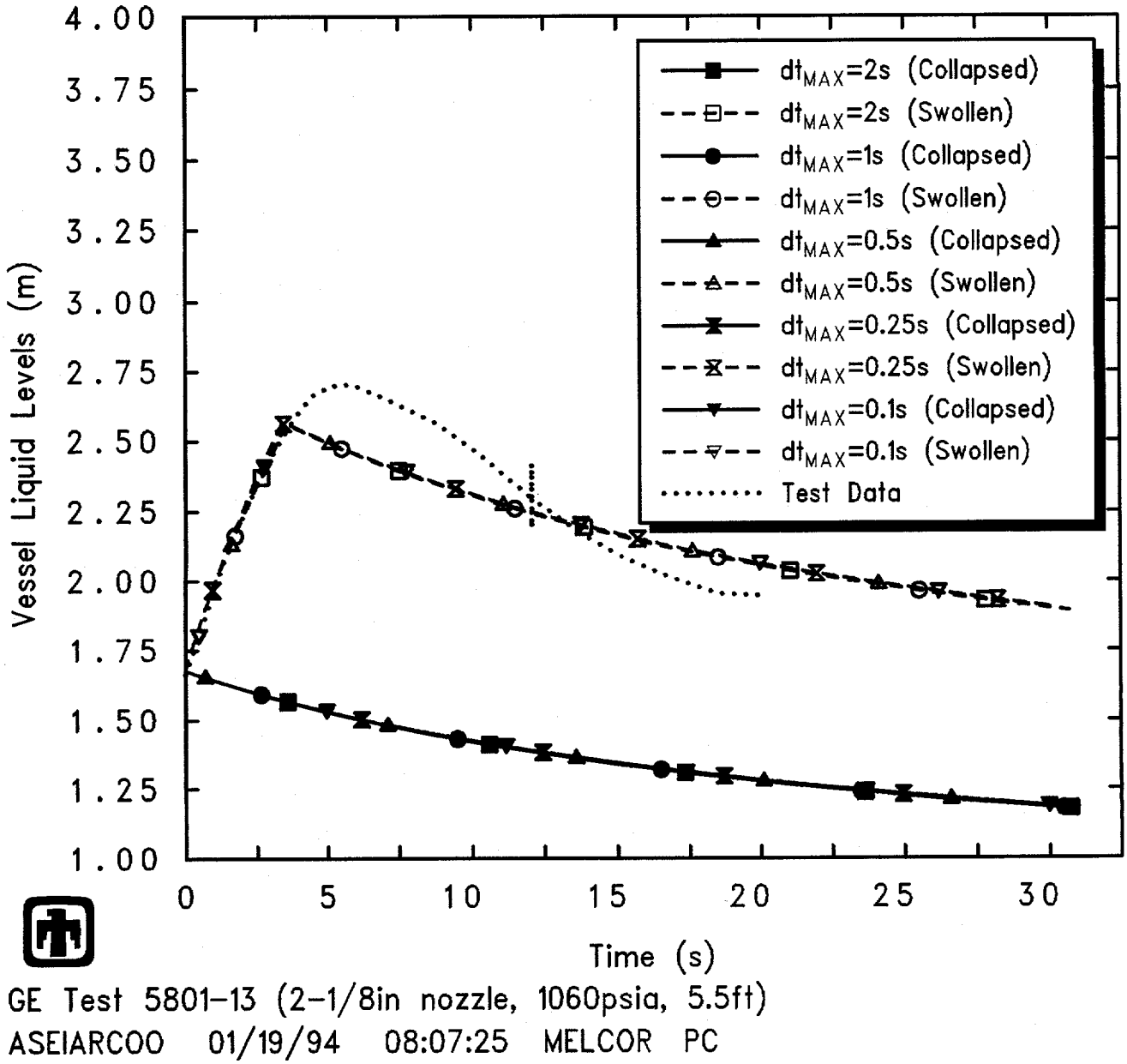

Figure 7.2.3. Vessel Liquid Levels for GE Large Vessel Top Blowdown Test 5801-13 – Time Step Sensitivity Study

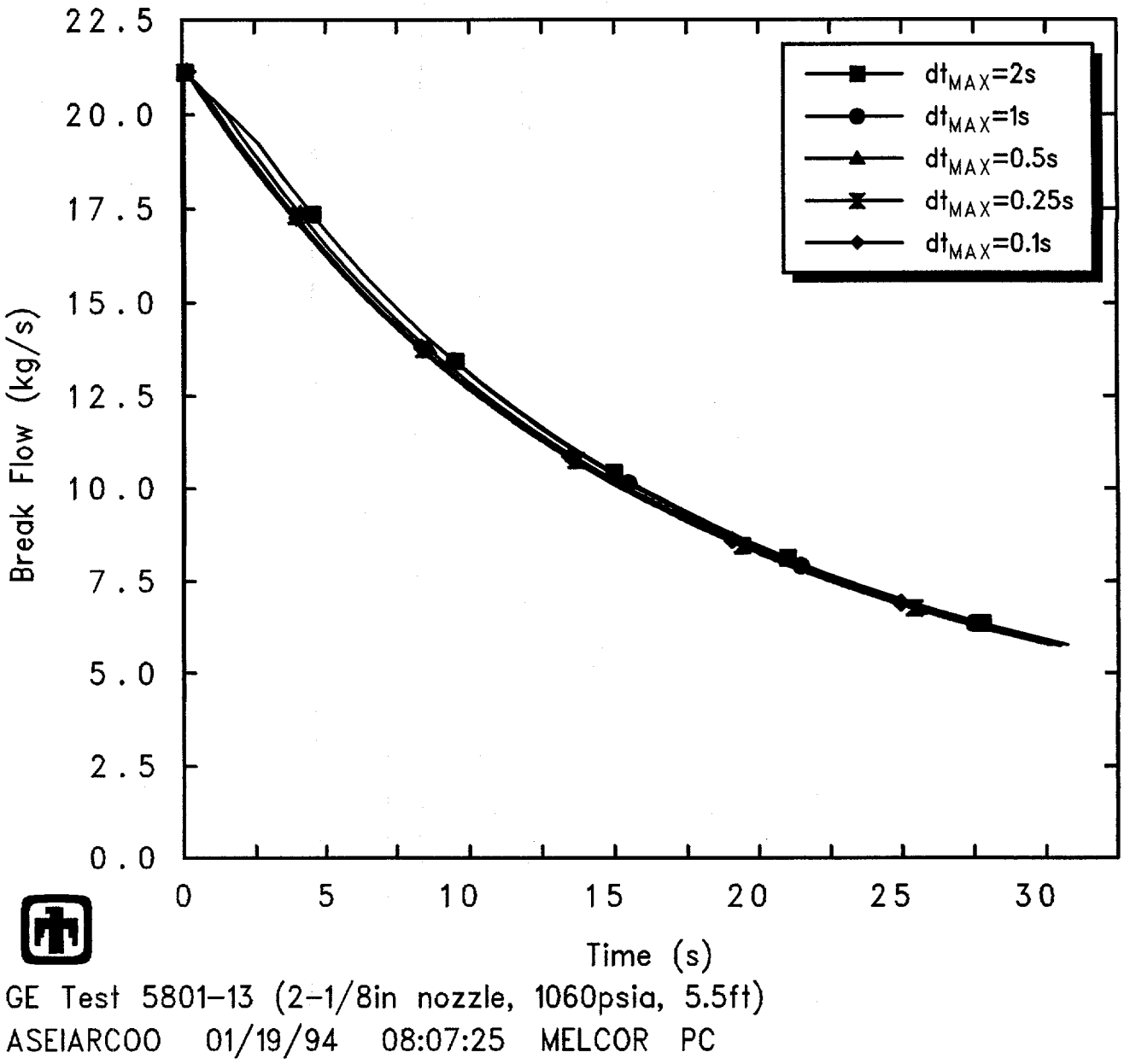

Figure 7.2.4. Blowdown Mass Flow for GE Large Vessel Top Blowdown Test 5801-13 – Time Step Sensitivity Study

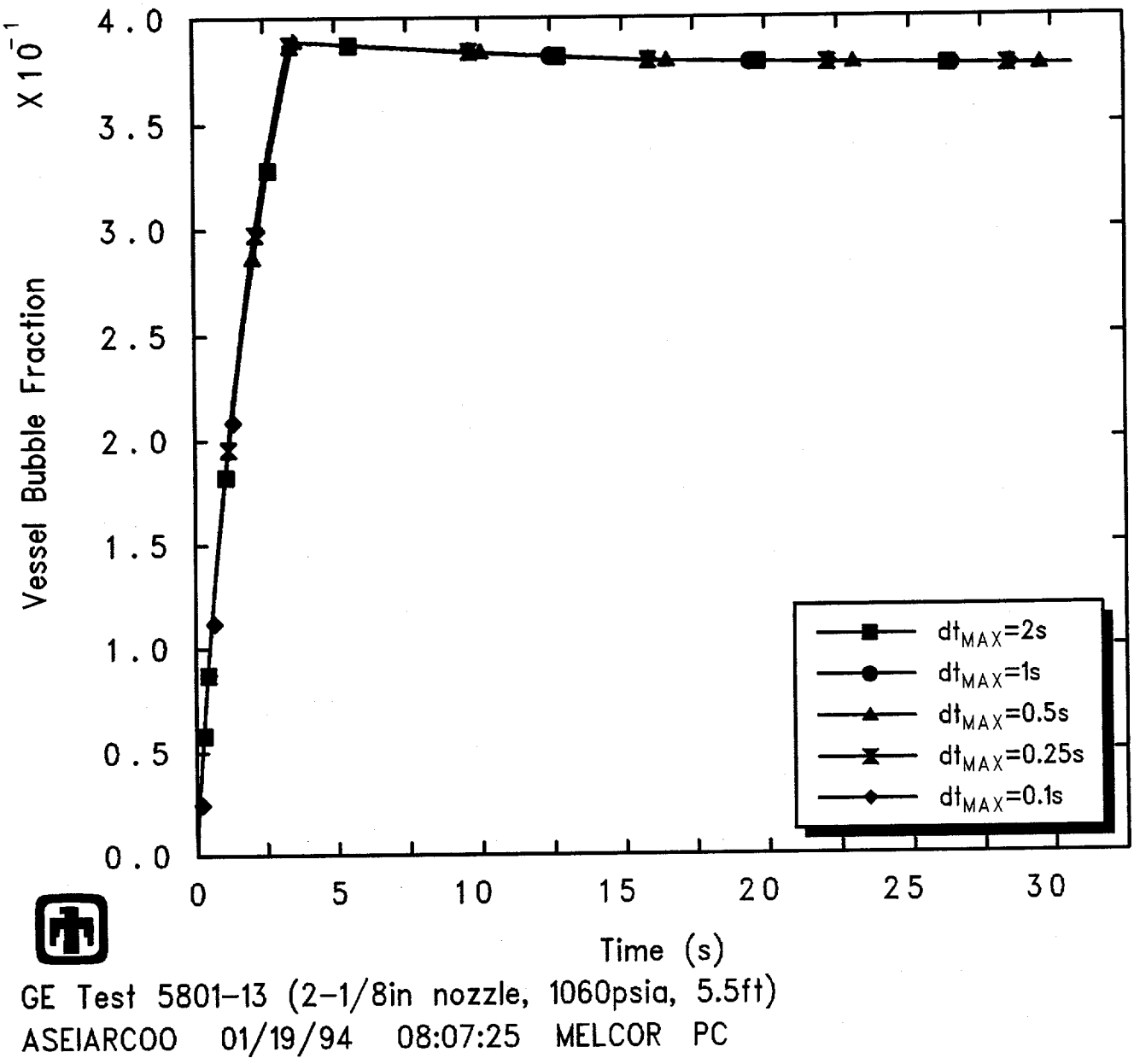

Figure 7.2.5. Vessel Two-Phase Liquid Bubble Fraction for GE Large Vessel Top Blowdown Test 5801-13 – Time Step Sensitivity Study

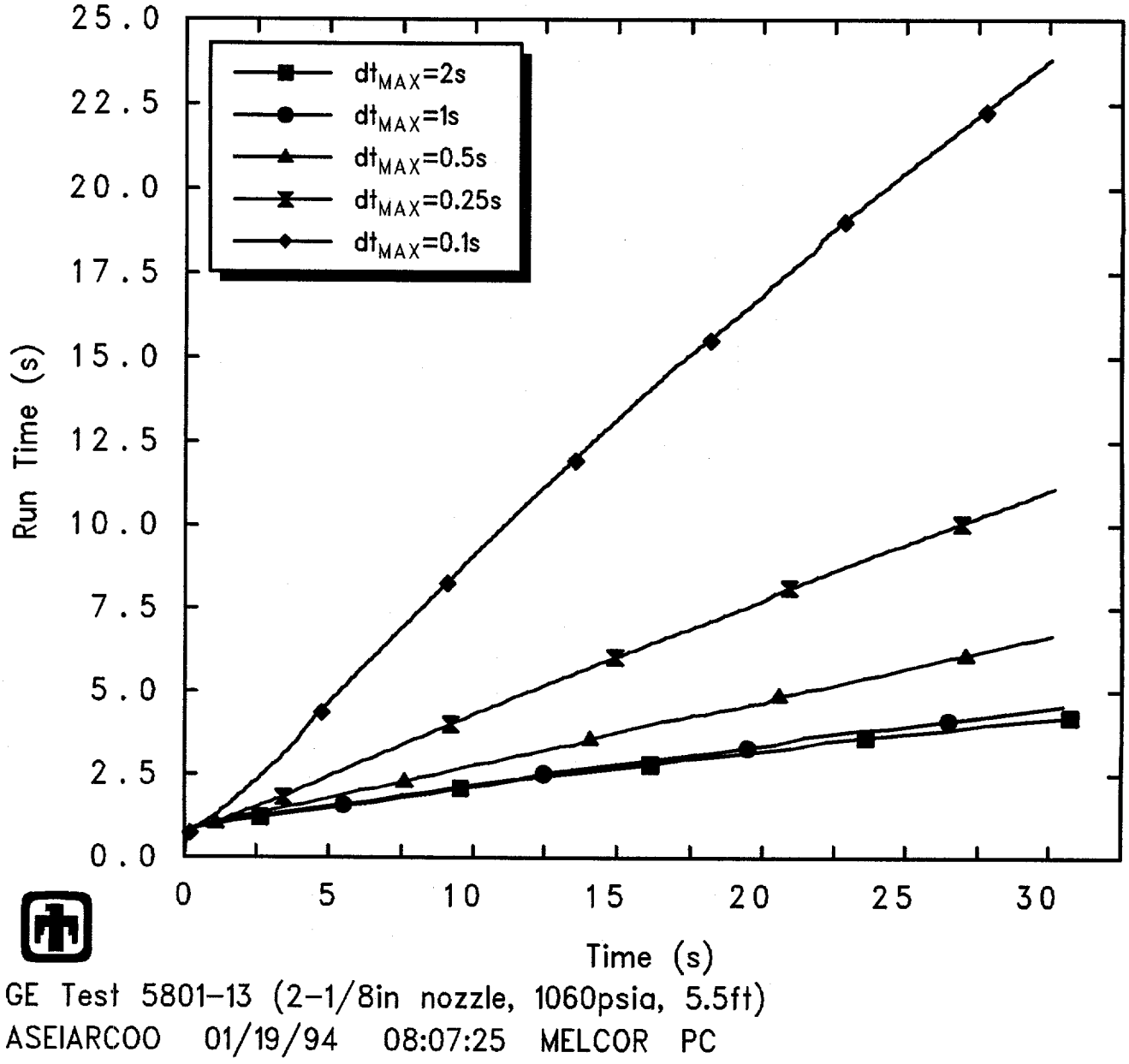

Figure 7.2.6. Total Run Time for GE Large Vessel Top Blowdown Test 5801-13 – Time Step Sensitivity Study

test 5801-13, the time step always began increasing smoothly from its initial value of 1ms at the maximum rate of increase allowed until reaching the user-specified maximum allowed Δt. The bottom blowdown test analyses then ran at the user-specified time step during the liquid and two-phase blowdown periods until the blowdown line became uncovered, when the code subsequently reduced the time step to $\leq$1s. Sensitivity study calculations with the user-specified maximum allowed time step set to 0.5s, 0.25s and 0.1s simply continued running at those maximum allowed values.

Figure 7.2.8 gives the corresponding vessel pressure histories (including test data, for comparison). There is no visible difference in results for the slow depressurization during liquid blowdown, but there is a spread in results beginning when the blowdown line uncovers, with slightly more rapid depressurization with larger time steps. Note that while the results are not converging (because the pressure history calculated with a 0.1s maximum allowed time step resembles the results with a 1-2s time step more than the results with a maximum allowed time step of 0.25s or 0.5s), the variation in results is not very great.

Figure 7.2.9 presents the collapsed and swollen vessel liquid levels calculated for test 5803-1 in this time step sensitivity study, together with the measured two-phase liquid level. There is very little difference visible in either curve set during most of the transient period simulated. The most visible difference, which is still quantitatively small, is in the collapsed liquid levels right at the time the blowdown line uncovers. This variation in collapsed liquid levels and hence vessel inventories corresponds to the divergence in vessel pressure histories at the time the blowdown line uncovers, noted in Figure 7.2.8.

Figure 7.2.10 compares the blowdown flow rates predicted for test 5803-1 using these different time step histories; experimental data are included for reference. These results indicate that the variations in vessel depressurization and in collapsed liquid levels are due to oscillations in the break flows being calculated in the blowdown line using different time steps.

The vessel pool bubble fractions calculated for this bottom blowdown test analysis in this time step sensitivity study are illustrated in Figure 7.2.11. The variations found in the pool bubble fraction reflect the variations in the liquid levels, shown in Figure 7.2.9. There is very little or no difference found during the liquid blowdown phase in the first $\leq$20s of the transient or during the vapor blowdown phase in the last $\leq$20s of the transient; most of the variation visible occurs during the uncovery of the blowdown line between about 20s and 30s.

Total run times required for this bottom blowdown test 5803-1 analysis various platforms are given in Figure 7.2.12, and are typical of the comparison seen for the other bottom blowdown test and for the top blowdown test analyses. As would be expected, reducing the time step and hence increasing the number of cycles increases the run times needed.

The results seen for this bottom blowdown test are characteristic of the behavior found for the other bottom blowdown test (5803-2), which are not shown.

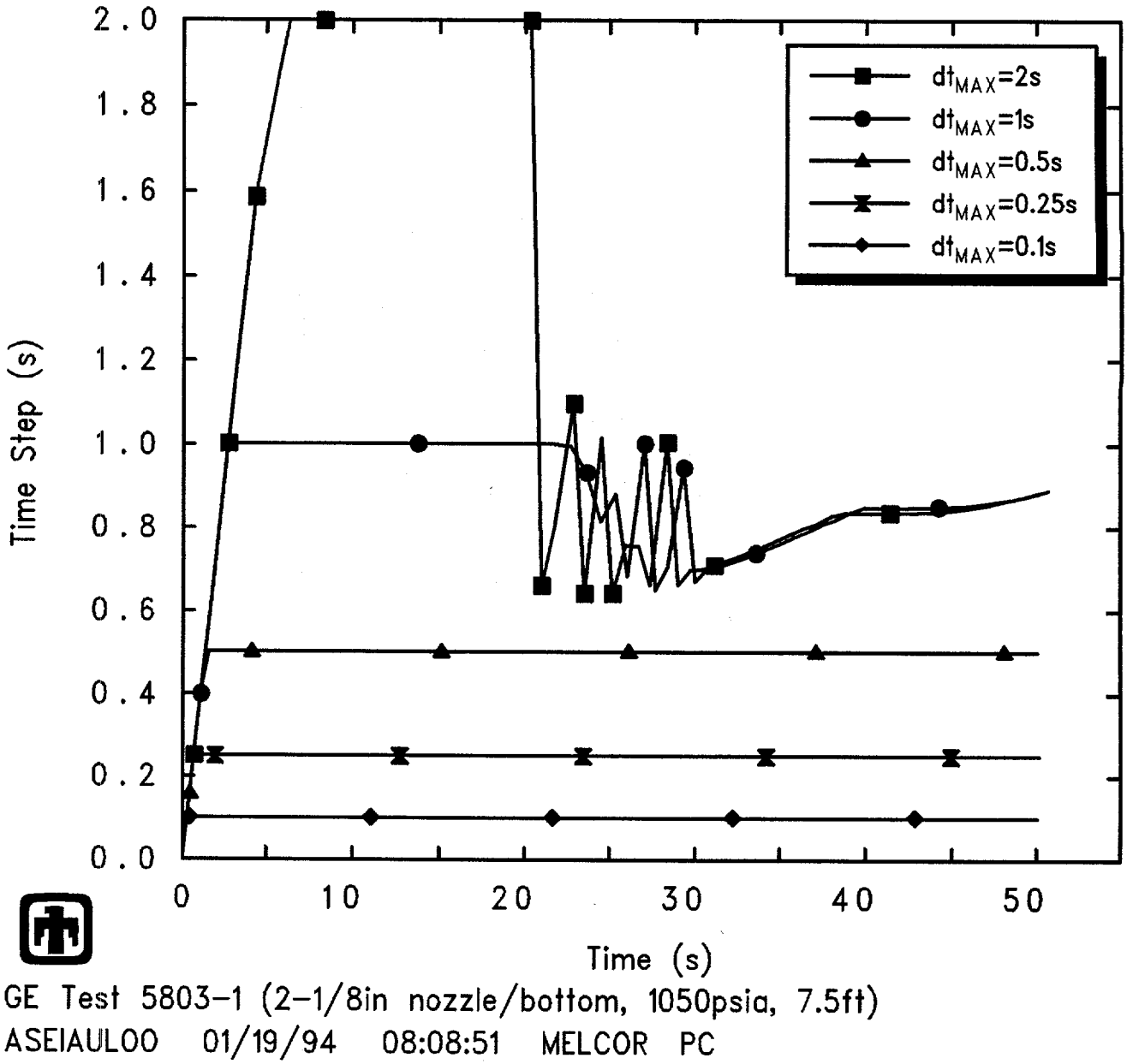

Figure 7.2.7. Time Steps for GE Large Vessel Bottom Blowdown Test 5803-1 – Time Step Sensitivity Study

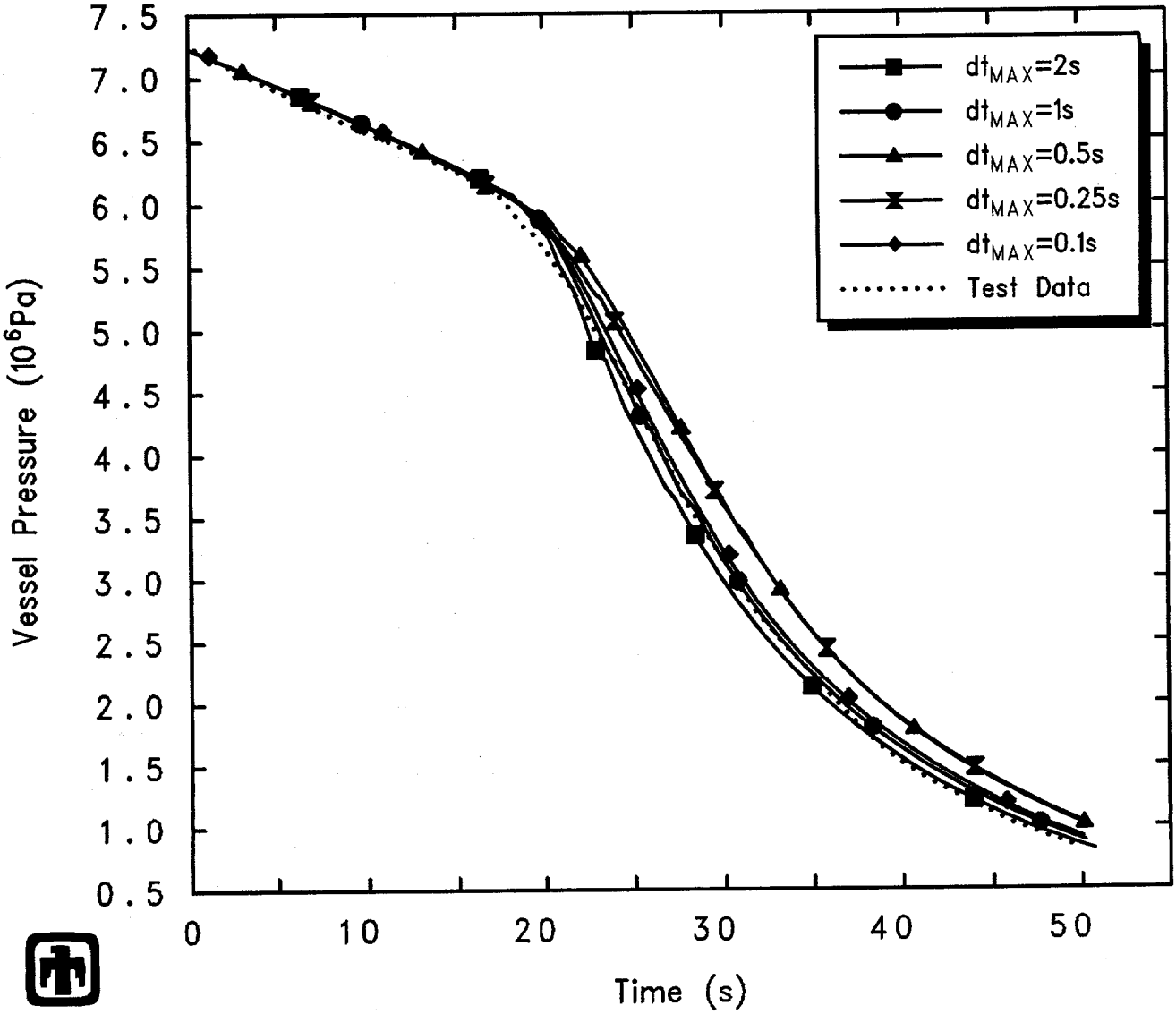

Figure 7.2.8. Vessel Pressure for GE Large Vessel Bottom Blowdown Test 5803-1 – Time Step Sensitivity Study

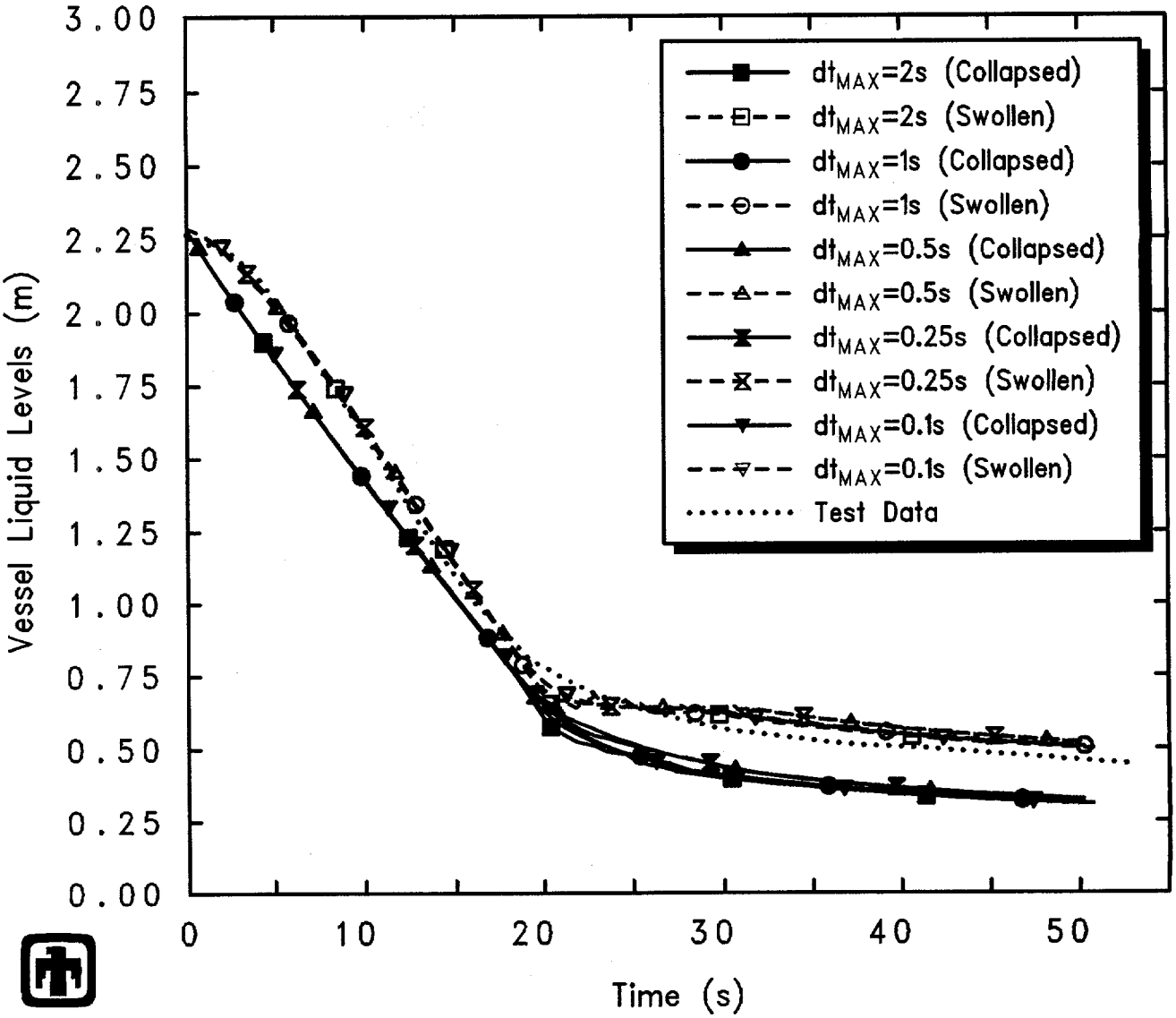

Figure 7.2.9. Vessel Liquid Levels for GE Large Vessel Bottom Blowdown Test 5803-1 – Time Step Sensitivity Study

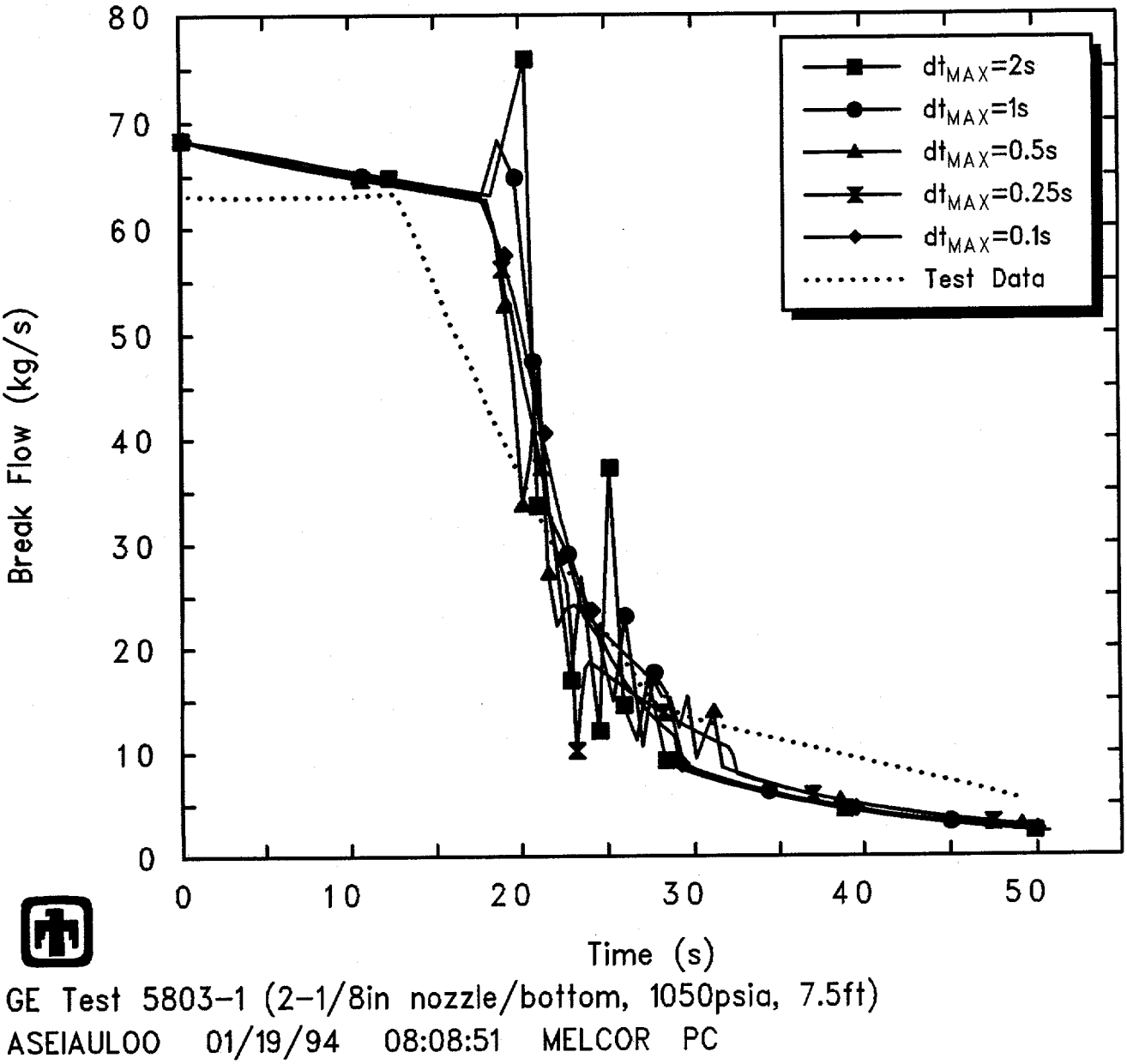

Figure 7.2.10. Blowdown Mass Flow for GE Large Vessel Bottom Blowdown Test 5803-1 – Time Step Sensitivity Study

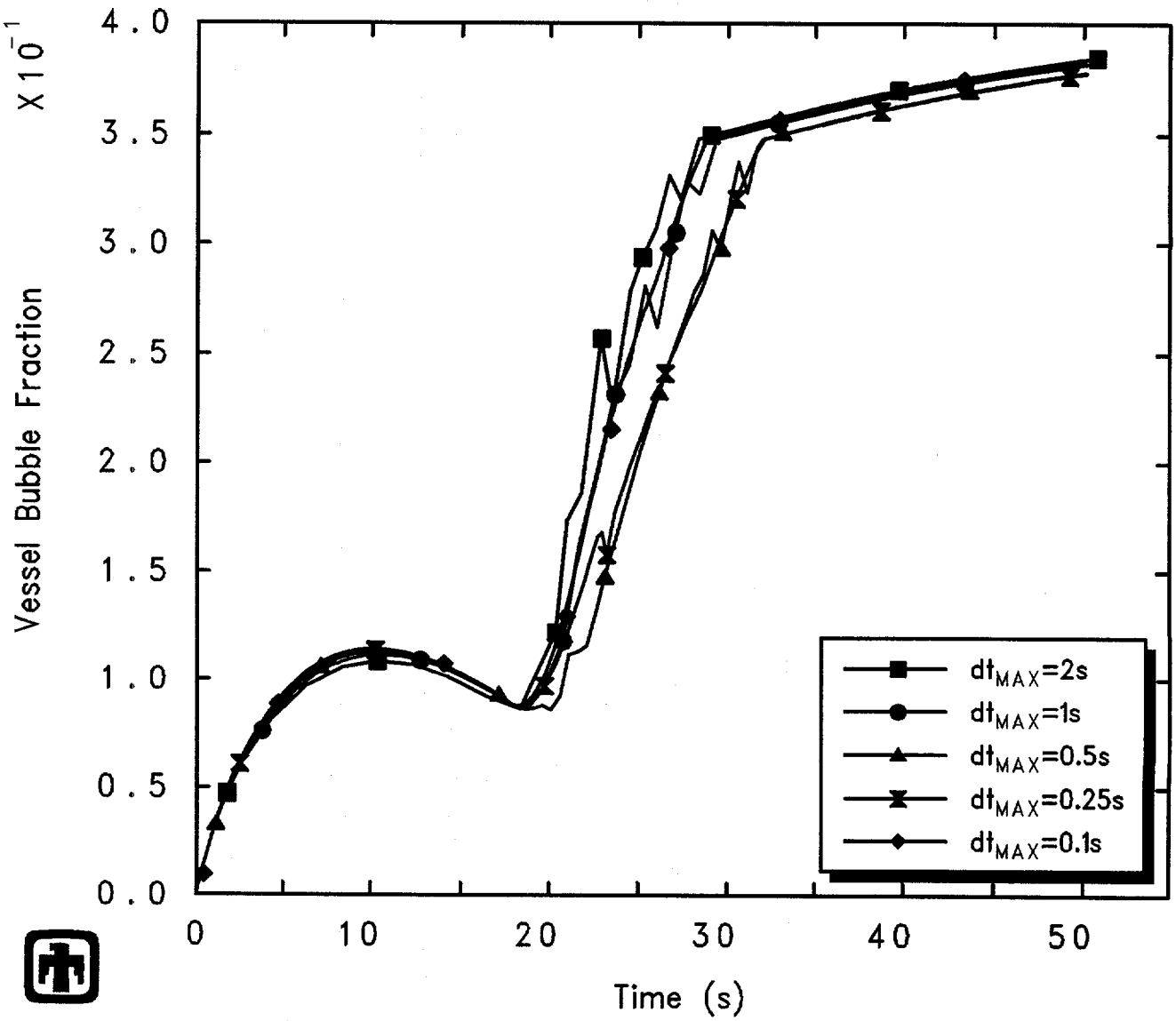

Figure 7.2.11. Vessel Two-Phase Liquid Bubble Fraction for GE Large Vessel Bottom Blowdown Test 5803-1 – Time Step Sensitivity Study

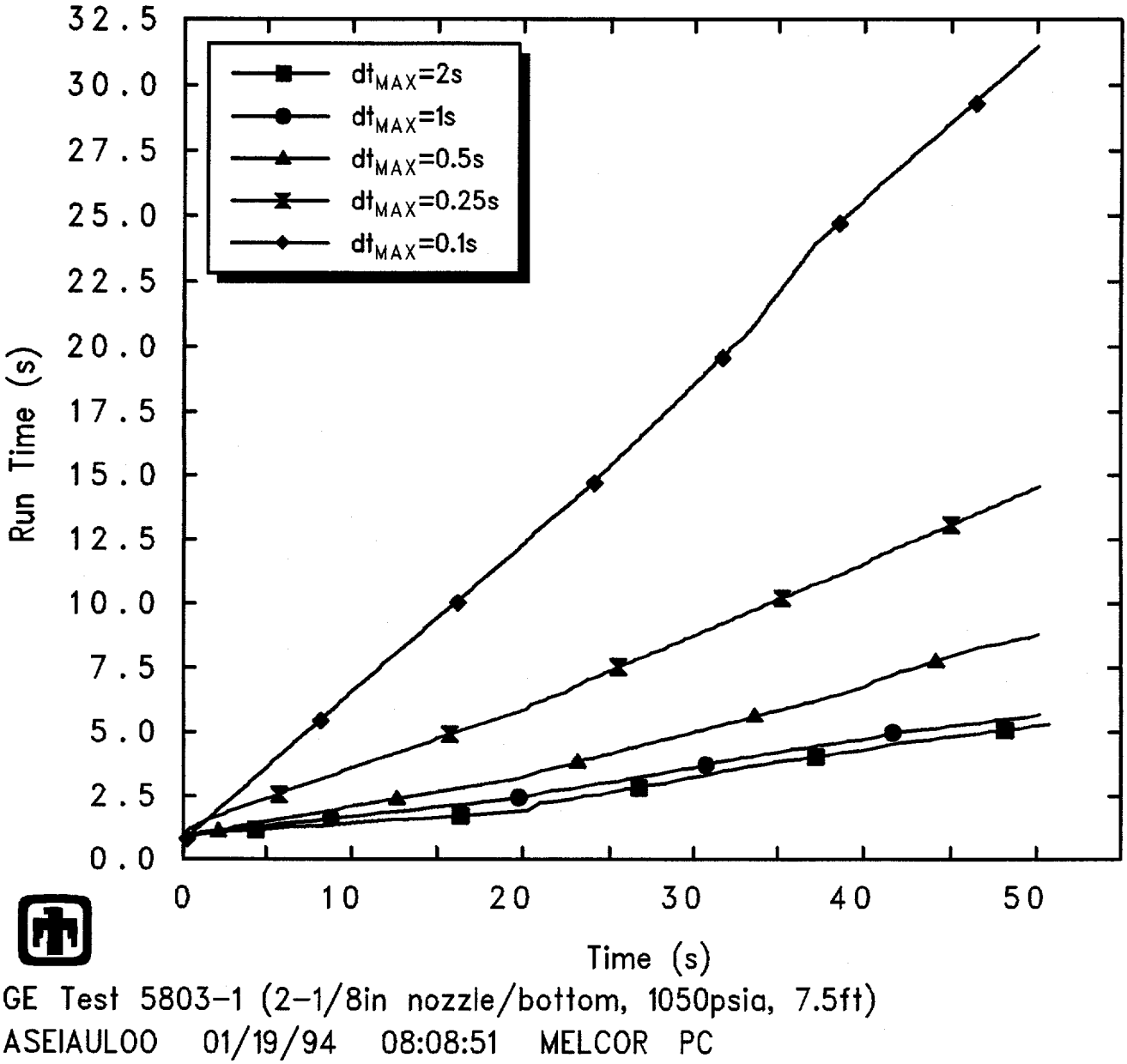

Figure 7.2.12. Total Run Time for GE Large Vessel Bottom Blowdown Test 5803-1 – Time Step Sensitivity Study

There is little time step dependence in these blowdown and level swell analyses partly becaue of the implicit bubble separation algorithm but also because these simulations are not subject to significant level fluctuations. The implicit bubble separation algorithm was implemented primarily to prevent severe numerical difficulties during uncovery or level swell in volumes with internal heat sources, while in this problem the level swell is produced only to flashing.

7.3 Code Version

MELCOR version 1.8OO was used for all the calculations described in this report, except for the calculations reported in this subsection. An implicit bubble separation algorithm has been implemented recently in the CVH package in MELCOR. Prior to the implementation of this algorithm, MELCOR was experiencing problems with natural circulation phenomena in the COR package; it is expected that the problems with calculating natural circulation will be eliminated with the implementation of the implicit bubble separation algorithm. A sensitivity study has been done on the effect of this implicit bubble separation algorithm comparing results from MELCOR version 1.8OO to results from the release version of MELCOR 1.8.2, which was MELCOR 1.8NM.

The vessel pressure predicted by MELCOR using the release version of MELCOR 1.8.2 is compared to the basecase results, obtained using version 1.8OO and the implicit bubble separation algorithm, and with test data in Figure 7.3.1, for the top blowdown experiment 5801-13; Figure 7.3.2 compares the corresponding calculated break flows. The pressure histories predicted by MELCOR using either version for this top blowdown test appear identical, as do the break flows predicted by MELCOR using these two versions. Figure 7.3.3 gives the swollen and collapsed liquid levels in the vessel control volume predicted by MELCOR using these two code versions for the top blowdown test 5801-13, together with test data on the two-phase mixture level, for reference. The corresponding vessel pool bubble fractions are presented in Figure 7.3.4. There is a slight change visible in the initial rate of increase of the vessel swollen level, with the level swelling somewhat faster with the release version of 1.8.2; however, the same value of maximum allowed pool bubble fraction in both versions causes the same longer-term level decline.

(The results and conclusions for the calculated pressures, break flows, vessel levels and pool bubble fractions in the other three top blowdown test analyses are very similar to the behavior noted for these test 5801-13 analyses, and are not shown here.)

Figure 7.3.5 shows the vessel depressurization histories calculated by MELCOR, using the release version of 1.8.2 and using a more recent version including the implicit bubble separation algorithm, compared to experimental data, and indicates a small difference in vessel depressurization histories predicted during the transition from liquid through two-phase to vapor blowdown in mid-transient. Figure 7.3.6 shows the break flows out the blowdown line and Venturi flow limiting nozzle causing the vessel depressurization, calculated by MELCOR using these different code versions, together with test data; the break flow calculated using the release version (1.8NM) is somewhat smoother and less

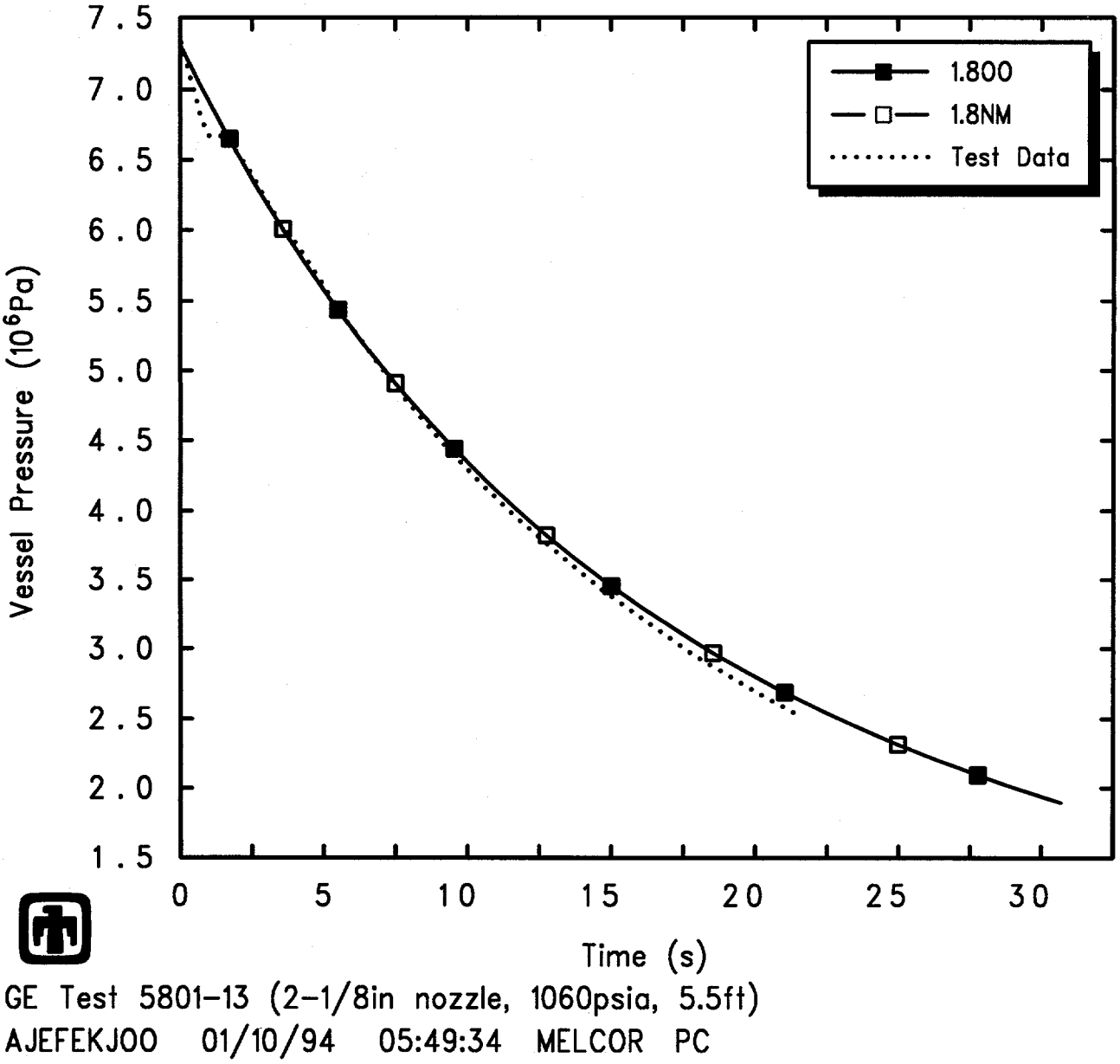

Figure 7.3.1. Vessel Pressure for GE Large Vessel Top Blowdown Test 5801-13 – Code Version Sensitivity Study

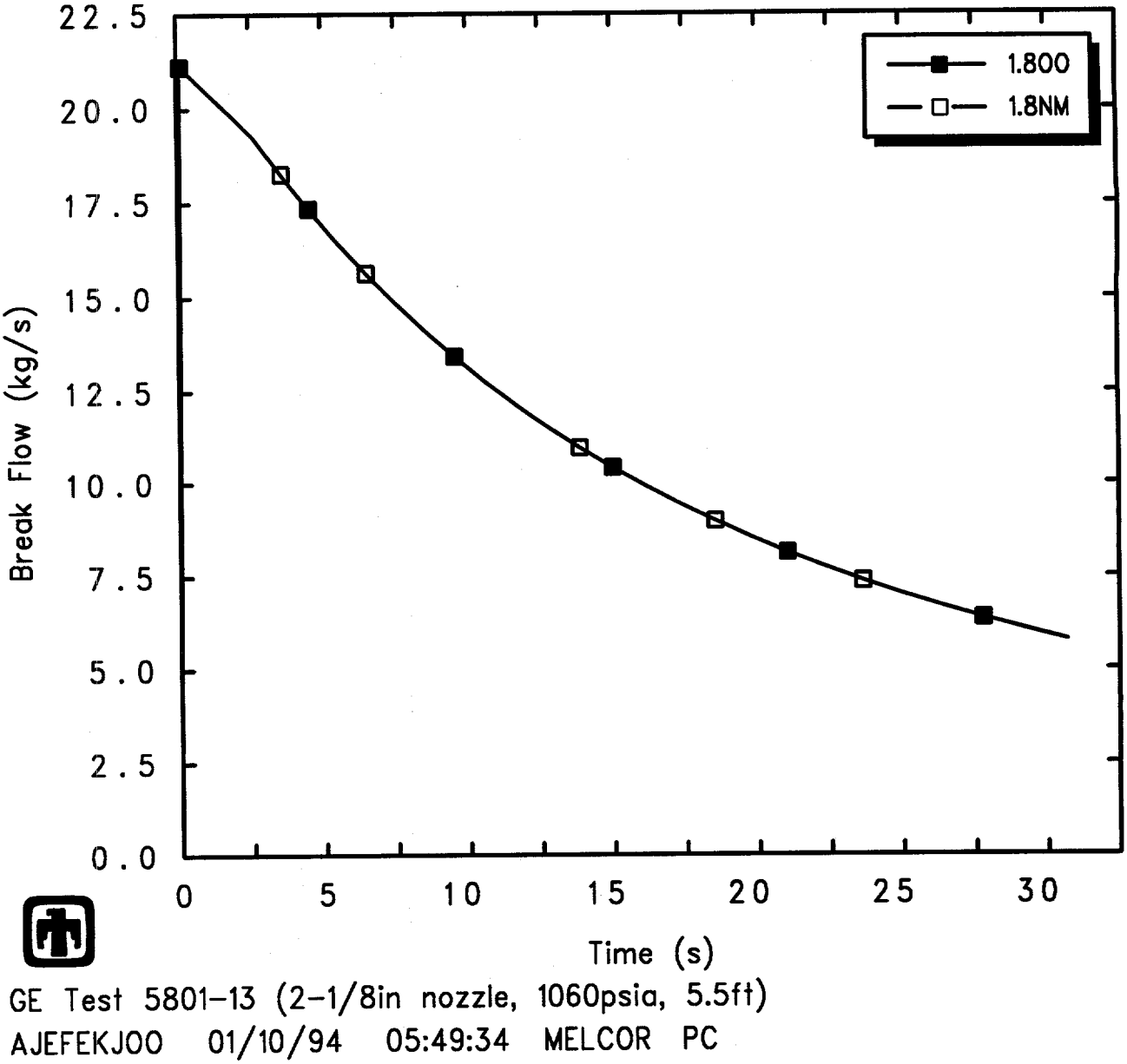

Figure 7.3.2. Blowdown Mass Flow for GE Large Vessel Top Blowdown 5801-13 – Code Version Sensitivity Study

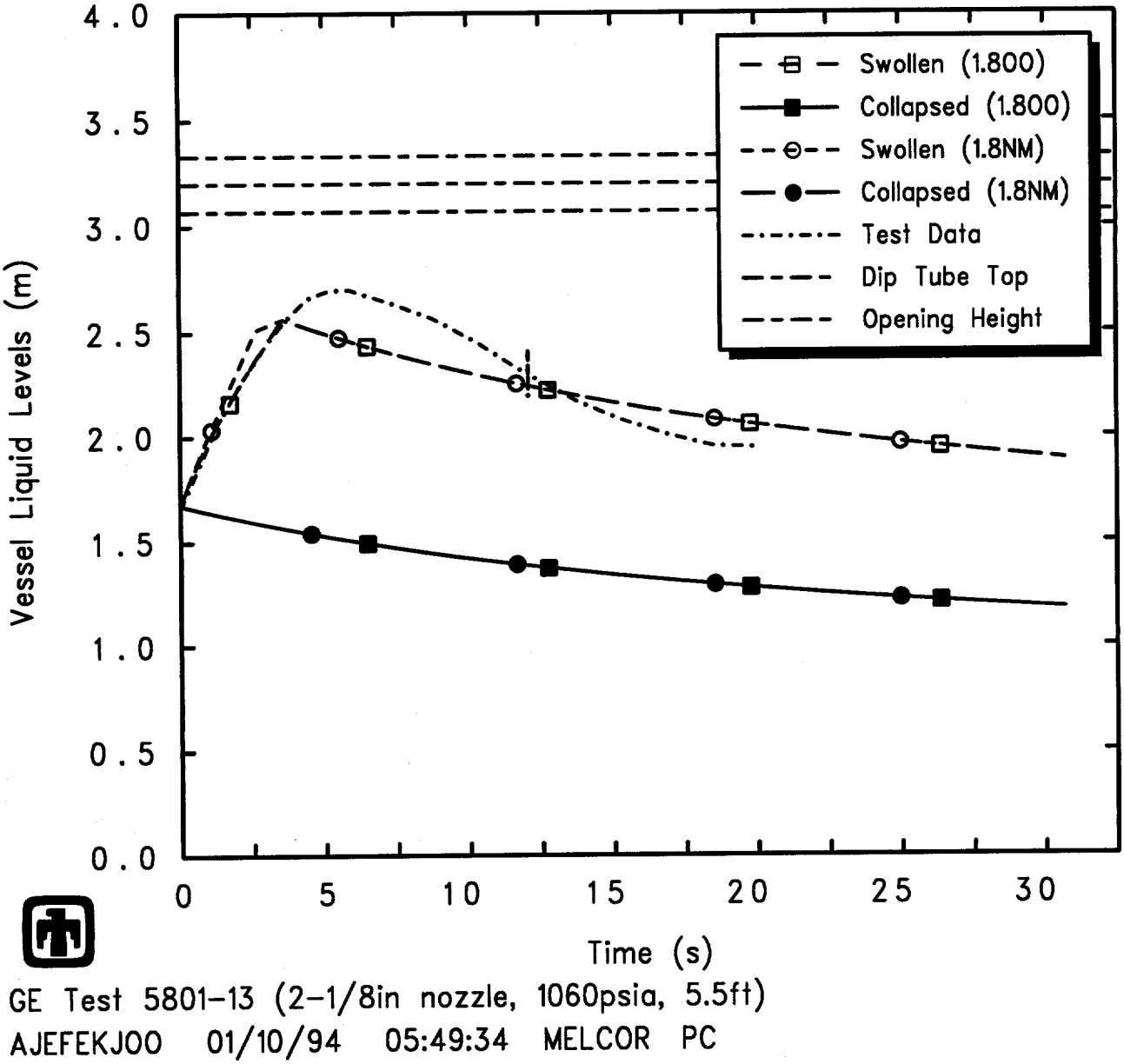

Figure 7.3.3. Vessel Liquid Levels for GE Large Vessel Top Blowdown Test 5801-13 – Code Version Sensitivity Study

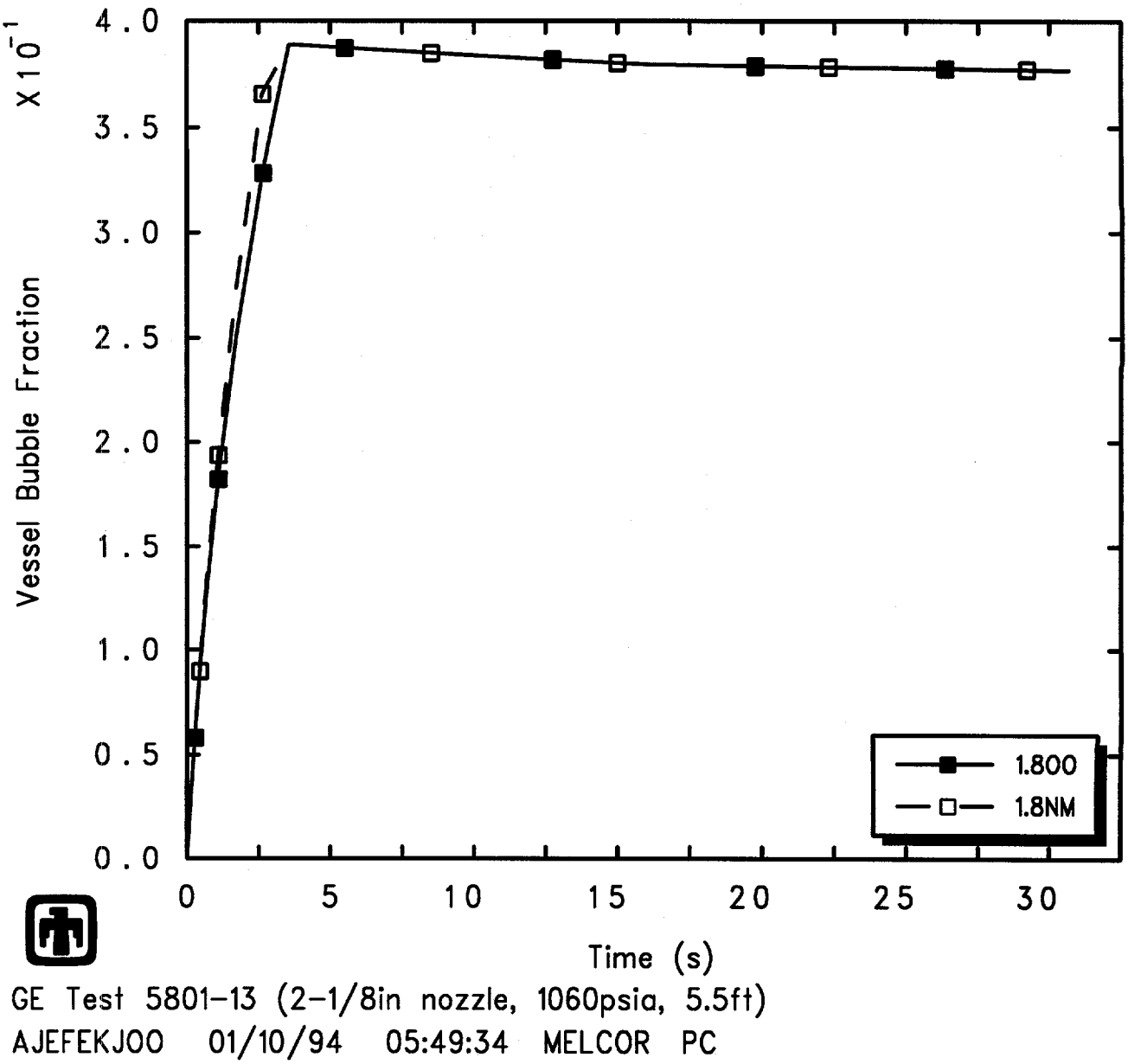

Figure 7.3.4. Vessel Two-Phase Liquid Bubble Fraction for GE Large Vessel Top Blowdown Test 5801-13 – Code Version Sensitivity Study

Table 7.3.1. Run Statistics for GE Large Vessel Top and Bottom Blowdown Test Analyses – Code Version Sensitivity Study

Test No.	1.8OO			1.8NM		
	Number of Cycles	Subcycles per Cycle	Fallbacks Requested	Number of Cycles	Subcycles per Cycle	Fallbacks Requested
5801-13	40	1.0	0	40	1.0	0
5801-15	47	1.0	0	47	1.0	0
5801-19	55	1.0	0	55	1.0	0
5702-16	65	1.0	0	65	1.0	0
5803-1	63	1.016	1	63	1.0	0
5803-2	95	1.011	1	98	1.010	1

oscillatory than the blowdown flow calculated in the basecase calculation including the implicit bubble separation algorithm during uncovery of the blowdown line.

The vessel collapsed and swollen (two-phase) liquid levels predicted by MELCOR using these different code versions, also compared to experimental data, are depicted in Figure 7.3.7, and the corresponding pool bubble fractions in the vessel volumes are illustrated in Figure 7.3.8. There are some minor differences visible in the late-time collapsed liquid levels calculated, but these appear generally quite small. There is less level swell predicted in the bottom blowdown test configuration in the basecase analysis, with the implicit bubble separation algorithm, than in the calculation with the released code version, particularly during the first half of the transient.

(The results obtained for a noding study on the bottom blowdown test 5803-2 analysis are similar to the results presented for test 5803-1, and are not shown here.)

Figures 7.3.9 and 7.3.10 show that there is a small run time increase associated with using the implicit bubble separation algorithm added after the release of version 1.8.2 for both the top and bottom blowdown test analyses, more noticeable for the top blowdown test analyses than for the bottom blowdown test analyses. Table 7.3.1 gives the number of cycles, the number of CVH subcycles and the number of fallbacks (*i.e.*, repeated cycles with reduced time steps) requested by CVH for these GE large vessel blowdown and level swell test analyses for the release version of 1.8.2 (1.8NM) and for a more recent code version (1.8OO) which includes the implicit bubble separation algorithm. There is no subcycling or fallback for any of the four top blowdown test analyses with either code version, and there is only a minor difference seen in the bottom blowdown test analyses. Most of the run time difference must therefore be due to more time per cycle, not due to more cycles or subcycles being requested.

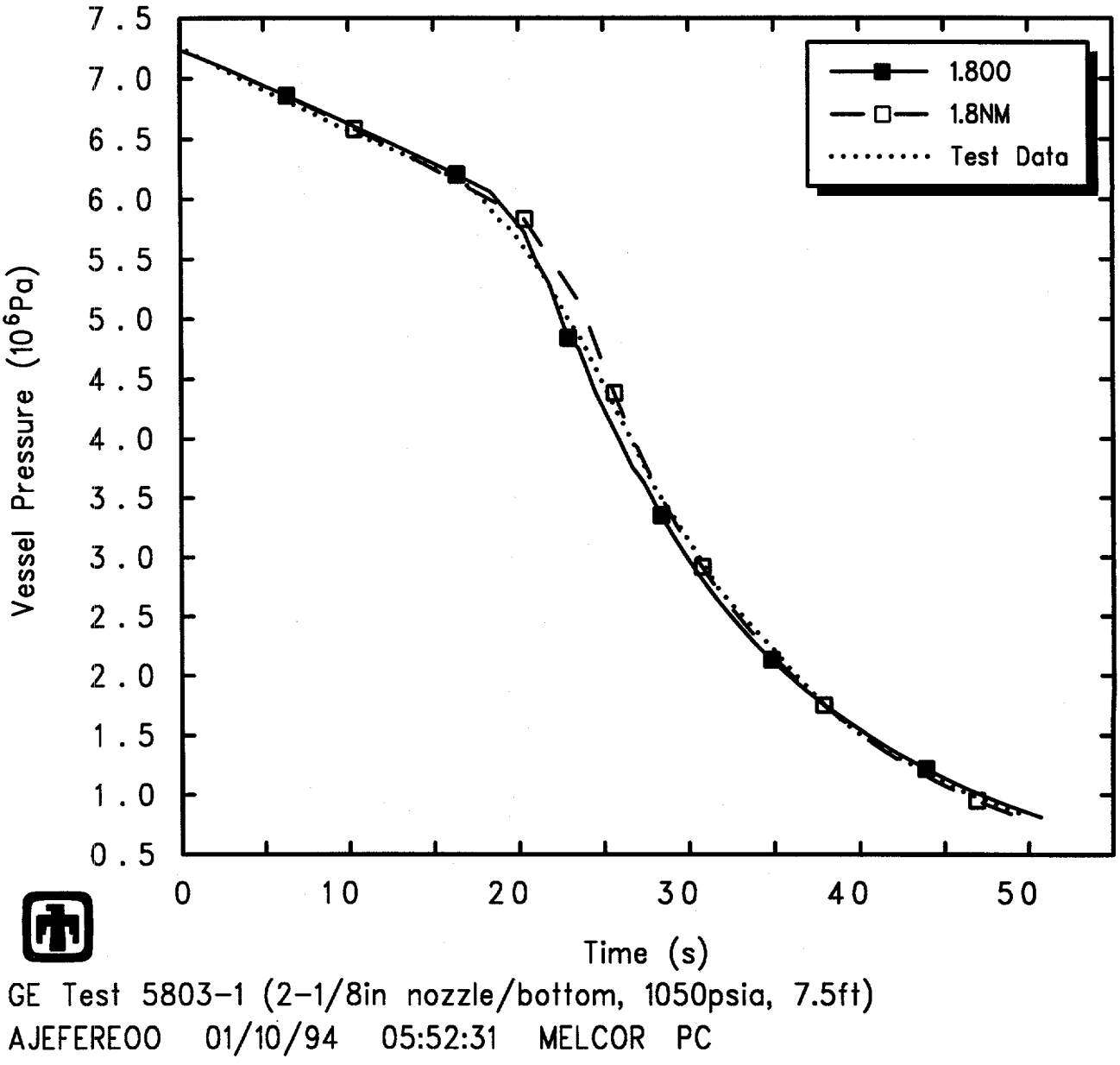

Figure 7.3.5. Vessel Pressure for GE Large Vessel Bottom Blowdown Test 5803-1 – Code Version Sensitivity Study

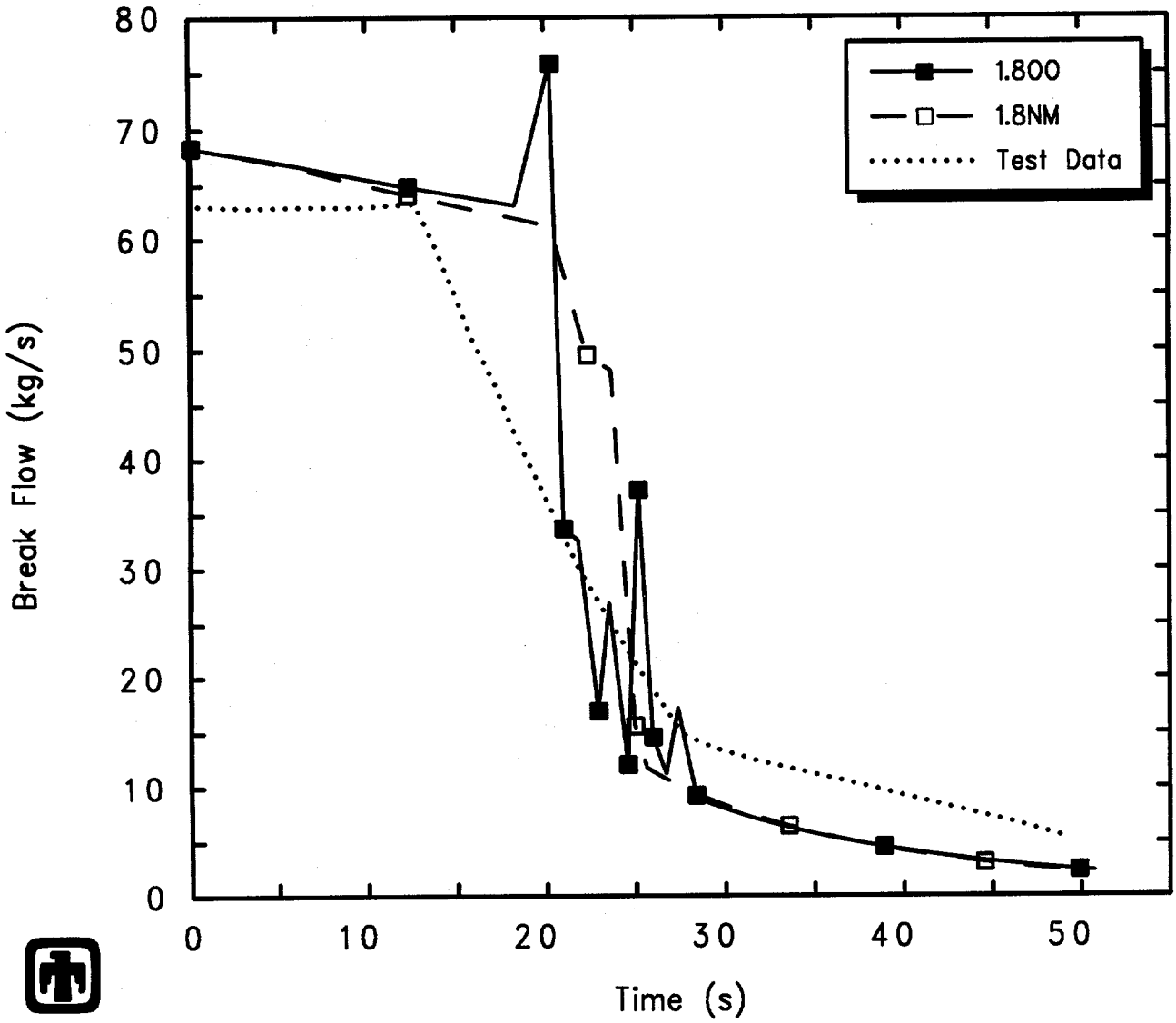

Figure 7.3.6. Blowdown Mass Flow for GE Large Vessel Bottom Blowdown Test 5803-1 – Code Version Sensitivity Study

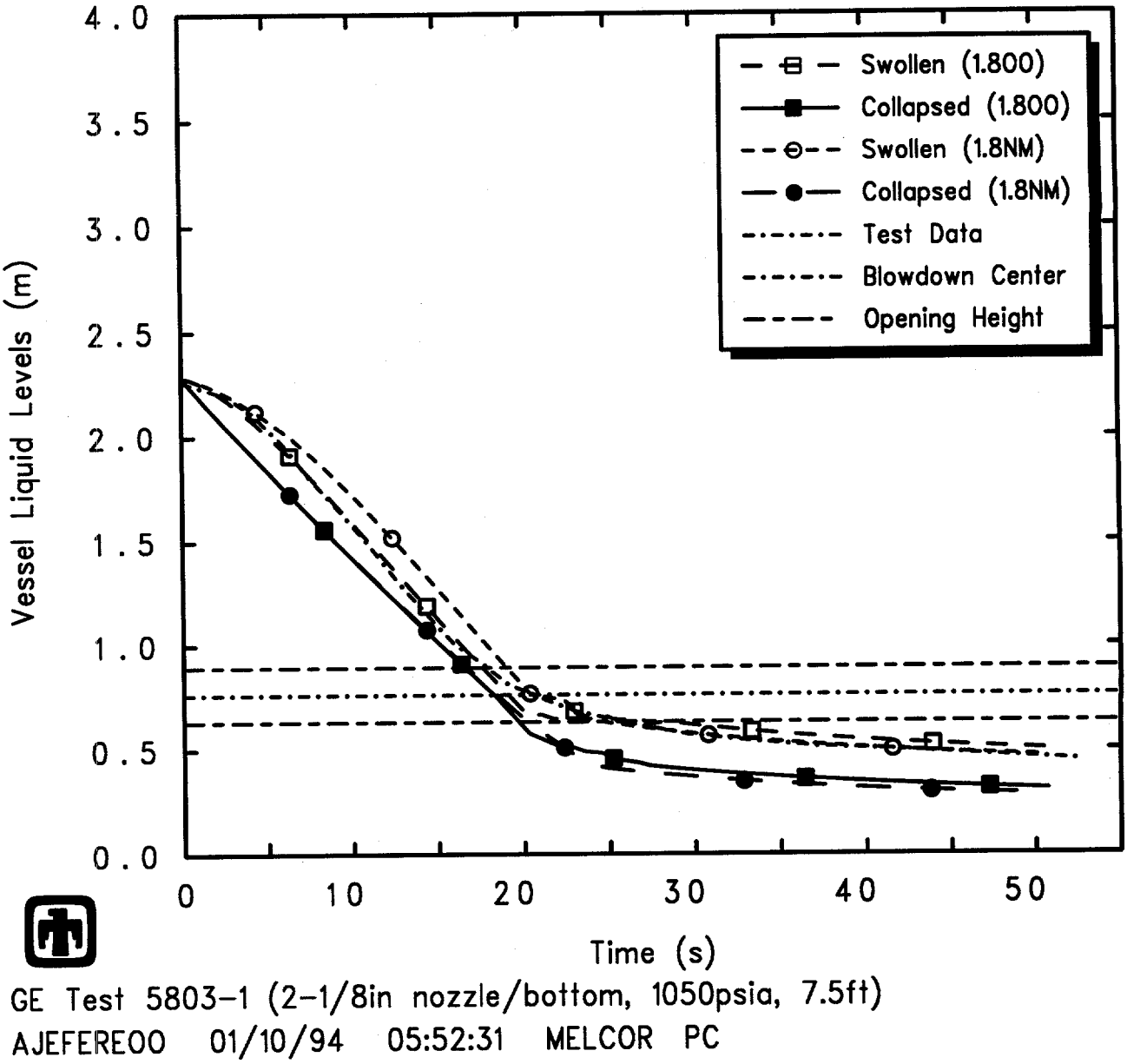

Figure 7.3.7. Vessel Liquid Levels for GE Large Vessel Bottom Blowdown Test 5803-1 – Code Version Sensitivity Study

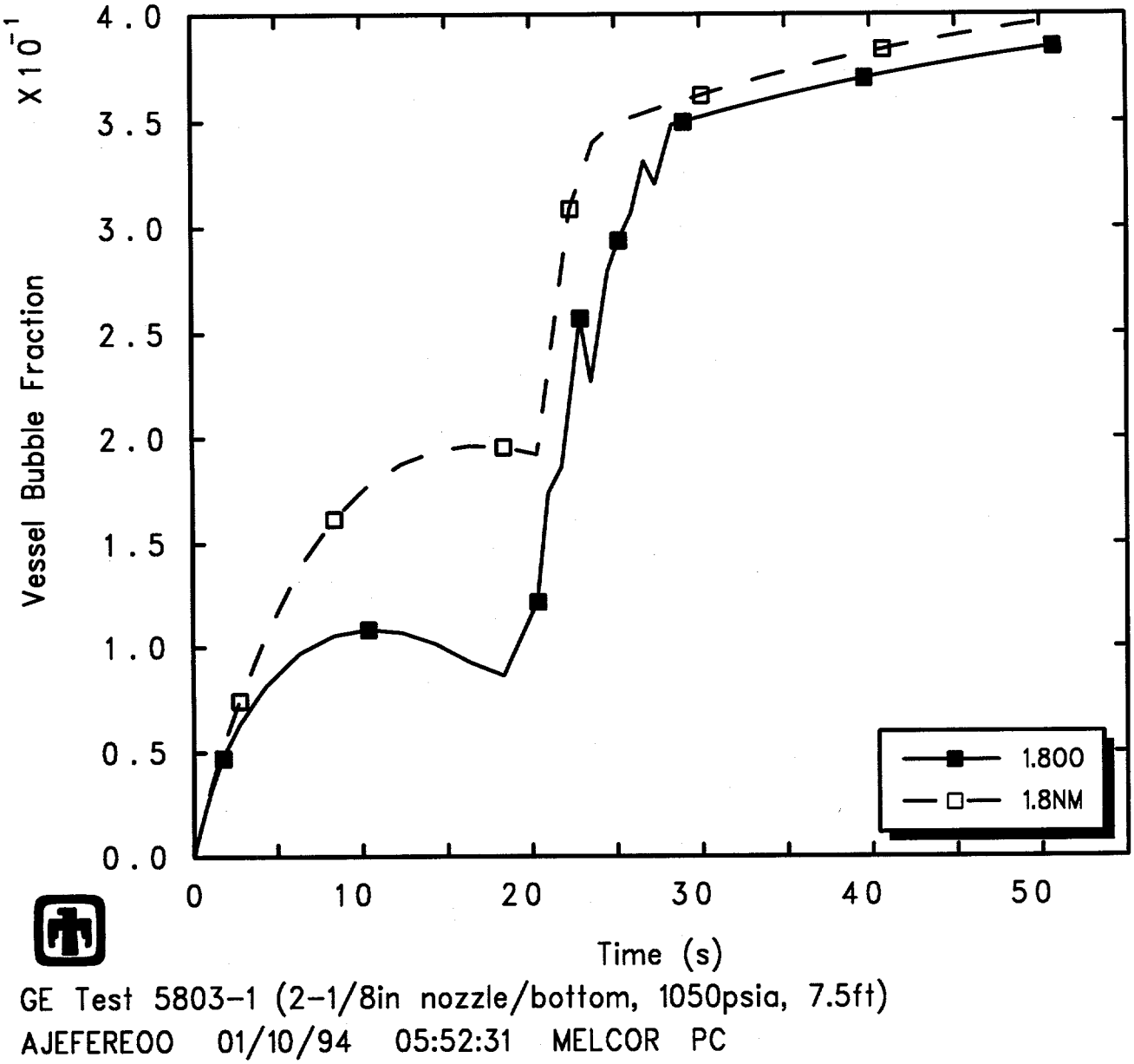

Figure 7.3.8. Vessel Two-Phase Liquid Bubble Fraction for GE Large Vessel Bottom Blowdown Test 5803-1 – Code Version Sensitivity Study

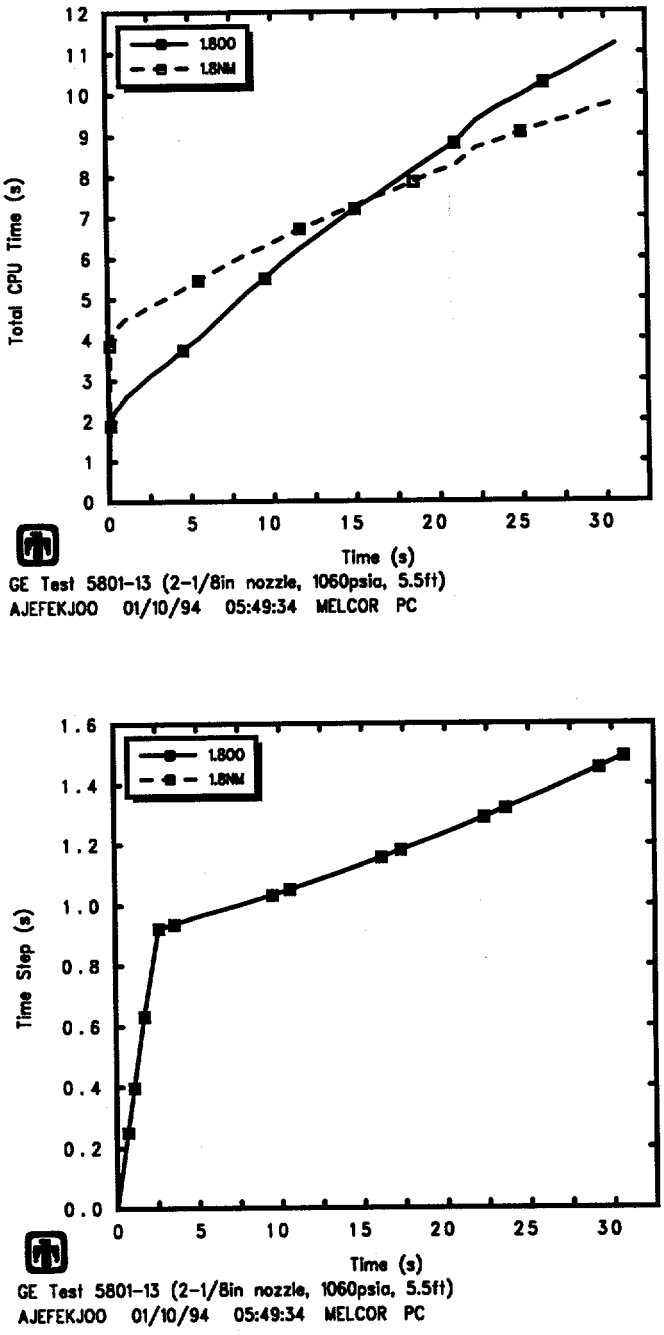

Figure 7.3.9. Total Run Time (top) and Time Step (bottom) for GE Large Vessel Top Blowdown Test 5801-13 – Code Version Sensitivity Study

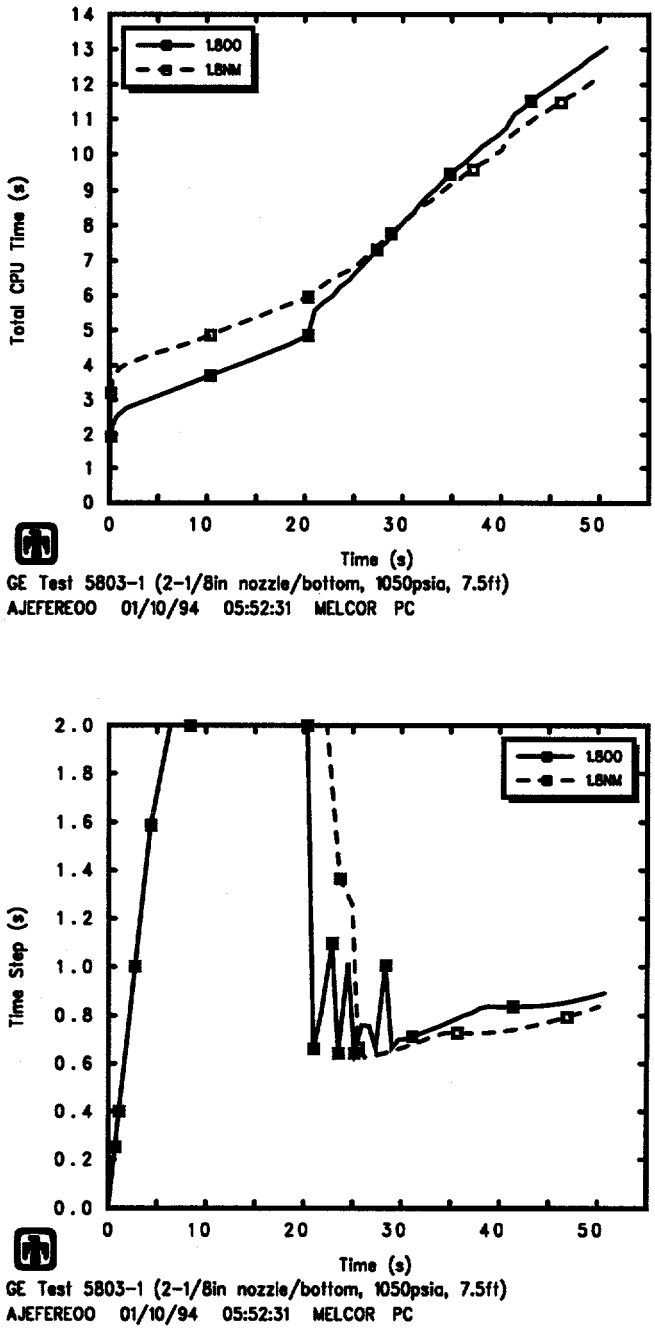

Figure 7.3.10. Total Run Time (top) and Time Step (bottom) for GE Large Vessel Bottom Blowdown Test 5803-1 – Code Version Sensitivity Study

There was generally little or no difference in results obtained using these two code versions for the various sensitivity studies done on these GE large vessel blowdown and level swell test analyses. The exception is the dependence on bubble rise velocity, described in Section 5.3 for the code version including the implicit bubble separation algorithm.

The effect of varying the pool bubble rise velocity in calculations using the release code (version 1.8NM) is shown in Figures 7.3.11 through 7.3.14, for the top blowdown test 5801-13. The results in these figures can be compared to corresponding results presented in Figures 5.3.1 through 5.3.4. There is relatively little effect found on the calculated vessel depressurization or blowdown outflow as the pool bubble rise velocity is varied, with either code version.

The noticeable difference is that with the release code the vessel pool bubble fraction always increases to the maximum allowed value, albeit more slowly for larger bubble rise velocities, while with the new implicit bubble separation algorithm the vessel pool bubble fraction equilibrates at lower values for the larger bubble rise velocities. With no difference in vessel depressurization, blowdown flow or collapsed liquid level, this results in higher swollen liquid levels calculated with the release code version than with the new implicit bubble separation algorithm for bubble rise velocities increased above the code default of 0.3m/s. (As already shown in Figure 7.3.3, there is not much difference in swollen liquid levels calculated with the release code version and with the new implicit bubble separation algorithm for the default bubble rise velocity of 0.3m/s.)

The behavior found for test 5801-13 is characteristic of the response in the other top blowdown test analyses, not shown here.

The effect of changing the pool bubble rise velocities for the bottom blowdown test 5803-1 in calculations using the release 1.8.2 code (version 1.8NM) is illustrated in Figures 7.3.15 through 7.3.18. (The results for test 5803-2 are similar.) Comparing these results to Figures 5.3.12 through 5.3.15 indicates that there is less difference in results calculated with the different code versions in the bubble rise velocity sensitivity study for the bottom blowdown tests than for the top blowdown tests, although some minor differences are visible. There is less effect of the implicit bubble separation algorithm in the bottom blowdown test analyses because those tests are not controlled by the maximum allowed pool bubble fraction until late in the transient, when little material or blowdown potential remains.

These sensitivity study calculations indicate that there are no major differences in vessel blowdown and/or level swell calculated by either the release version of MELCOR 1.8.2 (1.8NM) or by MELCOR version 1.8OO after an implicit bubble separation algorithm has been added. The implicit bubble separation algorithm was implemented primarily to prevent severe numerical difficulties during uncovery or level swell in volumes with internal heat sources, while in this problem the level swell is produced only to flashing. The results and conclusions of this assessment study therefore should apply equally well to the release version of 1.8.2 and to later code versions.

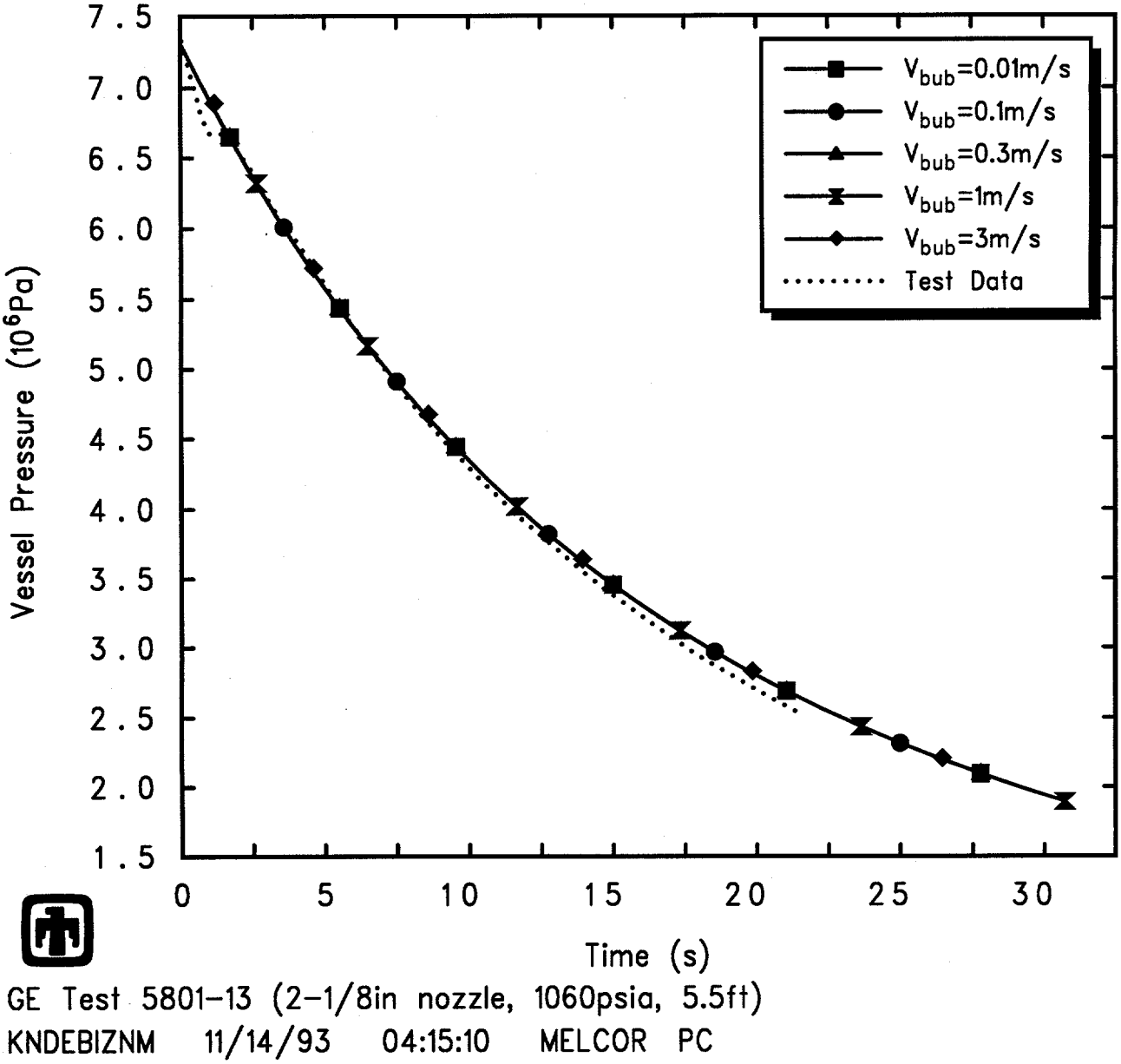

Figure 7.3.11. Vessel Pressure for GE Large Vessel Top Blowdown Test 5801-13 – Pool Bubble Rise Velocity Sensitivity Study (with Release Version of MELCOR 1.8.2)

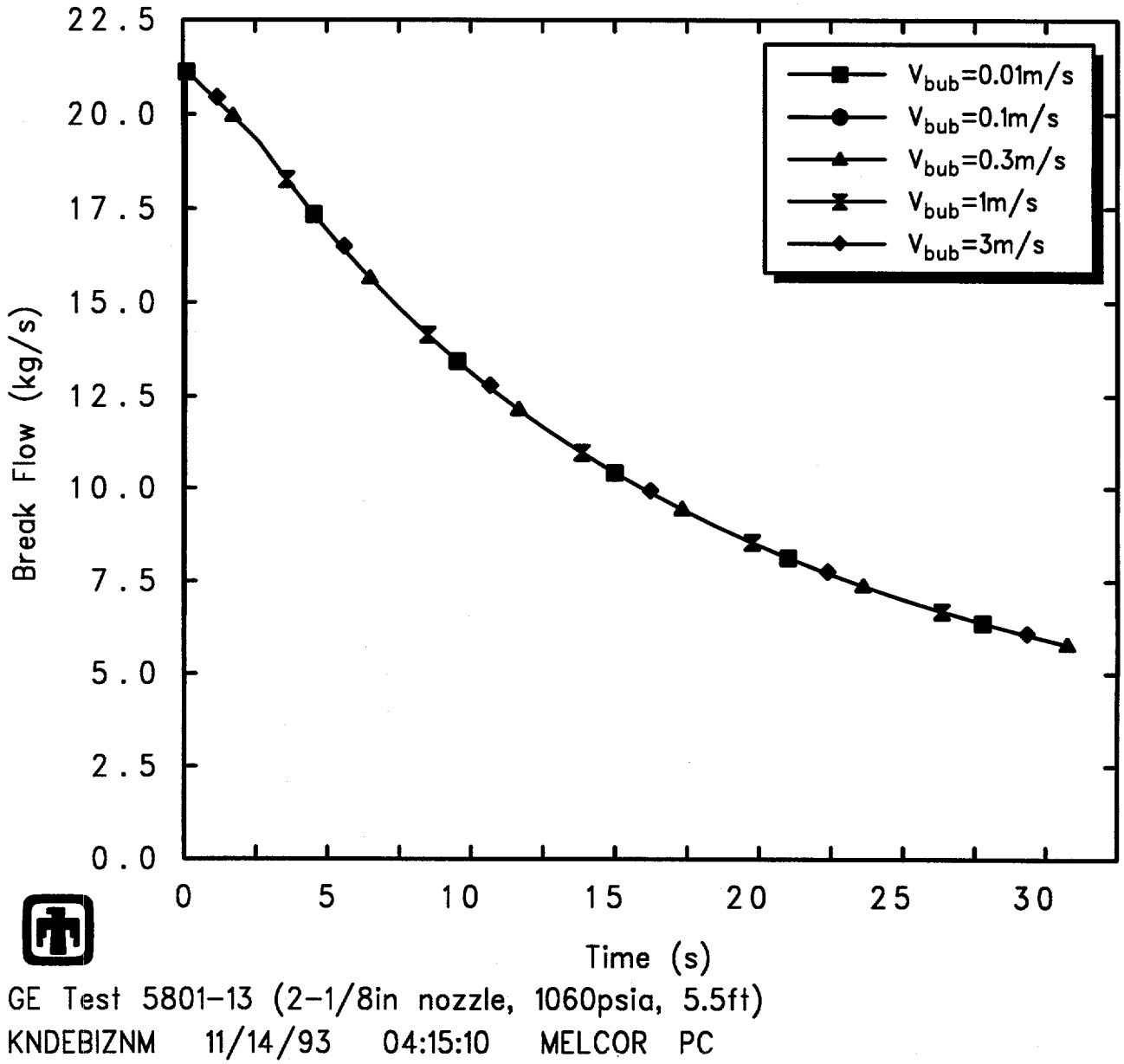

Figure 7.3.12. Blowdown Mass Flow for GE Large Vessel Top Blowdown Test 5801-13 – Pool Bubble Rise Velocity Sensitivity Study (with Release Version of MELCOR 1.8.2)

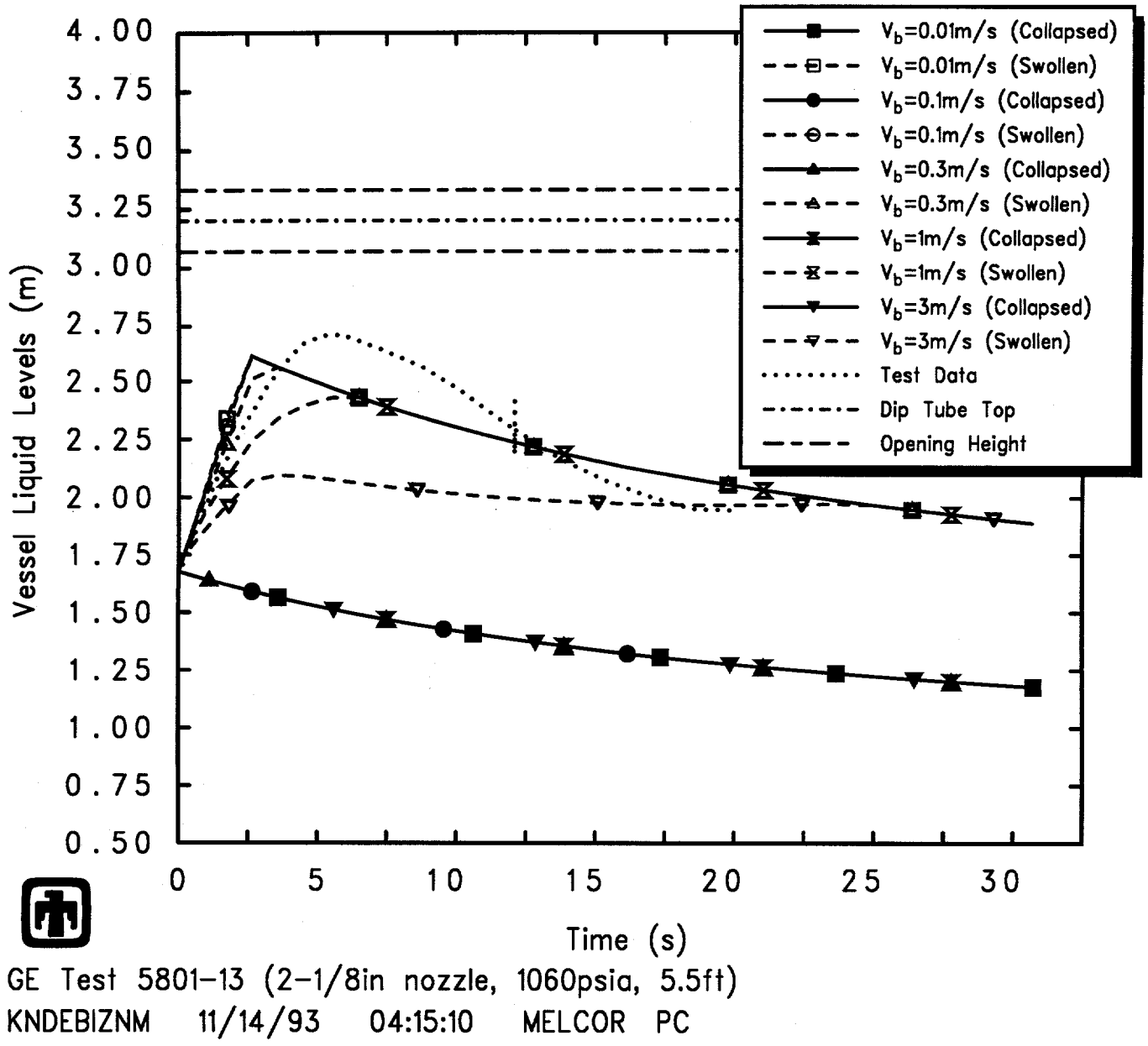

Figure 7.3.13. Vessel Liquid Levels for GE Large Vessel Top Blowdown Test 5801-13 – Pool Bubble Rise Velocity Sensitivity Study (with Release Version of MELCOR 1.8.2)

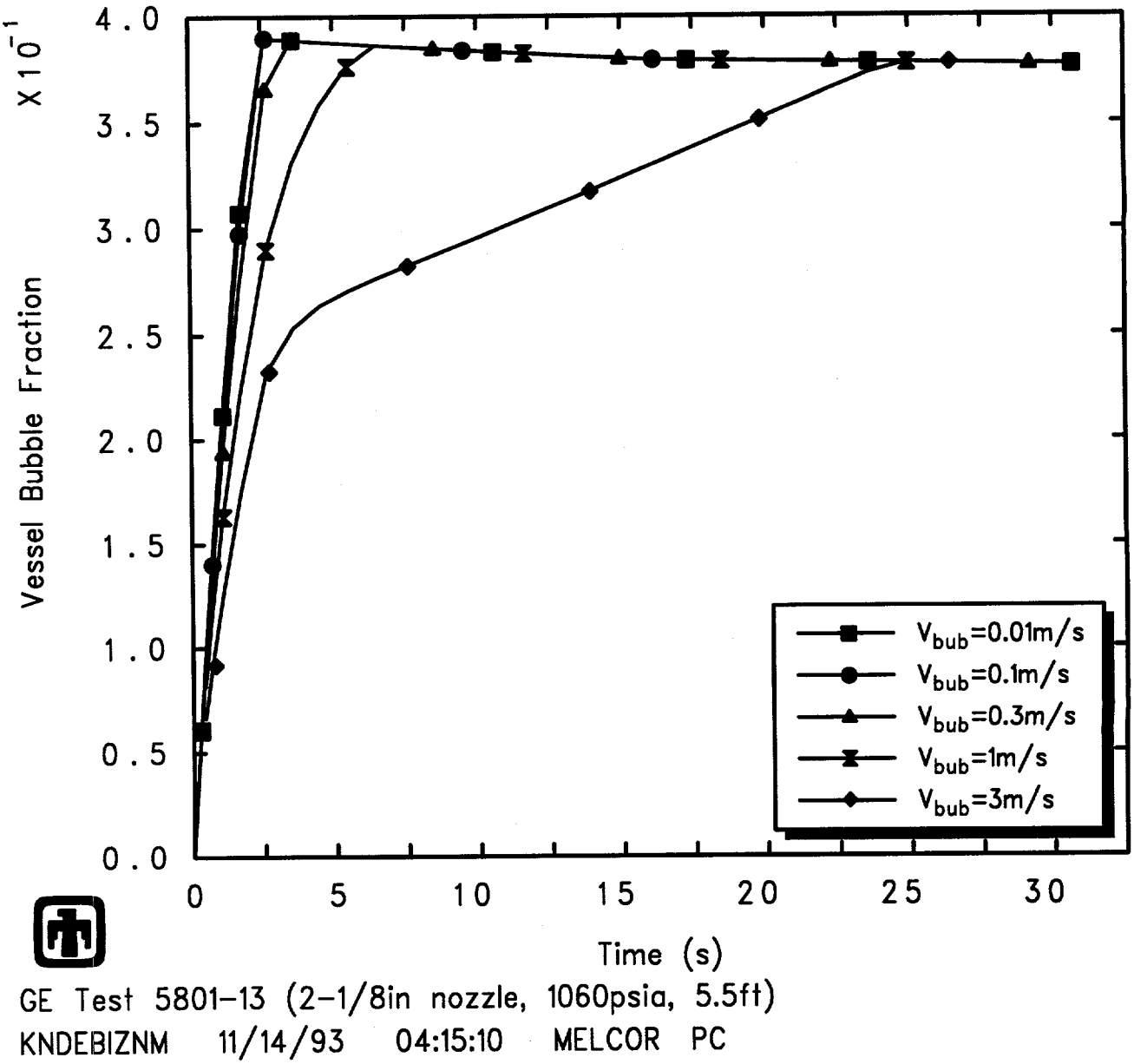

Figure 7.3.14. Vessel Two-Phase Liquid Bubble Fraction for GE Large Vessel Top Blowdown Test 5801-13 – Pool Bubble Rise Velocity Sensitivity Study (with Release Version of MELCOR 1.8.2)

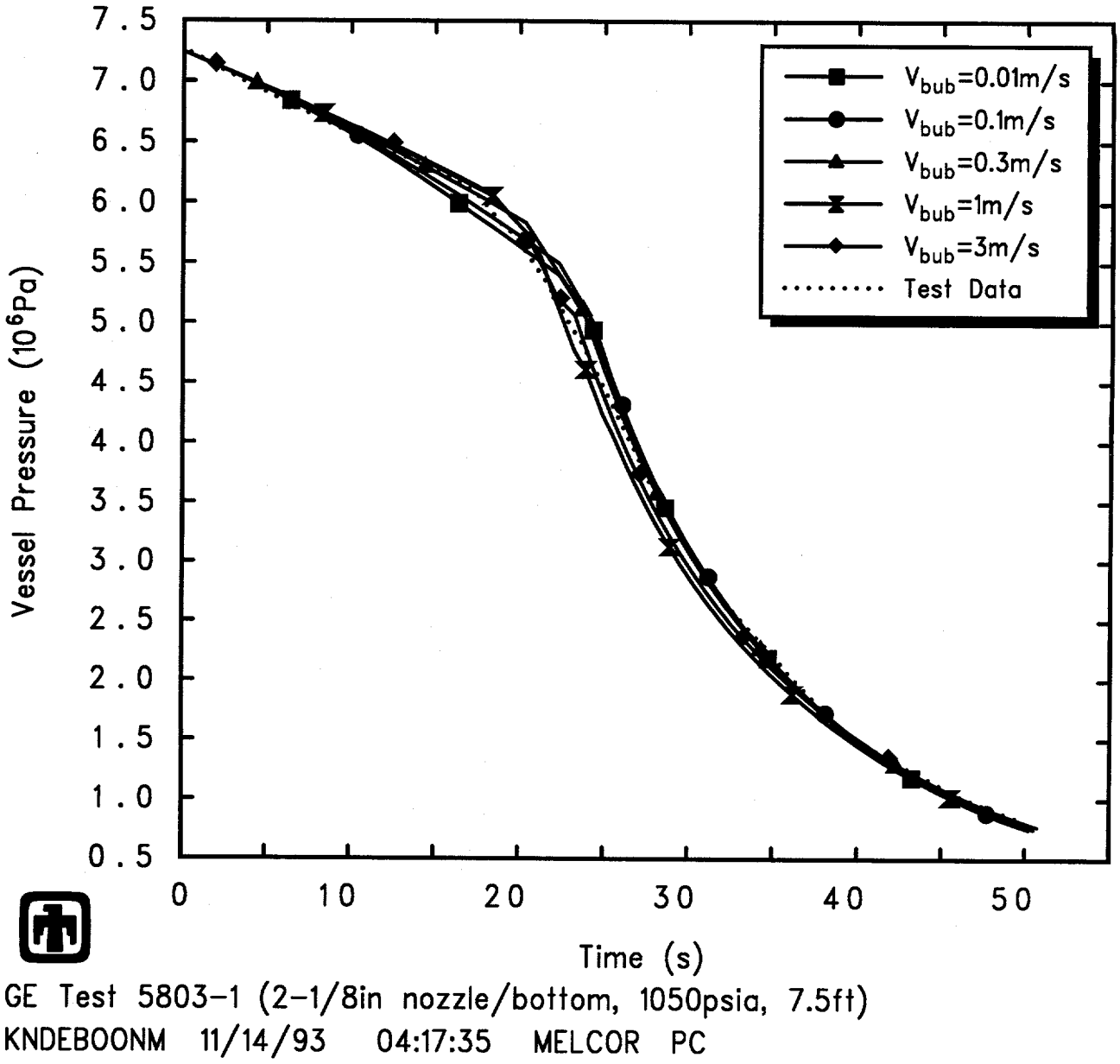

Figure 7.3.15. Vessel Pressure for GE Large Vessel Bottom Blowdown Test 5803-1 – Pool Bubble Rise Velocity Sensitivity Study (with Release Version of MELCOR 1.8.2)

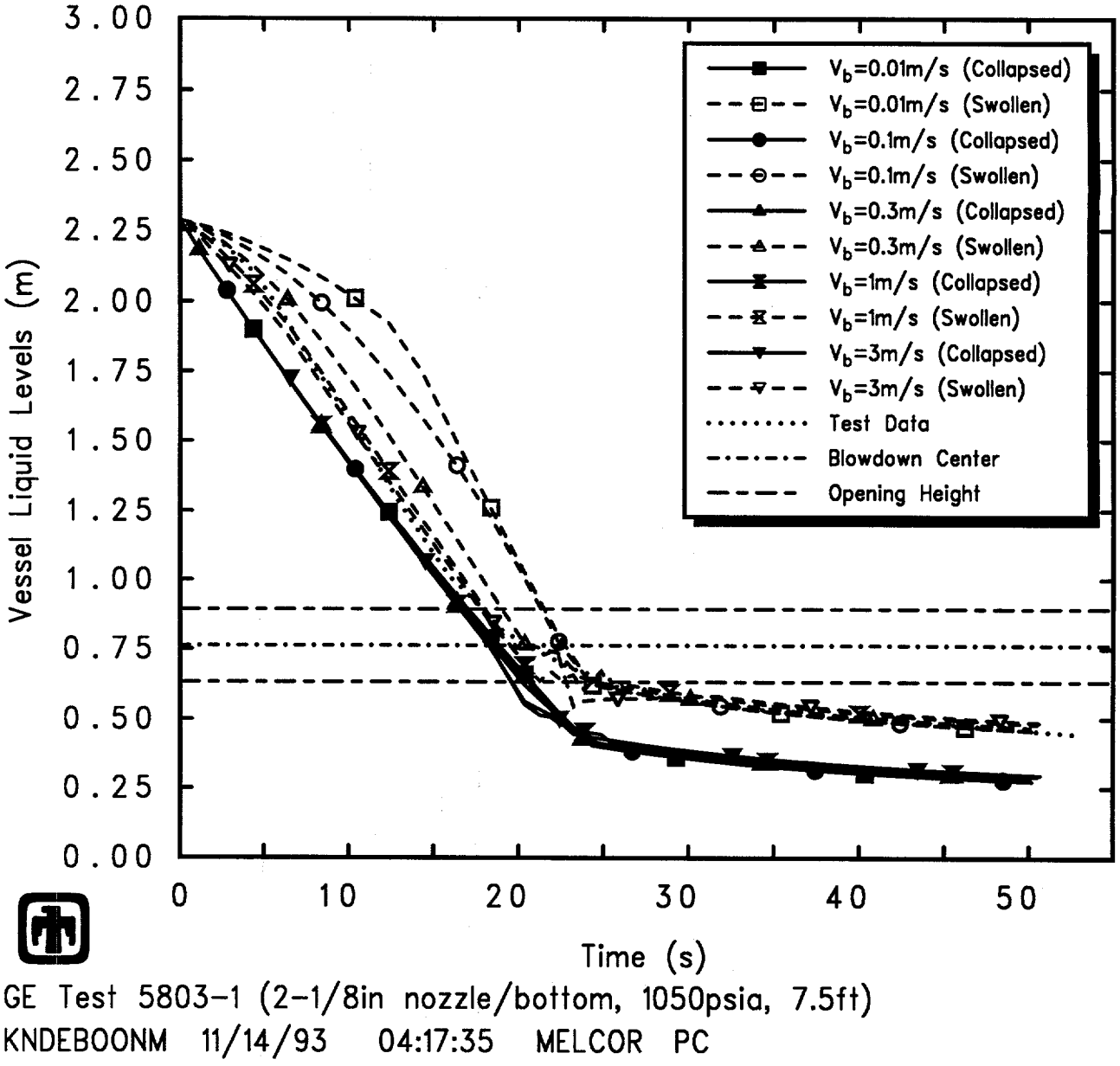

Figure 7.3.16. Vessel Liquid Levels for GE Large Vessel Bottom Blowdown Test 5803-1 – Pool Bubble Rise Velocity Sensitivity Study (with Release Version of MELCOR 1.8.2)

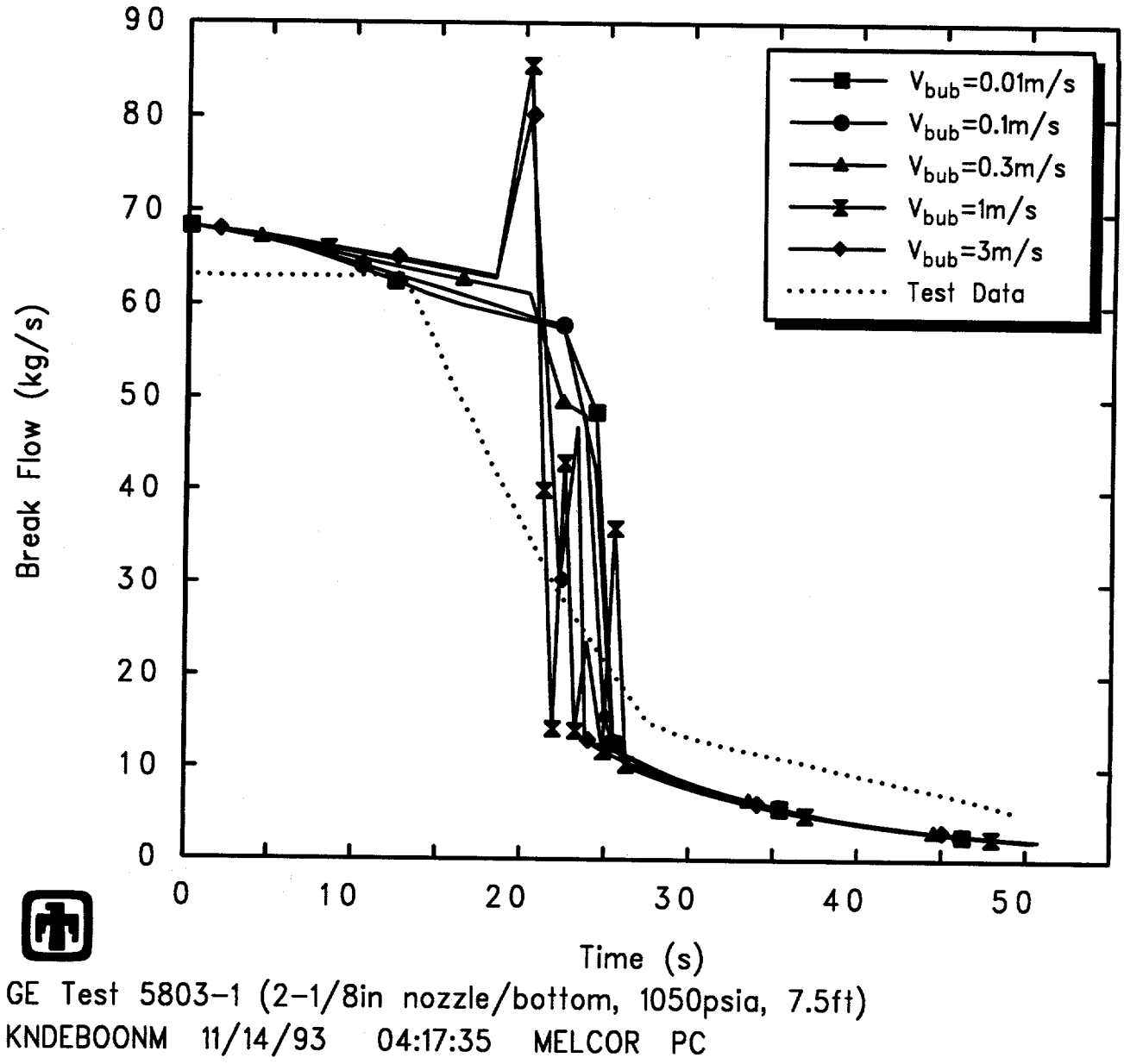

Figure 7.3.17. Blowdown Mass Flow for GE Large Vessel Bottom Blowdown Test 5803-1 – Pool Bubble Rise Velocity Sensitivity Study (with Release Version of MELCOR 1.8.2)

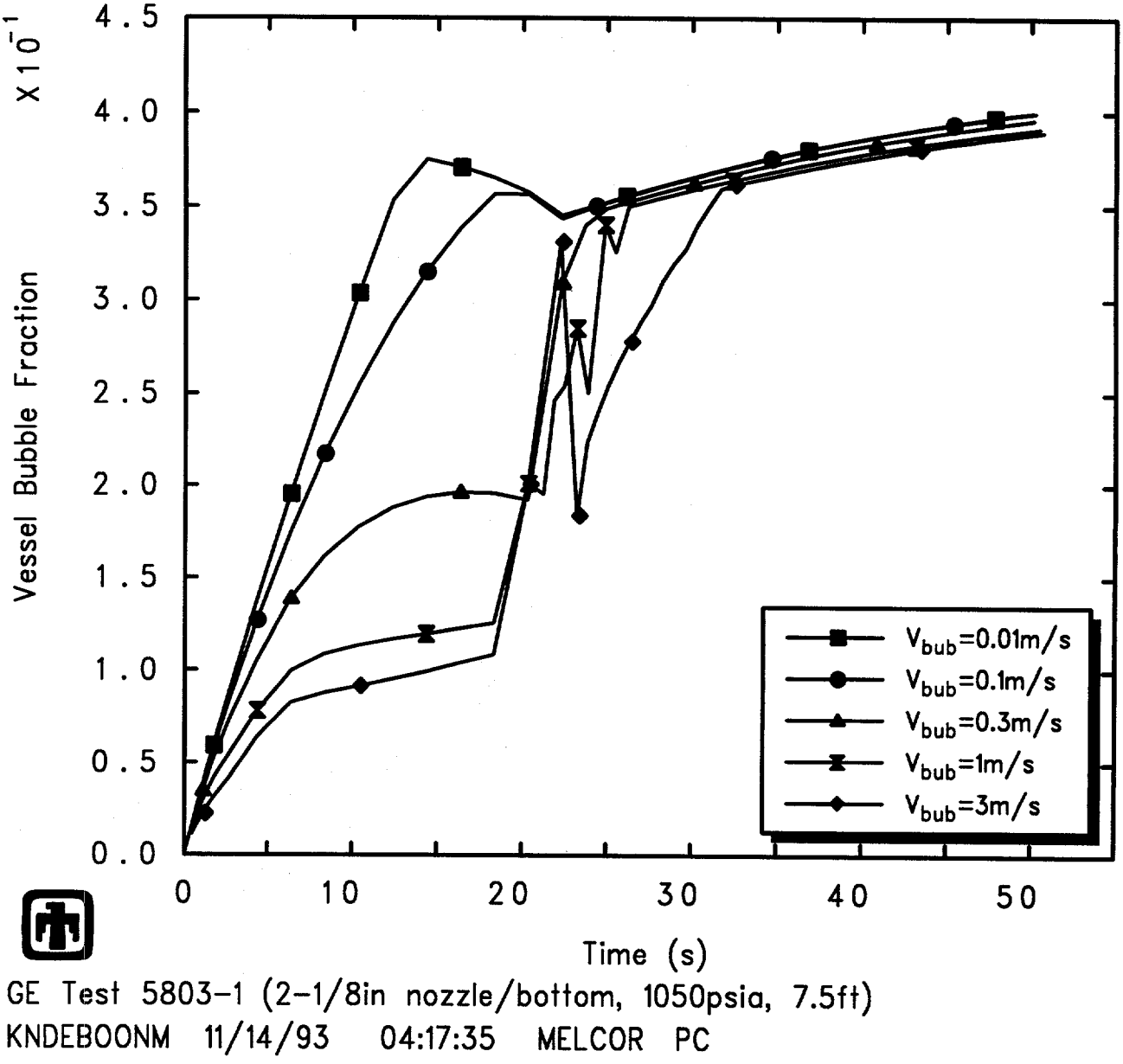

Figure 7.3.18. Vessel Two-Phase Liquid Level Bubble Fraction for GE Large Vessel Bottom Blowdown Test 5803-1 – Pool Bubble Rise Velocity Sensitivity Study (with Release Version of MELCOR 1.8.2)

8 Comparison to Other Codes

The GE large vessel blowdown and level swell tests have been used to validate both best-estimate thermal/hydraulics codes such as TRAC-B [13, 14, 15] and other engineering integrated, engineering-level severe accident analysis computer codes such as MAAP [16]. The results obtained with MELCOR are compared to results obtained using those other codes in this section.

8.1 TRAC-B

A early version of TRAC-B, TRACB02, a best-estimate BWR thermal/hydraulic code, was tested by performing assessment analyses for twelve separate effects and systems effects experiments [15], including the GE large vessel top blowdown test 5702-16. (Preliminary results of this assessment analysis were given in [13, 14].)

The test facility was nodalized using a VESSEL component for the pressure vessel and a PIPE component for the blowdown line and venturi. Fourteen axial levels, one radial ring and one theta sector were used in the vessel, essentially a one-dimensional model. Seven cells were used in the blowdown line pipe.

Figure 8.1.1 presents the two-phase liquid levels calculated within the vessel by these two codes, compared to test data and including the elevation of the dip tube opening, for reference. The system pressure calculated by TRAC-B is compared with test data and with the MELCOR basecase calculation for this test in Figure 8.1.2, while the total blowdown outflow calculated by TRAC-B is compared with test data and with the corresponding MELCOR basecase calculation result in Figure 8.1.3. (There was no break flow measurement for this test. The total break flow was estimated in [15] from the time-dependent vessel mass derived from vessel nodal pressure measurements. This figure is included for completeness, but the test data should not be considered quantitatively reliable.)

TRAC-B correctly reproduces the observed two-phase level behavior, with initial swelling of the level up to the break, due to flashing, followed by a drop in level due to inventory loss. TRAC-B thus calculates a relatively faster depressurization rate in the first few seconds corresponding to steam blowdown, slower depressurization as the mixture level swells up to the blowdown tube inlet which results in two-phase carryover, and finally sustained depressurization corresponding to high quality steam blowdown as the mixture level in the vessel drops back below the blowdown pipe inlet.

As already noted in Section 4.1, the two-phase mixture levels calculated by MELCOR correctly reproduce the observed initial swelling in each of the top blowdown tests; however, the vessel swollen levels calculated by MELCOR for the different nozzle dimensions all reach a similar maximum value which is significantly below the maximum two-phase levels in the test data, and the two-phase levels begin decreasing earlier in the calculations than observed in the test. (This discrepancy in measured *vs* calculated two-phase mixture levels in the MELCOR code is due to the limiting in the MELCOR

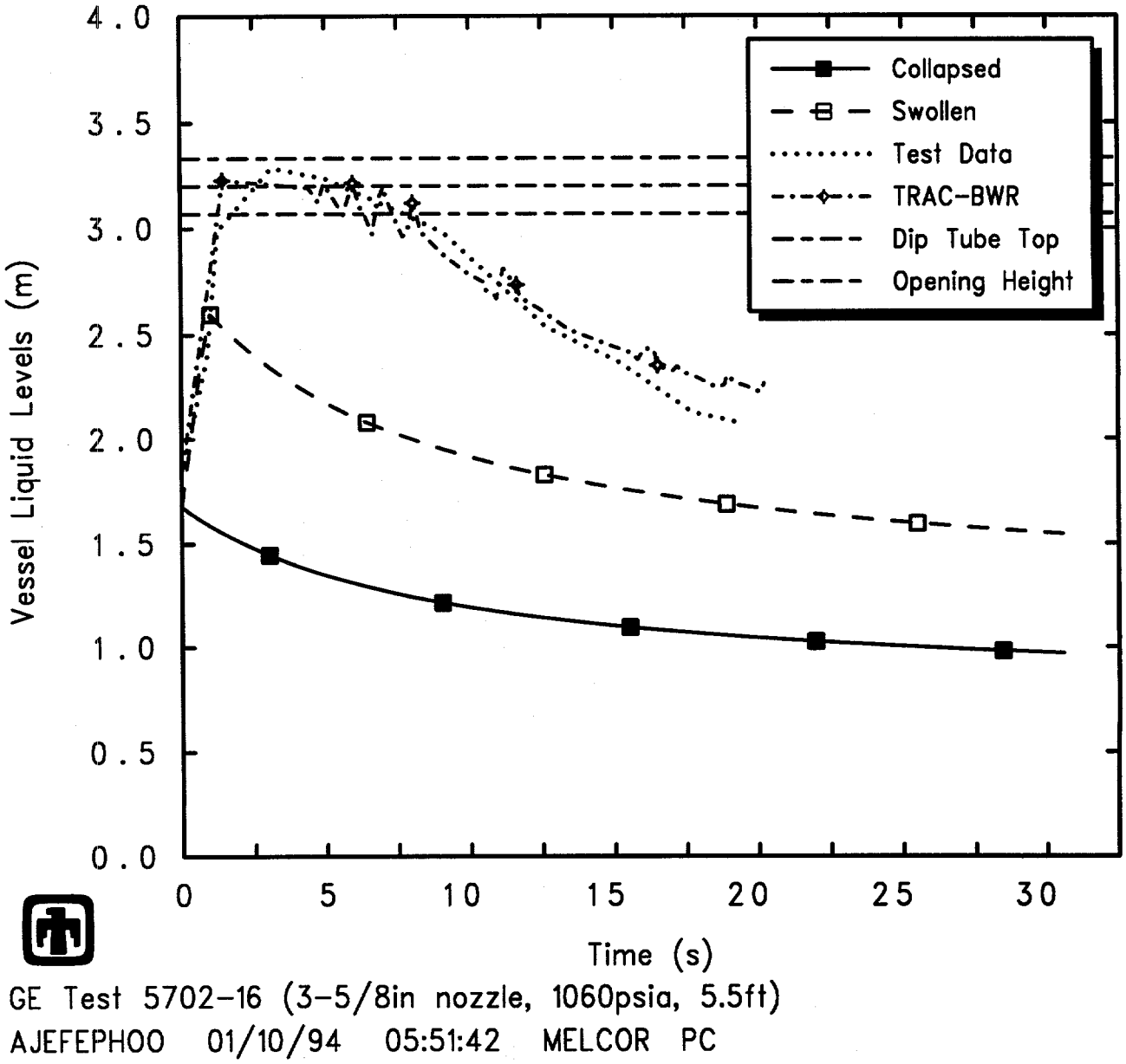

Figure 8.1.1. Vessel Liquid Levels for GE Large Vessel Top Blowdown Test 5702-16 – Code Comparison Sensitivity Study (with TRAC-B)

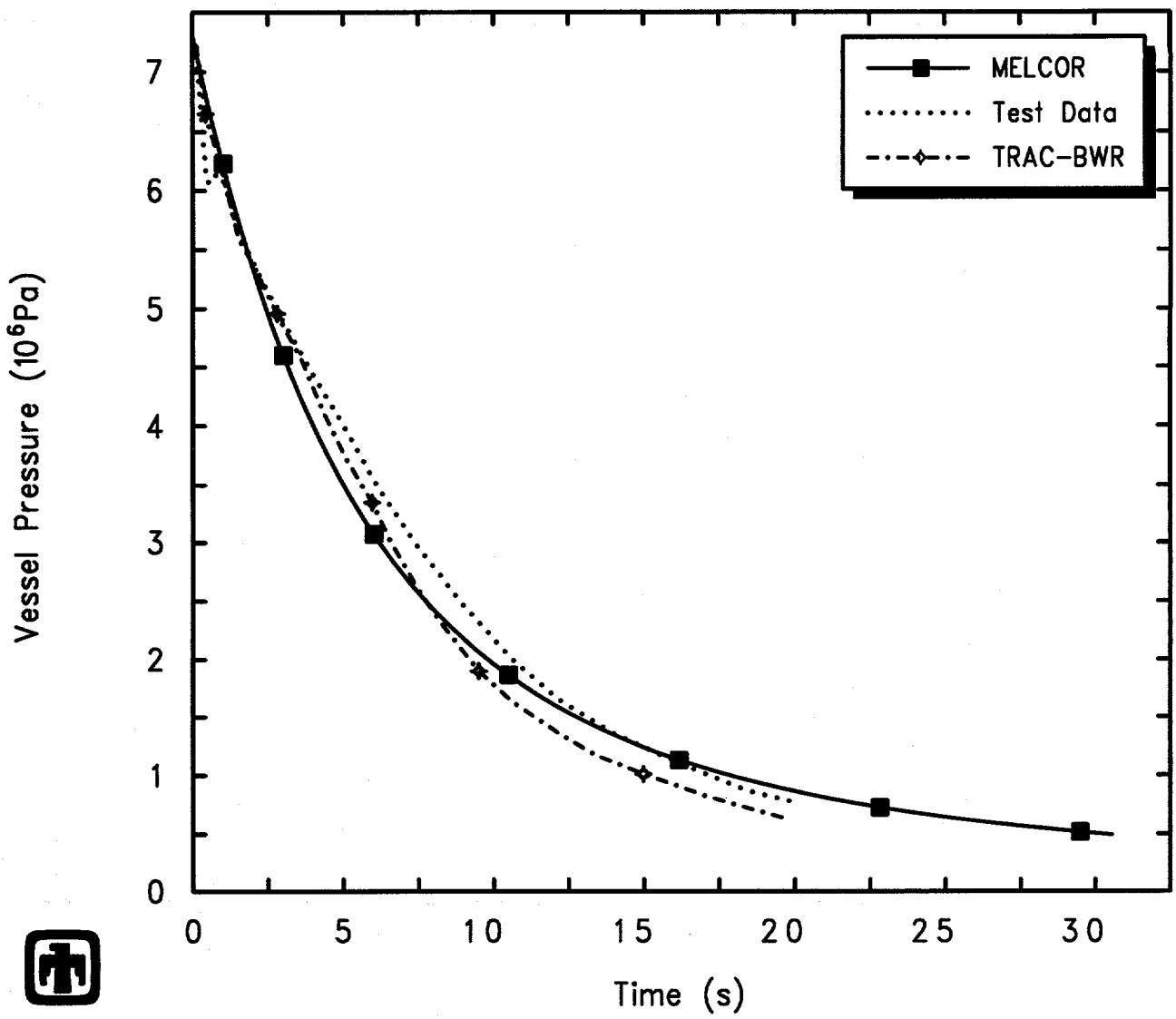

Figure 8.1.2. Vessel Pressure for GE Large Vessel Top Blowdown Test 5702-16 – Code Comparison Sensitivity Study (with TRAC-B)

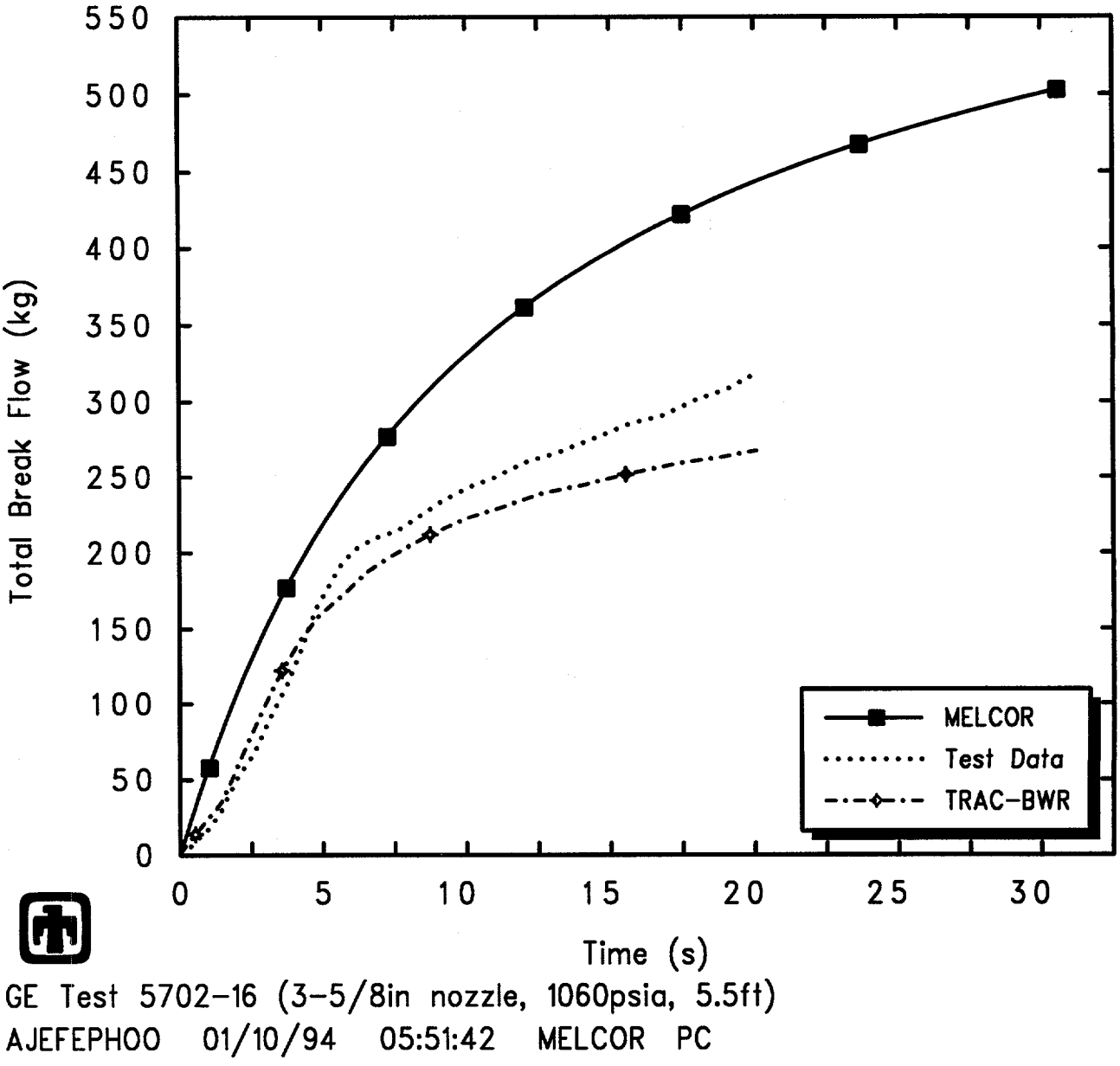

Figure 8.1.3. Total Break Flow for GE Large Vessel Top Blowdown Test 5702-16 – Code Comparison Sensitivity Study (with TRAC-B)

CVH package of the maximum allowed pool bubble fraction to 40%, as demonstrated in Section 5.2). MELCOR thus predicts only sustained steam blowdown, since the dip tube elevation remains uncovered throughout the calculation.

Neither code calculates the initial pressure dip and recovery observed because delayed nucleation is not modelled in either code. The TRAC-B calculation better matches the observed depressurization rate during the first <5s, when the vessel froth level has swollen up to the blowdown tube inlet elevation, resulting in two-phase outflow (which increases the mass outflow but decreases the volumetric outflow). The TRAC-B calculation then predicts a more rapid depressurization then measured, postulated to be due to underpredicting liquid pull-through in the blowdown line inlet. The MELCOR calculation yields a more rapid depressurization than measured earlier in the transient, due to pure steam outflow decreasing the mass outflow but increasing the volumetric outflow.

The best-estimate code, TRAC-B, clearly does a better job of predicting the observed level swell behavior in this test. However, the depressurization histories predicted by both codes are generally similar, despite the differences in calculated two-phase levels and total outflows.

8.2 MAAP

Analyses of the GE large vessel blowdown and level swell experiments were presented as part of a workshop on MAAP thermal/hydraulic qualifications and guidelines for plant application [16]. These tests were selected for qualification of the critical flow models in MAAP.

Two of the top blowdown tests were analyzed, as were the two bottom blowdown tests. Results from these calculations are compared to test data and to results from the corresponding MELCOR calculations in Figures 8.2.1 through 8.2.6.

Figures 8.2.1 and 8.2.2 show the pressure histories for the two top blowdown tests 5801-13 and 5801-19, with different Venturi nozzle throat diameters. MAAP predictions were given for both the actual break area and with a break multiplier of 0.7; in each figure, a set of MELCOR results are included, obtained using discharge coefficients varied from 1.0 to 0.6 (as described in Section 6.1). In both codes, reducing the break flow multiplier or discharge coefficient reduces the inventory loss and depressurization rate. For any given discharge coefficient, MELCOR predicts slightly slower depressurization than MAAP. A break flow multiplier of 0.7 was recommended for MAAP, based partly on these results. A discharge coefficient of 0.85 was used in the MELCOR basecase calculations for the top blowdown test analyses.

The pressure histories for the two bottom blowdown tests 5803-1 and 5803-2 are presented in Figures 8.2.3 and 8.2.4. For these bottom blowdown test analyses, MAAP results were available only for a break area multiplier of 0.7; in these figures, also, a set of MELCOR results are included for discharge coefficients varied from 1.0 to 0.6, with slower vessel depressurization for smaller discharge coefficients. As for the top blowdown

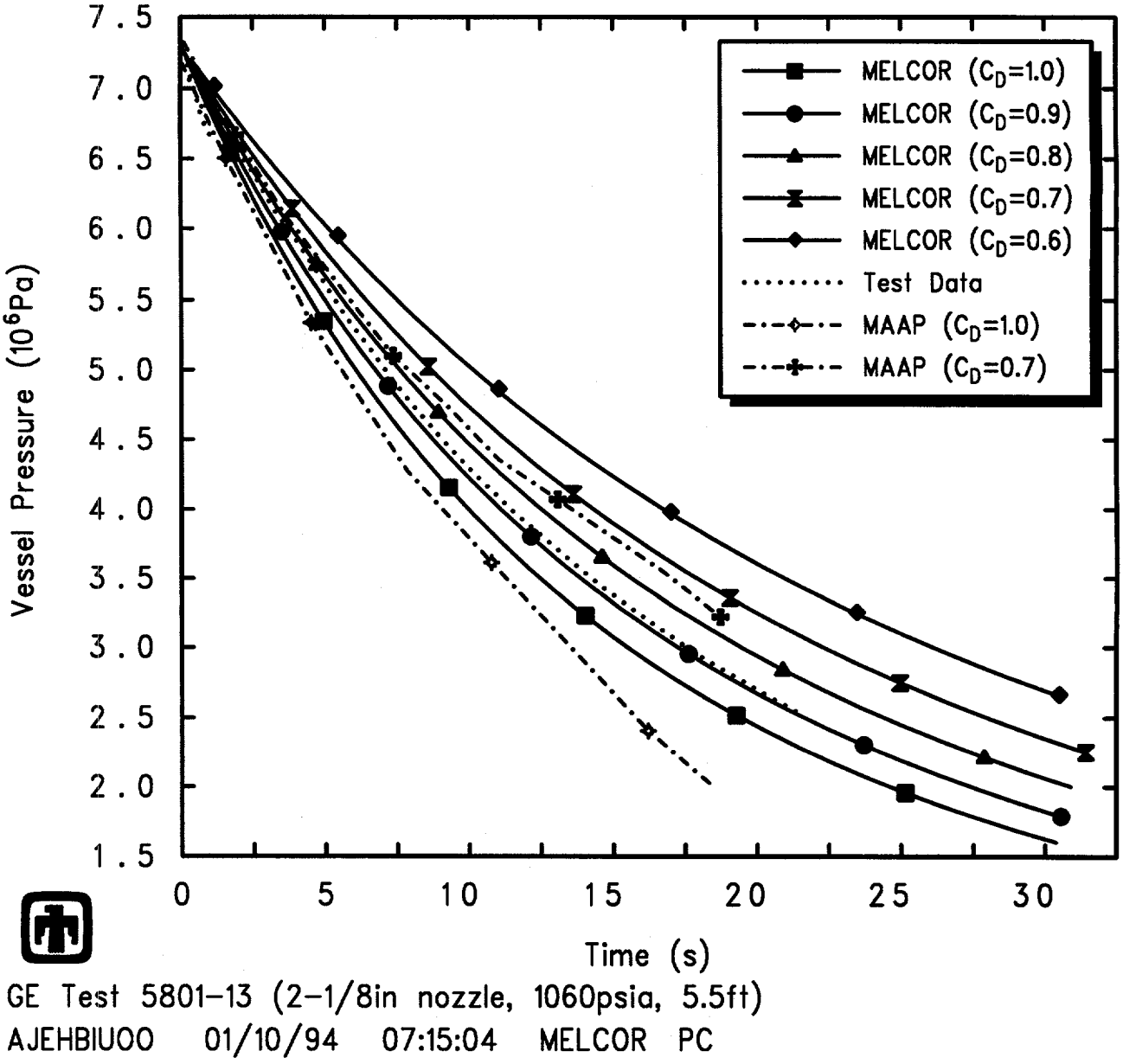

Figure 8.2.1. Vessel Pressure for GE Large Vessel Top Blowdown Test 5801-13 – Code Comparison Sensitivity Study (with MAAP)

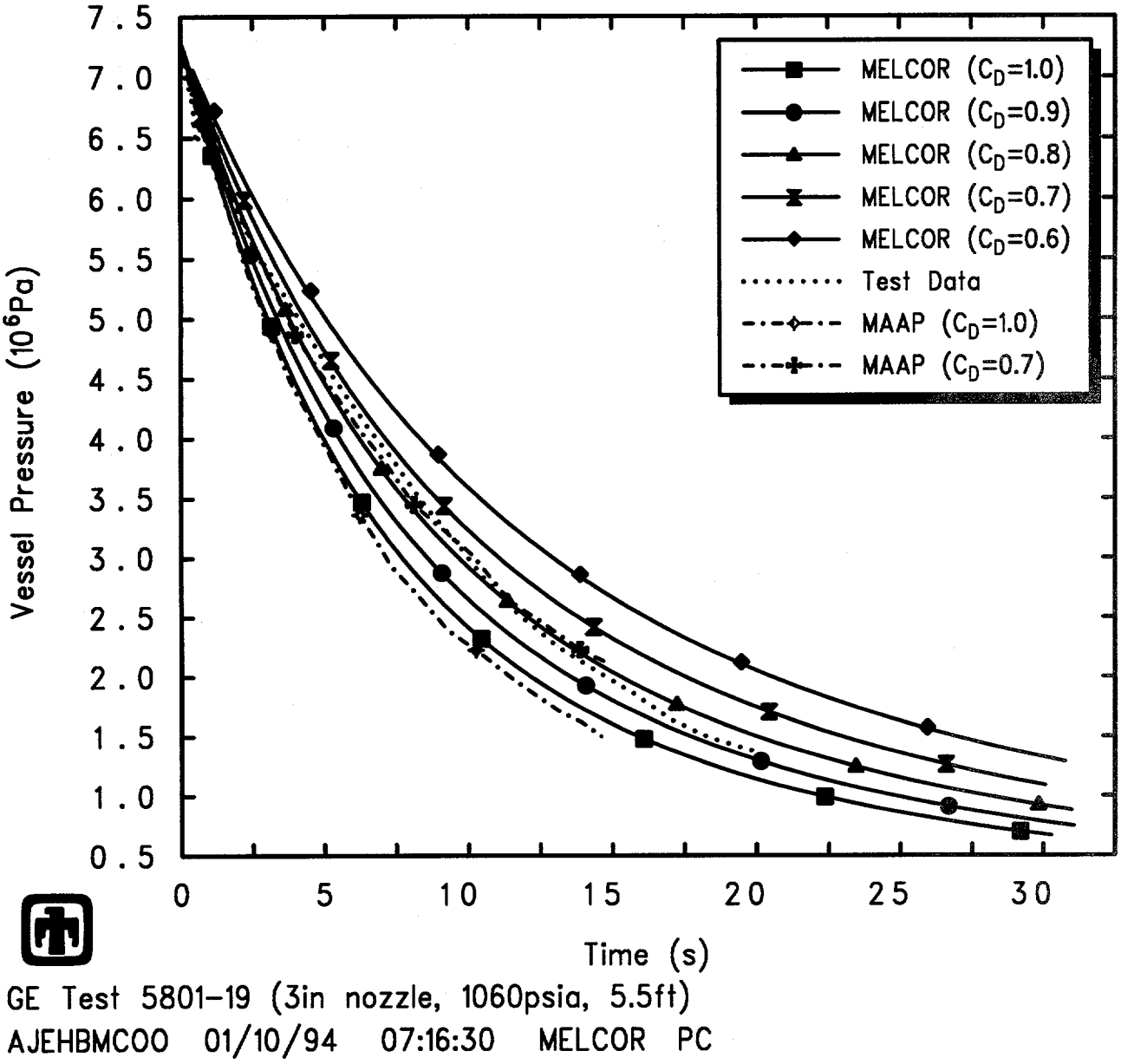

Figure 8.2.2. Vessel Pressure for GE Large Vessel Top Blowdown Test 5801-19 – Code Comparison Sensitivity Study (with MAAP)

test analyses shown in Figures 8.2.1 and 8.2.2, MELCOR predicts slightly slower depressurization for these bottom blowdown tests than MAAP for a given discharge coefficient (such as 0.7). A discharge coefficient of 0.75 was used in the MELCOR basecase calculations for the bottom blowdown test analyses. The MAAP vessel pressure prediction is in good agreement with test data during the early part of the blowdown, when the break is covered with liquid. After the break uncovers, MAAP underpredicts the test with the larger break diameter (5803-2) more than the test with the smaller break diameter (5803-1); the same trend is seen in the MELCOR results.

Figures 8.2.5 and 8.2.6 give the corresponding break flow comparisons for the two bottom blowdown tests. Both the MAAP and MELCOR calculations show an initial high break flow rate, as liquid is lost out the blowdown line, followed by a transition to pure steam outflow late in the blowdown transient. Both codes have a much sharper transition from liquid to vapor outflow than the more gradual transition found in the test data, indicating a much shorter period of two-phase flow in the calculations than in the experiments where, after break uncovery, more rapid depressurization increases the flashing in the remaining liquid and maintains two-phase outflow longer as the break partially recovers. The late-time break flows calculated by MAAP and MELCOR agree very well, but are less than the measured values, which may reflect some residual liquid entrainment even late in the transient.

The MAAP and MELCOR results for these GE large vessel blowdown and level swell tests are generally similar. Both codes underpredict the level swell observed at certain periods in the tests, but with little overall effect on the ability to calculate vessel depressurization during BWR accident scenarios.

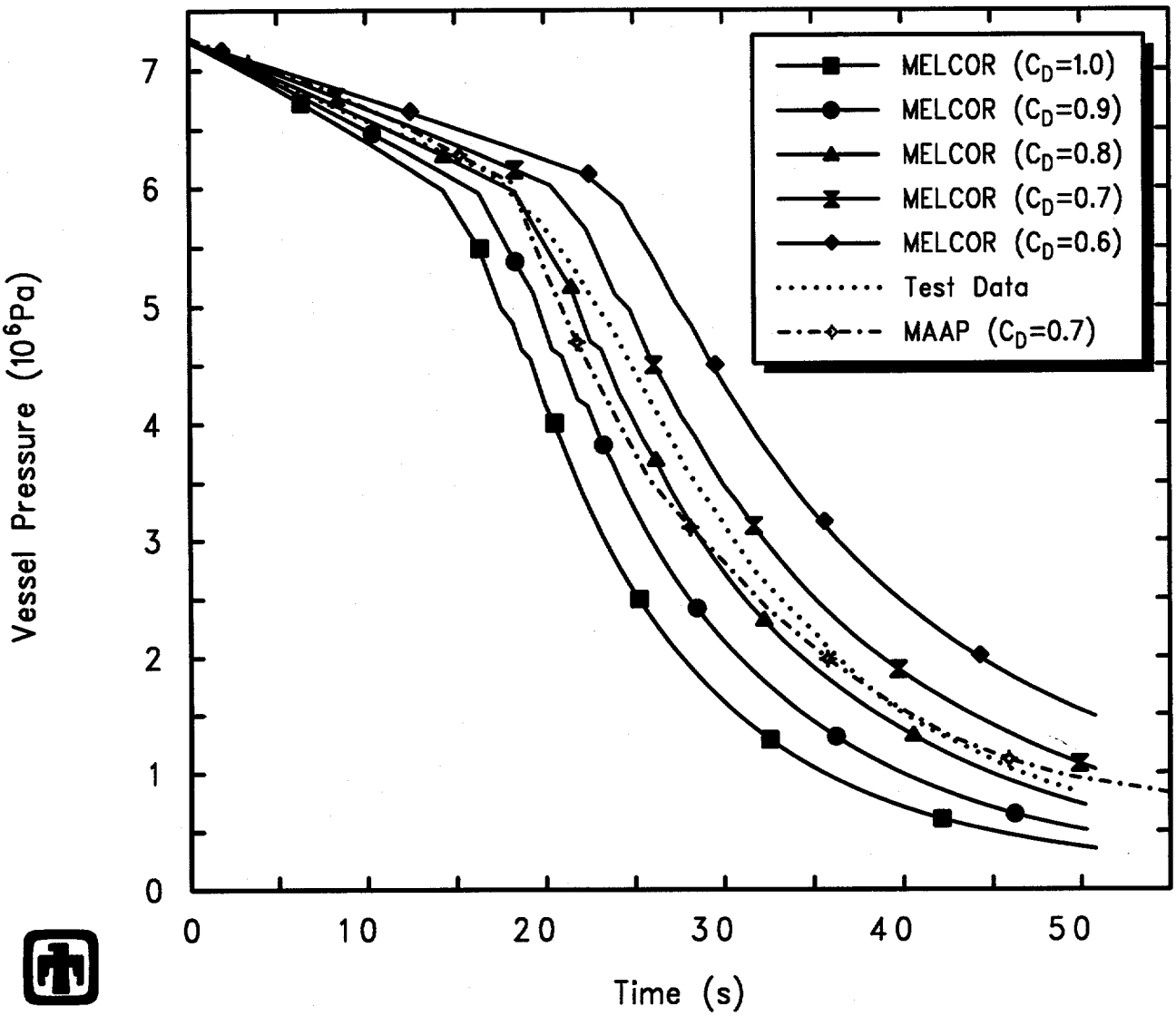

Figure 8.2.3. Vessel Pressure for GE Large Vessel Bottom Blowdown Test 5803-1 – Code Comparison Sensitivity Study (with MAAP)

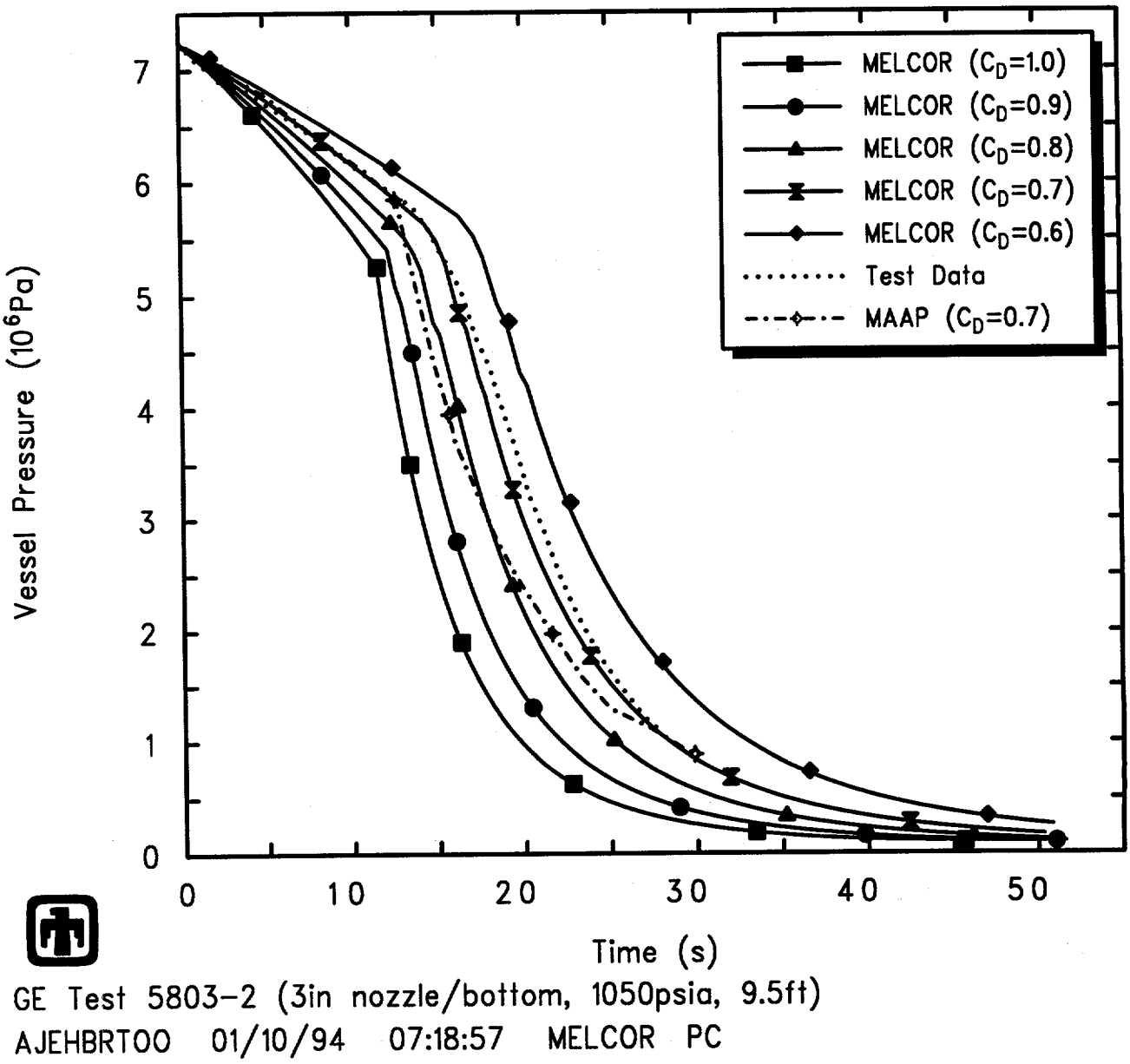

Figure 8.2.4. Vessel Pressure for GE Large Vessel Bottom Blowdown Test 5803-2 – Code Comparison Sensitivity Study (with MAAP)

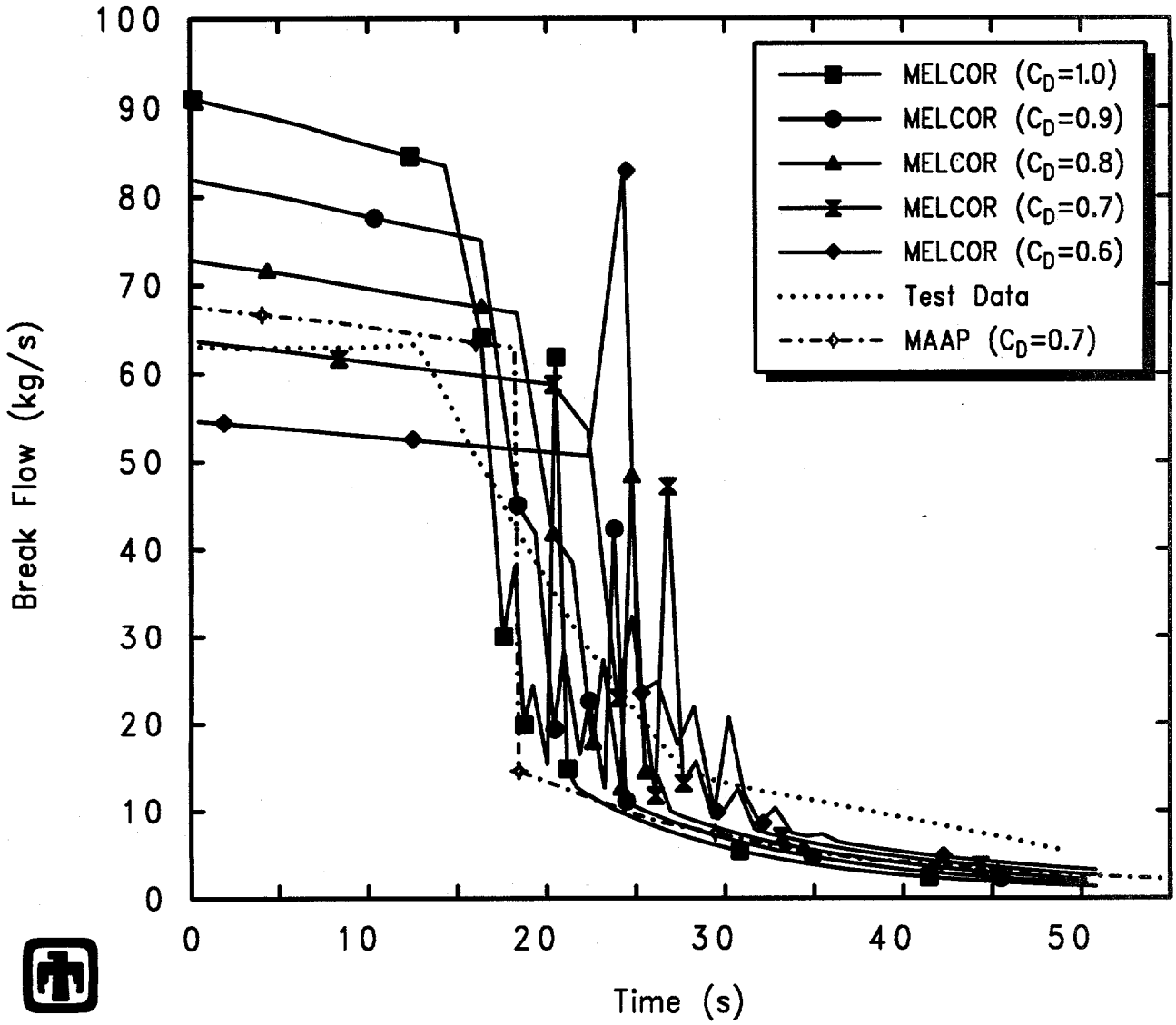

Figure 8.2.5. Blowdown Mass Flow for GE Large Vessel Bottom Blowdown Test 5803-1 – Code Comparison Sensitivity Study (with MAAP)

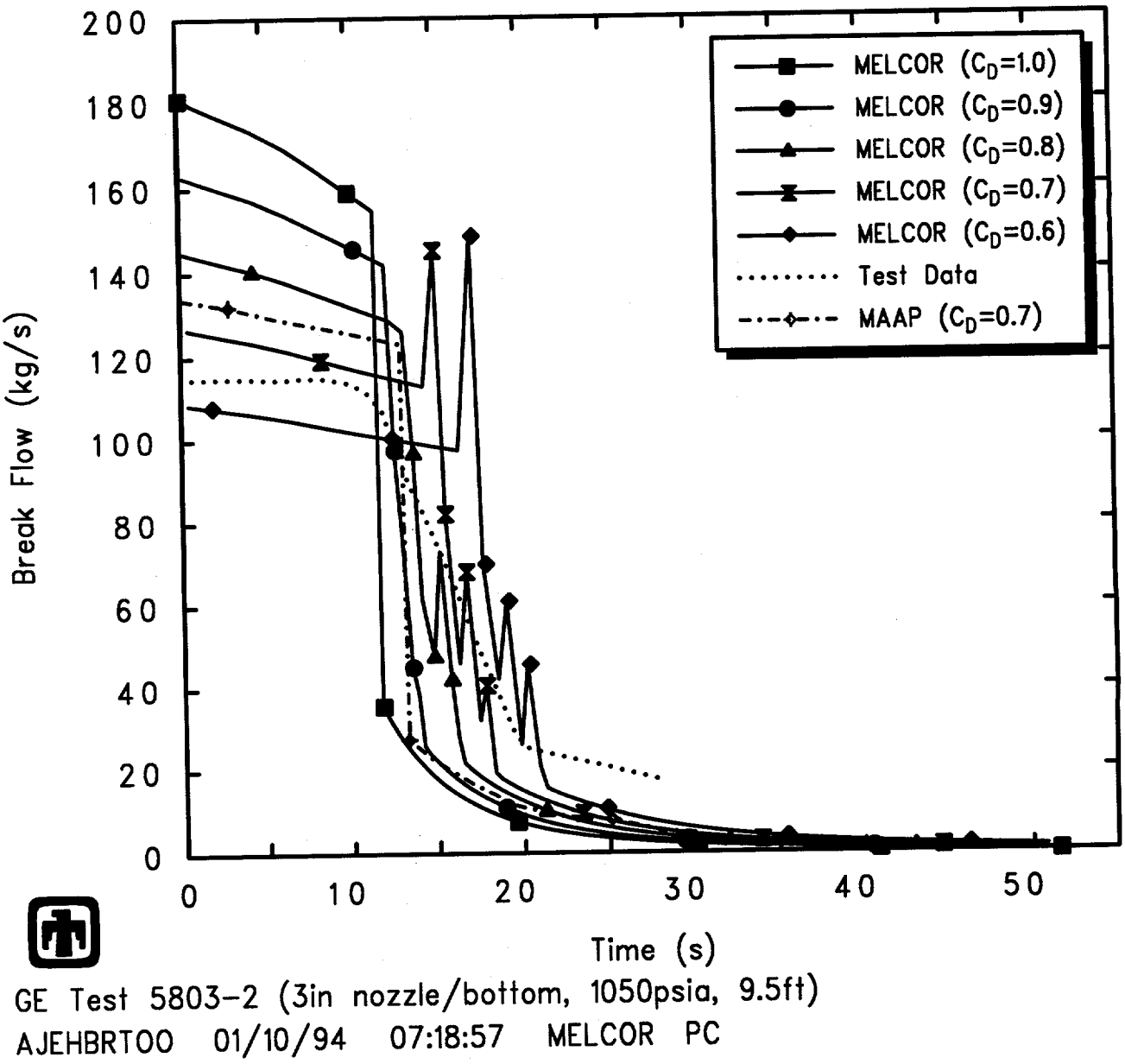

Figure 8.2.6. Blowdown Mass Flow for GE Large Vessel Bottom Blowdown Test 5803-2 – Code Comparison Sensitivity Study (with MAAP)

9 Summary and Conclusions

The MELCOR computer code has been used to analyze a series of blowdown tests performed in the early 1980s at General Electric (GE), as part of a code assessment program.

The GE large vessel blowdown and level swell experiments are a set of primary system thermal/hydraulic separate effects tests studying the level swell phenomenon for BWR transients and LOCAs. This experiment series includes both top blowdown tests with vapor blowdown, characteristic of accidents such as steam line breaks, and bottom blowdown tests with liquid and two-phase blowdown, more characteristic of recirculation line breaks. Assessment against this data allows an evaluation of the ability of MELCOR to predict the inventory loss, and hence time to core uncovery and heatup, in the early stages of transients and accidents in BWRs. Also, an implicit bubble separation algorithm has been implemented recently in the CVH package in MELCOR, since the release of MELCOR 1.8.2 in mid-1993. Analysis of the GE tests is intended to validate this algorithm for general use.

The calculated pressure transients generally agree well with the measurement. In the top blowdown tests, there is a relatively fast depressurization for the first few seconds, with progressively slower depressurization later in the transient. Qualitatively, the MELCOR calculations correctly reproduce the increase in vessel depressurization rate as the nozzle throat diameter and area increase, in the top blowdown experiment set. Quantitatively, there is progressively more difference between the calculated and measured vessel pressures as the nozzle throat diameter and area increases and the depressurization rate increases. This difference is due partly to the fact that the single value of form loss and discharge coefficients used in all these basecase calculations may not be optimum for all test conditions (as indicated by sensitivity studies), and partly due to increased discrepancies between measured and predicted level swelling as the nozzle throat diameter and area, and hence the depressurization rate, is increased.

The test data from the top blowdown tests show the two-phase mixture levels increasing more rapidly early in the transient as the nozzle throat diameter and area, and hence the depressurization rate, is increased, and also shows the two-phase mixture level reaching progressively greater maximum heights before beginning to drop off; for the test with the largest blowdown nozzle dimensions, the observed two-phase liquid level reaches above the top of the dip tube. The two-phase mixture, or swollen, levels calculated by MELCOR correctly reproduce the observed initial swelling, and the predicted two-phase levels initially increase at about the rate determined from measurement in each test; MELCOR correctly reproduces the qualitative trend seen in the test data that the measured two-phase liquid levels peak progressively earlier in the transient as the nozzle throat diameter and area, and hence the depressurization rate, is increased. However, the vessel swollen levels calculated by MELCOR for the different nozzle dimensions all reach a similar maximum value which is significantly below the maximum two-phase levels in the test data, and the two-phase levels begin decreasing earlier in the calculations than observed in the test. The swollen liquid levels in the calculation later decrease less rapidly

than observed for the measured two-phase liquid levels, for all these top blowdown tests. After the swollen levels begin to drop, the MELCOR calculations show progressively lower swollen levels at any particular time as the nozzle throat diameter and area, and hence the depressurization rate, is increased; the test data in contrast show the two-phase mixture levels in tests with larger blowdown nozzle diameters remaining above two-phase mixture levels in tests with smaller nozzle diameters throughout the entire period when test data are available.

The discrepancies found in measured *vs* calculated two-phase mixture levels in the basecase calculations for the top blowdown tests are generally all attributable to the limiting in the MELCOR CVH package of the maximum allowed pool bubble fraction to 40%. The maximum swollen levels in each of the four MELCOR top blowdown test analyses correspond to the bubble fraction in the pool reaching a value of $\leq$0.40. As the blowdown nozzle dimensions and hence the vessel depressurization rates increase, the swollen vessel level is predicted to reach that limiting value earlier in the transient and the swollen liquid level of the pool in the vessel then drops more rapidly as the vessel loses inventory more rapidly drops, due to continued inventory loss out the blowdown line, to maintain that pool bubble fraction of $\sim$0.40.

The calculated pressure transients generally agree very well with measurement for the bottom blowdown tests. There is a relatively slow depressurization for the first $\leq$20s seconds, followed by a more rapid depressurization beginning to slow again late in the transient. The relatively slow depressurization in the first phase of the transients corresponds to the time period where the two-phase mixture level is above the entrance to the blowdown line, so that liquid is being lost directly out the blowdown line. The subsequent more rapid depressurization begins when the mixture level drops below the blowdown line elevation, so that vapor blowdown can occur. As with the vessel pressure histories, the calculated mixture level transients for the bottom blowdown tests generally agree very well with measurement, both during the earlier liquid blowdown and the later vapor blowdown periods. The agreement of predicted level swell with test data is much better in this bottom blowdown test analysis than in any of the top blowdown test analyses because the pool bubble fraction is not being controlled within MELCOR by the maximum allowed value of 40%. There is significantly less level swell in this bottom blowdown test than in any of the top blowdown tests, and the pool bubble fraction is not affected by the maximum allowed value of 40% until very late in the transient, when little pool is left.

Sensitivity studies show that the blowdown flow and vessel depressurization are strongly dependent on the break discharge coefficient used, and weakly dependent on the form loss coefficient used in the blowdown line. The basecase calculations used a discharge coefficient of 0.85 for the top blowdown test analyses and 0.75 for the bottom blowdown test analyses, with a form loss coefficient of 1.5 applied to the nozzle throat area. Other sensitivity studies indicate that the nonequilibrium thermodynamics model must be enabled to calculate any level swell, and that the magnitude and timing of the level swell is dependent on the values used for the maximum allowed pool bubble fraction and for the bubble rise velocity assumed in the bubble separation model (not user input,

but variable through sensitivity coefficient input). Comparison to test data suggests that the default maximum allowed pool bubble fraction of 40% is too low for the top blowdown tests, but that the default bubble rise velocity of 0.3m/s produces generally good agreement with data for both top and bottom blowdown tests. The underprediction of level swell in the basecase calculations for the top blowdown tests does not appear to have any significant adverse effect on the code's ability to correctly calculate overall break flow and vessel depressurization.

The results proved insensitive to enabling the optional SPARC bubble rise physics model, which accounts for finite transit time through and interaction with any intervening water pool in the downstream volume. This bubble rise model does not contribute to the behavior response being predicted by MELCOR for these blowdown and level swell experiment analyses, even though two-phase conditions exist for significant periods in the test vessel, because the model only affects vapor flowing out of a flow path into a two-phase pool region; in the GE large vessel blowdown and level swell experiments, the two-phase conditions are on the upstream, inlet side of the flow path and the downstream sink volume consists of only atmosphere.

The basecase MELCOR input model for these GE large vessel blowdown and level swell experiments used a single control volume for the test vessel. This is standard modelling in MELCOR, where multiple control volumes are used to subdivide regions only if there is some obvious change in geometry or flow pattern. Unlike best-estimate codes such as TRAC or RELAP, MELCOR does not necessarily give better results if components or volumes are subdivided; most MELCOR models assume large, lumped component volumes. A sensitivity study was done in which the single vessel control volume was subdivided into a stack of multiple control volumes, with vertical flow paths added as needed to connect the stacked volumes. The heat structure modelling the vessel cylinder was subdivided correspondingly, also. This is a noding more typical of TRAC and/or RELAP than for MELCOR analyses. Since there is no obvious geometrically "correct" value for junction opening heights in flow paths connecting such a stack of volumes in MELCOR, both large (1ft) and small (1cm) junction opening heights were tried.

Subdividing the blowdown vessel into a stack of multiple control volumes has no significant effect on the vessel depressurization in the top blowdown test analyses. The results for two-phase level calculated using the single-volume basecase noding are in better quantitative agreement with test data in all of these top blowdown experiment analyses than the swollen levels calculated using a subdivided, stacked, multiple control volume model, even though the exact degree of level swelling is underpredicted with the basecase model. For bottom blowdown tests, using a subdivided noding yields small differences in depressurization history, a smoother break flow, and little or no difference in overall vessel level swell compared to test data or to basecase results when large junction opening heights are used. For both the top and bottom blowdown test analyses, using large junction opening heights (equal to the volume heights) in the flow paths connecting the subdivided, stacked control volumes in the finer noding produced much better agreement with both test data and with the 1-volume basecase results than did using small junction

opening heights. However, the results of this sensitivity study demonstrate no significant improvement in agreement with test data using a subdivided, stacked, multiple control volume vessel model rather than a single large volume. The results with the subdivided finer noding show more level swell at the bottom of the stack than further up, which seems counterintuitive. There appear to be no benefits and significant drawbacks found in subdividing the vessel into multiple, stacked control volumes, especially given the increased run times required.

There has been a lot of concern in the past about numeric effects seen in various MELCOR calculations [17], producing either differences in results for the same input on different machines or differences in results when the time step used is varied. Several calculations have been done to identify whether any such effects existed in our GE large vessel blowdown and level swell assessment analyses. We also compared results obtained with a recent code version (1.8OO) which includes a new implicit bubble separation algorithm with results obtained using the release version of MELCOR 1.8.2, 1.8NM (in which the bubble rise calculation is explicitly coupled to the rest of the thermal/hydraulics analysis).

The GE large vessel basecase calculations were rerun, using the same code version and input models, on an IBM RISC-6000 Model 550 workstation, on an HP 755 workstation, on a SUN Sparc2 workstation, on a CRAY Y-MP8/864, and on a 50MHz 486PC (IBM clone). There is very little or no difference found in the results obtained on any of these hardware platforms. The SUN and PC are always slowest in run time required; the IBM, HP and Cray are all significantly faster with the Cray the fastest by a small fraction for these analyses. There is also generally little or no difference found in the results obtained as the user-specified maximum allowed time step is progressively reduced and, as would be expected, reducing the time step and thus increasing the number of cycles required correspondingly increases the run times required.

An implicit bubble separation algorithm has been implemented recently in the CVH package in MELCOR. Prior to the implementation of this algorithm, MELCOR was experiencing problems with natural circulation phenomena in the COR package; it is expected that the problems with calculating natural circulation will be eliminated with the implementation of the implicit bubble separation algorithm. A sensitivity study has been done on the effect of this implicit bubble separation algorithm comparing results from MELCOR version 1.8OO to results from the release version of MELCOR 1.8.2, which was MELCOR 1.8NM. The results of that study indicate that there are no major differences in vessel blowdown and/or level swell calculated by either the release version of MELCOR 1.8.2 (1.8NM) or by MELCOR version 1.8OO after an implicit bubble separation algorithm has been added. The results and conclusions of this assessment study should apply equally well to either the release version of 1.8.2 or to later versions.

One noticeable difference is that with the release code the vessel pool bubble fraction always increases to the maximum allowed value, albeit more slowly for larger bubble rise velocities, while with the new implicit bubble separation algorithm the vessel pool bubble fraction equilibrates at lower values for the larger bubble rise velocities. With no difference in vessel depressurization, blowdown flow or collapsed liquid level, this results

in higher swollen liquid levels calculated with the release code version than with the new implicit bubble separation algorithm for bubble rise velocities increased above the code default of 0.3m/s. (There is not much difference in swollen liquid levels calculated with the release code version and with the new implicit bubble separation algorithm for the default bubble rise velocity of 0.3m/s.)

The GE large vessel blowdown and level swell tests have been used to validate both best-estimate thermal/hydraulics codes such as TRAC-B [13, 14, 15] and other engineering integrated, engineering-level severe accident analysis computer codes such as MAAP [16]. The results obtained with MELCOR have been compared to available results obtained using those other codes. The MAAP and MELCOR results for these GE large vessel blowdown and level swell tests are generally similar. Both codes underpredict the level swell observed at certain periods in the tests, but with little overall effect on the ability to calculate vessel depressurization during BWR accident scenarios.

TRAC-B correctly reproduces the observed two-phase level behavior, with initial swelling of the level up to the break, due to flashing, followed by a drop in level due to inventory loss. TRAC-B thus calculates a relatively faster depressurization rate in the first few seconds corresponding to steam blowdown, slower depressurization as the mixture level swells up to the blowdown tube inlet which results in two-phase carryover, and finally sustained depressurization corresponding to high quality steam blowdown as the mixture level in the vessel drops back below the blowdown pipe inlet. As already noted, the two-phase mixture levels calculated by MELCOR correctly reproduce the observed initial swelling in each of the top blowdown tests; however, the vessel swollen levels calculated by MELCOR for the different nozzle dimensions all reach a similar maximum value which is significantly below the maximum two-phase levels in the test data, and the two-phase levels begin decreasing earlier in the calculations than observed in the test. (This discrepancy in measured *vs* calculated two-phase mixture levels in the MELCOR code is due to the limiting in the MELCOR CVH package of the maximum allowed pool bubble fraction to 40%.) MELCOR thus predicts only sustained steam blowdown, since the dip tube elevation remains uncovered throughout the calculation. The best-estimate code, TRAC-B, clearly does a better job of predicting the observed level swell behavior in this test. However, the depressurization histories predicted by both codes are generally similar, despite the differences in calculated two-phase levels and total outflows.

The overall results for these GE large vessel blowdown and level swell test assessment analyses show that MELCOR does reasonably well calculating break flow and vessel depressurization for typical BWR accident conditions. While the level swell is underpredicted at certain periods in the tests, this discrepancy appears to have little effect on the code's overall ability to calculate vessel blowdown during BWR accident scenarios.

Bibliography

[1] R. M. Summers *et al.*,"MELCOR 1.8.0: A Computer Code for Severe Nuclear Reactor Accident Source Term and Risk Assessment Analyses", NUREG/CR-5531, SAND90-0364, Sandia National Laboratories, January 1991.

[2] C. D. Leigh, ed.,"MELCOR Validation and Verification – 1986 Papers", NUREG/CR-4830, SAND86-2689, Sandia National Laboratories, March 1987.

[3] L. N. Kmetyk, "MELCOR 1.8.1 Assessment: LACE Aerosol Experiment LA4", SAND91-1532, Sandia National Laboratories, September 1991.

[4] L. N. Kmetyk, "MELCOR 1.8.1 Assessment: FLECHT SEASET Natural Circulation Experiments", SAND91-2218, Sandia National Laboratories, December 1991.

[5] L. N. Kmetyk, "MELCOR 1.8.1 Assessment: ACRR Source Term Experiments ST-1/ST-2", SAND91-2833, Sandia National Laboratories, April 1992.

[6] L. N. Kmetyk, "MELCOR 1.8.1 Assessment: LOFT Integral Experiment LP-FP-2", SAND92-1273, Sandia National Laboratories, December 1992.

[7] R. J. Gross, "MELCOR 1.8.1 Assessment: PNL Ice Condenser Experiments", SAND92-2165, Sandia National Laboratories, June 1993.

[8] L. N. Kmetyk, "MELCOR 1.8.1 Assessment: Marviken-V Aerosol Transport Tests ATT-2b/ATT-4", SAND92-2243, Sandia National Laboratories, January 1993.

[9] T. J. Tautges, "MELCOR 1.8.2 Assessment: the DF-4 BWR Fuel Damage Experiment", SAND93-1377, Sandia National Laboratories, October 1993.

[10] L. N. Kmetyk, "MELCOR 1.8.2 Assessment: IET Direct Containment Heating Tests", SAND93-1475, Sandia National Laboratories, October 1993.

[11] L. N. Kmetyk, "MELCOR 1.8.2 Assessment: Surry PWR TMLB' (with a DCH Study)", SAND93-1899, Sandia National Laboratories, to be published.

[12] G. L. Sozzi, "Description of Void Fraction Distribution and Level Swell during Vessel Blowdown Transients", App. A-C in "BWR Refill-Reflood Program Task 4.8 – Model Qualification Task Plan", NUREG/CR-1899, EPRI NP-1527, GEAP-24898, General Electric Co., August 1981.

[13] M. Alamgir, "BWR Refill-Reflood Program Task 4.8 – TRAC-BWR Model Qualification for BWR Safety Analysis; Final Report", NUREG/CR-2571, EPRI NP-2377, GEAP-22049, General Electric Co., October 1983.

[14] J. G. M. Andersen, K. H. Chu, J. C. Shaug, "BWR Refill-Reflood Program Task 4.7 – Model Development; Basic Models for the BWR Version of TRAC", NUREG/CR-2573, EPRI NP-2375, GEAP-22051, General Electric Co., September 1983.

[15] Y. K. Cheung, V. Parameswaran, J. C. Shaug, "BWR Refill-Reflood Program Task 4.7 – Model Development; TRAC-BWR Component Models", NUREG/CR-2574, EPRI NP-2376, GEAP-22052, General Electric Co., September 1983.

[16] J. M. Healzer, "MAAP Comparison to Separate Effects Tests", in "Proceedings: MAAP Thermal-Hydraulic Qualifications and Guidelines for Plant Application Workshop", EPRI NP-7515, EPRI, October 1991.

[17] B. E. Boyack, V. K. Dhir, J. A. Gieseke, T. J. Haste, M. A. Kenton, M. Khatib-Rahbar, M. T. Leonard, R. Viskanta, "MELCOR Peer Review", LA-12240, Los Alamos National Laboratory, March 1992.

A Test 5801-13 Basecase Calculation Input Deck

```
*
*eor* melgen
*
title, 'GE Test 5801-13 (2-1/8in nozzle, 1060psia, 5.5ft)'
*
allowreplace
*
outputf      5801-13.gout
diagf        5801-13.gdia
plotf        5801-13.ptf
restartf     5801-13.rst
*
dttime       0.001
*
**************************************************************************
*
* noncondensible gases input
*
**************************************************************************
*
ncg000     o2  4
ncg001     n2  5
ncg002     h2  6
ncg003     co  7
ncg004     co2  8
ncg005     ch4  9
*
**************************************************************************
*
* control volume input
*
**************************************************************************
*
cv10000  'vessel'  2  1  4
cv10003  1.119
cv100a0  3
cv100a1  zpol  1.6764  pvol  7.306e6  tatm  561.98
cv100b1  0.0     0.0
cv100b2  0.4572  0.38896
cv100b3  2.134   2.2653
cv100b4  3.810   4.0273
cv100b5  4.268   4.5306
*
cv99900  'resevoir'  2  1  6
cv99901  0  -1
```

```
cv999a0  3
cv999a1  pvol  1.013e5  tatm  300.0
cv999a2  mlfr.4  0.21  mlfr.5  0.79  rhum  1.0
cv999b1  0.0    0.0
cv999b2  10.0   10.0
*
**************************************************************************
*
* flow path input
*
**************************************************************************
*
fl00200  'dip-tube'  100  999  3.2  0.762
fl00201  0.0022946  3.035  1.0  0.01  0.2628
fl00202  3  0  1  1
fl00203  1.5  1.5  0.85  0.85
fl00204  0.0  0.0
fl002s1  0.05425    3.035   0.26281
*
**************************************************************************
*
* heat structure input
*
**************************************************************************
*
hs00100000  5  2  0
hs00100001  'vessel'
hs00100002  0.4572  1.0
hs00100100  -1  1  0.5969
hs00100101  0.6223  5
hs00100200  -1
hs00100201  stainless-steel  4
hs00100300  -1
hs00100400  1  100  int  0.0  1.0
hs00100401  0.8  gray-gas-a  1.0
hs00100500  12.3124  1.19  3.3528
hs00100600  0
*
.
*
*eor* melcor
*
title, 'GE Test 5801-13 (2-1/8in nozzle, 1060psia, 5.5ft)'
*
allowreplace
*
outputf      5801-13.out
```

```
diagf        5801-13.dia
messagef     5801-13.mes
plotf        5801-13.ptf
restartf     5801-13.rst
*
restart  -1
cpuleft  60.0
cpulim  10000.0
tend  30.0
*
time1  0.0  2.0  0.00001  20.0  0.1  60.0
*
.
*
*eor* hisplt
*
color,2,3,4,6,0
*
file=5801-13.ptf
*
vlabel,CPU Time (()s)
ulabel,Time (()s)
plot time cpu color=2 line=solid legend='Total'
cplot time cvh-cput color=5 line=mdash legend='CVH'
cplot time hs-cpuc color=6 line=dotdash legend='HS'
legend,ul
*
vlabel,Time Step (()s)
ulabel,Time (()s)
plot time dt line=solid symbol=! legend='Time Step'
legend,ur
*
vlabel,Pressure (()Pa)
ulabel,Time (()s)
plot time cvh-p.100 line=solid symbol=! legend='Vessel'
cplot time cvh-p.300 line=mdash symbol=> legend='Environment'
data line=dot legend='Test Data'
*readfile ge-level.dat p1
legend,ur
*
vlabel,Vessel Temperature (()K)
ulabel,Time (()s)
plot time cvh-tliq.100 line=solid symbol=! legend='Pool'
cplot time cvh-tvap.100 line=mdash symbol=& legend='Atms'
legend,bottom
*
vlabel,Vessel Liquid Levels (()m)
```

```
ulabel,Time (()s)
limits 1.0,-1.0  0.0,5.0
plot time cvh-cliqlev.100 line=solid symbol=! legend='Collapsed'
cplot time cvh-liqlev.100 line=mdash symbol=& legend='Swollen'
data line=dot legend='Test Data'
*readfile ge-level.dat 11
legend,ur
*
vlabel,Break Flow (()kg/s)
ulabel,Time (()s)
plot time fl-mflow.002 line=solid symbol=! legend='Dip Tube'
legend,ur
*
```

External Distribution:

U. S. Nuclear Regulatory Commission (18)
Attn: Y. S. Chen, NLN-344
M. A. Cunningham, NLS-372
F. Eltawila, NLN-344
R. B. Foulds, NLN-344
S. Basu, NLN-344
C. Gingrich, NLN-344
C. G. Tinkler, NLN-344
R. O. Meyer, NLN-353
J. A. Mitchell, NLS-314
C. P. Ryder, NLS-372
L. Soffer, NLS-324
W. Hodges, NLS-007 (??)
J. A. Murphy, NLS-007
L. M. Shotkin, NLN-353
N. Lauben, NLN-353
R. Landry, OWFN 11D23
Washington, DC 20555

S. Y. Chen
Argonne National Laboratory
9700 South Cass Avenue
Argonne, IL 60439

Battelle Columbus Laboratories (3)
Attn: P. Cybulskis
M. Carmel
R. S. Denning
505 King Avenue
Columbus, OH 43201

Brookhaven National Laboratory (2)
Attn: I. K. Madni
T. Pratt
Bldg. 130
32 Lewis
Upton, NY 11973

Idaho National Engineering Laboratory (5)
Attn: A. Brown
R. J. Dallman
D. W. Golden
S. E. Reed
G. W. Johnsen
EG&G Idaho
P. O. Box 1625
Idaho Falls, ID 83404

D. Jones
EI International
P. O. Box 50736
Idaho Falls, ID 83405

Electric Power Research Institute (3)
Attn: E. Fuller
R. N. Oehlberg
P. O. Box 10412
Palo Alto, CA 94303

Los Alamos National Laboratory (2)
Attn: B. E. Boyack, K-551
D. R. Liles, K-553
P. O. Box 1663
Los Alamos, NM 87545

Oak Ridge National Laboratory (11)
P. O. Box 2009
Oak Ridge, TN 37831-8057
Attn: S. R. Greene, MS-8057
R. H. Morris, MS-8057
S. E. Fisher, MS-8057
R. Sanders, MS-8057
T. L. Heatherly, MS-8057
S. A. Hodge, MS-8057
C. R. Hyman, MS-8057
B. W. Patton, MS-8057
D. B. Simpson, MS-8057
R. P. Taleyarkhan, MS-8057
M. L. Tobias, MS-8088

Andrzej Drozd
Nuclear Regulatory Commission
OWFN, MS 8E1
11555 Rockville Pike
Rockville, MD 20852

W. P. Barthold
Barthold & Associates
132 Seven Oaks Drive
Knoxville, TN 37922

K. C. Wagner
Science Applications Intl. Corp.
2109 Air Park Rd. SE
Albuquerque, NM 87106

Savannah River Laboratory (2)
Attn: B. DeWald
D. Allison
Westinghouse Savannah River Co.
Bldg. 773-41A
Aiken, SC 29808-0001

Westinghouse Hanford Co. (2)
Attn: D. Ogden
O. Wang
P. O. Box 1970
Richland, WA 99352

General Electric Company (3)
Knolls Atomic Pwer Laboratory
Attn: D. F. McMullan
G. H. Epstein
E. Mennard
Bldg. F3, Room 8
P. O. Box 1072
Schenectady, NY 12301-1072

Bettis Atomic Power Laboratory (3)
Attn: Mark Riley
Jow Semanchik
Vincent Baiamonte
P. O. Box 79
West Mifflin, PA 15122

Mohsen Khatib-Rahbar
Energy Research Inc.
P. O. Box 2034
Rockville, MD 20852

V. K. Dhir
2445 22nd Street
Santa Monica, CA 90403

R. Viskanta
Purdue University
Heat Transfer Laboratory
School of Mechanical Engineering
West Lafayette, IN 47907

Dr. Jim Gieseke
Battelle Memorial Institute
505 King Ave.
Columbus, Ohio 43201

M. A. Kenton
Gabor, Kenton & Associates
770 Pasquinelli Drive
Suite 426
Westmont, IL 60559

University of California
Attn: T. Theofanous
ERC-CRSS
Santa Barbara, CA 93106

Professor K. B. Cady
Nuclear Science and Engineering
Cornell Universioty
Ward Laboratory
Ithaca, NY 14853-7701

F. E. Haskin
University of New Mexico
Department of Chemical and Nuclear Engineering
Albuquerque, NM 87131

J. C. Lee
University of Michigan
Dept. of Nuclear Engineering
Cooley Building, North Campus
College of Engineering
Ann Arbor, MI 48109-2104

University of Wisconsin (2)
Dept. of Nuclear Engineering
Attn: M. L. Corradini
G. A. Moses
Engineering Research Building
1500 Johnson Drive
Madison, WI 53706

Ramu K. Sundaram
Manager, LOCA Analysis Group
Nuclear Engineering
Yankee Atomic Electric Company
580 Main Street
Bolton, MA 01740

John Bolin
CEGA
P. O. Box 85608
San Diego, CA 92186-9784

M. Plys
Fauske & Associates
16W070 West 83rd Street
Burr Ridge, IL 60521

Nick Trikouros
GPU Nuclear Corporation
One Upper Pond Road
Parsippany, NJ 07054

B. Raychaudhuri
Nebraska Public Power District
PRA & Engineering Review Group
P. O. Box 499
Columbus, NE 68601

Frank Elia
Stone & Webster Engineering Corp.
245 Summer Street
Boston, MA 02210

Prof. Dr. Johann Korkisch
Institute of Analytical Chemistry
University of Vienna
A-1090 Vienna, Währingerstrasse 38
AUSTRIA

Samir S. Girgis
Atomic Energy of Canada Limited
CANDU Operations
Sheridan Park Research Community
Mississagua, Ontario
CANADA L5K1B2

Paul J. Fehrenbach
Chalk River Nuclear Laboratories
Fuel Engineering Branch, RSR Division
Chalk River, Ontario
CANADA KOJ1J0

Dr. Bohumír Kujal
Department of Reactor Technology
Nuclear Research Institute Řeˇz plc
250 68 Řež
CZECH REPUBLIC

Andrej Mitro
Institute of Radioecology and Applied Nuclear Techniques
Garbiarska 2
P. O. Box A-41
040 61 Košice
CHECHOSLOVAKIA

Shih-Kuei Cheng
Institute of Nuclear Energy Research
P. O. Box 3-3
Lung-Tan, Taiwan
REPUBLIC OF CHINA

Mr. Yi-Bin Chen
Department of Nuclear Technology
Atomic Energy Council
67, Lane 144
Keelung Road, Section 4
Taipei, Taiwan 106
REPUBLIC OF CHINA

Technical Research Centre of Finland (3)
Nuclear Engineering Laboratory
Attn: Lasse Mattila
Ilona Lindholm
Esko Pekkarinen
P. O. Box 208 (Tekniikantie 4)
SF-002151 Espoo
FINLAND

Jorma V. Sandberg
Finnish Center Radiation & Nucl. Safety,
Dept. of Nuclear Safety
P. O. Box 268
SF-00101 Helsinki
FINLAND

Akihide Hidaka
Safety Research Department
Reactor Accident Studies and Modelling Branch
DRS/SEMAR
Cadarache Nuclear Center
13108 Saint-Paul-Lez-Durance Cedex
FRANCE

Dr. Lothar Wolf
Battelle Institute EV
AM Romerhof 35
D-6000
Frankfurt/Main90
GERMANY

Gesellschaft fur Anlagen- und Reaktorsicherheit (3)
Attn: Ulrich Erven
Walter Erdmann
Manfred Firnhaber
Schwertnergasse 1
D-5000 Koln 1
GERMANY

Kernforschungzentrum, Karlsruhe (3)
Attn: P. Hofmann
Werner Scholtyssek
Philipp Schmuck
P. O. Box 3640
D-7500 Karlsruhe 1
GERMANY

Udo Brockmeier
University of Bochum
Energietechnik
IB-4-128
D-4630 Bochum
GERMANY

György Gyenes
Central Research Institute for Physics
Institute for Atomic Energy Research
H-1525 Budapest, P. O. Box 49
HUNGARY

Joint Research Center
Commission of the European Communities
Attn: Alan Jones
Iain Shepherd
Safety Technology Institute
21020 Ispra (Va)
ITALY

Giovanni Saponaro
ENEA
Natl. Comm. for R&D of Nuclear Energy
Via Vitaliano Brancati, 48
00144 Rome
ITALY

Japan Atomic Energy Research Institute (3)
Attn: Kunihisa Soda
Jun Sugimoto
Norihiro Yamano
Tokai-mura, Naka-gun, Ibaraki-ken
319-11, JAPAN

Dr. Masayoshi Shiba, Director General
Institute of Nuclear Safety
Nuclear Power Engineering Corporation
Fujita Kankou Toranoman Bldg. 7F
3-17-1, Toranoman
Minato-Ku, Tokyo, 105
JAPAN

Masao Ogino
Mitsubishi Atomic Power Industries
4-1 Shibakoen 2-Chome
Minatoku Tokyo
JAPAN

Hidetoshi Okada
Nuclear Power Engineering Corporation
3-17-1, Toranomon Bldg. 5F
Minato-ku, Tokyo 105
JAPAN

Hirohide Oikawa
Toshiba Corporation
8, Shin-Sugita, Isogo-ku
Yokohama
JAPAN

Korea Atomic Energy Research Inst. (3)
Attn: Kun-Joong Yoo
Song-Won Cho
Dong-Ha Kim
P. O. Box 7, Daeduk Danji
Taejon
SOUTH KOREA 305-353

Jae Hong Park
Safety Assessment Department
Korea Atomic Energy Research Institute
P. O. Box 16, Daeduk-Danji
Taejon
SOUTH KOREA 305-353

Netherlands Energy Research Foundation (2)
Attn: Karel J. Brinkmann
E. J. Velema
P. O. Box 1
1755 ZG Petten
THE NETHERLANDS

Dr. Valery F. Strizhov
Russian Academy of Science
Institute of Nuclear Safety
Moscow, G. Tulsky, 52
113191, RUSSIA

Dr. B. Mavko
Institut Josef Stepan
Odsek za Reaktorsko Tehniko
61111 Ljubljana
Jamova 39
P. O. Box 100
SLOVENIA

Universidad Politecnica de Madrid (2)
Attn: Augustin Alonzo Santos
Francisco Martin
E.T.S. Ingenieros Industriales
Jose Gutierrez Abascal, 2
28006 Madrid
SPAIN

Juan Bagues
Consejo de Seguridad Nuclear
Justo Dorado, 11
28040, Madrid
SPAIN

Oddbjörn Sandervåg
Statens Kärnkraftinspektion
Swedish Nuclear Power Inspectorate
Box 27106 102 52 Stockholm
SWEDEN

L. Hammar, Director
Division of Research
Swedish Nuclear Power Inspectorate
Statens Karnkraftinspektion
Sehlstedtsgatan 11
Box 27106
S-102-50 Stockholm
SWEDEN

B. Raj Sehgal
Department of Nuclear Power Safety
Royal Institute of Technology
Brinellvagen 60
S-100 44 Stockholm
SWEDEN

Swiss Federal Nuclear Safety Inspectorate (4)
Attn: S. Chakraborty
Sang Lung Chan
U. Schmocker
H. P. Isaak
CH-5232 Villigen-HSK
SWITZERLAND

United Kingdom Atomic Energy Agency (3)
Winfrith Technology Center
Attn: T. Haste
S. R. Kinnersley
D. W. Sweet
Winfrith, Dorchester, Dorset
UNITED KINGDOM, DTS 8DH

C. Wheatley
United Kingdom Atomic Energy Authority
Safety & Reliability Directorate
Wigshaw Lane, Culcheth, Warrington
Cheshire, WA3 4NE
UNITED KINGDOM

Geoffrey Brown
AEA Technology
Consultancy Services
Thomson House
Risley, Warrington WA3 6AT
UNITED KINGDOM

Internal Distribution:

MS1328 R. S. Longenbaugh, 6342
MS0736 N. R. Ortiz, 6400
MS0744 W. A. von Riesemann, 6403
MS0744 D. A. Powers, 6404
MS0747 A. L. Camp, 6412
MS0747 S. E. Dingman, 6412
MS0748 F. T. Harper, 6413
MS0742 J. E. Kelly, 6414
MS0745 S. L. Thompson, 6418 (10 copies)
MS0745 R. K. Cole, 6418
MS0745 A. A. Elsbernd, 6418
MS0745 L. N. Kmetyk, 6418 (10 copies)
MS0745 R. C. Smith, 6418
MS0745 D. S. Stuart, 6418
MS0745 R. M. Summers, 6418
MS0899 Technical Library, 7141 (5 copies)
MS0619 Technical Publications, 7151
MS0100 Document Processing for DOE/OSTI, 7613-2 (10 copies)
MS9018 Central Technical Files, 8523-2

*U.S. GOVERNMENT PRINTING OFFICE 1994-0-573-026/00008